iJERGS International Journal of Engineering Research And General Science

Journal which deals with research, Innovation and Originality

International Journal Of Engineering Research and General Science

ISSN 2091 - 2730

Table of Content

CHIEF EDITOR BOARD

Message from IJERGS

This is the Forth Issue of the Sixth Volume of International Journal of Engineering Research and General Science. A total of 15 research articles are published and we sincerely hope that each one of these provides some significant stimulation to a reasonable segment of our community of readers.

In this issue, we have focused mainly on the Innovative Ideas. We also welcome more research oriented ideas in our upcoming Issues.

Author's response for this issue was really inspiring for us. We received many papers from many countries in this issue but our technical team and editor members accepted very less number of research papers for the publication. We have provided editors feedback for every rejected as well as accepted paper so that authors can work out in the weakness more and we shall accept the paper in near future.

Our team have done good job however, this issue may possibly have some drawbacks, and therefore, constructive suggestions for further improvement shall be warmly welcomed.

IJERGS Team,

International Journal of Engineering Research and General Science

E-mail – feedback@ijergs.org

International Journal of Engineering Research and General Science Volume 6, Issue 4, July-August, 2018
ISSN 2091-2730

COMPARITIVE STUDY OF SPECIES ANALYSIS OF SEMI-CRYOGENIC PROPELLANTS

Danish Parvez, Samadarshi Adhikari

Amity University Gurugram, Danishparvez003@gmail.com

Abstract— Different computational software's were used for species analysis of various semi-cryogenic propellants. After analyzation the ideal and estimated values of various different parameters were calculated. Rocket Propulsion Analysis, a software developed by NASA was used for computing the ideal and estimated values as well as plotting of graphs with respect to different species. The adiabatic temperature of the species was also calculated by performing calculations on Microsoft Excel. In the end 1,1,1,2-tetraflouroethane, a semi-cryogenic propellant was used in order to draw comparison with other species such as Hydrogen, Methane, RPA-1. Graphical representation of the main variables such as pressure, temperature, density, specific heat etc. with respect to the different nozzle positions was also done.

Keywords— Cryogenics, Cryogenic Engines, Cryogenic Propellants, Semi-Cryogenic Propellants, Species Analysis, RPA Analysis, Hydrogen (H_2), Methane (CH_4), RP1($C_{13}H_{28}$), 1,1,1,2-Tetra Floro Ethane (CH_2FCF_3).

INTRODUCTION

The branch of physics dealing with the production of very low temperature as well as their effect on matter is known as cryogenics. In Cryogenics the gas is cooled by compressing the gas, which in turn releases heat and later when allowed to expand produces ultra-low temperatures. Cooling can also be accomplished by magnetocaloric effect which is a magneto thermodynamic phenomenon in which exposing the material to a changing magnetic field causes a change in temperature. Cryogenic propellant is a type of liquid propellant that is kept at very low temperatures to remain liquid [1]. The commonest examples are liquid hydrogen(LH_2) and liquid oxygen(LOX). Special insulated containers and vents are used to store Cryogenic propellants in order to allow gas from the evaporating liquids to escape. Liquid fuel and oxidizer from the storage tanks are fed to an expansion chamber and then injected into the combustion chamber with proper feeding system, where they are further mixed and ignited by a flame or spark.

Low temperatures of cryogenic propellants make them difficult to store over long periods of time. For example, LH_2 has a very low density (0.59 pounds per gallon) and therefore, requires a storage volume greater than other fuels. The high efficiency of cryogenic propellants despite these drawbacks makes them the ideal choice, when reaction time and storability are not too critical.

United States of America in 1963 was the first country to develop the Cryogenic Rocket Engine (CRE) with the use of RL 10 engines employed on Atlas-V rocket [2]. Indian Space and Research Organization (ISRO) plans to develop a 2000 Kn Semi Cryogenic Engine (SCE) using LOX and ISROSENE (propellant-grade kerosene) for space applications. LOX and Kerosene are environmentally friendly and low-cost propellants. This Semi-Cryogenic engine will be used as the booster engine for the Common Liquid Core of the future heavy-lift Unified Launch Vehicles (ULV) and Reusable Launch Vehicles (RLV).

The liquid stages of PSLV and GSLV engines use toxic propellants that are harmful to the environment. The drift across the globe is to change over to eco-friendly propellants [3]. The green propellant candidates are plentiful and include combinations like LOX –LH_2 and LOX - pure hydrocarbons. 1112-Tetrafluoroethane also known as norflurane (INN), is a halo alkane refrigerant with insignificant ozone depletion potential and a lower global warming potential [4][5].1,1,1,2-Tetrafluoroethane is a non-flammable gas whose other uses include plastic foam blowing, cleaning solvent, etc. It is also used as a solvent in organic chemistry, both in liquid and supercritical fluid. It is also used for other types of particle detectors. [6][7].

LITERATURE SURVEY

CRYOGENIC ROCKET ENGINE

A rocket engine that uses cryogenic fuel or oxidizer is known as a cryogenic rocket engine. Its fuel or oxidizer (or both) are gases that are liquefied and stored at very low temperatures. These engines require high mass flow rate of both oxidizer and fuel to generate sufficient thrust. Oxygen and low molecular weight hydrocarbons are used as oxidizer and fuel pair. They are in gaseous state at room temperature and pressure. Theoretically, if we store propellants as pressurized gases, the size and mass of the tanks would severely decrease rocket efficiency, therefore in order to get the required mass flow rate the propellants must be cooled down to cryogenic temperatures (below −150 °C, −238 °F)[8]. This converts them from gaseous state to liquid state. All cryogenic rocket engines by definition are, either liquid-propellant rocket engines or hybrid rocket engines. The most widely used combination amongst the numerous cryogenic fuel-oxidizer combinations is that of liquid hydrogen (LH_2) as fuel and liquid oxygen (LOX) as oxidizer. These components when burned have one of the maximum entropy releases by combustion. They produce a specific impulse up to 450 s with an effective exhaust velocity of 4.4 km/s [9].

(Fig.1 Cryogenic engine /Source; Cryogenic Technology Development for Exploration Missions by David J. Chato)

COMPONENTS

Cryogenic rocket engine comprises of a combustion chamber, fuel cryopumps, oxidizer cryopumps, gas turbine, cryo valves, regulators, pyrotechnic igniter, fuel injector, fuel tanks, and rocket engine nozzle. Cryogenic rocket engines work in either an expander cycle, a gas generator cycle, a staged combustion cycle, or the simplest pressure-fed cycle in order to feed the propellants to the combustion chamber. Looking at this aspect, engines can be differentiated into a main flow or a bypass flow configuration [10].

WORKING

Cryogenic Engines are rocket motors that are designed for liquid fuels held at cryogenic temperatures. Hydrogen and Oxygen are used typically which need to be held below 20°K (-423°F) and 90°K (297°F) in order to remain liquid. The engine components are also cooled so that the fuel doesn't boil and change to gaseous form in the feeding system. Thrust is generated due to the rapid expansion from liquid to gaseous state, with the gas emerging from the motor at very high speed. Cryogenic engines are the highest performing rocket motors. However, one disadvantage of cryogenic engines is that the fuel tanks tend to be bulky since they require heavy insulation to store the propellant. This disadvantage is however compensated by their high fuel efficiency. Ariane 5 uses oxygen and hydrogen, both stored as a cryogenic liquid, to produce its power. Liquid nitrogen, stored at -320 degrees Fahrenheit, is vaporized with the help of heat exchanger. Nitrogen gas formed in the heat exchanger then expands to about 700 times the volume of its liquid form. The force of the nitrogen gas is converted into mechanical power when the highly pressurized gas is fed to the expander.

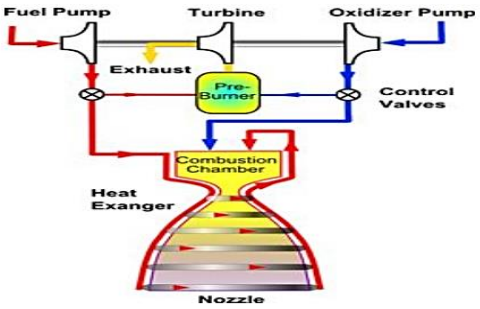

(Fig.2 Working principle of cryogenic engine /

Source; Richard Cohn, Developments in Liquid Rocket Engine Technology, Air Force Research Laboratory, 2012.)

CRYOGENIC PROPELLANTS

The fuel and the oxidizer are in the form of very cold, liquefied gases in a cryogenic propellant. Since they stay in liquid form even though they are at a temperature lower than their freezing point these liquefied gases are referred to as super cooled. Thus cryogenic fuels are super cooled gases used as liquid fuels. These propellants however are gases at normal atmospheric conditions. Because of their very low densities storing these propellants aboard a rocket is a very difficult task. Hence in order to store the propellants extremely huge tanks are required. Although their density can be increased by cooling and compressing them into liquids hence, making it possible to store them in large quantities in smaller tanks. The propellant combination of liquid oxygen and liquid hydrogen is normally used, Liquid oxygen being the oxidizer and liquid hydrogen being the fuel. [11].

CRYOGEN	TRIPLE POINT [k]	NORMAL B.P. [k]	CRITICAL POINT [k]
METHANE (CH_4)	90.7	111.6	190.5
OXYGEN (O_2)	54.4	90.2	154.6
ARGON	83.3	87.3	150.9
NITROGEN	63.1	77.3	126.2
NEON	24.6	27.1	44.4
HYDROGEN (H_2)	13.8	20.4	33.2
HELIUM	2.2	4.2	5.2

.

(TABLE 1; Characteristic Temperature of Cryogenic fluids;

Source; International Journal of Aerospace and Mechanical Engineering Volume 2 – No.5, August 2015, Cryogenic Technology & Rocket Engines)

The trend worldwide is to change over to eco-friendly propellants. Already known combinations like LOX - LH2 and LOX - pure hydrocarbons are amongst the numerous green propellant candidates. Solid propellant boosters could be also replaced by green liquid propellants but green solid candidates exist also. A first review of candidate chemical products revealed that no perfect green exist. The maximum allowable concentration in air for workers is sometimes very low for some green candidates. Other can form very easily explosive mixtures with air. Some risks should be accepted when greens are selected and they could be mitigated by appropriate measures.

ROCKET PROPULSION ANALYSIS (RPA)

RPA stands for Rocket Propulsion Analysis. It is an easy-to-use multi-platform tool used for the performance prediction of rocket engines. Along with convenient grouping of the input parameters and analysis results it also features an intuitive graphical user interface. Based on NASA's Glenn thermodynamic database RPA utilizes an expandable chemical species library. This library includes data for numerous fuels and oxidizers, such as liquid hydrogen and oxygen, kerosene, hydrogen peroxide and many others. The users can also easily define new propellant components, or import components from PROPEP or CEA2 species databases with embedded species editor.

The program obtains chemical equilibrium composition of combustion products by providing a few engine parameters such as combustion chamber pressure, used propellant components, and nozzle parameters, as well as determines its thermodynamic properties. It also predicts the theoretical rocket performance. These calculations are used in the designing process of combustion chambers, gas generators and preburners. Based on robust, proven and industry-accepted Gibbs free energy minimization approach the calculation method is used to obtain the combustion composition. Further analysis of nozzle flows with shifting and frozen chemical equilibrium, and calculation of engine performance for a finite and infinite-area combustion chambers is also done. RPA is written in C++ programming language using following libraries: Qt, Qwt, libconfig++ [12][13]. * Ambient condition for optimum expansion: H=0.00 km, p=1.000 atm.

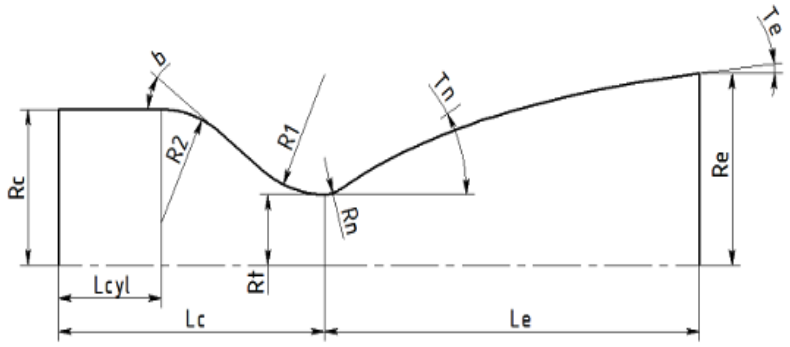

Rc ***;*** *Chamber radius*

Lcyl; *Length of cylinder*

R2; *Contraction of throat radius*

B; *Contraction angle*

Rt; *Throat radius*

Lc; *Distance from start of nozzle to throat*

R1; *Radius of throat profile*

Rn; *Projected radius*

Tn; *Divergent angle*

Le; *Distance from throat to exit nozzle*

Re; *Exit radius*

Te; *Exit angle*

(Fig 3. Contour of exhaust nozzle; Source: RPA Analysis)

HYDROGEN (H2)

Component	Temperature (K)	Mass fraction	Mole fraction
H2(L)	20.27	0.18	0.77
O2(L)	90.17	0.82	0.23
	Total	1.00	1.00

Exploded propellant formula:	$O_{0.455}$ $H_{1.545}$
O/F =	4.672
O/F^0 =	7.937 (stoichiometric)
α_{ox} =	0.589 (oxidizer excess coefficient)

(Table 3: Propellant Specification; Source: RPA Analysis)

Species	Injector	Injector	Nozzle inlet	Nozzle inlet	Nozzle throat	Nozzle throat	Nozzle exit	Nozzle exit
	mass fractions	mole fractions	mass fractions	mole fractions	mass fractions	mole fractions	mass fractions	mole fractions
H	0.001413	0.015825	0.001413	0.015825	0.000919	0.010344	1E-07	1.4E-06
H2	0.072028	0.403252	0.072028	0.403252	0.072095	0.40569	0.072519	0.411333
H2O	0.911701	0.571154	0.911701	0.571154	0.918903	0.578609	0.927481	0.588666
H2O2	5.4E-06	1.8E-06	5.4E-06	1.8E-06	1.8E-06	6E-07		
HO2	5.5E-06	1.9E-06	5.5E-06	1.9E-06	1.5E-06	5E-07		
O	0.00029	0.000205	0.00029	0.000205	0.000106	7.53E-05		
O2	0.000321	0.000113	0.000321	0.000113	0.00012	4.25E-05		
OH	0.014237	0.009448	0.014237	0.009448	0.007855	0.005239		

(Table 4. Fractions of the combustion products; Source: RPA Analysis)

Parameter	Injector	Nozzle inlet	Nozzle throat	Nozzle exit	Unit
Pressure	15.0000	15.0000	8.5217	0.1013	MPa
Temperature	3230.2733	3230.2733	2982.6784	1345.8039	K
Enthalpy	-1122.2620	-1122.2620	-2412.6981	-9208.9043	kJ/kg
Entropy	19.4372	19.4372	19.4372	19.4372	kJ/(kg·K)
Internal energy	-3502.0145	-3502.0145	-4598.8717	-10187.5188	kJ/kg
Specific heat (p=const)	6.0388	6.0388	5.4520	3.4860	kJ/(kg·K)
Specific heat (V=const)	5.1144	5.1144	4.5998	2.7588	kJ/(kg·K)
Gamma	1.1807	1.1807	1.1853	1.2636	
Isentropic exponent	1.1730	1.1730	1.1805	1.2636	
Gas constant	0.7367	0.7367	0.7330	0.7272	kJ/(kg·K)
Molecular weight (M)	11.2861	11.2861	11.3437	11.4342	
Molecular weight (MW)	0.01129	0.01129	0.01134	0.01143	

Density	6.3032	6.3032	3.8980	0.1035	kg/m³
Sonic velocity	1670.7359	1670.7359	1606.5095	1112.0076	m/s
Velocity	0.0000	0.0000	1606.5095	4021.6022	m/s
Mach number	0.0000	0.0000	1.0000	3.6165	
Area ratio	infinity	infinity	1.0000	15.0390	
Mass flux	0.0000	0.0000	6262.1399	416.3936	kg/(m²·s)
Mass flux (relative)	0.000e-04	0.000e-04			kg/(N·s)
Viscosity	9.575e-05	9.575e-05	9.033e-05	4.855e-05	kg/(m·s)
Conductivity, frozen	0.6134	0.6134	0.5689	0.2625	W/(m·K)
Specific heat (p=const), frozen	4.316	4.316	4.256	3.486	kJ/(kg·K)
Prandtl number, frozen	0.6737	0.6737	0.6758	0.6446	
Conductivity, effective	1.087	1.087	0.8943	0.2626	W/(m·K)
Specific heat (p=const), effective	6.039	6.039	5.452	3.486	kJ/(kg·K)
Prandtl number, effective	0.5321	0.5321	0.5506	0.6445	

(Table 5. Thermodynamic properties; Source: RPA Analysis)

Parameter	Sea level	Optimum expansion	Vacuum	Unit
Characteristic velocity		2395.35		m/s
Effective exhaust velocity	4021.60	4021.60	4264.94	m/s
Specific impulse (by mass)	4021.60	4021.60	4264.94	N·s/kg
Specific impulse (by weight)	410.09	410.09	434.90	s
Thrust coefficient	1.6789	1.6789	1.7805	

(Table 6. Theoretical (ideal) performance; Source: RPA Analysis)

Parameter	Sea level	Optimum expansion	Vacuum	Unit
Characteristic velocity		2390.91		m/s
Effective exhaust velocity	3913.47	3913.47	4156.81	m/s
Specific impulse (by mass)	3913.47	3913.47	4156.81	N·s/kg
Specific impulse (by weight)	399.06	399.06	423.88	s
Thrust coefficient	1.6368	1.6368	1.7386	

(Table 7. Estimated delivered performance; Source: RPA Analysis)

METHANE (CH4)

Component	Temperature (K)	Mass fraction	Mole fraction
CH4(L)	111.64	0.23	0.37
O2(L)	90.17	0.77	0.63
Total		1	1
Exploded propellant formula:	$O_{1.252}$ $C_{0.374}$ $H_{1.495}$		
O/F =	3.341		

O/F^0 =	3.989 (stoichiometric)		
α_{ox} =	0.837 (oxidizer excess coefficient)		

(Table 8: Propellant Specification; Source: RPA Analysis)

Parameter	Injector	Nozzle inlet	Nozzle throat	Nozzle exit	Unit
Pressure	10	10	5.7838	0.1013	MPa
Temperature	3590.9374	3590.9374	3411.3432	2191.902	K
Enthalpy	-1593.6405	-1593.6405	-2326.6326	-6502.1	kJ/kg
Entropy	12.0987	12.0987	12.0987	12.0987	kJ/(kg·K)
Internal energy	-2975.6995	-2975.6995	-3623.2121	-7288.6	kJ/kg
Specific heat (p=const)	6.6033	6.6033	6.3784	2.4822	kJ/(kg·K)
Specific heat (V=const)	5.6286	5.6286	5.4759	2.1053	kJ/(kg·K)
Gamma	1.1732	1.1732	1.1648	1.179	
Isentropic exponent	1.1335	1.1335	1.1307	1.178	
Gas constant	0.3849	0.3849	0.3801	0.3588	kJ/(kg·K)
Molecular weight (M)	21.6031	21.6031	21.8756	23.1716	
Molecular weight (MW)	0.0216	0.0216	0.02188	0.02317	
Density	7.2356	7.2356	4.4608	0.1288	kg/m³
Sonic velocity	1251.6157	1251.6157	1210.7803	962.5474	m/s
Velocity	0	0	1210.7803	3133.196	m/s
Mach number	0	0	1	3.2551	
Area ratio	infinity	infinity	1	13.3805	
Mass flux	0	0	5401.0443	403.6499	kg/(m²·s)
Mass flux (relative)	0.00E+00	0.00E+00			kg/(N·s)
Viscosity	0.000114	0.000114	0.0001103	8.16E-05	kg/(m·s)
Conductivity, frozen	0.396	0.396	0.3782	0.2502	W/(m·K)
Specific heat (p=const), frozen	2.348	2.348	2.336	2.191	kJ/(kg·K)
Prandtl number, frozen	0.6759	0.6759	0.681	0.7147	
Conductivity, effective	1.387	1.387	1.276	0.3145	W/(m·K)
Specific heat (p=const), effective	6.603	6.603	6.378	2.482	kJ/(kg·K)
Prandtl number, effective	0.5428	0.5428	0.551	0.644	

(Table 9. Thermodynamic properties; Source: RPA Analysis)

Species	Injector	Injector	Nozzle inlet	Nozzle inlet	Nozzle throat	Nozzle throat	Nozzle exit	Nozzle exit
	mass fractions	mole fractions	mass fractions	mole fractions	mass fractions	mole fractions	mass fractions	mole fractions
CO	0.2381517	0.1836771	0.2381517	0.183677	0.227494	0.177671	0.1666726	0.137882
CO2	0.2577548	0.1265249	0.2577548	0.126525	0.274536	0.136463	0.3701455	0.194887
COOH	0.0000392	0.0000188	0.0000392	1.88E-05	2.27E-05	0.000011		
H	0.0009841	0.0210931	0.0009841	0.021093	0.000833	0.018087	0.0000654	0.001503
H2	0.0079433	0.085124	0.0079433	0.085124	0.007528	0.081686	0.0068581	0.078831

H2O	0.4112356	0.4931347	0.4112356	0.493135	0.420785	0.510953	0.4548955	0.585096
H2O2	0.0000391	0.0000248	0.0000391	2.48E-05	2.27E-05	1.46E-05		
HCHO	0.0000009	0.0000007	0.0000009	7E-07	5E-07	4E-07		
HCO	0.0000238	0.0000177	0.0000238	1.77E-05	1.29E-05	9.8E-06		
HCOOH	0.0000075	0.0000035	0.0000075	3.5E-06	4.2E-06	0.000002		
HO2	0.0001861	0.0001218	0.0001861	0.000122	0.000111	7.39E-05		
O	0.00624	0.0084255	0.00624	0.008426	0.004687	0.006409	0.0000141	2.04E-05
O2	0.0276826	0.0186891	0.0276826	0.018689	0.022651	0.015485	0.000088	6.37E-05
O3	0.0000002	0.0000001	0.0000002	1E-07				
OH	0.0497109	0.0631438	0.0497109	0.063144	0.04131	0.053135	0.0012605	0.001717

(Table 10. Fractions of the combustion products; Source: RPA Analysis)

Parameter	Sea level	Optimum expansion	Vacuum	Unit
Characteristic velocity		1851.49		m/s
Effective exhaust velocity	3133.2	3133.2	3384.22	m/s
Specific impulse (by mass)	3133.2	3133.2	3384.22	N·s/kg
Specific impulse (by weight)	319.5	319.5	345.09	s
Thrust coefficient	1.6923	1.6923	1.8278	

(Table 11. Theoretical (ideal) performance; Source: RPA Analysis)

Parameter	Sea level	Optimum expansion	Vacuum	Unit
Characteristic velocity		1826.69		m/s
Effective exhaust velocity	3008.78	3008.78	3259.8	m/s
Specific impulse (by mass)	3008.78	3008.78	3259.8	N·s/kg
Specific impulse (by weight)	306.81	306.81	332.41	s
Thrust coefficient	1.6471	1.6471	1.7845	

(Table 12. Estimated delivered performance; Source: RPA Analysis)

RP1($C_{13}H_{28}$)

Component	Temperature (K)	Mass fraction	Mole fraction
RP-1	298.15	0.27	0.46
O2(L)	90.17	0.73	0.54
	Total	1.00	1.00

Exploded propellant formula:	$O_{1.083}\ C_{0.458}\ H_{0.894}$
O/F =	2.704
α_{ox} =	0.794 (oxidizer excess coefficient)
O/F^0 =	3.406 (stoichiometric)

(Table 13: Propellant Specification; Source: RPA Analysis)

Parameter	Injector	Nozzle inlet	Nozzle throat	Nozzle exit	Unit
Pressure	10.0000	10.0000	5.7793	0.1013	MPa
Temperature	3740.7309	3740.7309	3553.8958	2354.4877	K
Enthalpy	-773.5330	-773.5330	-1462.4738	-5389.633	kJ/kg
Entropy	11.0335	11.0335	11.0335	11.0335	kJ/(kg·K)
Internal energy	-2071.588	-2071.588	-2678.6198	-6139.435	kJ/kg
Specific heat (p=const)	6.3447	6.3447	6.2320	2.4608	kJ/(kg·K)
Specific heat (V=const)	5.3499	5.3499	5.2979	2.1040	kJ/(kg·K)
Gamma	1.1860	1.1860	1.1763	1.1695	
Isentropic exponent	1.1370	1.1370	1.1330	1.1670	
Gas constant	0.3470	0.3470	0.3422	0.3185	kJ/(kg·K)
Molecular weight (M)	23.9606	23.9606	24.2971	26.1087	
Molecular weight (MW)	0.02396	0.02396	0.0243	0.02611	
Density	7.7038	7.7038	4.7521	0.1351	kg/m³
Sonic velocity	1214.8433	1214.8433	1173.8361	935.4050	m/s
Velocity	0.0000	0.0000	1173.8361	3038.4536	m/s
Mach number	0.0000	0.0000	1.0000	3.2483	
Area ratio	infinity	infinity	1.0000	13.5853	
Mass flux	0.0000	0.0000	5578.1922	410.6035	kg/(m²·s)
Mass flux (relative)	0.000e-04	0.000e-04			kg/(N·s)
Viscosity	0.0001149	0.0001149	0.0001111	8.418e-05	kg/(m·s)
Conductivity, frozen	0.355	0.355	0.3396	0.2354	W/(m·K)
Specific heat (p=const), frozen	2.019	2.019	2.011	1.924	kJ/(kg·K)
Prandtl number, frozen	0.6537	0.6537	0.658	0.688	

Conductivity, effective	1.419	1.419	1.333	0.3623	W/(m·K)
Specific heat (p=const), effective	6.345	6.345	6.232	2.461	kJ/(kg·K)
Prandtl number, effective	0.5138	0.5138	0.5193	0.5718	

(Table 14. Thermodynamic properties; Source: RPA Analysis)

(Table 15.

Species	**Injector**	**Injector**	**Nozzle inlet**	**Nozzle inlet**	**Nozzle throat**	**Nozzle throat**	**Nozzle exit**	**Nozzle exit**
	mass fractions	**mole fractions**	**mass fractions**	**mole fractions**	**mass fractions**	**mole fractions**	**mass fractions**	**mole fractions**
CO	0.3484917	0.298109	0.3484917	0.2981093	0.3354517	0.290984	0.260107	0.242449
CO2	0.3023635	0.164619	0.3023635	0.1646193	0.3229032	0.178271	0.441354	0.261833
COOH	0.0000529	2.82E-05	0.0000529	0.0000282	0.0000313	1.69E-05	3E-07	2E-07
H	0.0010981	0.026103	0.0010981	0.0261033	0.0009493	0.022883	0.000127	0.003297
H2	0.0059015	0.070145	0.0059015	0.0701451	0.0056439	0.068025	0.005212	0.0675
H2O	0.2507053	0.333442	0.2507053	0.333442	0.2582547	0.348306	0.290187	0.420554
H2O2	0.000032	2.25E-05	0.000032	0.0000225	0.0000191	1.37E-05		
HCHO	0.0000011	9E-07	0.0000011	0.0000009	0.0000006	5E-07		
HCO	0.0000389	3.21E-05	0.0000389	0.0000321	0.0000216	1.81E-05	2E-07	1E-07
HCOOH	0.0000075	3.9E-06	0.0000075	0.0000039	0.0000043	2.3E-06		
HO2	0.0002046	0.000149	0.0002046	0.0001485	0.000127	9.35E-05	2E-07	2E-07
O	0.0091408	0.013689	0.0091408	0.0136892	0.0071031	0.010787	7.16E-05	0.000117
O2	0.0330513	0.024749	0.0330513	0.0247487	0.0279008	0.021185	0.000371	0.000302
O3	0.0000004	2E-07	0.0000004	0.0000002				
OH	0.0489102	0.068907	0.0489102	0.0689066	0.0415892	0.059415	0.002571	0.003947

Fractions of the combustion products; Source: RPA Analysis)

Parameter	Sea level	Optimum expansion	Vacuum	Unit
Characteristic velocity		1792.70		m/s
Effective exhaust velocity	3038.45	3038.45	3285.22	m/s
Specific impulse (by mass)	3038.45	3038.45	3285.22	N·s/kg
Specific impulse (by weight)	309.84	309.84	335.00	s
Thrust coefficient	1.6949	1.6949	1.8326	

(Table 16. Theoretical (ideal) performance; Source: RPA Analysis)

Parameter	Sea level	Optimum expansion	Vacuum	Unit
Characteristic velocity		1770.67		m/s
Effective exhaust velocity	2921.29	2921.29	3168.06	m/s
Specific impulse (by mass)	2921.29	2921.29	3168.06	N·s/kg
Specific impulse (by weight)	297.89	297.89	323.05	s
Thrust coefficient	1.6498	1.6498	1.7892	

(Table 17. Estimated delivered performance; Source: RPA Analysis)

1,1,1,2-TETRA FLORO ETHANE (CH2FCF3)

Parameter	Sea level	Optimum expansion	Vacuum	Unit
Characteristic velocity		1856.2		m/s
Effective exhaust velocity	3112.32	3112.32	3363.33	m/s
Specific impulse (by mass)	3112.32	3112.32	3363.33	N·s/kg
Specific impulse (by weight)	317.37	317.37	342.96	s
Thrust coefficient	1.6767	1.6767	1.8119	
Characteristic velocity		1830.91		m/s
Effective exhaust velocity	2987.92	2987.92	3238.93	m/s
Specific impulse (by mass)	2987.92	2987.92	3238.93	N·s/kg
Specific impulse (by weight)	304.68	304.68	330.28	s
Thrust coefficient	1.6319	1.6319	1.769	

(Table 18. Theoretical (ideal) & Estimated delivered performance; Source: RPA Analysis)

Parameter	Injector	Nozzle inlet	Nozzle throat	Nozzle exit	Unit
Pressure	10	10	5.6395	0.1013	MPa
Temperature	4196.836	4196.836	3851.7631	2590.4963	K

Enthalpy	258.8972	258.8972	-535.4484	-4584.36	kJ/kg
Entropy	9.862	9.862	9.862	9.862	kJ/(kg·K)
Internal energy	-1198.423	-1198.423	-1854.882	-5365.586	kJ/kg
Specific heat (p=const)	2.9785	2.9785	3.2869	6.9664	kJ/(kg·K)
Specific heat (V=const)	2.3921	2.3921	2.6521	5.899	kJ/(kg·K)
Gamma	1.2451	1.2451	1.2394	1.1809	
Isentropic exponent	1.2135	1.2135	1.2041	1.1273	
Gas constant	0.3472	0.3472	0.3426	0.3016	kJ/(kg·K)
Molecular weight (M)	23.9443	23.9443	24.2721	27.5703	
Molecular weight (MW)	0.02394	0.02394	0.02427	0.02757	
Density	6.8619	6.8619	4.2742	0.1297	kg/m³
Sonic velocity	1329.807	1329.807	1260.4322	938.4393	m/s
Velocity	0	0	1260.4322	3112.3166	m/s
Mach number	0	0	1	3.3165	
Area ratio	infinity	infinity	1	13.346	
Mass flux	0	0	5387.3535	403.6677	kg/(m²·s)
Mass flux (relative)	0.00E+00	0.00E+00			kg/(N·s)
Viscosity	0.000129	0.000129	0.0001217	9.16E-05	kg/(m·s)
Conductivity, frozen	0.2649	0.2649	0.2482	0.1773	W/(m·K)
Specific heat (p=const), frozen	1.454	1.454	1.444	1.414	kJ/(kg·K)
Prandtl number, frozen	0.7065	0.7065	0.7086	0.7307	
Conductivity, effective	0.5773	0.5773	0.5069	0.7119	W/(m·K)
Specific heat (p=const), effective	2.979	2.979	3.287	6.966	kJ/(kg·K)
Prandtl number, effective	0.6642	0.6642	0.7895	0.8967	

(Table 19. Thermodynamic properties: Source; RPA Analysis)

Species	**Injector**	**Injector**	**Nozzle inlet**	**Nozzle inlet**	**Nozzle throat**	**Nozzle throat**	**Nozzle exit**	**Nozzle exit**
	mass fractions	**mole fractions**	**mass fractions**	**mole fractions**	**mass fractions**	**mole fractions**	**mass fractions**	**mole fractions**
C	0.000054	0.000108	0.000054	0.0001076	1.29E-05	2.61E-05		

C2	1.29E-05	1.29E-05	0.0000129	0.0000129	0.000002	2.1E-06		
C2F	0.000314	0.000175	0.0003135	0.0001745	0.000114	6.41E-05		
C2F2	0.008911	0.003441	0.0089114	0.0034405	0.00747	0.002923	0.000138	6.14E-05
C2F3	1.71E-05	5.1E-06	0.0000171	0.0000051	1.19E-05	3.6E-06		
C2F4	7.3E-06	1.8E-06	0.0000073	0.0000018	9.9E-06	2.4E-06	5E-07	1E-07
C2F6							1.1E-06	2E-07
C2H	3.5E-06	3.4E-06	0.0000035	0.0000034	4E-07	4E-07		
C2H2,acetylene	3E-07	2E-07	0.0000003	0.0000002				
C2HF	0.00011	5.99E-05	0.0001101	0.0000599	3.58E-05	1.97E-05		
C2HF3	4E-07	1E-07	0.0000004	0.0000001				
C2O	2.37E-05	1.42E-05	0.0000237	0.0000142	0.000007	4.2E-06		
C3	9.9E-06	6.6E-06	0.0000099	0.0000066	1.4E-06	9E-07		
CF	0.020129	0.015543	0.0201294	0.0155433	0.011309	0.008852	0.000107	9.54E-05
CF+	4.4E-06	3.4E-06	0.0000044	0.0000034	1.4E-06	1.1E-06		
CF2	0.085608	0.04099	0.085608	0.0409903	0.097496	0.047321	0.024069	0.01327
CF3	0.00548	0.001902	0.0054799	0.0019015	0.008319	0.002926	0.004709	0.001881
CF3+	1.6E-06	6E-07	0.0000016	0.0000006	1.4E-06	5E-07		
CF4	0.002841	0.000773	0.0028408	0.0007729	0.009209	0.00254	0.19659	0.061588
CH	6E-07	1.1E-06	0.0000006	0.0000011	1E-07	1E-07		
CH2F	3E-07	2E-07	0.0000003	0.0000002				
CHF	7.63E-05	0.000057	0.0000763	0.000057	2.39E-05	1.82E-05		
CHF2	6.93E-05	3.25E-05	0.0000693	0.0000325	3.67E-05	1.75E-05		
CHF3	4.91E-05	1.68E-05	0.0000491	0.0000168	5.22E-05	1.81E-05	5.8E-06	2.3E-06
CO	0.356872	0.30507	0.3568719	0.3050699	0.356457	0.308886	0.353059	0.347515
CO2	6.62E-05	0.000036	0.0000662	0.000036	6.28E-05	3.46E-05	6.83E-05	4.28E-05
COF2	0.001972	0.000715	0.0019722	0.0007154	0.003333	0.001226	0.012443	0.005197
COHF	4.3E-06	2.1E-06	0.0000043	0.0000021	2.3E-06	1.2E-06		
F	0.20602	0.259654	0.2060201	0.2596535	0.193853	0.247664	0.096853	0.140552
F-	3.2E-06	0.000004	0.0000032	0.000004	1.3E-06	1.6E-06		
F2	0.000225	0.000142	0.0002253	0.000142	0.00018	0.000115	1.26E-05	9.1E-06
FCO	0.001078	0.000549	0.0010776	0.0005489	0.00086	0.000444	8.98E-05	5.27E-05
FO	3E-07	2E-07	0.0000003	0.0000002				
H	8.32E-05	0.001976	0.0000832	0.001976	3.34E-05	0.000804	4E-07	1.04E-05
H2	6.7E-06	7.97E-05	0.0000067	0.0000797	0.000002	2.45E-05		
H2F2	0.003893	0.00233	0.0038932	0.0023298	0.002273	0.001379	5.16E-05	3.56E-05
HCO	2.3E-06	1.9E-06	0.0000023	0.0000019	6E-07	5E-07		
HF	0.306036	0.366274	0.3060358	0.3662741	0.308823	0.374669	0.311801	0.429685
O	1.23E-05	1.84E-05	0.0000123	0.0000184	5.3E-06	0.000008	1E-07	2E-07
OH	0.000001	1.4E-06	0.000001	0.0000014	3E-07	5E-07		

(Table 20. Fractions of the combustion products; Source; RPA Analysis)

RESULT

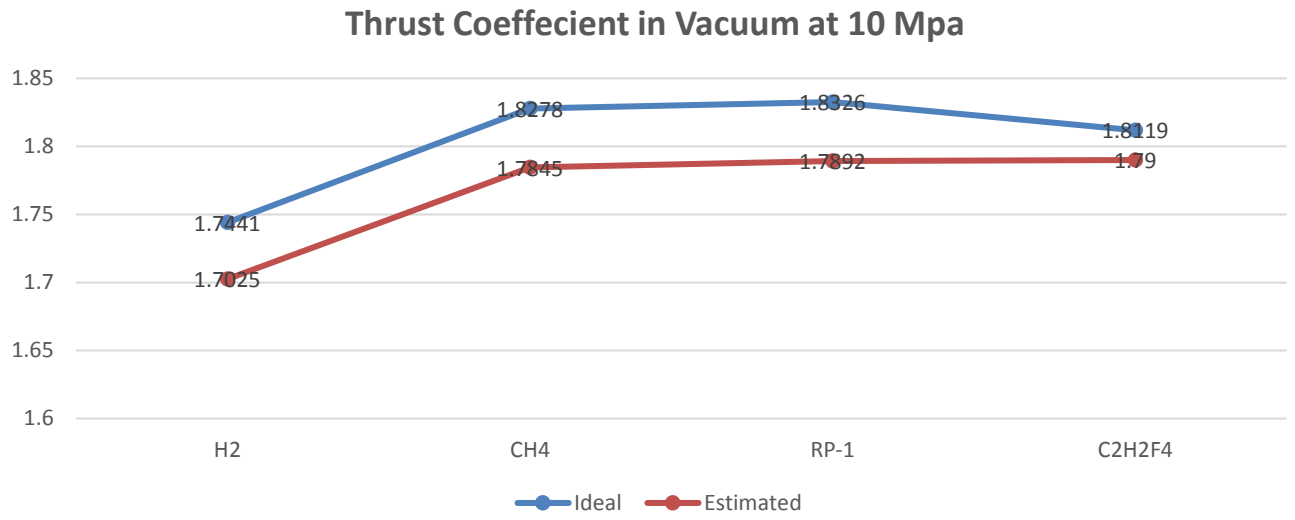
Thrust Coeffecient in Vacuum at 10 Mpa
1.85
1.8
1.75
1.7
1.65
1.6
1.8278
1.8326
1.8119
1.7845
1.7892
1.79
1.7441
1.7025
H2
CH4
RP-1
C2H2F4
Ideal
Estimated

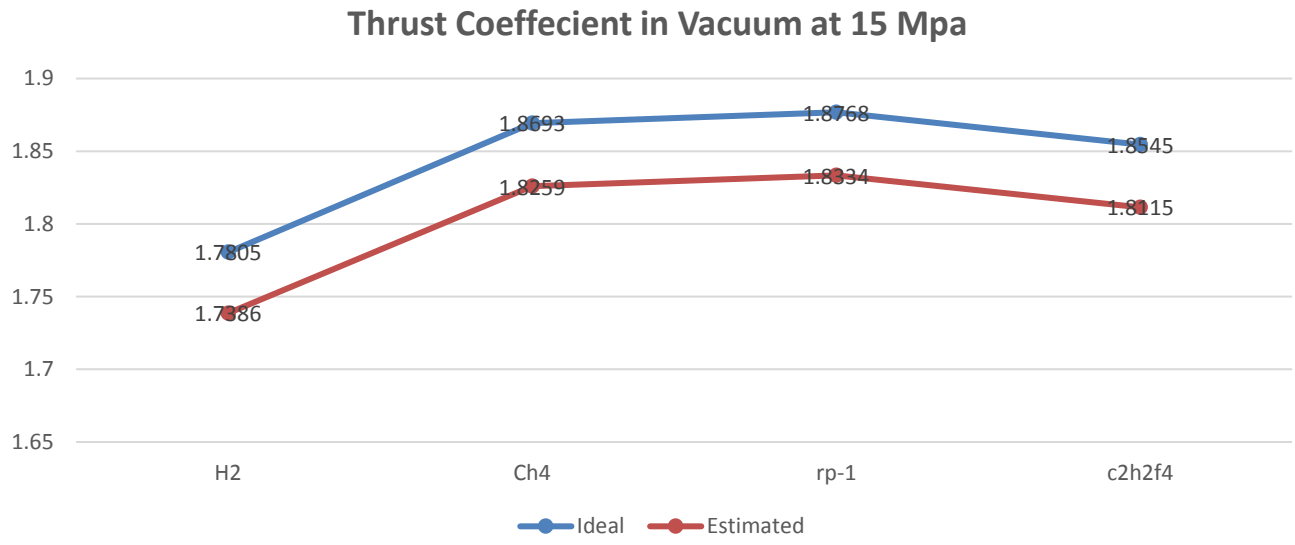
Thrust Coeffecient in Vacuum at 15 Mpa
1.9
1.85
1.8
1.75
1.7
1.65
1.8693
1.8768
1.8545
1.8259
1.8334
1.8115
1.7805
1.7386
H2
Ch4
rp-1
c2h2f4
Ideal
Estimated

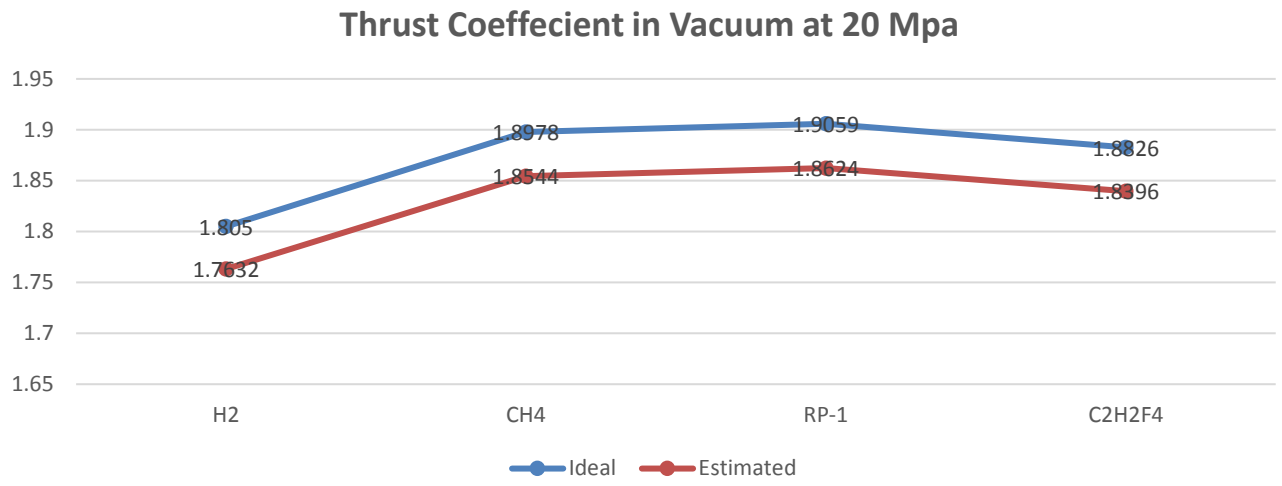
Thrust Coeffecient in Vacuum at 20 Mpa
1.95
1.9
1.85
1.8
1.75
1.7
1.65
1.805
1.8978
1.9059
1.8826
1.7632
1.8544
1.8624
1.8396
H2
CH4
RP-1
C2H2F4
Ideal
Estimated

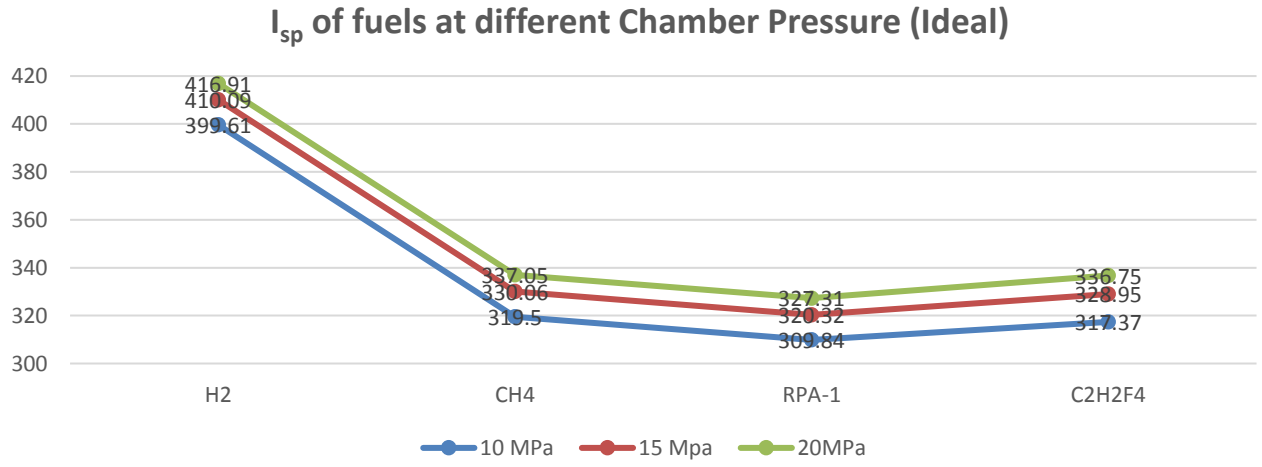
Isp of fuels at different Chamber Pressure (Ideal)
420
400
380
360
340
320
300
416.91
410.09
399.61
337.05
330.06
319.5
327.31
320.32
309.84
336.75
328.95
317.37
H2
CH4
RPA-1
C2H2F4
10 MPa
15 Mpa
20MPa

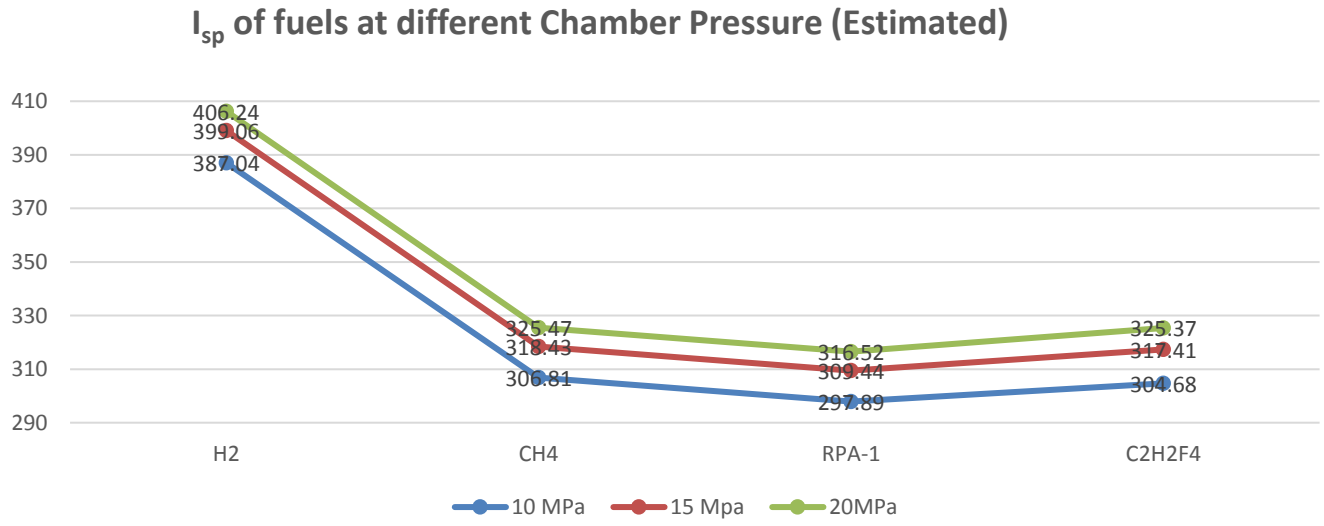
Isp of fuels at different Chamber Pressure (Estimated)
410
390
370
350
330
310
290
406.24
399.06
387.04
325.47
318.43
306.81
316.52
309.44
297.89
325.37
317.41
304.68
H2
CH4
RPA-1
C2H2F4
10 MPa
15 Mpa
20MPa

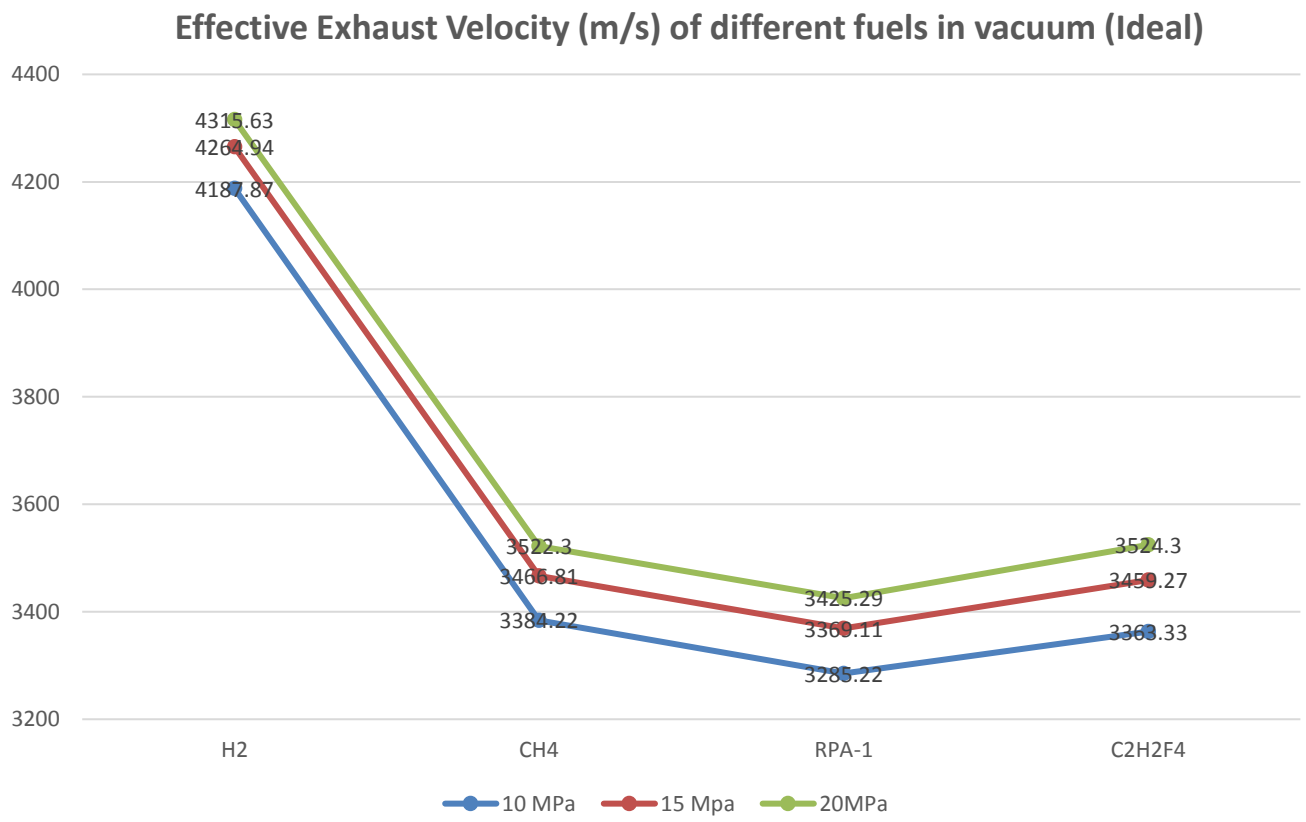
Effective Exhaust Velocity (m/s) of different fuels in vacuum (Ideal)
4400
4200
4000
3800
3600
3400
3200
4315.63
4264.94
4187.87
3522.3
3466.81
3384.22
3425.29
3369.11
3285.22
3524.3
3459.27
3363.33
H2
CH4
RPA-1
C2H2F4
10 MPa
15 Mpa
20MPa

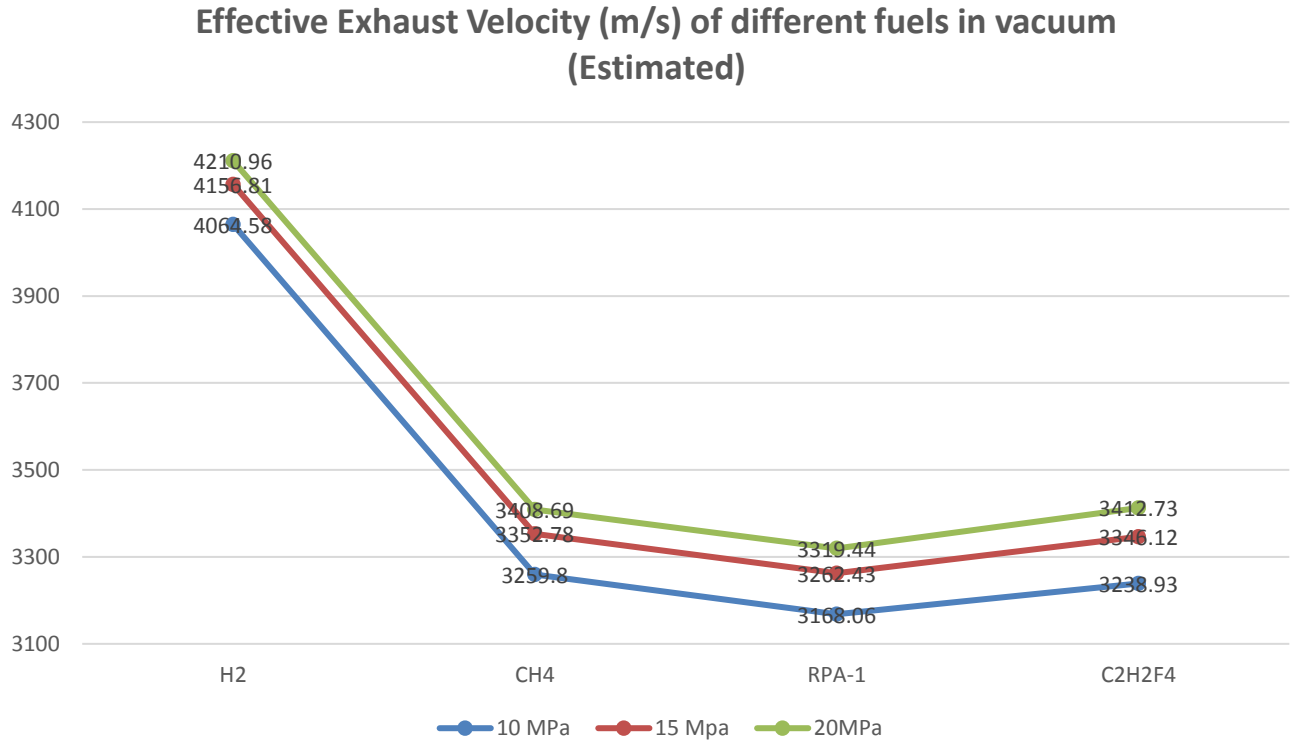
Effective Exhaust Velocity (m/s) of different fuels in vacuum (Estimated)
4300
4100
3900
3700
3500
3300
3100
4210.96
4156.81
4064.58
3408.69
3352.78
3259.8
3319.44
3262.43
3168.06
3412.73
3346.12
3238.93
H2
CH4
RPA-1
C2H2F4
10 MPa
15 Mpa
20MPa

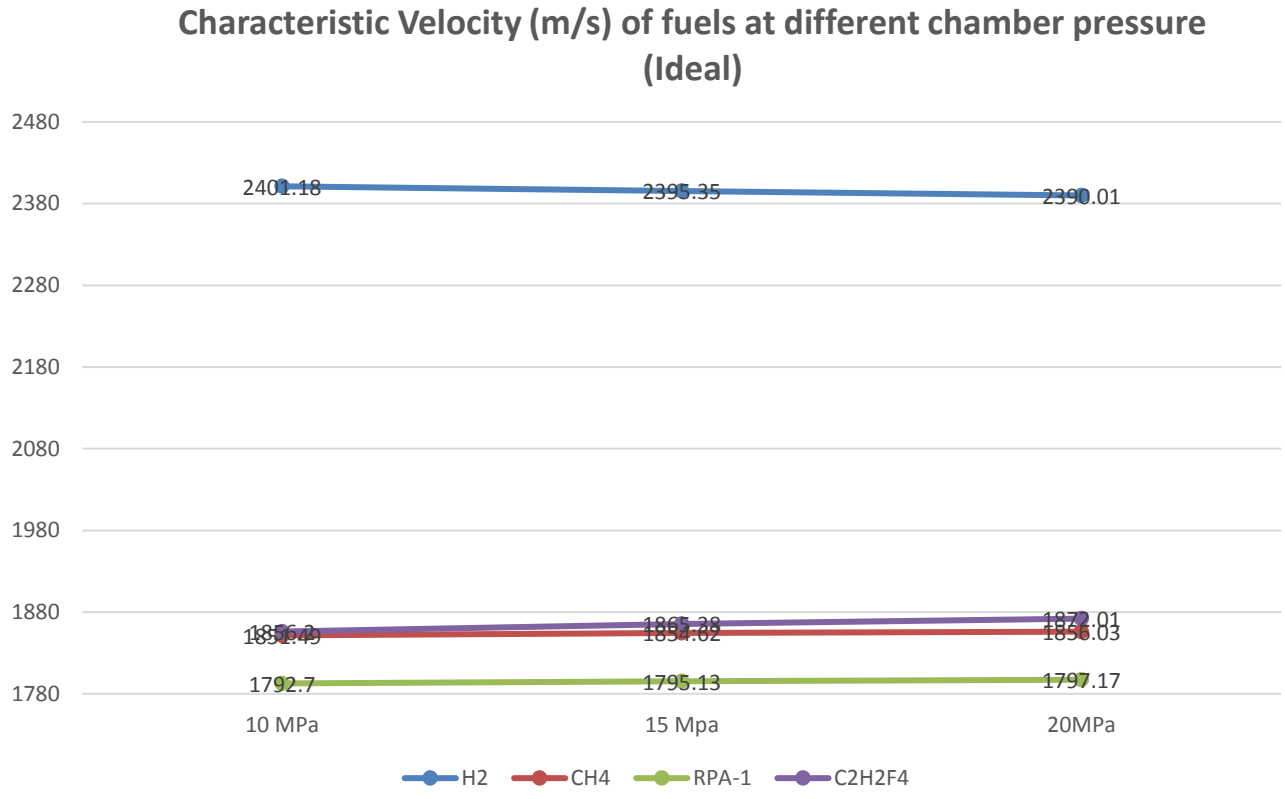
Characteristic Velocity (m/s) of fuels at different chamber pressure (Ideal)
2480
2380
2280
2180
2080
1980
1880
1780
2401.18
2395.35
2390.01
1792.7
1795.13
1797.17
10 MPa
15 Mpa
20MPa
H2
CH4
RPA-1
C2H2F4

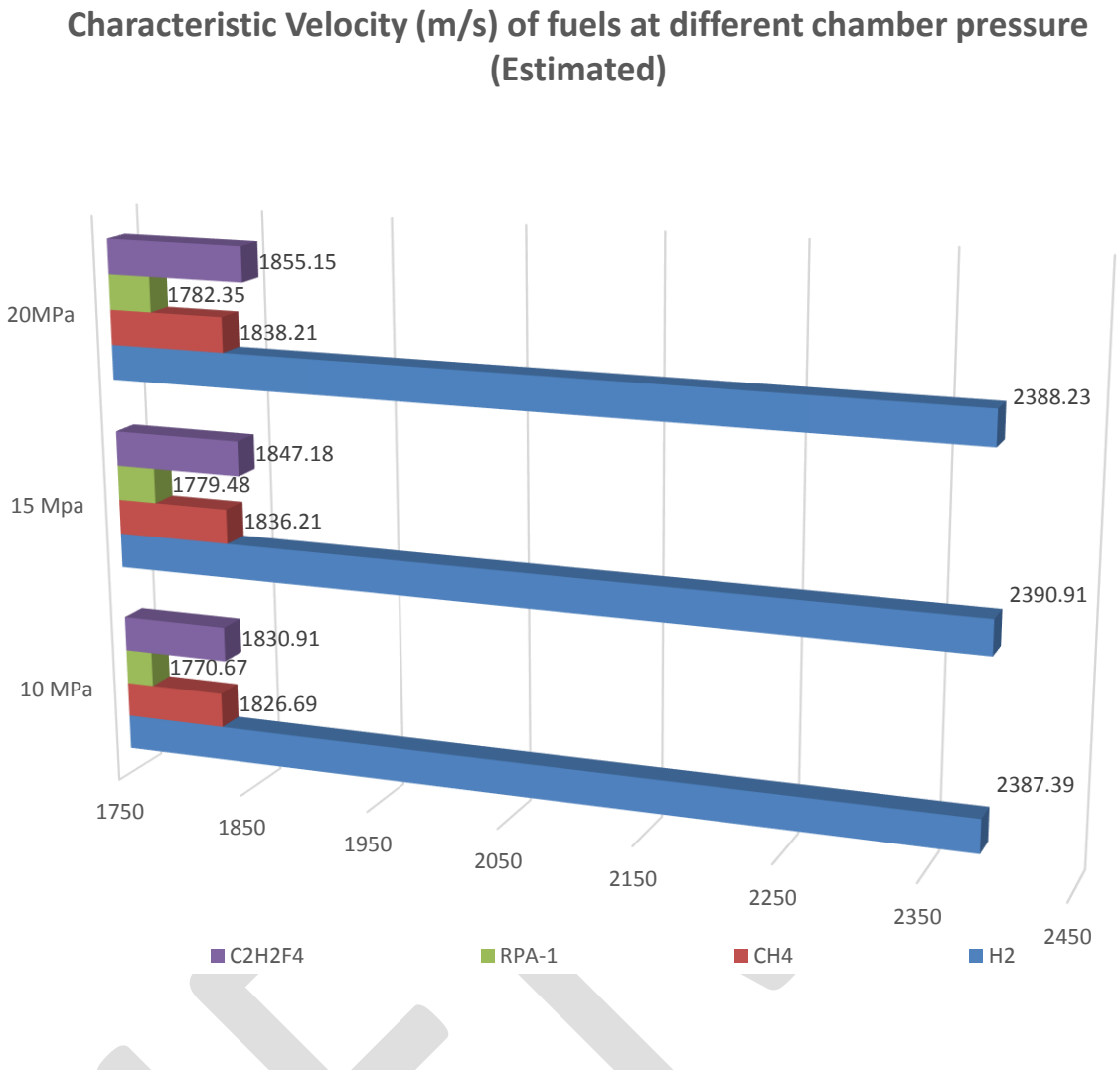
Characteristic Velocity (m/s) of fuels at different chamber pressure (Estimated)
20MPa
15 Mpa
10 MPa
1855.15
1782.35
1838.21
2388.23
1847.18
1779.48
1836.21
2390.91
1830.91
1770.67
1826.69
2387.39
1750
1850
1950
2050
2150
2250
2350
2450
C2H2F4
RPA-1
CH4
H2

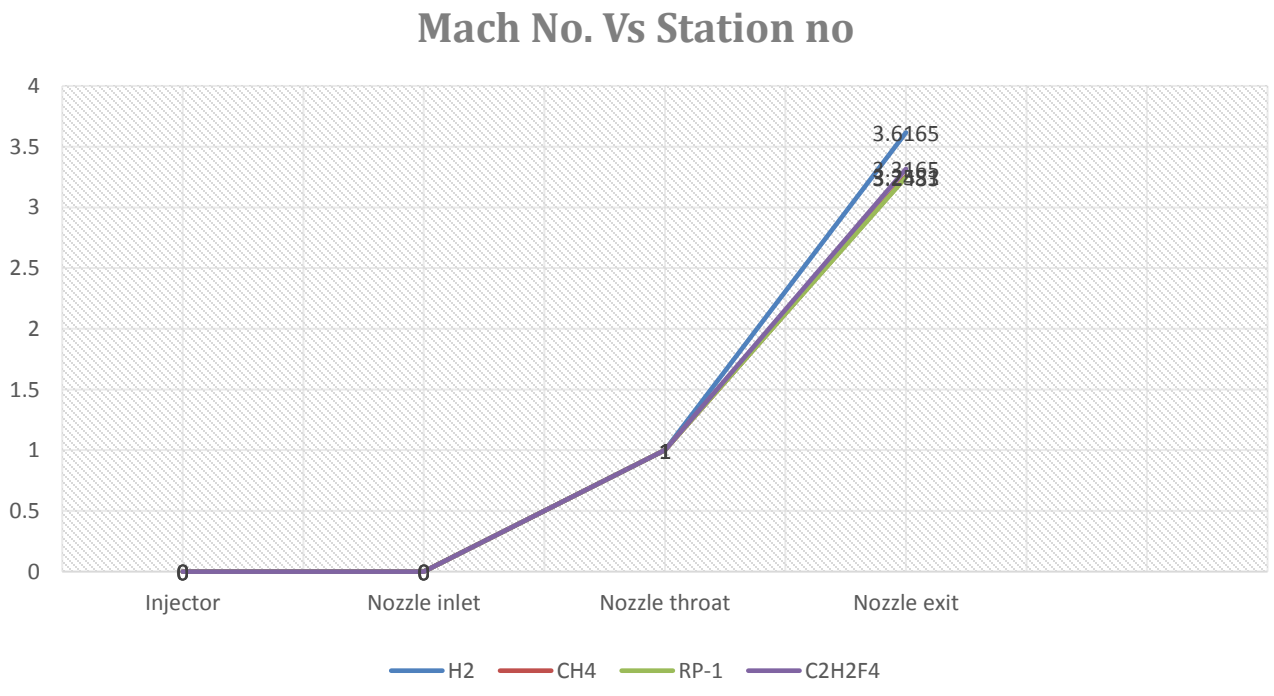
Mach No. Vs Station no
4
3.5
3
2.5
2
1.5
1
0.5
0
3.6165
0
0
1
Injector
Nozzle inlet
Nozzle throat
Nozzle exit
H2
CH4
RP-1
C2H2F4

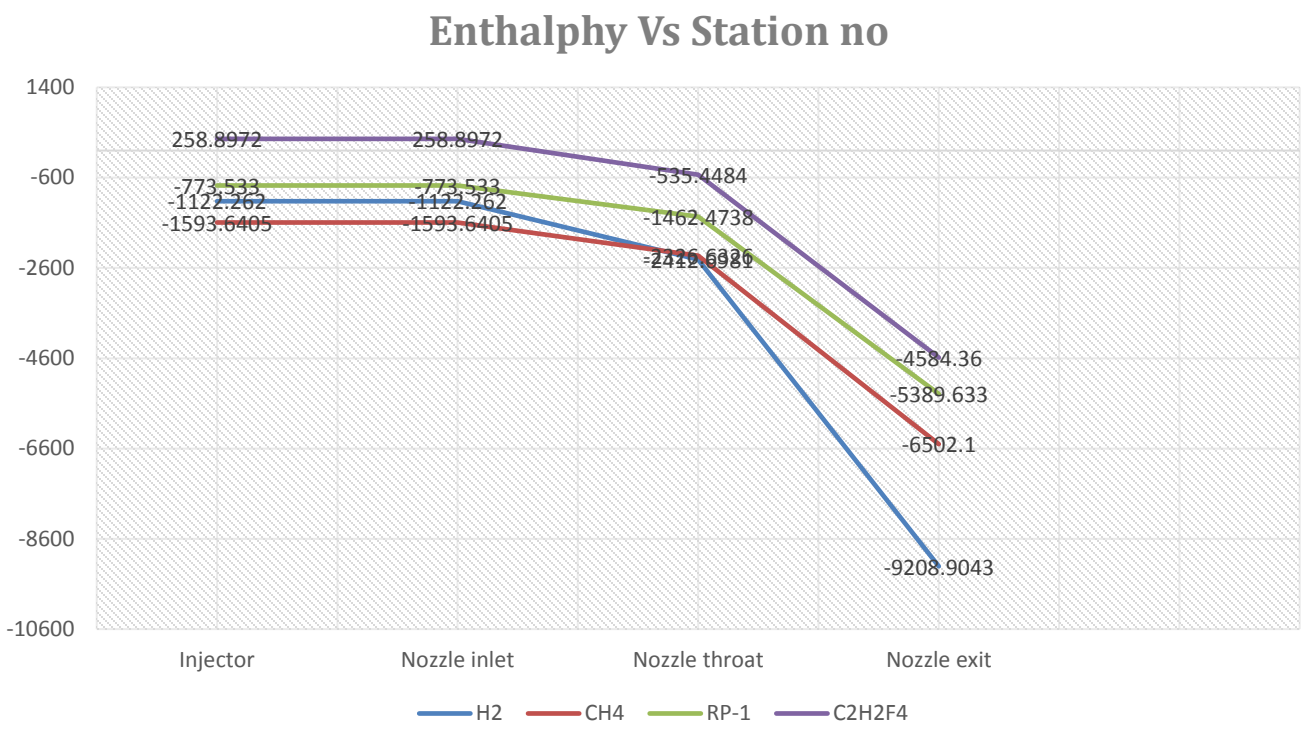
Enthalpy Vs Station no
1400
-600
-2600
-4600
-6600
-8600
-10600
258.8972
258.8972
-535.4484
-773.533
-773.533
-1462.4738
-1122.262
-1122.262
-1593.6405
-1593.6405
-4584.36
-5389.633
-6502.1
-9208.9043
Injector
Nozzle inlet
Nozzle throat
Nozzle exit
H2
CH4
RP-1
C2H2F4

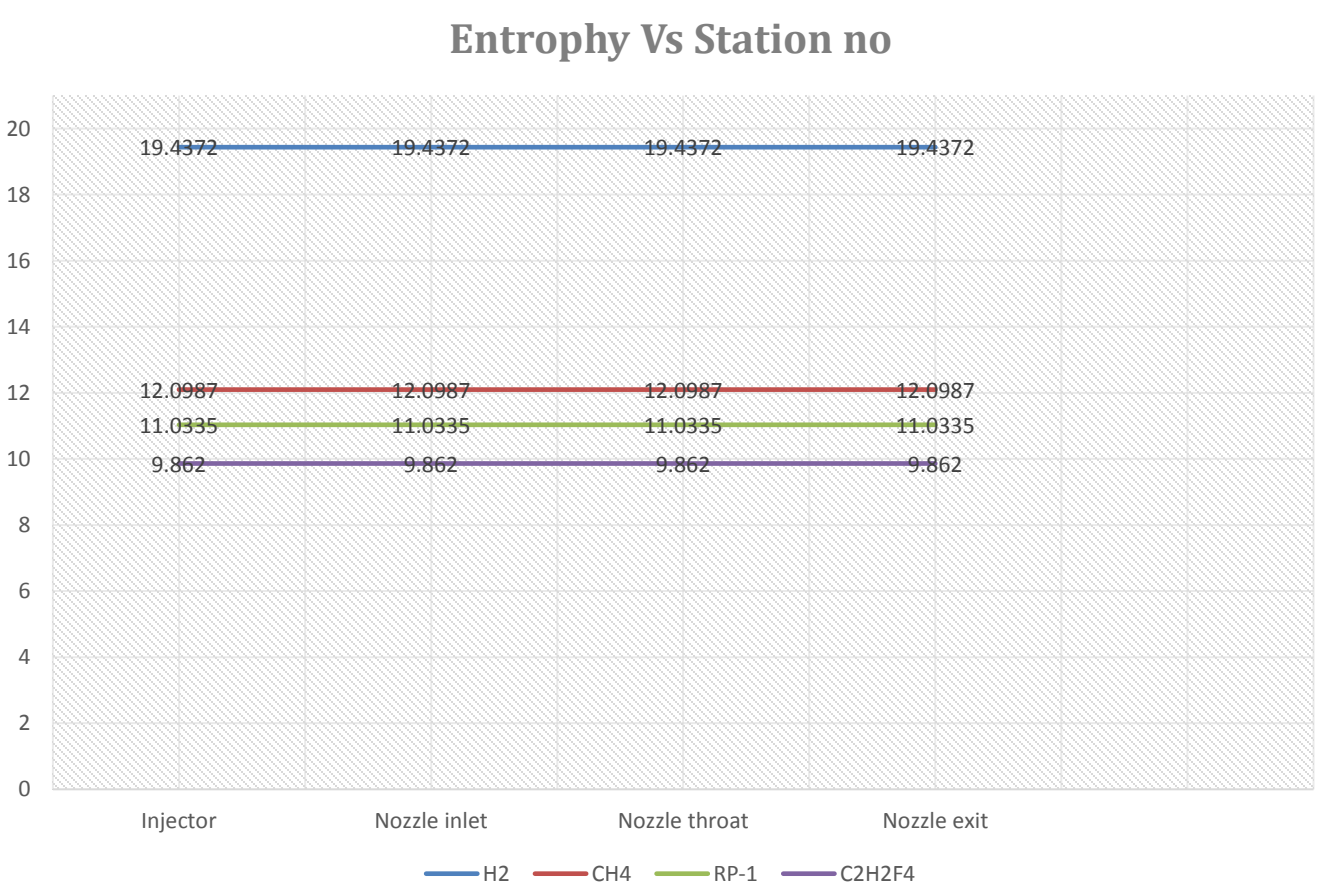
Entrophy Vs Station no
20
18
16
14
12
10
8
6
4
2
0
19.4372
19.4372
19.4372
19.4372
12.0987
12.0987
12.0987
12.0987
11.0335
11.0335
11.0335
11.0335
9.862
9.862
9.862
9.862
Injector
Nozzle inlet
Nozzle throat
Nozzle exit
H2
CH4
RP-1
C2H2F4

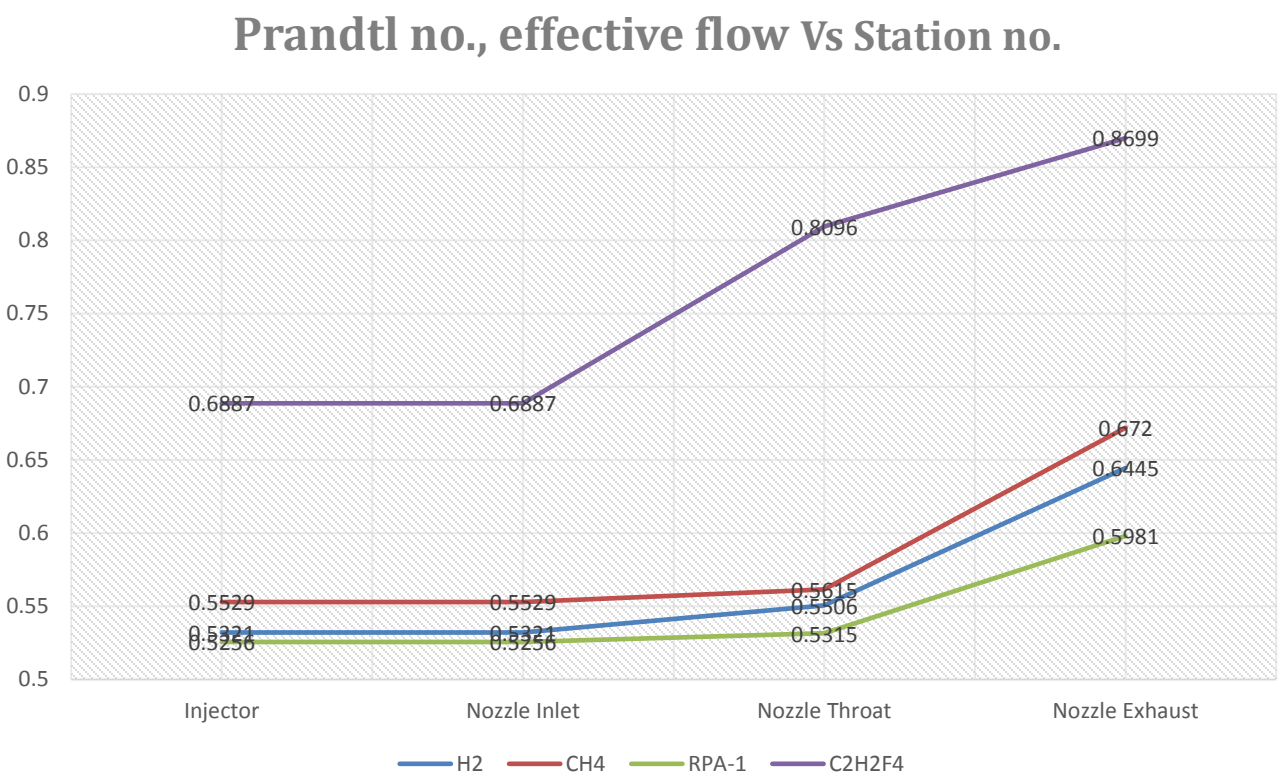
Prandtl no., effective flow Vs Station no.
0.9
0.85
0.8
0.75
0.7
0.65
0.6
0.55
0.5
0.6887
0.6887
0.8096
0.8699
0.5529
0.5529
0.5615
0.672
0.5321
0.5321
0.5506
0.6445
0.5256
0.5256
0.5315
0.5981
Injector
Nozzle Inlet
Nozzle Throat
Nozzle Exhaust
H2
CH4
RPA-1
C2H2F4

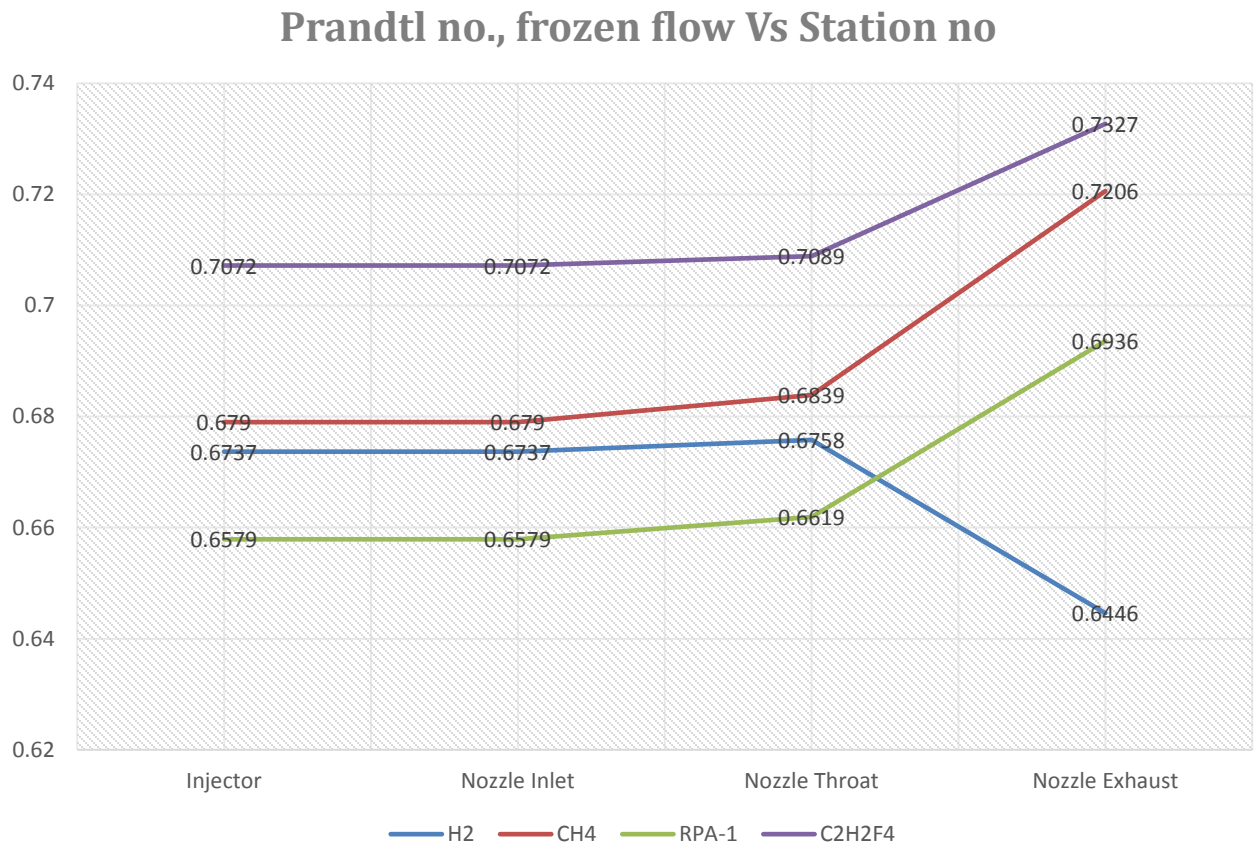
Prandtl no., frozen flow Vs Station no
0.74
0.72
0.7
0.68
0.66
0.64
0.62
0.7072
0.7072
0.7089
0.7327
0.7206
0.679
0.679
0.6839
0.6737
0.6737
0.6758
0.6936
0.6579
0.6579
0.6619
0.6446
Injector
Nozzle Inlet
Nozzle Throat
Nozzle Exhaust
H2
CH4
RPA-1
C2H2F4

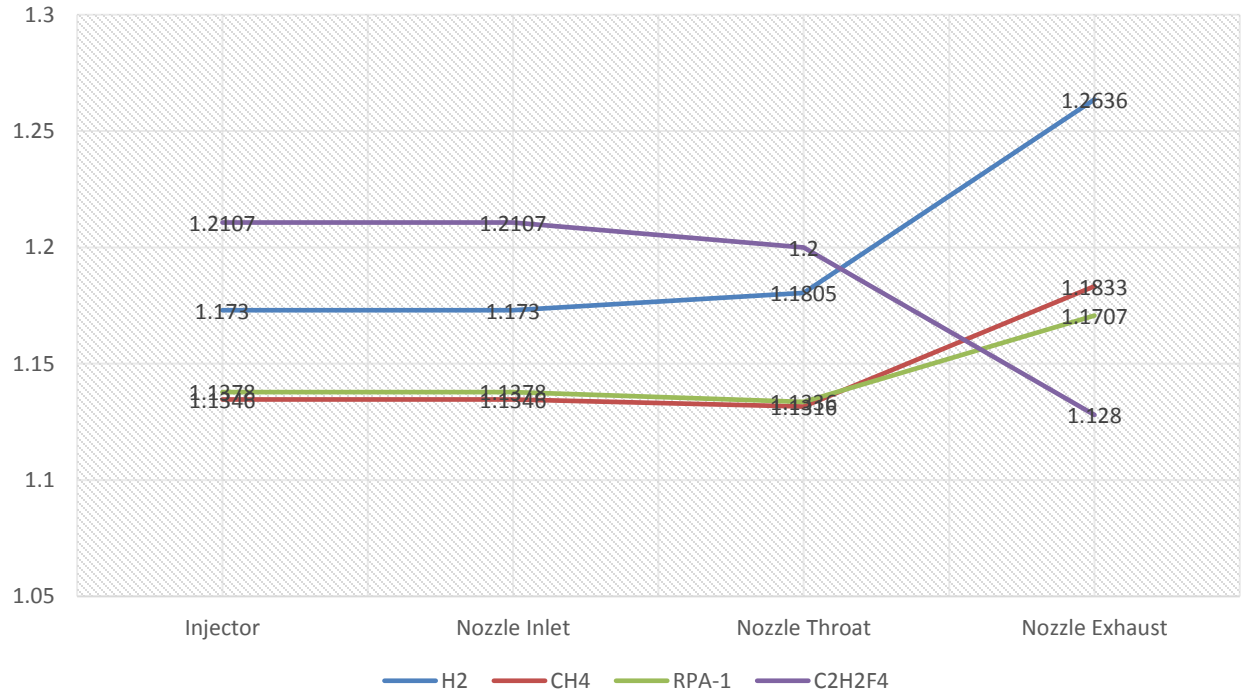
Isentropic Exponent Vs Station no
1.3
1.25
1.2
1.15
1.1
1.05
1.2107
1.2107
1.2
1.2636
1.173
1.173
1.1805
1.1833
1.1707
1.1378
1.1378
1.1340
1.1340
1.1310
1.128
Injector
Nozzle Inlet
Nozzle Throat
Nozzle Exhaust
H2
CH4
RPA-1
C2H2F4

FUTURE SCOPE OF WORK

There are many different ways of analysing propellants with respect to different parameters hence widening the scope of the work to a vast extent. Further Analysis of the propellant can be made on the below mentioned areas:

- ❖Multi-phase flow analysis
- ❖Two phase flow
- ❖Eulerian analysis
- ❖Eulerian – Lagrangian analysis
- ❖Chemical kinetics analysis
- ❖Combustion characteristics analysis

CONCLUSION

The analyzation of species and their comparison with each other shows the difference in their thermodynamic properties. The deviation in the thrust coefficient of hydrogen, methane and RPA-1 is considerably large as compared to that of 1,1,1,2-tetraflouroethane at 10MPa. As the chamber pressure increases, thrust coefficient of all the species increases simultaneously. Hydrogen has the highest Isp at 20MPa whereas RPA-1 has the lowest.

The effective exhaust velocity of the species is lower at estimated condition whereas in ideal condition hydrogen's velocity is way higher than other species. The deviation between 1,1,1,2-tetraflouroethane and methane increases as the chamber pressure increases with increase in their characteristic velocity in ideal condition whereas the velocity increases very minutely in the case of the estimated condition.

REFRENCES:

[1]. B. Podgornik, F. Majdic, Leskovesk, J.Vizintin, Improving properties of tool steels through combination of deep cryogenic treatment and plasmanitriding, Wear, (2011), doi: 10.116/j. wear. 2011.4.001

[2]. Engineering Materials & Metallurgy by V. Jaya Kumar, A. R. S. Publication.

[3]. G. P. Sutton: Rocket Propulsion Elements, Seventh Edition, Wiley, New York, (2001).

[4]. Cryogenic Engine in Rocket Propulsion (PDF).

[5]. Ronald W. Humble, N. Henry Gary: Space Propulsion Analysis and Design, McGraw-Hill, United States, (1997).

[6]. Richard Cohn (2012), "Developments in Liquid Rocket Engine Technology", Air Force Research Laboratory.

[7]. International Journal of Aerospace and Mechanical Engineering Volume 2 – No.5, August 2015

27, ISSN (O): 2393-8609, Cryogenic Technology & Rocket Engines.

[8]. S. Zhirafar, A. Rezaeian, M. Pug, Effect of cryogenic treatment on the mechanical properties of 4340 steel, Journal of Materials Processing Technology 186 (2007) 298-303, doi: 1016/j, j matprotec. 2006. 12. 046.

[9]. Richard Cohn (2012), "Developments in Liquid Rocket Engine Technology", Air Force Research Laboratory.

[10]. Ronald W. Humble, N. Henry Gary: Space Propulsion Analysis and Design, McGraw-Hill, United States, (1997).

[11]. International Journal of Aerospace and Mechanical Engineering, Cryogenic Technology & Rocket Engines.

[12]. Concise International Chemical Assessment Document 11, 1112-Tetrafluoroethane.

[13]. Rocket Propulsion Analysis v.2.3, User Manual, NASA.

International Journal of Engineering Research and General Science Volume 6, Issue 4, July-August, 2018
ISSN 2091-2730

High Speed and Energy Efficient Carry Skip Adder

[1]Neenu Kuriakose, [2]Dr.Gnana Sheela K

APJ Abdul Kalam Technological University, Kerala, India

Abstract— In this paper a novel carry skip adder structure of 32 bit has been proposed that have better speed and less power consumption than the conventionally used. In this we are analysing the delay, area and power consumption of currently available different carry skip structures, firstly analyse conventional carry skip structure, then we modified the structure for better performance by using the concatenation and incrementation scheme. Then analyze the hybrid variable latency carry skip adder by replacing the nucleus stage of concatenation and incrementation scheme with parallel prefix adder. Later we uses different CSKA implementations in convolver for performing a convolution function along with 16 x 16 reversible Vedic multiplier and the delay and energy consumption of each one is studied. Verilog HDL is used for designing the circuits and Xilinx software tool is used for estimating the delay and power consumption.

Keywords— Carry Skip Adder , Convolver, Delay, Hybrid Variable Latency, Skip technique ,UrdhvaTiryakbhyam sutra, , VHDL.

INTRODUCTION

Adders are digital circuit that executes addition of numbers. In numerous computers and other types of processors adders are used in the arithmetic logic units or ALU. They are also applied in other parts of the processor, where they are used to compute addresses, table indices, increment and decrement operators, and similar operations. Adders are a key building block in arithmetic and logic units (ALUs) and hence increasing their speed and reducing their power/energy consumption strongly affect the speed and power consumption of processors. There are many works on the subject of optimizing the speed and power of these units. Obviously, it is highly desirable to achieve higher speeds at low-power/energy consumptions, which is a challenge for the designers of general purpose processors. One of the effective techniques to lower the power consumption of digital circuits is to reduce the supply voltage due to quadratic dependence of the switching energy on the voltage. There are different types of adders are available according to our demands. They are normally two types of adders: binary adders and multiple bit adders. Carry skip adders are multiple bit adders which is also known as a carry-bypass adder. It is a skip the logic in propagation of carry and its operation is to speed up the additional operation and to adding the propagation of carry bit around portion of complete adder where it is an adder implementation that increases on the delay of a ripple-carry adder with little effort related to other adders. The enhancement of the worst-case delay is attained by using several carry-skip adders to form a block-carry-skip adder. In this paper we estimates delay and power consumption of different carry skip adders using these adders in convolver for performing the convolution function in digital signal processing. There are different adder families are available for estimation of delay and power including Ripple Carry Adder (RCA), Carry Select Adder(CSLA),Carry Skip Adder(CSKA) etc. From these CSKA is more efficient in case of delay and power consumption.

The CSKA consist of chain of Full Adders(FAs), RCA and 2:1 multiplexer. These multiplexers are used to connect RCAs.The delay of CSKA is depends on number of Fas .There are many methods are suggested for determining optimum delay .It uses the VSS (variable stage size) to minimize the delay. In [17] proposes new technique to reduce the optimal path delay. There are some methods are proposed to improve performance of adder at low voltage levels. It examines the CLSA better performance. Finally uses the hybrid structure to improve the efficiency and speed of adder.

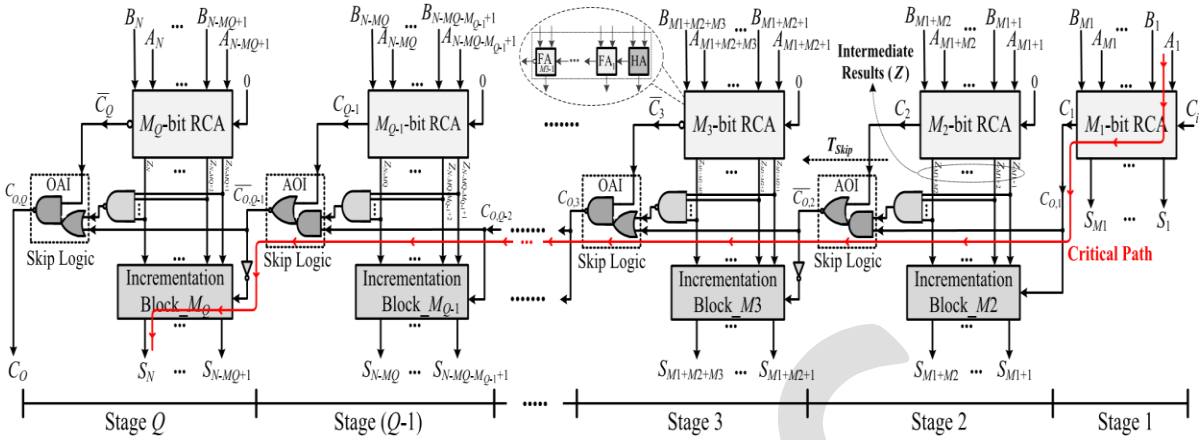

Fig 1: Structure of CI CSKA

CONVENTIONAL CARRY SKIP ADDER

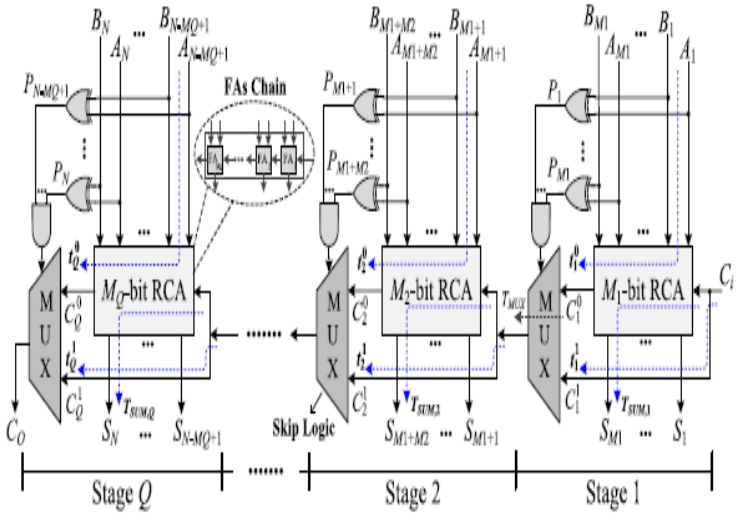

Fig 2: Conventional CSKA

The structure of conventional carry skip adder is shown in fig 2,which is based on blocks of RCAs.In addition to RCA blocks ,there is chain of FAs in each stage and skip logic using 2:1 multiplexer. In the CSKA, the carry skip logic detects the situation, and makes the carry ready for the next stage without waiting for the operation of the FA chain to be completed. The skip operation is performed using the gates and the multiplexer shown in the figure 1.The CSKA can be implemented by VSS and FSS .Where VSS CSKA is more efficient.

A. Fixed Stage Size CSKA

In this CSKA, assumes that each stage of CSKA contains M FAs ,then for N bit CSKA there is Q number of stages i.e Q =M/N ,where Q is an integer. The critical path of CSKA consists of FA chain of first stage, multiplexer on intermediate stage and FA chain on last stage.

B. Variable Stage Size CSKA

Thus using the variable sizes to each stage we can increase the speed which is shown in fig 3.It is achieved by lowering the delays of first and third terms in fig 1.These delays are minimized by lowering the size of first and last RCA blocks.

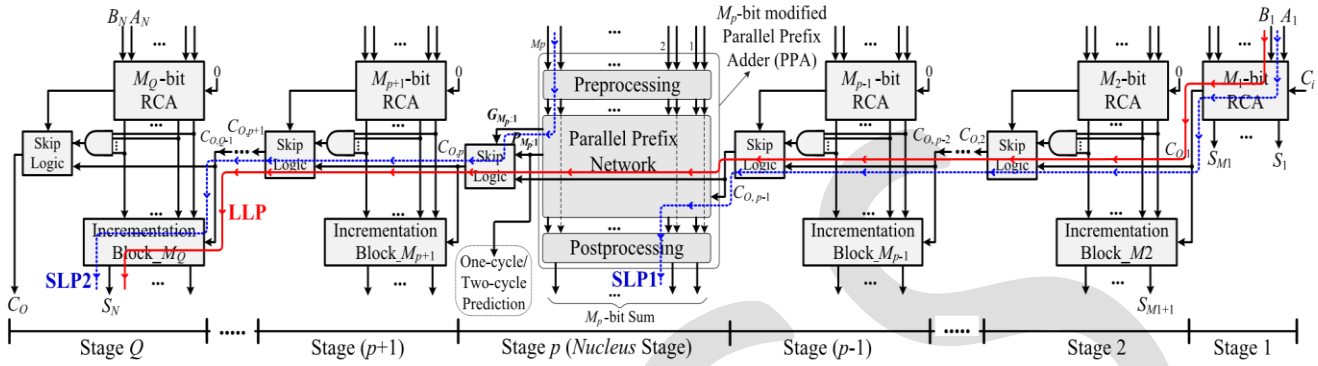

Fig. 3.Structure of hybrid variable latency CSKA

V.HYBRID VARIABLE LATENCY CSKA

Hybrid variable latency adder structure is similar to CI CSKA structure which is shown in fig 3.For making the hybrid variable latency structure to CSKA ,we have to replace some of the middle stages of CI CSKA with PPA(parallel prefix adder).This structure has higher speed than conventional one. The figure 5 shows the hybrid variable latency structure. In this structure we are using parallel prefix network of brent kung adder [4] is used .One of the advantages of using this PPA is that it uses forward paths ,so longest carry is calculated faster than others anf fan out is also lesser than other ones.The PPA has used in nucleus stage of CI CSKA .It has three levels of operation ,first the preprocessing level where propagate signals and generate signal for inputs are calculated.In the next level we are using brent kung adder parallel prefix network to calculate all intermediate signals.Finally in postprocessing stage final summation is calculated which is shown in fig 4.

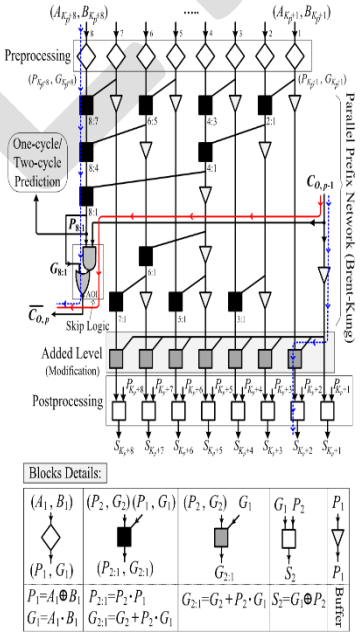

Fig 4. Internal structure of hybrid variable latency CSKA.

Convolution is assumed to be the necessary operation used in most of the signal processing applications. Convolution is a mathematical operation executed on two functions, producing a third function that is typically observed as an efficiently modified version of one of the two original functions. It is used for different applications comprising probability, statistics, computer vision, language processing, image and signal processing, engineering, and differential equations. So it is very important to develop a technique which improves the speed of convolution operation.

Vedic mathematics is traditional mathematical form used by Aryans. It increases the speed of operation, and the algorithms are based on mind calculations. The calculations are based on 16 sutras, of which UrdhvaTiryakbhyam sutra is used for Vedic multiplication. The proposed design uses reversible logic, therefore the power dissipation and delay reduces greatly. In this paper, the delay, area and power of existing design is compared with proposed design.

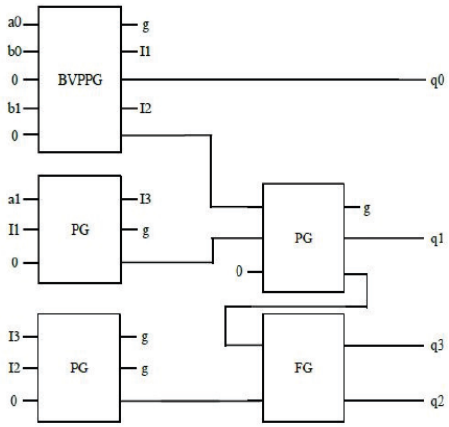

Fig 5: Reversible 2x2 UrdhvaTiryakbhyam multiplier

PROPOSED DESIGN

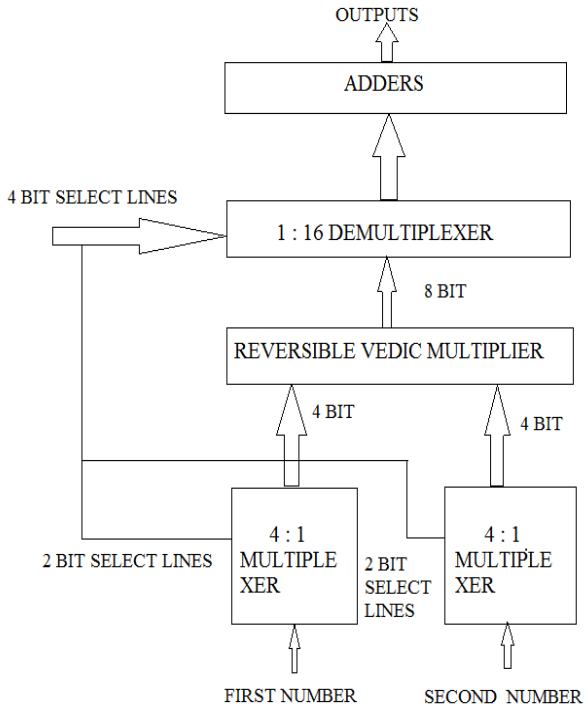

Fig 6. Block Diagram of Convolver

The convolution of two 4-bit numbers is calculated and realised using reversible logic. The multiplier and multiplicand are selected using two 4:1 multiplexers. Then the multiplication operation, that is, the Vedic multiplication is performed and is stored using 1:16 demultiplexer. The first two bit of four bit select line of demultiplexer is the select line of first 4:1 multiplexer. And the last two bits are the select line of second 4:1 multiplexer. Then the corresponding products are added in the adder section. The block diagram of the proposed design is shown in Figure 6. For the addition of two numbers carry look skip adder is selected.

RESULTS AND DISCUSSION

Simulation results obtained from Xilinx ISE design suite is observed and compare the delay and power consumption of different CSKAs.By analysing different CSKAs its evident that hybrid variable latency adder has lesser delay compared to other ones.But area is larger for this CSKA .

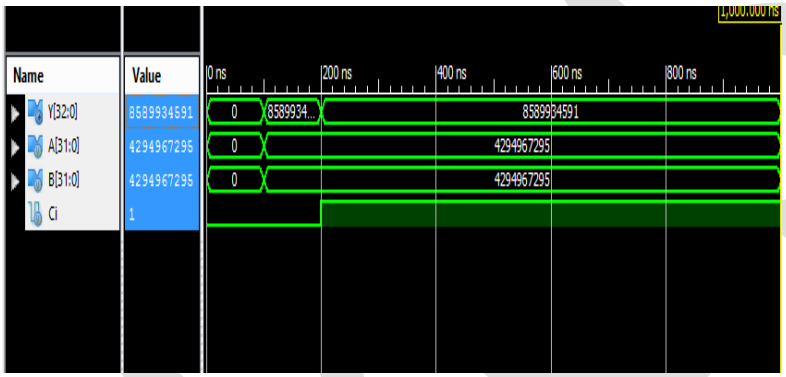

Fig 7. Simulation Result of CSKA

From the simulation results of different CSKAs,itscler that Conv CSKA occupies less space but delay is higher. In CI CSKA delay is less than CONV CSKA,butno.of LUTs used is higher than conventional one. In Hybrid Variable Latency CSKA also the delay is further reduced but no.of LUTs increased.

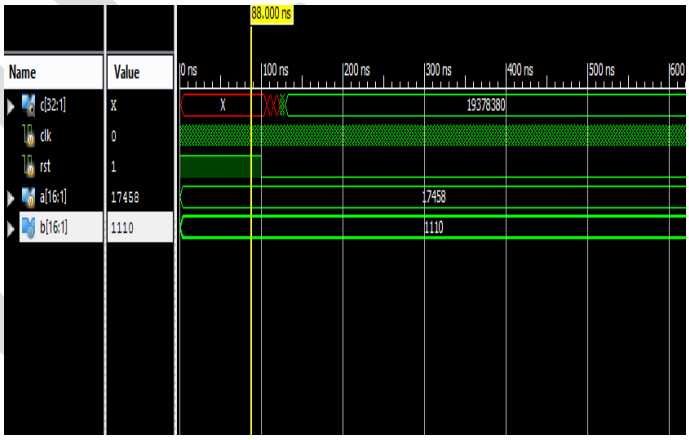

Fig 8. Simulation of Convolution using CSKAs.

Power dissipation is calculated using Xilinx Xpower Analyzer Tool. Energy consumption is product of delay and power dissipation and is tabulated in table 1.

Table 1. Comparison of various CSKA

ADDER DESIGN	NO.OF LUTS	DELAY(ns)	ENERGY(nJ)
CONV - CSKA	49	21.089	1.82
CI - CSKA	75	20.234	1.56
HYBRID CSKA	67	18.170	1.04

CONCLUSION

In this paper, different CSKA structures are analyzed using XILINX software and there delays and energy consumption are estimated. Then for better analyses we are using a convolver for performing convolution function ,where we are using different CSKA structures in convolver. From the analyses it's clear that Hybrid variable latency adder has higher speed and power consumption is also less. But area is larger than other ones.

REFERENCES:

[1] V. G. Oklobdzija, B. R. Zeydel, H. Dao, S. Mathew, and R. Krishnamurthy, "Energy-delay estimation technique for high performance microprocessor VLSI adders," in *Proc. 16th IEEE Symp.Comput. Arithmetic*, Jun. 2003, pp. 272–279.

[2] M. Alioto and G. Palumbo, "A simple strategy for optimized design of one-level carry-skip adders," *IEEE Trans. Circuits Syst. I, Fundam.Theory Appl.*, vol. 50, no. 1, pp. 141–148, Jan. 2003.

[3] S. Jia*et al.*, "Static CMOS implementation of logarithmic skip adder," in *Proc. IEEE Conf. Electron Devices Solid-State Circuits*, Dec. 2003, pp. 509–512.

[4] H. Suzuki, W. Jeong, and K. Roy, "Low-power carry-select adder using adaptive supply voltage based on input vector patterns," in *Proc. Int.Symp. Low Power Electron. Design (ISLPED)*, Aug. 2004, pp. 313–318.

[5] Y. Chen, H. Li, K. Roy, and C.-K. Koh, "Cascaded carry-select adder (C2SA): A new structure for low-power CSA design," in *Proc. Int. Symp.Low Power Electron. Design (ISLPED)*, Aug. 2005, pp. 115–118.

[6] V. G. Oklobdzija, B. R. Zeydel, H. Q. Dao, S. Mathew, and R. Krishnamurthy, "Comparison of high-performance VLSI adders in the energy-delay space," *IEEE Trans. Very Large Scale Integr. (VLSI)Syst.*, vol. 13, no. 6, pp. 754–758, Jun. 2005.

[7] Y. Chen, H. Li, J. Li, and C.-K. Koh, "Variable-latency adder (VL-adder): New arithmetic circuit design practice to overcome NBTI," in *Proc. ACM/IEEE Int. Symp. Low Power Electron.Design (ISLPED)*, Aug. 2007, pp. 195–200.

[8] Y. He and C.-H. Chang, "A power-delay efficient hybrid carry lookahead/ carry-select based redundant binary to two's complement converter," *IEEE Trans. Circuits Syst. I, Reg. Papers*, vol. 55, no. 1, pp. 336–346, Feb. 2008.

[9] R. Zlatanovici, S. Kao, and B. Nikolic, "Energy–delay optimization of 64-bit carry-lookahead adders with a 240 ps 90 nm CMOS design example," *IEEE J. Solid-State Circuits*, vol. 44, no. 2, pp. 569–583, Feb. 2009.

[10] S. Ghosh, D. Mohapatra, G. Karakonstantis, and K. Roy, "Voltage scalable high-speed robust hybrid arithmetic units using adaptive clocking," *IEEE Trans. Very Large Scale Integr. (VLSI) Syst.*, vol. 18, no. 9, pp. 1301–1309, Sep. 2010.

[11] Y. Liu, Y. Sun, Y. Zhu, and H. Yang, "Design methodology of variable latency adders with multistage function speculation," in *Proc. IEEE 11th Int. Symp. Quality Electron. Design (ISQED)*, Mar. 2010, pp. 824–830.

[12] MiladBahadori*et al.* "High-Speed and Energy-Efficient Carry Skip Adder Operating Under a Wide Range ofSupply Voltage Levels" *IEEE Trans on Very Large Scale Integration (vlsi) Systems*, vol. 24, no. 2, Feb 2016

[13] Anuja Georgeand Sreethu Raj "Speedy Convolution Using Reversible Vedic Multiplier" International Journal of Scientific and Research Publications, Volume 6, Issue 9, September 2016 .

International Journal of Engineering Research and General Science Volume 6, Issue 4, July-August, 2018
ISSN 2091-2730

Design and fabrication of 3-axis CNC Milling machine

Sriranga V Deshpande[1], P U Karthik[2], Naveen Kumar D[3], Dr Vijendra Kumar[4], Dr K. S Badrinaryan[5]

1.Student, department of mechanical engineering, srirangadeshpande296@gmail.com

2.Student, department of mechanical engineering, karthikpu99@gmail.com

3. Asst. Professor, Department of mechanical engineering, M S Engineering College, dnaveenmech@gmail.com

4. Professor and H.O.D, Department of mechanical engineering, M S Engineering College, vijendravk@gmail.com

5.Professor and Principal, M S Engineering College, principal@msec.ac.in

Abstract— Nowadays with a digital control it's became more and more useful to use such a machine tools with a coded software. This paper will present the design and fabrication of 3-axis milling machine. computer numerically-controlled (CNC) machine which comprise the use of Arduino micro controller to produce pulse-width modulation (PWM) outputs in order to run the stepper motors that will be used in this work. A milling 3-axis CNC is previously used precisely surfaced designed for snapping of wood, plastic sheet and thin sheet of metal alloy by using a rotating drill bit which its accuracy is much lesser than using a lesser cutter technique this machine tool is portable and it's controlled by computer (PC). Design and Fabrication of CNC with precision Stepper motors that contacted with the lead screw moment along 3 -axis.

Keywords— Stepper motor, spindle motor, leadscrew, ball bearings, flexible coupling, and control system by Arduino micro controller in Easel software.

INTRODUCTION

Computer Numerical Control or CNC machine is a conventionally machine where an operator decides and adjusts various machines parameters like feed, depth of cut etc. depending on type of job, and controls the slide movements by hand. It also is a specialized and versatile form of a Soft Automation and its applications cover many kinds, although it was initially developed to control the motion and operation of machine tools. A CNC machine takes codes from a computer and converts the code using software into electrical signals. The signals from the computer are then used to control motors. Since the motors can turn very small amounts the machine is able to move in highly precise movements over and over again. The 3-axis CNC machine; these machines nowadays have range size in the open market

Over decades, industrial technology has transformed many aspects of daily life. Several studies have been carried out for the development of such a (CNC) machine on smaller thinner, lighter weighted and budget cost. From the related journal and research, the main idea in carrying out this work of CNC development. As the technology of CNC machine characterized by accessible price and technology so rip that even individuals can design and construct CNC controlled machine [2]. Advanced facility and precision of control of CNC tools, if it's compare with usual machine, has had a significant influence on the development of function components, frame body, stepper motors, and control circuits. Construction and evaluation of Low-cost table CNC milling machine by using low-price milling cutter for the main spindle due to a low voltage supply of the main cutting forces it is possible to use the tools of smaller dimension to machine materials like wood, aluminum and plastic materials. Design and Implementation of Three-Dimensional CNC Machine [3] where it discusses the design of low cost three dimensional CNC. The main function is a microcontroller-based CNC machine and its communication between personal computer (PC) and CNC machine by Software sub system that gets a set of commands and fetch it to the mechanical sub system in order to be control the 3-axis. Software sub system that is a PC that provides easy to use interface for user to program commands in such a language that microcontroller accepts.

RESEARCH METHOD

The first step in the operation of CNC machine was calibrating the tool, it was aimed to know whether the stepper motor and any other system were working according to the program that has been configured. Followed by setting the starting position of the spindle drill on the CNC machine using Universal G-code Sender software both automatically and manually by hand spinning. Spindle drill speed can be set up to a maximum speed of 12000 rpm (rotation per minute). After the CNC machine is calibrated, the design with the *G-code extension format was uploaded using Universal G- code Sender to Arduino Uno with serial communication. The microcontroller will read the data as a command and provide logic to the A4988 motor driver. The data received by the motor driver was used to drive 4 Nema 23 X, Y and Z axis stepper motors, so that a pattern will be formed on the object.

OBJECTIVE

The idea behind fabrication of low cost CNC Milling Machine is to full fill the demand of CNC machines from small scale to large scale industries with optimized low cost. A major new development in computer technology is the availability of low-cost open source hardware, such as the Arduino microcontroller. An advantage of open source hardware is that a wide variety of ready-to-use software is

available for them on the Web; therefore, the prototyping and development times are drastically reduced. Moreover, a wide range of low-cost interfaces and accessories such as Arduino shields are also available. However, for the development of low-cost models of CNC machines, such tools may be quite adequate from the viewpoint of machine control. In this project, the development of a prototype 3-axis CNC Milling Machine using Arduino-based control system is presented with the following specification.

- Low cost
- Easily operable
- Easy interface
- Flexible
- Low power consumption

METHODOLOGY

The structural design of the machine including to wiring connection and the software adopted to generate codes and C+ language. Finally, but not last is Development the base of the design that has been achieved.

A. Structure Design

The machine structure is the vital part of the machining tool. It merges all machine components into a single complete system. The machine structure is vital to the efficiency of the machine since it's directly affecting the total dynamic stiffness and also affecting the damping response. Perfectly designed structure can afford high stiffness, which leads to precise operation. Mini scaled machine tool required more precise stiffness than the regular large-scale machine tool as shown in Fig. 2

The initial design will be drafting or sketching then when the design satisfied. The next level will be deciding the criteria required which is firstly the length travel. The length travel is the length of the X, Y and Z axis that travels from one point to another. The X axis move left & right, Y axis move front & back, Z axis moves Up and Down. Travel length that is to be designed is X axis 3.5 foot and Y axis 2.5 foot and Z axis will be 0.984 foot. This structure comes with less materials hence it's very less expensive to build which it's designed to cut wood plastic and aluminum.

Fig 1 structure of CNC machine

B. Components

Stepper motor & Accessories: It's a combination of stepper motor drive connected with pillow bearing with lead screw that is mechanical linear bar and linear bearings that drives rotational motion into liner motion with minimum friction. The stepper motor as represented in Fig. 5 have 1/30 step angle and the speed is directly proportional to the pulse frequency where it stands of the higher the output voltage from the easy driver the more level of torque drive. Microcontroller Board: Uno it's an Arduino Board it's selected to be the control unit in this project, which it's used as a motion control board. The Arduino Uno is a microcontroller board based as shown in Fig. 6. It has 14 digital input/output pins (of which 6 can be used as PWM outputs), 6 analog inputs, a 16 MHz ceramic resonator, a USB connection, a power jack, an ICSP header, and a reset button. It contains everything needed to support the microcontroller; simply connect it to a computer with a USB cable or power it with an AC-to-DC adapter or battery to get started.

Fig 2. chromium rod and lead screw

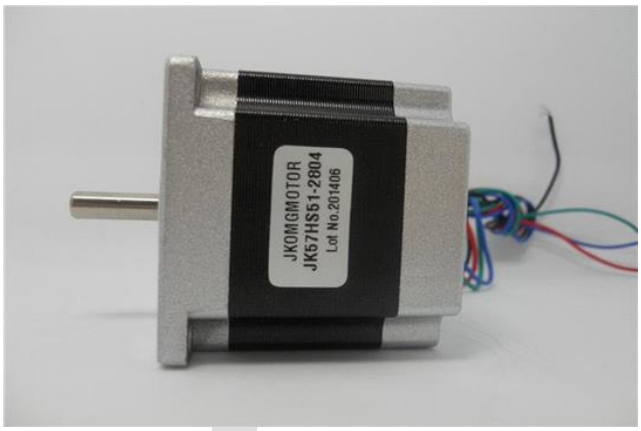

Fig.3.stepper motor

. Power Supply: 12V SMPS (Switch mode Power Supply) is used for stepper motor driver. 2V SMPS is used to power the microcontroller board (Arduino Uno3). The microcontroller is flashed with GCODE interpreter firmware written in optimized 'C' language.

Fid 4. Arduino Uno board

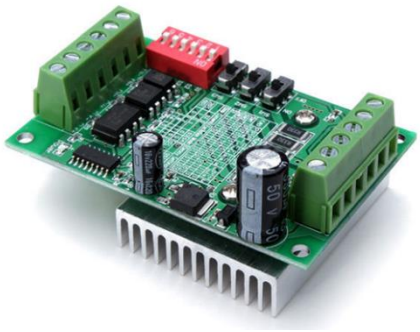

Fig 5. stepper motor driver

Stepper Motor Drivers: It's kind of driver that receive steps signal from microcontroller and convert it into voltage electrical signals that turn the motor. This driver is called Easy Driver V4.5 as shown in Figure.4 that required 6V – 30V supply to power the motor which can power any type of step motors

C. Software development

The CNC machine uses easel software for motion control of the axis. Easel converts any design given or G-code, where certain commands are used that stepper motor driver will easily understand.

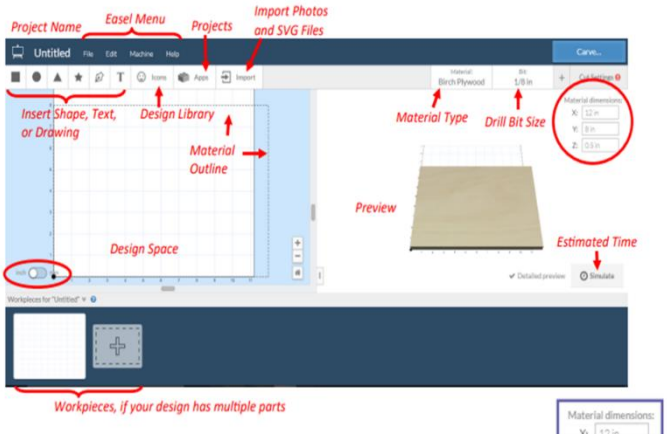

Fig 6. Easel software

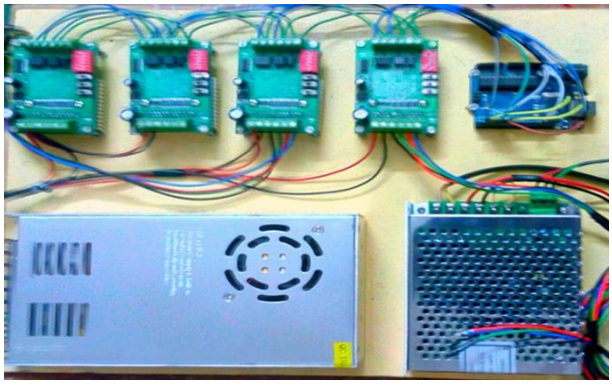

Fig.7. circuit connections

In order to begin programming it's required for IDE Arduino software to make it easier and friendlier to generate G-code the best way is to use "Easel" combined with laser engraver plug-in which is an open source graphical editor. There are three easy drivers in this

project electronic circuit each driver is connected individually to the Arduino PWM output on terminal number 3,5,6 which according to Arduino Uno datasheet and is shown in Fig. 9. Stepper motor that is used in X, Y and Z axis in this project uses with 4 wire connections that is each stepper motor are connecter to one easy driver respectively as shown in Fig. 10.

D. CNC Structure Assembly

After gathering all required parts and accessories for assembly, step by step procedure for making the CNC is noted below.

a) Start from lower-deck which is the base table.
b) Install 4 rubber bush lever
c) Assemble the upper-deck which is Y-axis base.
d) joining of aluminum extrusion of 40x40 rod
e) Assembly the Frame using aluminum stand.
f) Completion of the Frame.
g) Assemble the gantry which is X-axis support.
h) connecting c-channel
i) putting the sliding wheel in the c channel.
j) Assembly the Cutting-Head Slider which is a tool mount.

E. CNC Structure Assembly

To begin with the help of online source the EASEL controller to PC that it's used to send G-code to CNC it is user friendly and free open source to Arduino to give a virtual command to control moment of machine using easy driver, and the interface of the easel software connected to Arduino. For compilation the easel to Arduino it's don't required to download a software source code to be added into Arduino library folder by following the steps from easel website. After having easel library stetted up into Arduino IDE next is flashing the CNC .hex file Firmware to Arduino using X loader application which required to be download and open to select the COM port connected to Arduino with correct baud rate for Arduino Uno: 115200 to upload the hex file.

ACKNOWLEDGMENT

The successful completion of any work will be incomplete without complementing those who made it possible and whose encouragement made my effort successful. At the very outset, Firstly I would like to be highly grateful towards the college, M S Engineering College, Bangalore, for providing us with all the necessary help and grooming up in to being Bachelor of Engineering.

I express my sincere gratitude to Dr. K S Badarinarayan, Principal, MSEC, and Professor Department of Mechanical Engineering, Bangalore, for providing the required facility.

I express my sincere gratitude to Dr. Vijendra Kumar, HOD, MSEC, and Professor Department of Mechanical Engineering, Bangalore, for providing the required facility.

I also extend my sincere thanks to our Guide NAVEEN KUMAR D, assistant Professor, Mechanical Engineering, MSEC, Bangalore, for his encouragement and support throughout the project.

Last but not least I extend, my thanks to the entire Teaching and Non-teaching faculty members of Department of Mechanical Engineering, MSEC Bangalore, who has encouraged us directly and indirectly throughout the course of my Bachelor Degree. Finally I thank my parents and friends for their continuous encouragement and support.

CONCLUSION

From this project, we learned the principle of CNC machine. We gained better understanding in the modes of operation of CNC machine. There is various type of modern CNC machines use in industry. Automatic generation of different preparatory (G codes) and miscellaneous function (M codes) is used in CNC part programming for completing a successful CNC program. Specifically, CNC milling machine works with a computer numerical control that writes and read G-code instructions to drive machine tool to fabricate components with a proper material removal rate. G-codes are commands for CNC machines to follow so that they can operate on their own without human control. Zero set up is very important step to obtain an accurate geometry of the work piece.
From this project, we would conclude that it gives an idea for the beginners to understand on how the CNC machines work virtually.

REFERENCES:

1. Sundar pandain et al (2014), demonstrated an open source G-code interpreter i.e. GRBL controller which acts as an inspiration to work on the production system with low cost [1].
2. Dr.J.B. Jayachandraiah et al (2014) provide the idea to develop the low-cost Router system which is capable of 3 Axis simultaneous interpolated [2].
3. Torjus spilling (2014), presented his master's thesis on self-improving CNC machine [3].

4. Alian Albert (2011) has studied history of CNC machines, information regarding CAD/CAM software's and suggested for various components used in a router [4].
5. Rajendra rajput et al (2016), demonstrated the comparison of CNC controller viz., Fanuc 21M 840D, Heidenhain TNC426. Kajal Madekar et al (2016) [5].
6. Ahmed A.D Sarhan in this paper, an initial CNC gantry milling machine structure with the potential to produce the high surface finish has been designed and analysed 2015 [6].

International Journal of Engineering Research and General Science Volume 6, Issue 4, July-August, 2018
ISSN 2091-2730

Bacteriological quality of effluents from the University Clinics of Kinshasa treated in UASB

Lubieno Okieng Louis[1], Weya Mazinkene Alfa[1], Ndaywel N. Olivier[1], Biey Makaly Emmanuel[1]*

[1]University of Kinshasa, Faculty of Science, Department of Environmental Sciences, P.O. Box 190 Kin XI
*Corresponding Author: biey.makaly@unikin.ac.cd

Abstract- The analysis of wastewater from the University Clinics of Kinshasa has shown that they are filled in considerable proportion the total germs, total coliforms, faecal coliforms, Staphylococci (*Staphylococcus sp*. and *Staphylococcus aureus*); the Enterobacteriaceae (*Entérobacter agglomerans*, *Entérobacter cloaceae*, *Providencia*, *Klebsiella pneumoniae*, *Proteus vulgaris*) multi-resistant to antibiotics, responsible for nosocomial infections. As a result of a treatment by UASB, it was noted a total reduction of germs (total germs from 10.6x 10^6 CFU/L to 32x10^4 CFU/L; 2.1x 10^6 CFU/L of total coliforms to 0 CFU/L and from 1.5x10^6 CFU/L of faecal coliforms to 0 CFU/L), and an elimination to 100% of Entérobacter which proves the effectiveness of the UASB system for the treatment of effluents from the hospital environments.

Key words: UASB, Bacteriological Quality, Effluents, nosocomial infections, Enterobacteriaceae

Introduction

Linking health and the environment is a highlight for the opinion, but it is still a challenge for anybody looking for reliable and accurate information. The Environmental health therefore relies partly on the assessment and risk management from where the emergency of the precautionary principle that it is now seeking to introduce in addition to the protection and prevention health (Fatiha Elmoumen, 2010). All health institutions produce a large quantity of waste. It will be observed in the framework of the DRC, that the hospital wastes are a threat to the environment. The hospital waste are all biological waste or not, eliminated without any intention to be reused (Kasuku and Kitambala, 2016).

The problem of discharges of hospital effluents becomes increasingly significant. Indeed, these institutions generate large volumes of liquid effluents that contain specific substances and are likely to spread of pathogenic germs. These effluents are usually evacuated in urban networks without prior treatment, in the same way as traditional domestic wastewater (Boillot Clotilde, 2008).

The microbiological pollution, toxicological, and genotoxic, added to the importance of volumes of effluent products (of the order of 1 m^3/day/active bed) lead to raise several questions on their potential risk to man and his environment on the one hand and on their negative influence on the biological treatment in Step on the other hand (Jehannin, 1999). Leprat (1998), indicates that a level of global pollution higher than household effluent, associated with the systematic presence of germs having acquired the characters of resistance to antibiotics and to the presence of ad hoc typically strains in hospital. On the microbiological level, the concentrations of pilot germs are lower in the hospital effluents that in urban effluents, which is probably related to higher concentrations of disinfectants and antibiotics. One finds an average between 10^4 and 10^6 germs/ml.

The level of contamination is very variable depending on the time, day, or the flow rate at the sampling time. That is why it is important to keep a extreme vigilance in regards to the security of the internal network. The hospital strains are characterized by their resistance to antibiotics. Their survival in the environment is poorly known; research of parasites is not currently practiced.

According to Tilley E. and al. (2014), the use of a UASB process in a treatment station is due to the very high organic loads discharged by the source of production in the sewage system. The UASB uses a anaerobic process while forming a coverage of granular sludge which is suspended in the tank. The wastewater flows upward through the cover and are processed (degraded) by the anaerobic microorganisms. The UASB reactors generally feet to dilute the currents of wastewater (TSS to 3% with a particle size > 0.75 mm).

This research has had as objective to characterize the bacteriological pollution of the effluent from clinics, to count and identify the substances germs responsible for the biological pollution of these hospital effluents, and to see the effect of a treatment by UASB on

the Microbiological quality of hospital effluent hospital as well as the effect of a treatment by UASB on the Microbiological quality of the hospital effluent.

Study area, Material and Methods

Study area

The University Clinics of Kinshasa (CUK) have been created by the University Lovanium in 1957, currently the University of Kinshasa, placed under the Scientific Authority of the Faculty of Medicine, but having a clear management autonomy and dependent, to do this, directly to the Board of Directors of the University.

They are built on the site of the University of Kinshasa (UNIKIN) behind the Faculty of Medicine.

They have a triple mission: the dispensing of high quality care, the teaching practice of medicine intended as well to the students of the Faculty of Medicine as to the pupils of the nurses school and other paramedical, and, finally, that of scientific research.

Built for a capacity of 1,000 beds, they currently have 800 beds whose 545 effectively functional divided into ten departments and the occupation of beds varies from 50% to 70%. The duration of hospitalization is of ± 3 days for the maternity and ± 17 days in hospitalization. The CUK are classified in the highest level having the rank of the tertiary hospital of last reference for the country.

As soon as the opening of the University Clinics of Kinshasa, the sewage system unit was with three main sewer including two poured waters in front of the clinics to the FUNA valley and the third behind the technical building of the clinics laying the effluent into the Kemi river.

The sewers which were evacuating the technical waters and valves are out of use. A separatist system was introduced with the implementation of three septic tanks, which contain the technical waters, and valves of some services. Despite the presence of these pits, which are located elsewhere in a state of very advanced decay, these waters are poorly contained. Only the storm water continue to be evacuated through the old sewer.

Material

The effluents of the infectious and tropical diseases services from the university clinics of Kinshasa were collected in four sites of rejection and treated in the laboratory of Ecotoxicology and environmental Biotechnology of the Department of Environmental Sciences, Faculty of Sciences of the University of Kinshasa by the UASB system. The UASB reactor mounted in glass at the Faculty of Polytechnics of the UNIKIN had a volume of one litre. It was adjusted to a HRT of 13 hours by the technique of gravity.

The microbiological characterization of the effluents was held before and after treatment by UASB.

Sampling

These samples were taken at 4 main glances of evacuation of the whole of the wastewater of the clinics, in March 2017.

➢ the site 1 deals with the effluents of the central administrative services, the emergency rooms, the central pharmacy, physiotherapy, and on the upstairs the consulting rooms;

➢ Site 2 receives effluent from emergency services and the block containing the gynaecology and paediatrics;

➢ the site 3 collects the effluent from the internal medicine, the surgical blocks and general pharmacy;

➢ the Site 4 is the glance, which drains the effluents of the technical building;

➢ the 5th sample was made up of the whole of effluents from these 4 mixed sampling points;

➢ the 6th sample was obtained after treatment of all the samples in the Pilot UASB set up system.

For bacteriological analysis of effluents from CUK, samples were collected in glass bottles of 200 ml each previously sterilized. The sign S1, S2, S3, S4, S5, S6, identified each sample.

The samples were transported directly to the laboratory in an insulated box at a temperature of 4°C and kept in the fridge for bacteriological analysis.

In order to isolate the germs contained in the effluent from the university clinics, two culture media (Ando agar and nutrient agar) have initially been prepared. The technique of Multiple dilutions in tubes has been applied using the Sterile physiological water, up to the ten thousandth. In total, 6 samples E1 - E6 were treated with 4 repetitions, and diluted up to ten-thousandth.

Microbial growth is characterized by the appearance of the troubles in the dilution tubes.

Petri dishes containing culture media Nutrient agar were seeded with 100 microliters per sample. The medium nutrient agar was used to isolate to a thousandth the total germs and the Ando agar at a tenth near for total and faecal coliforms.

a) Culture Medium Lactose broth

On the quantitative level, it has been applied the approach or the most probable number method in achieving the successive dilutions of the samples from hospital effluent hospital and those treated in UASB, in the lactose broth, general environment in which grow all the germs.

The principle is to place a series of four tubes containing 9 ml of lactose broth, numbered T1, T2, T3, T4 by proceeding with the addition of 1 ml of sample from the medium to the T1, then from T1 to T2 and so on. A blank tube was planned, without adding sample.

b) test of confirmation by the culture medium in broth Brilliant green bile

After incubation at 37°C and check for the presence of gas in the tubes of Durham after 24 to 48 hours, it was proceeded to the insulation by the planting of the positive samples on the culture media Mac-Conkey and Mannhutol Salt Agar (MSA) in order to respectively isolate Enterobacteriaceae and Staphylococcus. The insulation of faecal coliforms was done on the Peptone Water medium

The identification of *Staphylococcus aureus* was made on the test of related free coagulation.3. Results and discussion

3.1. Results

Table 1: Bacteriological characterization (total coliforms and germs) of effluents from Cuk

	First Laboratory			**Second laboratory (presence)**				**interpretation** bact/ml
	Germes (CFU/l)			**10^{-1}**	**10^{-2}**	**10^{-3}**	**10^{-4}**	
Sample	TG	TC	FC	+	+	+	+	10^4
S1	8.10^5	0	0	+	+	+	+	10^4
S2	$9.4.10^6$	$2.1x10^6$	$1.5x10^6$	+	+	+	+	10^4
S3	$10.6x10^6$	33.10^4	12.10^4	+	+	+	+	10^4
S4	$10.1x10^5$	0	0	+	+	+	+	10^4
S5	9.10^6	73.10^4	$11.2x10^6$	+	+	+	+	10^4
S6	32.10^4	0	0	+	+	+	-	10^3

It is clear from this table that the site 3 presents $10.6x10^6$CFU/L of total germs, followed by the Site 4 with $10.1x10^5$ CFU/L, and the Site 2 with $9.4x10^6$ CFU/L. The mixed sample then comes with 9.10^6 CFU/L, and finally the Site 1 with 8.10^5 CFU/L.

With regard to the total coliforms, apart from the site 1 and 4 not having presented the CFU, the second site has presented $21,3.10^5$ CFU/L, followed by the mixed sample with 73.10^4 CFU/L and the third site was 33.10^4 CFU/L.

The Faecal coliforms were found in the mixed effluent with a concentration of $11.2x10^6$ CFU/L, the effluent of sites 2 and 3 respectively with 15,1.105 CFU/L and 12.104 CFU/L, whereas the Sites 1 and 4 were lacking. After treatment (S6), in addition to the total germs, which have been present with $32.1O^4$ CFU/L, total and faecal coliforms were not isolated in our sample, which shows a processing efficiency of 60% for the total germs and 100% for faecal coliforms but one has assisted to the emergency of other germs.

Table 2: isolation of staphylococci

N°	Sample	MSA and coagulase test
1	1st site	-
2	2nd site	*Staphylococcus sp*
3	3rd site	*Staphylococcus aureus*
4	4th site	*Staphylococcus sp*
5	5th sample (mixde)	*Staphylococcus sp* and *Staphylococcus aureus*
6	After treatment	-

The presence of Staphylococcus was noted in the Sites 2, 4, and 5.

Table 3: Isolation and identification of germs (Enterobacteria)

N°	Samples	Identification						
		Kligler			Gaz	Citrate	indole	germs
		gluc	lac	H_2S				
1	1st site	+	-	-	+	+	+	*Entérobacter agglomerans*
2	2nd site	+	±	-	+	+	+	*providencia*
3	3rd site	+	-	-	-	-	-	*Klebsiella pneumoniae*
4	4th site	+	-	+	+	+	+	*Proteus vulgaris*
5	mixed sample	+	±	+	+	+	+	*Klebsiella Pneumoniae et providencia cloaceae*
5	After treatment	-	-	-	-	-	-	-

After culture of the samples of effluent from CUK, certain biochemical parameters (tests) (glucose, lactose, H_2S, gas, citrate and indol) were observed whose some positive and the other negative. Using the Table of Identification of Enterobacteriaceae, the germs below were isolated according to the sampling site: *Entérobacter agglomerans* to the first, Providencia at the second site, *Klebsiella pneumoniae* at the third site, Proteus vulgaris at the fourth site; the mixed sample contained *Klebsiella pneumoniae* and *Providencia*, the *Entérobacter* were not found on the effluent after treatment.

Table 4: Isolation of faecal streptococci on the Bilsculine medium

N°	Samples	Bilsculine medium
1	1st site	No blackening
2	2nd site	Blackening
3	3rd site	No blackening
4	4th site	Blackening
5	After treatment	No blackening

The samples from sites 2 and 4 went black in the tube containing 5 ml of Bilsculine thus showing that there was growth of germs (faecal streptococci) in this environment.

Table 5: Isolation of Escherichia coli on the peptone water medium

N°	Samples	Peptone water medium
1	1st site	presence of red ring
2	2nd site	presence of red ring
3	3rd site	presence of red ring

4	4th site	presence of red ring
5	After treatment	No ring

The results in this table show the presence of Escherichia coli in all sites except for the treated effluent.

Discussion

The enumeration of total germs in the effluent of the University Clinics of Kinshasa has given respectively $10.6x10^6$ CFU/L and $10x10^6$ CFU/L at Sites 3 and 4. The study of KASUKU and KITAMBALA (2016), conducted on the effluents of the Department of Gynecology of the University Clinics of Kinshasa, gave a concentration of 3.1×10^3 CFU/L of bacterial flora.

With regard to the total coliforms, apart from the site 1 and 4 not having presented the CFU, the second site has presented $21.3x10^5$CFU/L, followed by the mixed sample with $73x10^4$ CFU/L and the third site was $33x10^4$ CFU/L. This is consistent with the idea of Fatiha Elmoumen (2010), which declares that the total coliforms are present in large numbers in the faeces of humans and animals ($2\ 10^9$ coliforms /day/capita) and it is considered as an indicator of the control of the general quality of the water. It is possible that they are found in large numbers in the effluent of a hospital. These are of indicator bacteria of pollution of microbial contamination (Edberg et al, 2000).

The analyzes on the faecal coliforms have revealed the presence of germs in the second and third site with respectively $15,1x10^5$ CFU/L and $12x10^4$ CFU/L. The presence of coliforms in water indicates that this water may be contaminated by pathogens. The coliform bacteria are used as indicators of the contamination of the water because many of them live in abundance in the digestive tract of man (Midian and Martinko, 2007).

Améziane and Benaabidate (2014) have obtained in their studies the annual mean values of the load of the traditional pilot bacteria of faecal pollution in the effluent from the hospital Mohamed V in the following way: TC: $10,6x10^7$ CFU/L, FC: $7,44x10^6$ CFU/L and FS: $2,28.10^6$ CFU/L.

The results obtained after treatment, in addition to the total germs, which have been present (32.1 O4 CFU/L), coliform bacteria were not isolated in this sample. The installation of our pilot UASB station has folded back the bacterial load where the coliforms were eliminated; the installation of a treatment plant within the hospital would reduce the load of the river in the city.

Finally it is even within the hospital that the fate of liquid waste must be supported, by sensitizing the staff on the impact of these discharges. Given the bacterial load of these effluents, the need for a treatment plant within the hospital is useful.

The culture of the CUK effluent samples made in the MSA and MC media has shown that the sample taken at site 1 and after treatment did not present germs in the MSA medium whereas the 2nd, 3rd, 4th have shown the presence of germs and all samples had a positive result in the Mac-Conkey. The bacteriological quality of the water is evaluated by the search for pilot bacteria of faecal contamination. The culture of effluents from the services of care presents pathogenic germs that are often polyrésitants to antibiotics such as Salmonella, bacteria responsible for nosocomial infections (*Staphylococcus aureus, Pseudomonas aeruginosa, Escherichia coli*, etc.), viruses, parasites (Boillot C, 2008).

In the samples of effluent from CUK, bacteriological analyzes have highlighted the staphylococcus sp and the *Staphylococcus aureus*, responsible for nosocomial infections at the hospitals. These results confirm the hypothesis of Evans (2004), which indicates that the wastewater produced by the establishments of health care can serve as a vector to agents of transmission of nosocomial infections. As to Schlosser (1999), if for most of the researchers the hospital waters would not be more polluted than the urban wastewater, the specific species such as *Pseudomonas aeruginosa* and pathogenic *Staphylocci* would make exception (more than 10 times higher for Pseudomonas).

After culture of the samples from the CUK effluent, analyzes of some biochemical parameters (tests) have enabled using the Identification table for Enterobacteriaceae, isolate the germs such as the *Entérobacter agglomerans*, *Entérobacter cloaceae*, the

providencia , *Klebsiella pneumoniae*, and *Proteus vulgaris*. The enterococci, Staphylococci, Enterobactériaceae and heterotrophic bacteria are used as indicators of the presence of multi-resistant bacteria to the antibiotics in the network of hospital sanitation (Evans, 2004).

The observation made on the results obtained after isolation of streptococci in the effluent of CUK is that, the samples in the site 2 and site 4 have presented the darkness in the tube containing the Bilsculine and this means the growth of germs (faecal streptococci) in this environment. The parasitological or bacteriological pollution of water remains the main problem of developing countries (Fatiha Elmoumen, 2010).

During the identification of *Escherichia coli* in the effluent of the CUK having to undergo a treatment by UASB, it was noted the presence of a red ring on the whole of the samples, which characterizes the growth of Escherichia coli except the treated sample. *Escherichia coli* is an enteric bacterium living in the digestive tract; when they are excreted in the water, coliforms eventually die. But they die less rapidly than several pathogens (Madigan and Martinko, 2007). In order to avoid that all pollutants from hospital effluent be found in the environment, they should be treated upstream. Due to the fact that the hospital effluents contain a lot of germs, they are part of infectious wastes (KASUKU and KITAMBALA, 2016).

Regarding the performance of the wastewater treatment plant, it is clear from the microbiological analyzes, that the amount of total coliforms and faecal coliforms were greatly reduced by the treatment in our pilot UASB unit.

The UASB process is complex but very effective to eliminate the organic content of wastewater (Tony Davies, 2005). The anaerobic treatment offers several advantages for developing countries because of its merits such as the high efficiency, profitability and simplicity in the construction and operation (Abdullah Yasar and Bari Amtul Tabinda, 2009).

In a study on the effluents of the Department of Gynecology of the University Clinics in Kinshasa, a concentration of bacterial flora 3.1 x 10^3 per 100 ml has been found (KASUKU and KITAMBALA, 2016). According to the authors, by lack of standards established in this regard in the DRC, they could not compare this value. In the identification, several colonies of faecal coliforms and streptococci were counted; and in the insulation the effluents have shown the presence of Escherichia coli, Klebsiella, Salmonella and Enterococcus.

Conclusion

Wastewater from the university clinics in Kinshasa have shown significant concentrations of bacteria responsible for nosocomial infections and multi-resistant to antibiotics such as *Klebsiella pneumoniae* and *Staphylococcus aureus*.

The highest concentration was that of total germs obtained at $10.6x10^6$ CFU/L, faecal coliforms with $15,1x10^5$ CFU/L and total coliforms with $21.3.10^5$ CFU/L

The UASB treatment applied to these waters eliminates the coliforms in general to almost 60% and the *Entérobacter* to 100% but this gives rise to the establishment of a new bacterial community different from that of departure, due to anaerobic conditions that settle in the reactor.

The bacteriological analyzes carried out allowed to deduct that microbiological load of effluents from the University Clinics in Kinshasa constitutes a health risk that could potentially be hazardous especially where these effluents are used for the irrigation of crops consumed by the populations.

It is therefore necessary to limit the discharges of hospital effluents in the environment without prior treatment.

However, despite the fact that bacteriological analyzes represent only a fraction of the total load of contaminants from the Hospital, it is recognized the danger of microorganisms among all other contaminants from the CUK.

REFERENCES:

1. **Abdullah Yasar et Amtul Bari Tabinda, 2009.** Anaerobic Treatment of Industrial Wastewater by UASB Reactor Integrated with Chemical Oxidation Processes; an Overview, Sustainable Development Study Center GC University Lahore Pakistan
2. **Agrawal LK., Ohashi Y., Mochida E., Okui H., Ueki Y., Harada H., A. Ohashi, 1997.** Traitement des matières premières : les eaux usées dans un climat tempéré en utilisant un réacteur UASB
3. **Ameziane, N.E et Benaabidate, L., 2014.** Caractérisation microbiologique des effluents de l'hôpital Mohamed V de Meknès et étude de leur impact sur l'environnement, Laboratoire de Géoressources et Environnement, Faculté des Sciences et Techniques, B.P. 2202, Route d'Imouzzer Fès, Maroc, Revue « Nature & Technologie ». C- Sciences de l'Environnement, n° 10/Janvier 2014. Pp 31 - 38
4. **Boillot, C, 2008.** Evaluation des risques écotoxicologiques liées aux rejets d'effluents hospitaliers dans les milieux aquatiques. Contribution à l'amélioration de la phase « caractérisation des effets ». domain other. L'Institut National des Sciences Appliquées de Lyon (INSA), France. N° d'ordre 2008 ISAL 0021
5. **Coralie Darsy, Irène Lescure, Véronique PAYOT, et Géraldine Rouland, 2002.** Effluents des établissements hospitaliers : teneur en microorganismes pathogènes, risques sanitaires, procédures particulières d'épuration et de gestion des boues, Office International de l'Eau Service National d'Information et de Documentation sur l'Eau (SNIDE)
6. **Duchesne D., Coallier J. et Lafrance P., 2000.** Méthode simple pour doser les coliformes totaux à la sortie d'une usine de traitement d'eau, Sciences et technique de l'eau.
7. **Edberg S., Rice E., Karlin R.J. et M.J. Allen, 2000.** Escherichia coli: The best biological drinking water indication for public health protection. Journal of Applied Microbiology, 88: 106S-116S.
8. **Evens E 2004.** Evaluations des risques sanitaires et écotoxicologiques liés aux effluents hospitaliers, l'institut national des sciences appliquées de lyon, formation doctorale : sciences et techniques du déchet école doctorale de chimie de lyon, Thèse de doctorat, France Limoge
9. **Fatiha Elmoumen, 2010.** Caractérisation et conséquences environnementales de la charge polluante des eaux usées de la ville de Tiznit (Maroc), Mémoire de Licence des Sciences et Technique, Eau et environnement, *Université Cadi Ayyad , Faculté des Sciences et Techniques- Marrakech* Hanging processus éponge cubes. Sciences de l'eau et La technologie. **36**, (6-7), 433.
10. **Hamsatou MOUSSA MOUMOUNI DJERMAKOYE, 2005.** Caractéristiques physico-chimiques, bactériologiques et impact sur les eaux de surface et les eaux souterraines, Faculté de Médecine de Pharmacie et d'Odonto-Stomatologie, Thèse de doctorat, Université de BAMAKO, République du MALI
11. **Jehannin Pascal, 1999.** Caractérisation et gestion des rejets liquides hospitaliers, étude particulière de la situation du C.H. de Hyères (Var), mémoire de fin d'études en formation d'ingénieur du génie sanitaire, école nationale de la santé publique (INSA) Rennes, Paris, France.
12. **Jules B. van Lier1, Anand Vashi2, Jeroen van der Lubbe3 and Barry Heffernan4, 2012.** Anaerobic Sewage Treatment using UASB Reactors: Engineering and Operational Aspects, Faculty of Civil Engineering and Geosciences, Department of Water Management, Delft University of Technology, The Netherlands
13. **Kasuku Z. et Kitambala A, 2016.** caractérisation biologique et chimique des effluents liquides des Clinique Universitaires de Kinshasa en RDC, faculté des sciences, unité de sciences de l'environnement, université libre de Bruxelles, campus de la plaine, CP 260
14. **Leprat, P., 1998.** Les rejets liquides hospitaliers, quels agents et quelles solutions techniques? In: Santé et environnement hospitalier, les Assises Nationales QUALIBO, Caen, 1998 pp. 10-12
15. **Madigan, M. et Martinko, J., 2007.** Biologie des micro-organismes, 6ème édition, Université Carbondale de l'Illinois du sud, nouveaux horizons-ARS, Paris, France ; traduction française de Daniel Prieur.
16. **Schlosser, O. 1999.** Exposition aux eaux usées et risques microbiologiques
17. **Tilley, E., Ulrich, L., Lüthi, C., Reymond, Ph., Zurbrügg, C., 2014.** Compendiun des systems et technologies de l'assainissement, 2ème éd. révisée ; Institut fédéral Suisse des sciences aquatiques et de la technologie (Eawag), Duebendorf, Suisse.
18. **Tony Davies,** 2005. Fonctionnement d'un réacteur de couverture de boues anaérobie (UASB), Campaspe Water Reclamation Scheme, Earthtech Engineering. Victorian.

International Journal of Engineering Research and General Science Volume 6, Issue 4, July-August, 2018
ISSN 2091-2730

ELECTRICAL FORGING MACHINE

Varun hegde1, Naveen Kumar D2, Dr Vijendra Kumar3, Dr K. S Badrinarayan4.

1. Student, department of mechanical engineering, varunhegde278@gmail.com

2. Asst. Professor, Department of mechanical engineering, M S Engineering College, dnaveenmech@gmail.com

3. Professor and H.O.D, Department of mechanical engineering, M S Engineering College, vijendravk@gmail.com

4. Professor and Principal, M S Engineering College, principal@msec.ac.in

Abstract—Here we are going to fabricate the automated forging machine. It's a new innovative concept Forging is the term for shaping metal by using localized compressive forces, This machine has been mainly developed for a metal forming to required shape and size. The aim of our project is to eliminate the manual method of forging into automated forging machine to overcome the problems like inaccuracy and manual errors.

Keywords— Forging machine, slider crank mechanism, 2hp motor,link, hammer.

INTRODUCTION

Forging is the application of compressive forces on the work piece to get desired shape and size. Forging is a manufacturing process involving the shaping of metal using localized compressive forces. Forging has been done by Smith's for traditional products kitchenware, hardware, hand tools, edged weapons, and jewelry. Forged parts are widely used in mechanics and machines whenever a component requires high strength.

The aim of our project is to eliminate the manual method of Forging into electrical forging machine. Usually forging is the process of shaping the work piece it is done by two methods hot forging and cold forging methods. In hot forging method work piece is forged at a very high temperatures and lot of man power is required. This machine has been mainly developed for a metal forming to required shape and size.

In present situation there is a problem regarding shortage of labors. To overcome these problems, we have come up with the electrical forging machine which requires zero-man power. Electrical Forging Machine helps to the labors and the students who are studying forging and laboratory.

RESEARCH METHOD

OBJECTIVE

1. The main objective of our project is to eradicate the manual methods of forging and replace it into the electrical system. Usually the forging machine is done by manual methods like hammering.
2. To minimize the labor availability problems and other financial expenditures spent on the labor. The cost spent on the labors are now a day increasing hence to minimize the labor cost Electrical Forging Machine is helpful.
3. To get the good surface finish compared with manual methods. The surface finish obtained by manual methods is not good hence to have a better surface finish this project can be used

METHODOLOGY

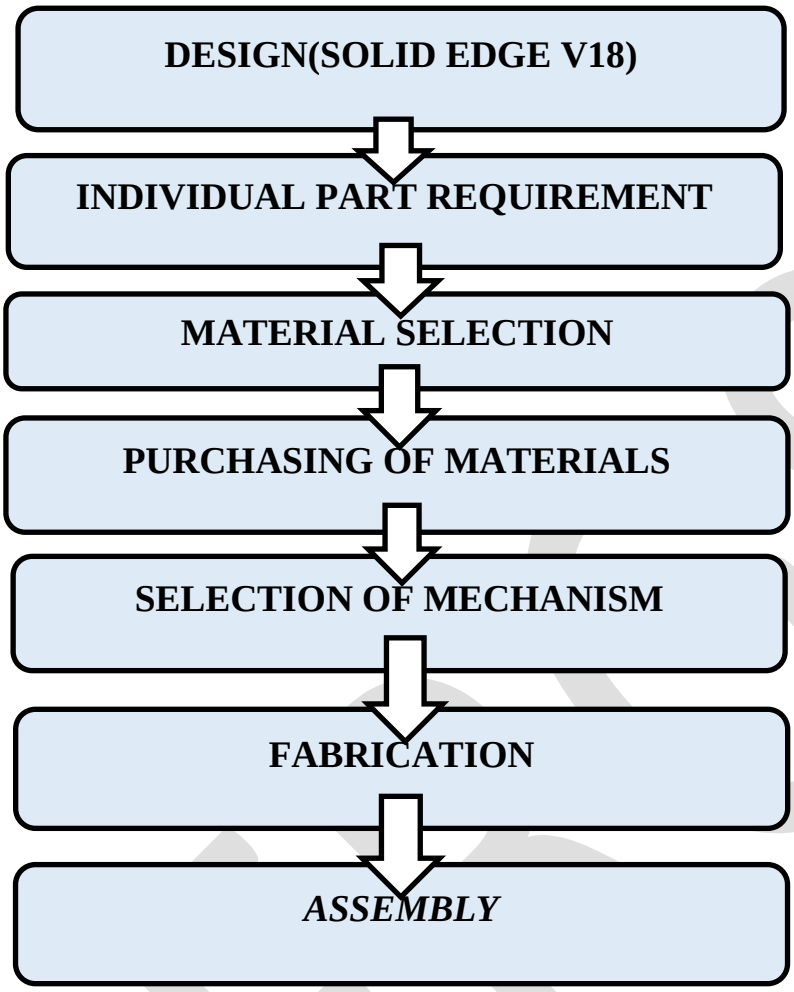

Flow chart: 4.1 methodologies

In the design and fabrication of any product the role of each and every part play a vital role. Each and every part is required for the final assembly of the project. The main objective of our project is to eradicate the manual methods of forging and replace it into the electrical system. Usually the forging is done by manual methods like hammering. To minimize the labor availability problems and others financial expenditures spent on the labors. The cost spent on the labors are nowadays increasing hence to minimize the labor cost Electrical Forging machine is helpful.

Some of the individual parts of the Electrical Machine is listed below.

- Motor
- Bearings
- V- Belts
- Pulley
- Hammer

- Base- C –Channel
- Links
- Anvil
- MS Pipe
- Supporting frame

Material Selection

Material selection is a step in the process of designing any physical object. In the context of product design, the main goal of material selection is to minimize cost while meeting product performance goals. Systematic selection of the best material for a given application begin with properties and costs of the candidate materials. For example, a thermal blanket must have poor thermal conductivity in order to minimize heat transfer for a given temperature difference. In the design and fabrication of any product the role of each and every part plays a vital role. Each and every part is required for the final assembly of the project. The main objective of our project is to eradicate the manual methods of forging and replace it into the automated system Materials selected for the automatic forging machine based on their characteristics is given below

- Motor- Seamless Steel (Treated with Epoxy Coatings).
- Bearings- Stainless Steel and Ceramic Material.
- V-belts- Rubber Impregnated Fabric.
- Pulley- Cast Iron.
- Hammer- High Carbon Steel.
- Base- C-Channel- Mild Steel (0.05%-0.025% Carbon).
- Links- polyurethane. ➢Anvil- wrought Iron.
- MS Pipe- Hollow Steel.
- Supporting Frame- MS Steel (0.05%-0.025% carbon).

Purchasing of Materials

Purchase is the main activity in area of material management. Purchasing refers to the procurement of the raw materials required for the particular objective. Purchase management is one of the most crucial are of the project.

Purchasing involve acquiring materials of right quality in a right quantity at a reasonable price and at right time.

DESIGN OF COMPONENTS

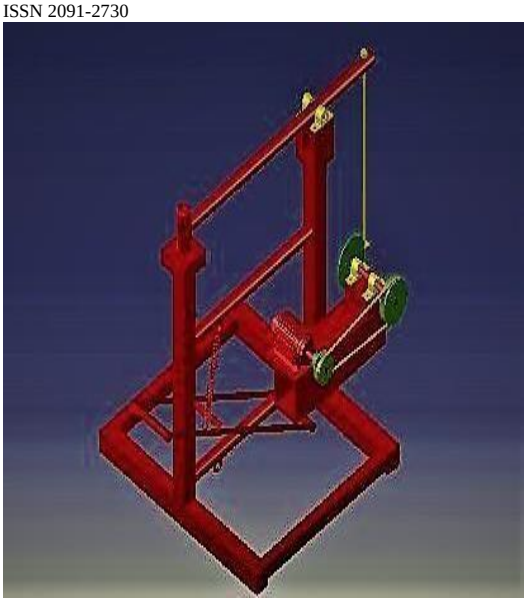

Machine model

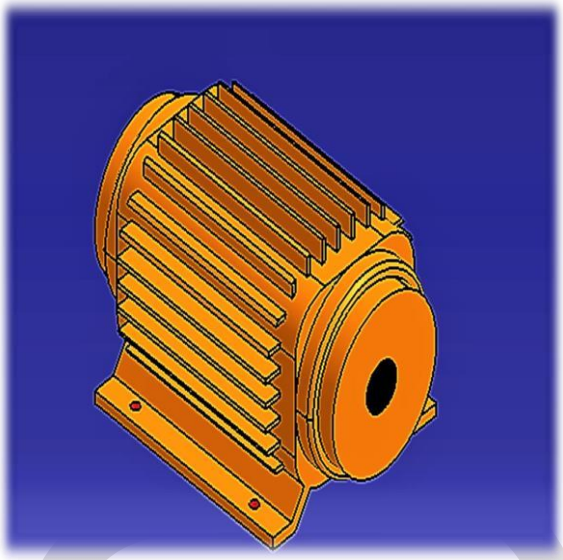

Motor

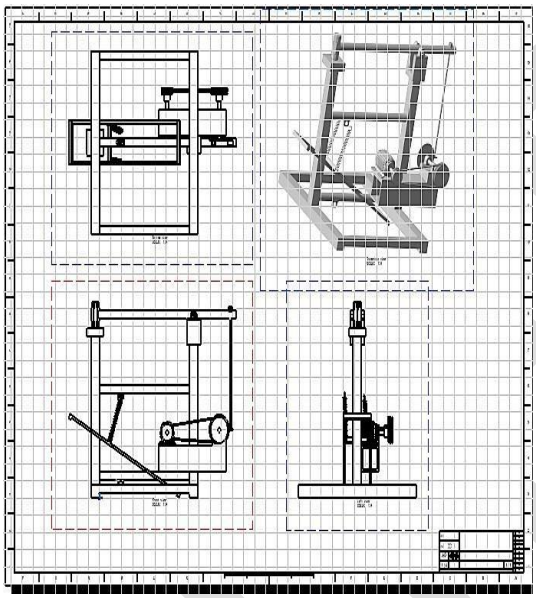

Drafting

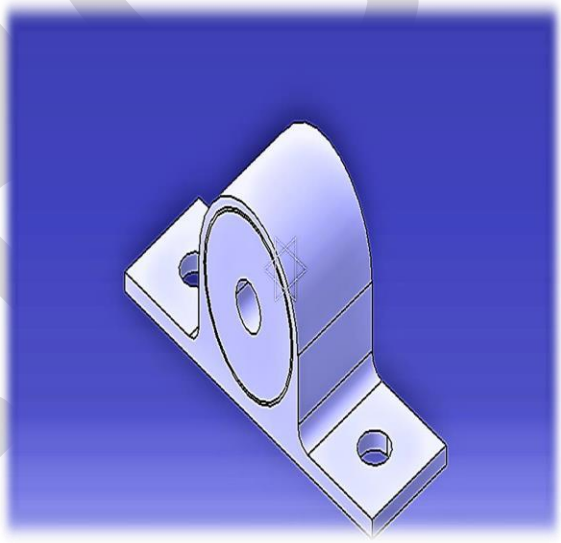

Bearing

ACKNOWLEDGMENT

The successful completion of any work will be incomplete without complementing those who made it possible and whose encouragement made my effort successful. At the very outset, Firstly I would like to be highly grateful towards the college, M S Engineering College, Bangalore, for providing us with all the necessary help and grooming up in to being Bachelor of Engineering.

I express my sincere gratitude to Dr. K S Badarinarayan, Principal, MSEC, and Professor Department of Mechanical Engineering, Bangalore, for providing the required facility.

I express my sincere gratitude to Dr. Vijendra Kumar, HOD, MSEC, and Professor Department of Mechanical Engineering, Bangalore, for providing the required facility.

I also extend my sincere thanks to our Guide NAVEEN KUMAR D, assistant Professor, Mechanical Engineering, MSEC, Bangalore, for his encouragement and support throughout the project.

Last but not least I extend, my thanks to the entire Teaching and Non-teaching faculty members of Department of Mechanical Engineering, MSEC Bangalore, who has encouraged us directly and indirectly throughout the course of my Bachelor Degree. Finally I thank my parents and friends for their continuous encouragement and support.

CONCLUSION

During working on project we have been gone through learning of many feasibility study production process and controlling with team work. Thus this project work is much useful in forging lab. For practical applications this is designed and fabricated for forging the work piece. In any manufacturing industries time is an important parameter and it should be utilized properly in order to reduce delivery lag time. This machine can save the processing time. Labor availability is a major problem faced nowadays hence the forging machine which is being automated can reduce the labor problems. The effort required by the man for the forging operation is high hence this machine can reduce the human efforts. This experience and knowledge will be further helpful to our professional career.

REFERENCES:

[1]. J. Kupta Et AI, united states patent office journals, application – December 2,1995, serial no. 550718, patented Oct 23,1957, published no.US2789540

[2]. Howard Terhune, Cleveland, Ohio, united states Patent office journals, application – September 27,2994, serial no. 555977, patented Oct 28,1947, published no. US2429780 **[3]. David A.Giardino,** utica; William K.Wallace,barneveld; Joseph R.Groshans,clinton,all of N.Y,united states patent office journals,application – September 25,1989,patented Jan.28,1992,patent no. 5083619 published no. US 5083619

[5]. Ulrich demuth, erbach- ernsbach; winrich hakbedane,diez, both of

Germany, united states patent office journals, application – November 30, 2996, patent August 39, 2000, patent no.6109364, published no. US006109364A

[6]. James kepnar , Lawrenceville,GA(US),united states patent office journals,application filled – March 23,2001,serial no.09/815,677,patented September 26,2002,published no.US 3002/0133997A1

[7]. Theory of machines by R.S.khurmi and J.K.gupta(pg. No.774to 832)4th edition

[8]. A textbook of machine design by R. S. Khurmi and J.K.gupta (pg.no 509 to 557, chapter 14.shaft, pg,no. 759 to 775,chapter21.chain drive,pg. No.996 to 1020,chapter 27. Bearings, pg no.1021 to 1124, chapter 28, 29,30,31)

[9]. Design data for machine elements by B.D.Shiwalker (pg.125to 132,pg.150 to 154.pg. 255 to 160,pg.39

International Journal of Engineering Research and General Science Volume 6, Issue 4, July-August, 2018
ISSN 2091-2730

A MOTIVATED METHOD FOR DETECTION OF DISTORTED TRAFFIC SIGN BOARD IMAGES

[1]Dr.Shubhangi D.C, [2]Supriya Mohrir

[1]Chairman, [2] P.G Student
[1]Department of PG Studies in Computer Science and engineering,
Visvesvaraya Technological University Centre for PG Studies, Kalaburagi, Karnataka, India

[2]Department of PG Studies in Computer Science and engineering,
Visvesvaraya Technological University Centre for PG Studies, Kalaburagi, Karnataka, India

1.drshubhangipatil1972@gmail.com , 2. supriyamohrir@gmail.com

ABSTRACT :In human general activities the movement from one place to another place is an important aspect. The use of vehicles is a main resource for the movement of the humans from one place to other place. It requires the person who is driving must be capable of handling the vehicle and also should have the knowledge regarding road driving rules. In accordance with this , traffic sign boards are displayed across the road side to avoid the collision on the roads. Detection of these sign board meaning is an important aspect in the maintenance of the road collision. If the user who is driving understands the sign , than the collision can be reduced significantly. Hence a traffic sign recognition system is introduced for the user who doesn't know the meaning of sign exactly. The system detects the sign board based on the features like shape and colour and later classifies the sign based on the Multilayer perception (MLP) classifier to give the result to user after interpretation.

Index Terms - MLP, HSV, DWT, HSV, DE noising, image acquisition, image processing.

I INTRODUCTION

Traffic sign recognition system is an important part of intelligence transportation systems, which can take images by the cameras installed on the front side of the motor vehicle and transfer images to the image processing module of the system. It plays an important role in drivers and pedestrian safety.The natural scene of the traffic board recognition exists in complex scenes: climate interference, illumination changes, dirt or blocked traffic sign board and skew distortions due to anthropogenic factors or disrepair. Therefore, the recognition of traffic sign board is of great significance in natural scenes.

Every country has its own sign boards in terms of signs, colors and designs in it etc. These standards are considered to be static or uniform in any part of the country. The Government has set the rules and regulations regarding these color and shape of the sign boards, colors like red, Green, blue , yellow, and the shapes such as diamond, triangular, square, circle and etc are to be used. Depending on these signs driver need to follow the instructions. These sign boards have been evolved to reduce the amount of accidents happening on the road. These signs have specific information regarding speed limit, terms ahead, school ahead, Hospital ahead and do not park etc. Proposed road sign recognition system uses the computer vision technology by grabbing the images from the frames, from the videos, and giving input to system for recognition of the sign boards. It is performed based on the assumptions of uniqueness of color and shape. There are many methods which have been developed for road sign recognition over many years. But a challenge of recognition of these sign boards in case of bad weather conditions has been challenging to the drivers due to blurriness of the board and even over speed can also cause collision of vehicles .

To overcome these problems many of the techniques have been proposed but still it is a expensive process as well as time consuming. A real time traffic sign recognition has been performed in following stages:

1. Acquisition of Image
2. Preprocessing of Image.

It consist of following steps:

a. Color module Conversion

b. Noise Filtering
c. Connect component labelling
d. Size filters.

3. Sign recognition or feature recognition.

4. Traffic sign Tracking.

The flow of the road types are as follows.

a. Warning

b. Prohibition

c. Obligation

d. Informative.

a. Warning: This type of sign boards are used to be generally in red color. It indicates a not to do a information to the users.

b. Prohibition: Sign boards generally circle in shape, white or blue in color generally located in area which public works.

c. Obligation: Generally Obligations are circle in shape in blue background. Which indicates no parking indications.

d. Informative: The sign board which indicates some informations like hospitals, schools etc.

II RELATED WORK

S. Maldonado-Bascón, et al.[1] has addressed the task of recognising the traffic sign by using a video input in the two components independently. In the initial stage the team, takes video input from the source and perform the same frame conversion from the video. H. Gomez-Moreno and team have performed Traffic Sign Recognition by using transformation of the features and support of classifier. Based on the reality of the images, every images are initially classified based on three classifications like distance, angle, environment etc. In [3] ,A. Ruta, F. Porikli et al. tried to achieve a real time classification of road signs by using a live camera which is embedded on the moving vehicles. They have emphasized a neural network for the classification stage to avoid the conflicts for the candidate selection. T. Michalke, et al. [4] have used a approach to recognise the traffic signs based on the patterns associated with each image like shapes, colors etc. The classifier SVM is used for classification of recognised sign boards. Images are acquired through the camera and it is invariable to size once it is scaled.L.-F. Liu, et al .[5] had concentrated mainly on shape of a sign boards to be classified based on the distance measure by using SVM classifier. They have given lot of interest in providing a safe and accurate measurement of the sign for the user to avoid the accidents. In[6],H. Chen, has used histogram based features like HOG and classifier like SVM for recognition and classification of road signs. This system recognises those candidates in the image which are stable in nature and gives good results under various lightning conditions. It also operate for high speed vehicles and bad weather performance. P. E. Hart, et al.[7] have used sensor based technology for the recognition of sign on a moving vehicle .They used the infrastructure based vehicle communication method with a vision sensor applied in it and used GPS based sensor to track the vehicle location and providing higher level of communication ,the experiment has been performed in day and night situation on number of vehicles provided with accuracy for detection 95%, and recognition 93% and consume time about 35milisecond per test. G. Loy et al .[8] have applied color based segmentation with adaboost classifier an HOG transformation method to perform the sign recognition easily and efficiently.

III METHODOLOGY

In the proposed work the requirement of digital image processing is the main criteria about the process. We use image process technologies which will allow the user to capture process recognised and classify the given input image of technologies available. The image processing technologies such as image acquisition, image transformation, Image classification has to be performed in order to get accurate and efficient results.

The Road sign boards has to be captured first by the use of digital camera later it is sent to the system by the help of image acquisition process. The input image is then processed based on the requirement of the user which is generally used to classify the road sign.

The processed image is then taken into consideration for the final classification of the system, later the result is interpreted to the user, then it can be processed for the later uses.

SYSTEM ARCHITECTURE

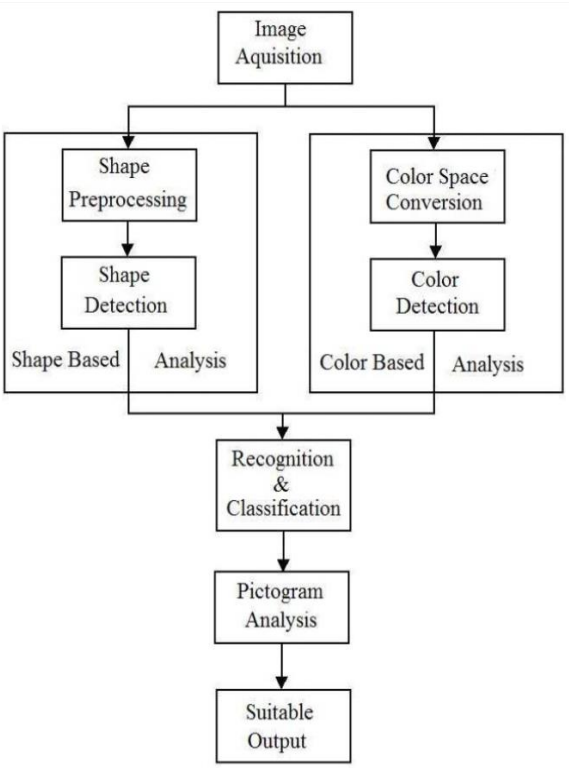

Fig 1 : System Architecture

Algorithm used for image denoising:

```
Begin
send true image;
Division process
Set Condition: pixel similarity
    If(pixel similarity = = TRUE)
        Return: "Compared to region"
    End
    If(pixel similarity = = FALSE)
        Return: "sub-areas of interest in turn"
    End
    For(i =begins of images, split cut)
SplitImage
    If(Splitting = = 0)
        Brake
Else split
End
    For (i = splitrregion ; split areas)
        Merge process
    Compare adjacent regions
    Merge of necessary
    End
End
Terminate;
```

Algorithm used for Interpretation:

```
Initially
    Read the image 'I'
        I = Imread(image)
    Convert Image to Binary
        B = im2Bw (I)
    For each pixel in image B
            If pixel in image is Red
                Current pixel to white
            End
    End
Create pixel to blue
    Perform Binary Image labelling
    Perform criteria selection
Extract clustersize 'C'
    For each cluster C in B
        If(Cluster > 100 & Cluster <3000)
            Then mark as Road sign
        End
      For each user.c

        If(Cluster is too small or high)
            Neglect objects;
        End
      End

      Merge pixel clusters 'C' and same or signImage.
```

Filtering of the image is carried out as follows :

A noise is a unwanted pixel present in the image which is caused due to many of the electronic issues, such as storage, transmission, recording etc.Hence filtering removes such noise present in the image, A kind of filter called split and merge is used in the proposed work.This filter removes the noise without blurring the image and does not remove the inter information of given input image.This filter may reduce block of pixels based on its nature and attempts to divide the image into the uniform regions and later merging them based on the neighborhood pixel values.

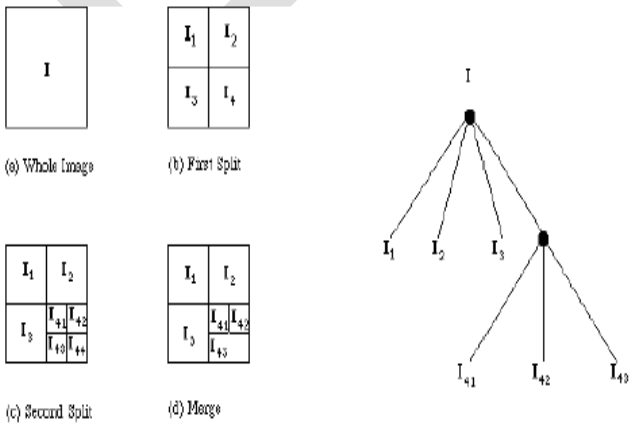

Fig 2 : Split and merge filter process

HSV color model :

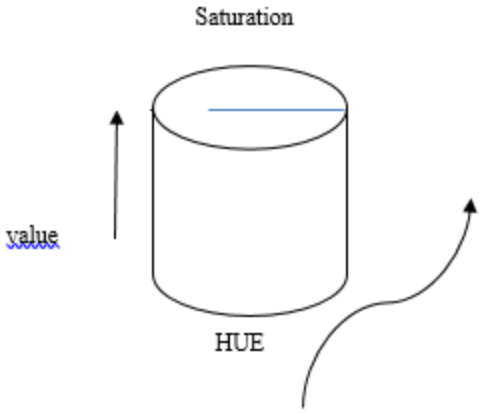

Fig 3 : HSV color model

The HSV color model is implemented in the proposed work, which is used to calculate the brightness, intensity of the image which is given from the dataset **.** The Hue (H) and saturation (S) , these two parameters are concerned with the wavelength of color model, used in the image and the value(V) ,is used to indicate the amount of brightness present in the light which ranges from 0 to 100 %.

For ex: In HSV the range are as follows.
For Red color.

- Here HUE is less than of 0.05 or also is greater than of 0.95.
- Saturation greater than of 0.5.
- Value also greater than of 0.01

The pixel ranges which above and below range of a threshold are eliminated and assign the value of 0 in the pixel values which are within the range of values are assigned value of 1.

IV GRAPHICAL ANALYSIS AND EXPERIMENTAL RESULT

Experimental Results

After analyzing the colors from different videos to the usual color ,HSV values are set in the table below:

Table 1

color	HSV values		
	HUE	Saturation	value
Red	0-58	0-90	0-90
Blue	0-60	0-107	98-255
Yellow	100-140	80-90	0-65
Black	150-160	110-150	0-120

Table 2

Table for Mismatched traffic sign

Sign color		Results		
	Inputs	Detected	Different Patterns	Mismatch percent

Red	74	40	34	0%
Blue	90	78	12	0%

Table 3

Table showing percentage of correct noise detection for the given input images

Sign code		Results	
	Inputs	Correct detection	Correct percentage
Red	40	39	97.35%
Blue	50	47	95%

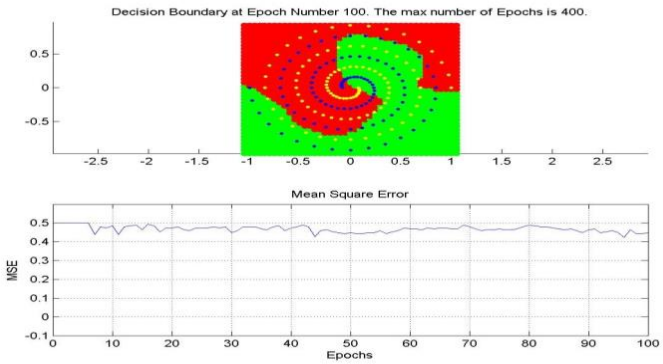

Fig 4 : Graphical analysis of image labeling

Fig 5 : Occluded Samples

V RESULT AND DISCUSSION

The Algorithm which are used for interpretation and image DE noising are implemented in step wise in order to recognize the traffic sign image efficiently. The De noising algorithm use the concept of split image and merge concept necessarily and interpretation algorithm uses Binary image labeling concept and gives the following efficient results.

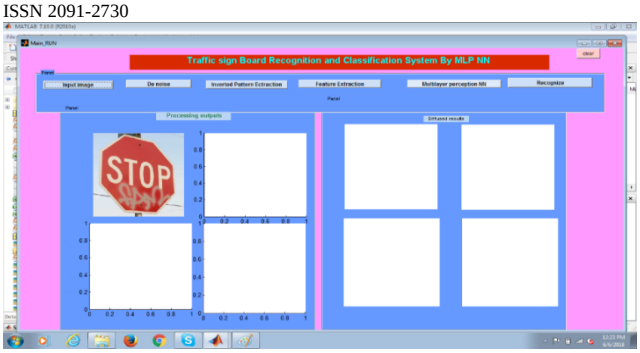

Fig 6: Input Image

The figure represents the Traffic Sign which is given as an input image to the system from the data set.

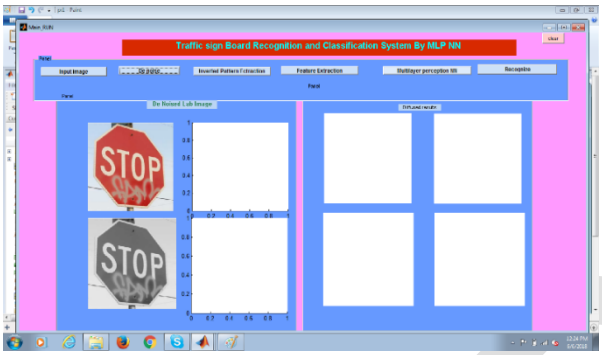

Fig 7: Input image from the traning data set.

The figure shows input image, which is preselected from the image database. The image which is given as input is STOP signal image which contains noise in it

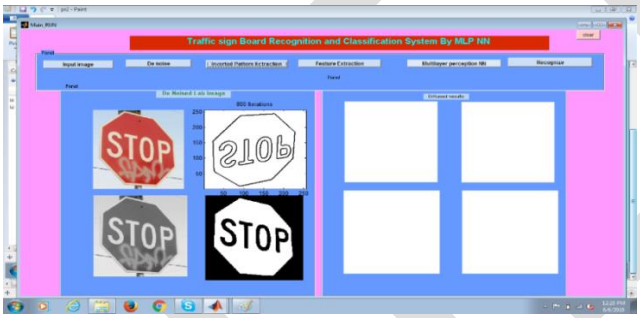

Fig 8 : Image preprocessing

Figure Perform the basic image processing operation from the given input image based on Training data set.

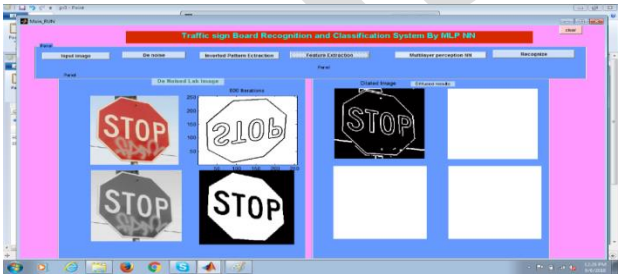

Fig 9 :Region based Feature Extraction

Figure shows, input image process the region based feature extraction and detects the boundaries of a given input image

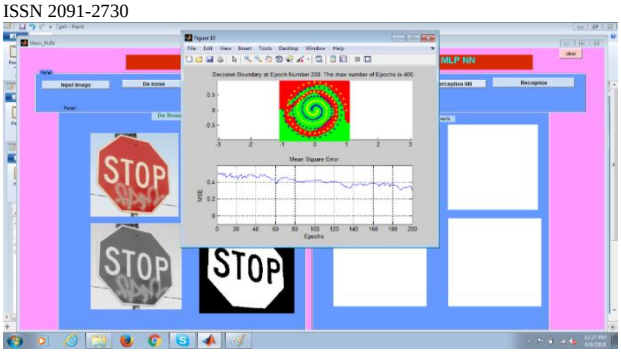

Fig 10: Image Color Band Labelling

Figure shows that preselected image pass the processed image set to the system and Image Labelling. Through this we get a least mean square error difference.

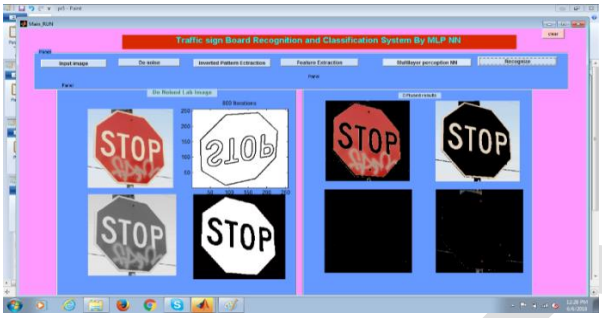

Fig 11: multilayer perception.

Figure shows that color and shape based feature extractions classify images by multilayer perception and recognition.

Fig 12 : Recognizing the type of the sign

CONCLUSION

The proposed system of multilayer perception for the Indian Road side Recognition and Classification has given the satisfactory results to the user. By using this system with the help of HSV color transformation the user can detect and classify the road sign images more accurately. This system which uses processing of road images has given accurate results, but the images have to be in the prescribed format ,with the help of processing method the system is capable of performing DE noising, reshaping, resizing type of basic image processing options.The feature extraction phase includes extraction of color and shape which can be used in the classification method .Future enhancement of the system is automatic video rendering and classification on road.Also need to include higher level of images and datasets in the system.

REFERENCES:

[1] S. Maldonado-Bascón, S. Lafuente-Arroyo, P. Gil-Jiménez, H. Gomez-Moreno, and F. Lopez-Ferreras, "Road-sign detection and recognition based on support vector machines," IEEE Trans. Intell. Transp. Syst., vol. 8, no. 2, pp. 264–278, Jun. 2007.

[2] H. Gomez-Moreno, S. Maldonado-Bascon, P. Gil-Jimenez, and S. Lafuente-Arroyo, "Goal evaluation of segmentation algorithms for traffic sign recognition," IEEE Trans. Intell. Transp. Syst., vol. 11, no. 4, pp. 917–930, Dec. 2010.

[3] A. Ruta, F. Porikli, S. Watanabe, and Y. Li, "In-vehicle camera traffic sign detection and recognition," Mach. Vis. Appl., vol. 22, no. 2, pp. 359–375, 2011.

[4] R. Kastner, T. Michalke, T. Burbach, J. Fritsch, and C. Goerick, "Attention-based traffic sign recognition with an array of weak classifiers," in Proc. IEEE Intell.Veh.Symp., San Diego, CA, USA, 2010, pp. 333–339.

[5] Y. Xie, L.-F.Liu, C.-H.Li, and Y.-Y. Qu, "Unifying visual saliency with HOG feature learning for traffic sign detection," in Proc. IEEE Intell.Veh.Symp., Xi'an, China, 2009, pp. 24–29.

[6] X. Yuan, J. Guo, X. Hao, and H. Chen, "Traffic sign detection via graphbased ranking and segmentation algorithms," IEEE Trans. Syst., Man, Cybern., Syst., vol. 45, no. 12, pp. 1509–1521, Dec. 2015.

[7] R. O. Duda and P. E. Hart, "Use of the Hough transformation to detect lines and curves in pictures," Commun. ACM, vol. 15, no. 1, pp. 11–15, 1972.

[8] G. Loy and A. Zelinsky, "Fast radial symmetry for detecting points of interest," IEEE Trans. Pattern Anal. Mach. Intell., vol. 25, no. 8, pp. 959–973, Aug. 2003.

[9] G. Loy and N. Barnes, "Fast shape-based road sign detection for a driver assistance system," in Proc. IROS, Sendai, Japan, 2004, pp. 70–75.[10] J. Greenhalgh and M. Mirmehdi, "Real-time detection and recognition of road traffic signs," IEEE Trans. Intell. Transp. Syst., vol. 13, no. 4, pp. 1498–1506, Dec. 2012.

[10] H. Li, F. Sun, L. Liu, and L. Wang, "A novel traffic sign detection method via color segmentation and robust shape matching," Neurocomputing, vol. 169, pp. 77–88, Dec. 2015.

[11] Stallkamp J., Schlipsing M., Salmen J., Igel C. "Man vs. computer: Benchmarking machine learning algorithms for traffic sign recognition" Neural Networks, Vol. 32, pp. 323–332, 2012.

[12] Fleyeh H., Dougherty M. "Road And Traffic Sign Detection And Recognition". Proceedings of the 16th Mini – EURO Conference and 10th Meeting of EWGT, pp. 644-653, 2007.

[13] Suzuki S., Abe K. "Topologival Structural Analysis of Degitized Binary. Images by Border Following CVGIP 30 1, pp. 32–46, 1985.

[14] Belaroussi R., Foucher P., Tarel J.P., Soheilian B., Charbonnier P.,Paparoditis N. "Road Sign Detection in Images". A Case Study, International Conference on Pattern Recognition (ICPR), pp. 484–488,2010.

[15] Houben S., Stallkamp J., Salmen J., Schlipsing M., Igel C. "Detection ofTraffic Signs in Real-World Images. The German Traffic Sign DetectionBenchmark".International Joint Conference on Neural Networks, 2013.

International Journal of Engineering Research and General Science Volume 6, Issue 4, July-August, 2018
ISSN 2091-2730

A FLYWHEEL ENERGY STORAGE SYSTEM INTEGRATED WITH PV FOR FRT SUPPORT OF GRID CONNECTED HVDC –BASED OFFSHORE WIND FARMS

[1]E.Damodar Reddy, PG Scholar, EEE, lakireddy Balireddy College of Engineering,

Email Id: erugala.damodarreddy@gmail.com

[2]Mr. J.V .Pavan Chand, Sr. Asst. Professor, EEE, lakireddy Balireddy College of Engineering ,

Email Id: pavanchand217@gmail.com

Abstract— For the sake of uninterrupted power supply (UPS) to the loads, here in this paper we are using the renewable energy source (RES).Among the RES, Photovoltaic and wind energy are most familiar and hence we are using both the energy source which comes under hybrid system or integrated system. The cause of using both the system is to meet the loads demand during off set of any one of the energy source where the balancing of power takes place. In addition to this we are also using a flywheel energy place storage system which is of large capacity and of low speed. It is a connected in shunt along with a VSC-HVDC which is present at grid side circuit based on squirrel cage induction motor. The VSC-HVDC transmission is chosen for the offshore wind farms. The main property of FESS is to absorb the excess amount of energy that reaches the load and also provision of the stored energy to the grid when there is a fault (or) when there insufficient amount of energy to meet the load demand at grid. From the above discussion it is clear that FESS is accomplished for monitoring of power (or) even out through normal and fault operating conditions. The outcomes for the projected system are attained by means of Matlab /Simulink during the normal and abnormal conditions.

Keywords— FESS, HVDC, Off Shore wind energy system integrated with PV, fault ride through system.

INTRODUCTION

Due to the random increase in population there is a greater degree of demand for electrical energy which tuned our interest towards the RES, Which are clean, pollution free and non-exhaustible. Generally there are three forms of RES. Among them solar and wind are very much familiar to the research and also to the power generator. The solar energy depends upon the temperature and irradiation of sun .Depending up on those two factors the energy will be generated. The solar cells are exposed to the sun for the generation of solar energy. Moving on to the wind energy the wind farms are installed onshore and off shore .The utilization of offshore wind farms is generally high because of high wind speed [1] when compared to on shore wind farms. The installation cost and maintenance of offshore wind farms is high when compared to the on shore wind farms and hence it is considered to be its limitation. Higher power transmission from offshore wind farms is a essential task. The transmission of higher voltage i.e. Dc (HVDC) for long distance from offshore wind farms is an substitute to ac communication. In general the HVDC system uses line-commutated converter (LCC) [2] which are appropriate for large power control request [3]. The LCC generates a large amount of harmonic and the conduction angle is dependent on non-unity displacement factor as there is large amount of harmonics, it requires filters at the ac side. The study of VSC based HVDC [2] was started by the developers in 1990. Moving on to the comparison between LCC HVDC, VSC-HVDC transmission has more and more benefits [3]-[4]. The VSC plays an vital role became the system stability depends upon the control of VSC ,which is a difficult task .the system stability in turn depends upon the transients and variations of ac systems. The deportment of ac system is considered as one of the vitiation under fault condition Even during(or) after the short circuit fault the wind farms need to be associated to meet the demand of grid [5]. Finally to make this clear FRT in VSC –HVDC for wind farms is necessary. There are many policies that takes place for FRT in VSC-HVDC in case of offshore wind system [4]-[5].

The utmost and the primary step is that, diminish the energy generated since by wind turbines. Basically here are two sorts of conditions to diminish the power that is produced by the wind turbine. Among them the first condition is to lower the torque of generator by controlling the frequency to be constant and useful active current component to be lower for the off shore converter [5]. Under this circumstance the diminishing of power generated by wind turbines is very slow and it's not adequate. The second condition is to obtain the grid frequency under that fault condition. The second strategy that exist for FRT VSC—HVDC is by creating or provision of short circuit at the offshore HVDC circuit in despite to stop the happening of onshore side near power spread. This can be done by diminishing the value of modulation index which in turn used to decrease the terminal voltage of offshore converter .even through there is a flow of high currents [6] across the converter which is consider to be its limitation. Ac side faults uses dc chopper along with the breaking resistor for avowing the igniting and power dissipation on dc side [6]-[7],which comes under third strategy. Among the mentioned strategies this is advantageous as it is reliable , but in accumulation to this the system price and energy losses increases. The above study

is made to obtain new fault ride through technique which is used to preserve the power during abnormal condition and also leveling of wind energy during and normal operation. The flywheel is nothing but the storage element which stores the energy in the form of kinetic energy resisting on the rotational speed and its mass. Therefore, from the above discussion we can say that FESS is surviving two basic needs which is nothing but balance of power during normal condition .from the above discussion we can say FESS acts as storage elements in addition to batteries and super capacitors . The performance of fess is similar to that of super capacitor .the life time and density of energy for charging and discharging is relatively high [8] to overcome the limitation of super capacitor [i.e. the cost for the energy stored in fess per kwh is less compared to super capacitor] we are going ahead for Fess. The foremost aim of the this report is employing a FESS for ac side faults ride through system, at grid side converter of VSC-HVDC transmission system. The Integration of FESS with PV for leveling and tracking of power during normal and abnormal conditions can be obtained through Matlab/Simulink software.

I. ILLUSTRATION OF THE PROPOSED SYSTEM

Despite of balancing the power during normal operation and tracking of the power during conditions the fess have high efficiency, low maintenance, simple in structure with high energy and power mass [9]. A fess eventually consists of flywheel, bearings, power convention system and an electrical machine [10]. As we know that kinetic energy is the products of mass and volume here the flywheel acts as a mass where the kinetic power is preserved to drive the electrical system. Hence the machine behave like a motorized during incriminating and as generator during discriminating. Generally the high speed flywheel are incorporated in permanent magnet machine [11] but Whereas the induction motor are incorporated with low speed flywheels [12]. For the sake of power conversion, the power electric circuits are employed at wind farms known as wind side converter along with flywheel in parallel to the system. Moving on to bearings they are used in all the machines for the free rotation of the motor. Basically here we are have two sorts of bearings such as conventional mechanical bearings and magnetic bearings. In conventional mechanical bearings the rotor is made up of steel which used for low speed application to increases the inertia which finally results in abundant fess but where as in the magnetic the rotor is composed of composite material [11] which is applied in high speed requirements.

II. OPERATION OF PROPOSED SYSTEM

Here in this proposed project flywheel energy storage of large capacity is used for little speed induction machine which is associated in shunt to the grid side circuit .The single line diagram of FESS integrated with PV and VSC-HVDC transmission system is represented in Figure 1. The operation of the single line diagram is as follows her the power production by wind farms is offshore power which uses the ac generators like double fed induction generators (DFIG) and permanent magnet synchronous generator (PMSG) which in turn this ac power is transformed to dc through the converter present at wind side. The dc energy produced by the offshore wind farms is conveyed to onshore system by converting that high dc level power into ac power by efficiently utilizing the grid side converter. The converted power can stay sustainable for high power applications, losses in power and the harmonic content present in the output [13]. The above discussed operation is similar to that of the batteries that were used in case of FESS [14].

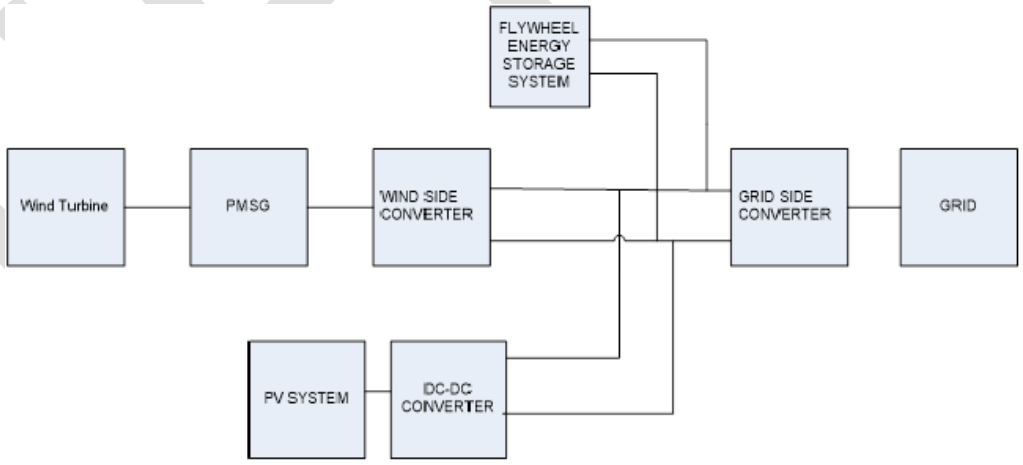

Fig 1. Single line strategy of planned system

The justification of the project is that both the wind energy and photovoltaic energy system are integrated with FESS. The integration of wind energy and Photovoltaic energy is to meet the demand at grid. For example if we consider only the wind energy (or) PV energy sometimes it is impossible to meet the demand at grid side even during the presence of flywheel In order to overcome that problem we are integrating both the energy system to meet the demand. If the generated energy by integrated systems is more (or) excess than the required demand at grid then the excess amount of energy is stored in fess which is connected in parallel with the wind side circuit. Apart from this the fess is also well known for leveling (or) balancing of power during normal condition. As discussed earlier that fess

stores the energy , stored energy is utilized during the fault condition in order to meet the demand at grid as it is necessary. During phase to ground short circuit faults which is considered to be a worst fault will takes place at the ac side will tend the energy to zero. Taking this circumstance into account it is important to design the fess converter as that of the ratings of wind farm to store , store the wind energy for the fault at ac side. Here a high power flywheel is direct through an induction machine for balancing of power conditioning applications even there is a presence of variation in the operating mode.

The induction machine and fess modeling is done using direct and quadrature frame is as follows

A) Modeling of induction machine and FESS using direct and quadrature frame:

The design of induction machine in d-q frame [7], and for FESS converter is illustrated in (1-7) mathematical equations.

The voltages at stator side are as follows.

$$v_{ds} = r_s i_{ds} + p\lambda_{ds} - w_e \lambda_{qs} \quad (1)$$

$$.v_{qs} = r_s i_{qs} + p\lambda_{qs} + w_e \lambda_{ds} \quad (2)$$

Since the overhead basic equation (1) and (2) we can obtain the torque and flux of stator as follows

$$P_s = \frac{3}{2}(v_{ds} i_{ds} + v_{qs} i_{qs})$$

$$= Pcu_{stator} + Pcu_{rotor} + Tm_{wm} \quad (3)$$

$$Q_S = \frac{3}{2}\left(v_{ds} i_{qs} - v_{qs} i_{ds}\right) = L_m w_e i^2{}_{ds} \quad (4)$$

$$T_m = \frac{3}{2}\frac{PL^2}{L_r} i_{qs} i_{ds} \quad (5)$$

$$P_{fw} = P_S \quad (6)$$

$$\lambda_s = L_m i_{ds} \approx \frac{V}{Ws} \quad (7)$$

B) Converter at grid side

The ac voltage of d-q frame which are fed to grid via grid side converter and power were as depicted below (8-10).

$$v_{dinv} = v_{dg} - r_g i_{dg} - L_g p i_{dg} - w L_g p i_{qg} \quad (8)$$

$$v_{qinv} = v_{qg} - r_g i_{qg} - L_g p i_{qg} + w L_g p i_{dg} \quad (9)$$

$$P_g = \frac{3}{2}(v_{dg} i_{dg} + v_{qg} i_{qg}) \quad (10)$$

Where, v_{inv}= Voltage across inverter

v_g= Grid voltage

δ =Grid angle

The total power that flows through the system is illustrated as

$$P_{fw} = P_s = P_{dc} - P_g \quad (11)$$

As there is a change in the energy that was stored in flywheel, it can be obtained as

$$\Delta E = \frac{1}{2} J(W^2{}_2 - W^2{}_1) = P_{fw} t_{disch} \qquad (12)$$

Where,

J = Moment of inertia for flywheel

W1,W2 =Initial and final speeds

t_{disch}=Discharging time of stored energy

We are well familiar to the power deposited in the capacitor as

$$E=\frac{1}{2} CV^2 \qquad (13)$$

Thus, From the equation (13) the voltage across the dc link is obtain as

$$V_{dc}(t) = \sqrt{\frac{2}{C}\int (P_{dc} - P_g - P_{fw})dt + c} \qquad (14)$$

The controlling of flywheel dc link power depends on the controlling of dc link voltage. Hence it is maintained constant

III. CONCEPT OF FAULT-RIDE THROUGH SYSTEM

Faults ride through system [FRT] is nothing but the system used to control the flywheel to operate during normal and fault condition. The flywheel drives the induction machine which depends up on the control indirect feed forward control [IFOC] [15].The basic sketch for the proposed fess based on IFOC is shown in Figure 2.

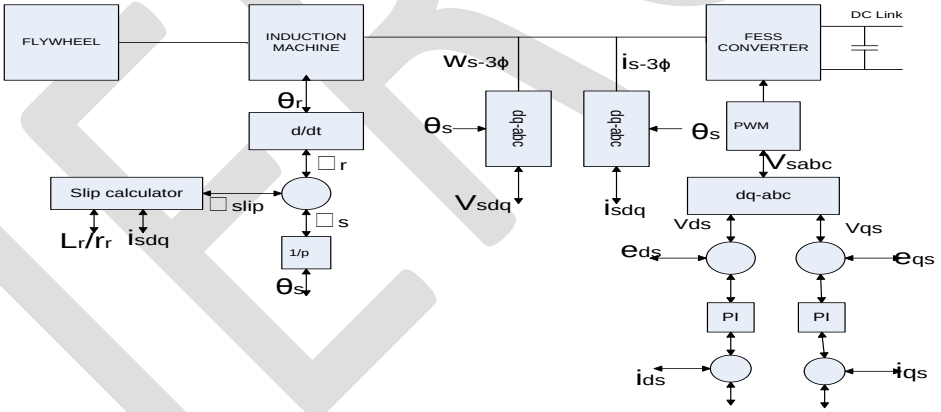

Fig.2 Sketch for proposed FESS based on IFOC

Figure 2 we can say that the dc link power sustains on the wind farm where in turn the fess control and grid side converter under normal operating condition control depends on dc link [16]. As we know that the flywheel has two conditions to be satisfied i.e balancing of power during normal operating conditions and control of dc voltage during faults conditions. The voltage control represents the controlling of torque component for quadrature axis current. The rating of machine [i.e voltage and current]are compared with the integrated power (PV, wind)and grid power to obtain the error which is applied controller in order to get the power across fess .The controller is PI controller as shown in Figure 3.

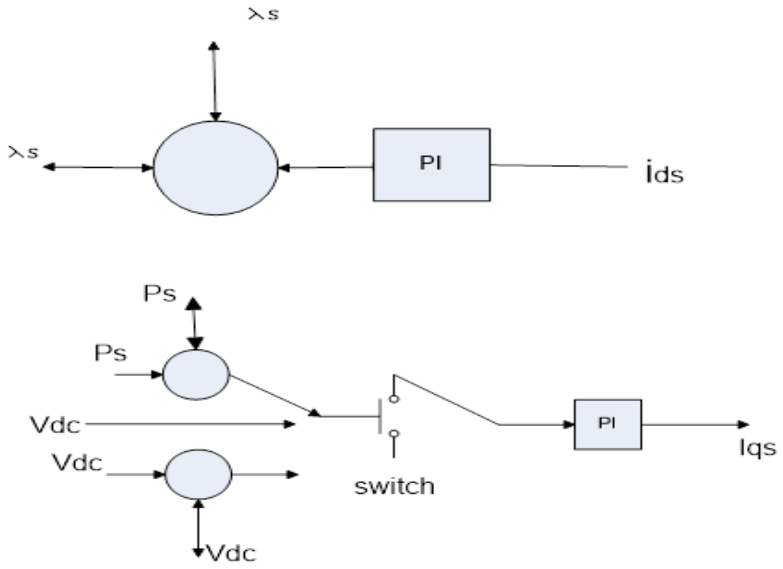

Fig. 3 Based on dc link voltage the switching between normal and abnormal conditions

IV. SIMULATION RESULTS

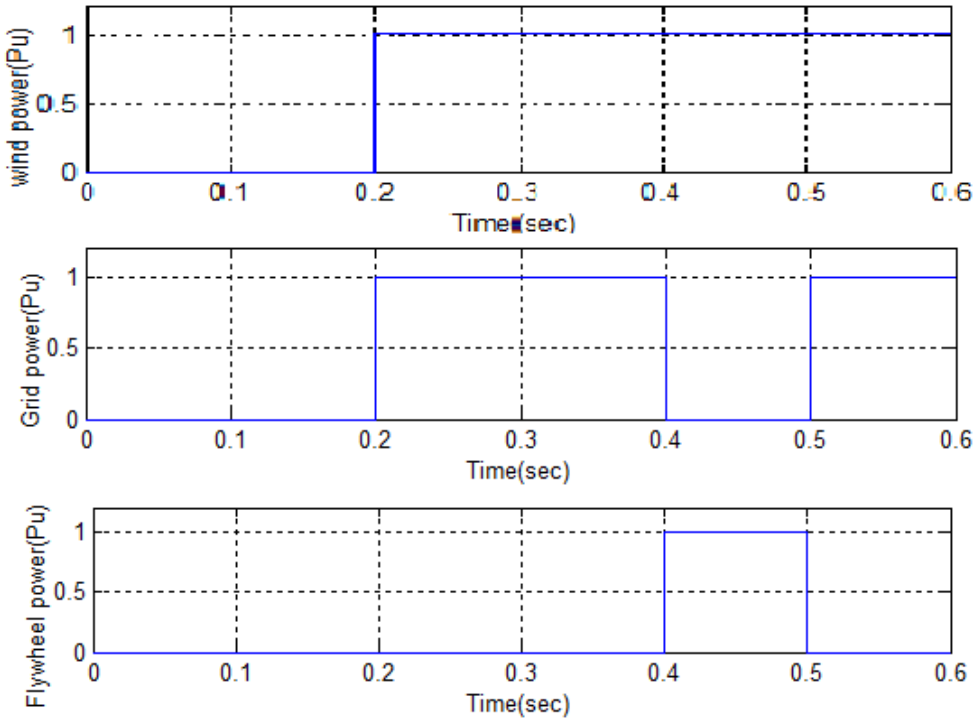

(a)Power profiles

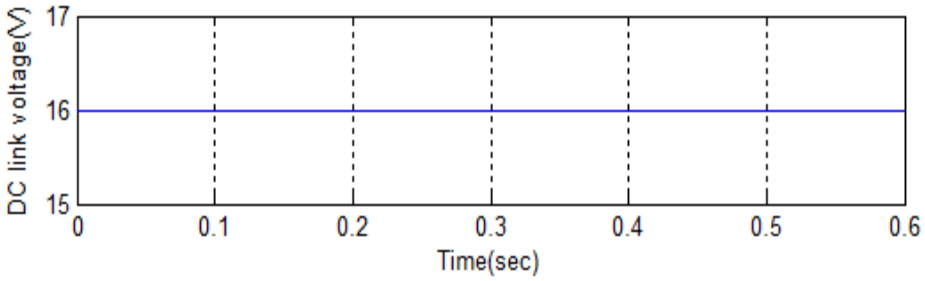

(b)DC link voltage

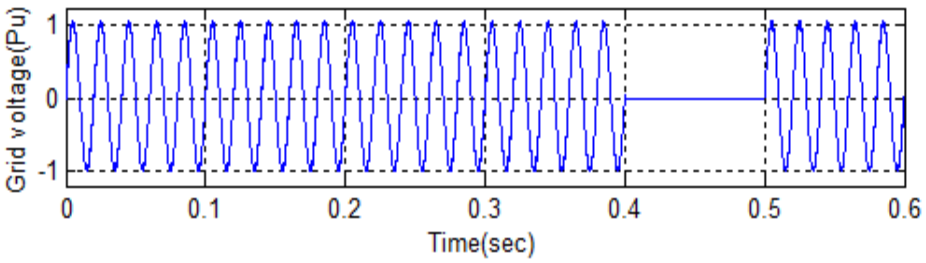

(c)Grid voltage

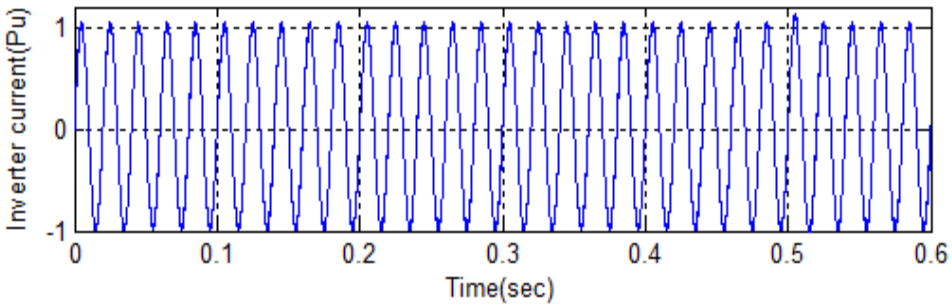

(d)Main inverter current

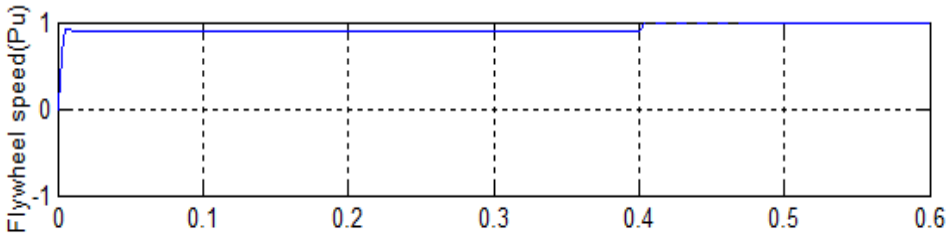

(e)Flywheel speed

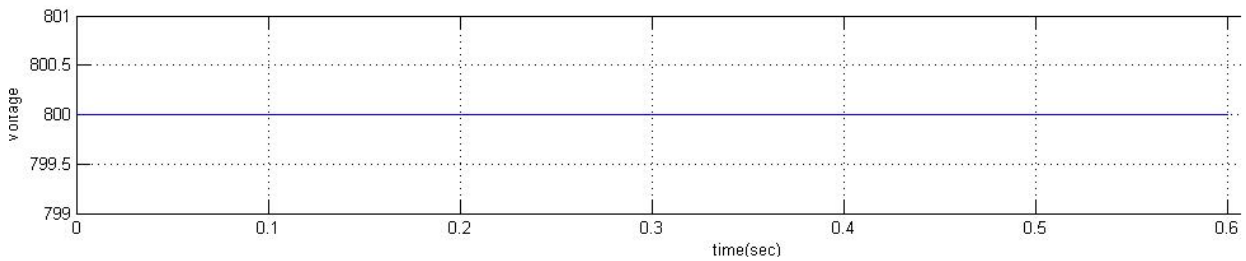

(f)Photovoltaic cell input energy

Simulation results when three phase to ground fault operation were considered (a)Power profiles(b)Dc-link voltage(c)Grid voltage(d)Main current of inverter(e)Speed of flywheel(f)PV cell input

V. CONCLUSION

An integrated system is used for meeting the requirement of demand at grid. Along with this integrated system a FESS is associated in shunt by a wind side converter which is driven by induction machine. Therefore, an integrated PV system along with fess is proposed in this paper in which the fess operates during the normal condition for balancing the power and discharging of power from fess the grid which was stored during normal condition.

REFERENCES:

[1] Rehana Perveen, Nand Kishor n , Soumya R. Mohanty., "Off-shore wind farm development: Present status and challenges," Renewable and Sustainable Energy Reviews, Vol. 29 , 2014, PP. 780–792.

[2] W. Long and S. Nilsson, "HVDC transmission: Yesterday and today," IEEE Power Energy Mag.,vol.5,no.2, pp. 22–31,Mar.–Apr.2007..

[3] **Alan Novak** "Ultra-High Voltage Transmission (UHV)–A New Way to Move Power", January 9th,2015under Power.. 2010

[4] Xiong guang Zhao, Qiang Song, Hong Rao, Xiaoqian Li, Xiaolin Li, and Wenhua Liu, "Control of Multi-Terminal VSC-HVDC System to Integrate Large Offshore Wind Farms," International Journal of Computer and Electrical Engineering, Vol. 5, No. 2, April 2013.

[5] A. Mullane, G. Light body, and R. Yacamini, "Wind-turbine fault ride through enhancement," IEEE Trans. Power Syst., vol. 20, no.4, pp. 1929–1937, Nov.2005. [6] S. K. Chaudhary, R. Teodorescu and P. Rodriguez, "Wind Farm Grid Integration Using VSC Based HVDC Transmission - An Overview," I Energy 2030 Conference, 2008. ENERGY 2008. IEEE,pp.1-7,2008.

[7] Ali Hagh ,Hamid Simorgh," Improving Fault Ride Through Capabilities For Offshore PMSG Wind Farms Connected To VSC-HVDC Transmission System". (February 2017), PP.14-24.

[8] S. Kim and S. Hahn, "Analysis and design of a induction generator with a superconducting bulk magnet rotor," IEEE Trans. Appl. Superconduct., vol. 10, no. 1, pp. 931–934, Mar. 2000.

[9] G. O. Cimuca, C. Saudemont, B. Robobyns, and M. M. Radulescu, "Control and performance evaluation of a flywheel energy-storage system associated to a variable speed wind generator", IEEE Trans. industrial electronics, vol.53, no.4, August 2006.

[10] Bitterly, J.G.; "Flywheel technology past, present, and 21st Century projections," Energy Conversion Engineering Conference, 1997. IECEC-97., Proceedings of the 32nd Intersociety, vol.4,no.,pp.2312-2315vol.,Aug1997…
[11] Lachs, W.R.; and Sutanto, D.; "Applications of Battery Energy Storage in Power Systems", IEEECatalogueNo.95TH8025,pp.700-705,.year.1995.

[12] M. Yamamoto and O. Motoyoshi, "Active and reactive power control for a doubly-fed wound-rotor induction generator," IEEE Trans. Power Electron., vol. 6, pp. 624–629, July 1991.

[13] F. Schettler, H. Huang, and N. Christl, "HVDC transmission systems using voltage sourced converters design and applications," in Proc. IEEE Power Eng. Soc. Summer Meeting, 2000, vol. 2,pp.715–720.

[14] S. Samineni, B.K. Johnson, H.L. Hess, and J.D. Law, "Modeling and analysis of a flywheel energy storage system for Voltage sag correction," IEEE Trans. Ind. Applicat., vol. 42, no. 1, pp. 42–52,Jan.–Feb.2006.

[15] R. Blasco-Gimenez, G. M. Asher, J. Cilia, and K. J. Bradley, "Field weakening at high and low speed for sensor less vector controlled induction machine," in Proc. IEE Int. Conf. PEVD, 1996,pp258–261. …

[16] L. Ran, D. Xiang, and J. Kirtley, "Analysis of electro mechanical interactions in a flywheel system with a doubly fed induction machine," IEEE Trans. Ind. Appl., vol. 47, no. 3, pp. 1498–1506, May/Jun. 2011.

International Journal of Engineering Research and General Science Volume 6, Issue 4, July-August, 2018
ISSN 2091-2730

DESIGN AND ANALYSIS OF MODULAR CASCADED H-BRIDGE MULTILEVEL INVERTER FOR MPPT BASED PV CONNECTED GRID APPLICATIONS

Sk. Nawaz shareef[1], G.Tabita[2]

[1]PG Scholar, EEE, lakireddyBalireddy College of Engineering,shareef.eee786@gmail.com

[2] Asst.Professor, EEE, lakireddyBalireddy College of Engineering

Abstract— this paper reports a modular cascaded H-bridge multilevel photovoltaic (PV) inverter for single- or three-phase grid-connected applications**.** The efficiency, flexibility and stability of the system has been increased and improved by the modular cascaded multilevel technique. The MPPT technique is used for both single and three phase multilevel inverters to essence extreme power energy from the PV segments, this MPPT technique is helpful for an individual control of each dc-link voltage. Due to the unbalanced power supply to the PV cells may lead to unbalanced grid current for three phase grid coupled applications. To overcome this problem in the three phase grid tied applications modulation compensation control technique is proposed .By using nine h-bridge modules, we can built a three phase seven level cascaded H-bridge inverter (three modules per phase). 185-W solar panel is tied to each h-bridge module. Simulation results are presented.

Keywords: Cascaded multi-level inverter, distributed maximum power point (MPP) tracking (MPPT), modular, modulation compensation, photovoltaic (PV)

INTRODUCTION

Due to the conventional power generation natural fuels consumption will reduce and climatically problems will increase. Geothermal power especially solar energy at present has turn into popular. The production of solar energy has been increased 20%-25% per Annam from the last 25 years and mostly the growth occurs in grid linked applications [1].The strange growth of market in PV systems the interest also increased for grid tied configurations. At fig1 five inverter families are shown to the separate formations of the PV system [2]-[7].

Several inverters are connected in series in cascaded inverters; due to combination of number of module inverters will give high power and high voltage. it will help in this scheme for small end bulky PV systems[8]-[10].which are connected to grid. 2 types of series inverters are present in this topology. The dc-dc converter association of PV segments are shown in fig.1 (e). This process combines the features of string inverters, ac-module inverters provides the advantages of individual segment MPPT, but it has lower and the efficiency is more than the ac module inverters[11]-[12].

But, in this configuration we have two power conversation phases. Additional series linked inverter is shown in fig. 1(f),it is also a dc to ac inverter, a PV panel is connected to it., then these inverters are joined in series to get high voltage level [13]. The benefits maintained by this cascaded inverter are of "per panel one converter," such as improved operation per PV module, the ability of merge the different source, and separation of the organization. In resulting, this dc/ac series connected inverters will eliminate the requirement of the dc bus and also the central dc/ac inverter, which improver's complete efficiency.

The integrated cascaded multilevel h-bridge inverter that needs an isolated dc source for each h-bridge. Independent voltage control is possible by the division of dc links in multilevel inverter. As a result, in each PV module individual MPPT control is achieved, and

maximum energy is gathered from the PV panels. Temporarily, the low cost and the modularity of multilevel converters will place them as primary aspirant for the following generation of capable, and dependable grid tied solar power electronics.

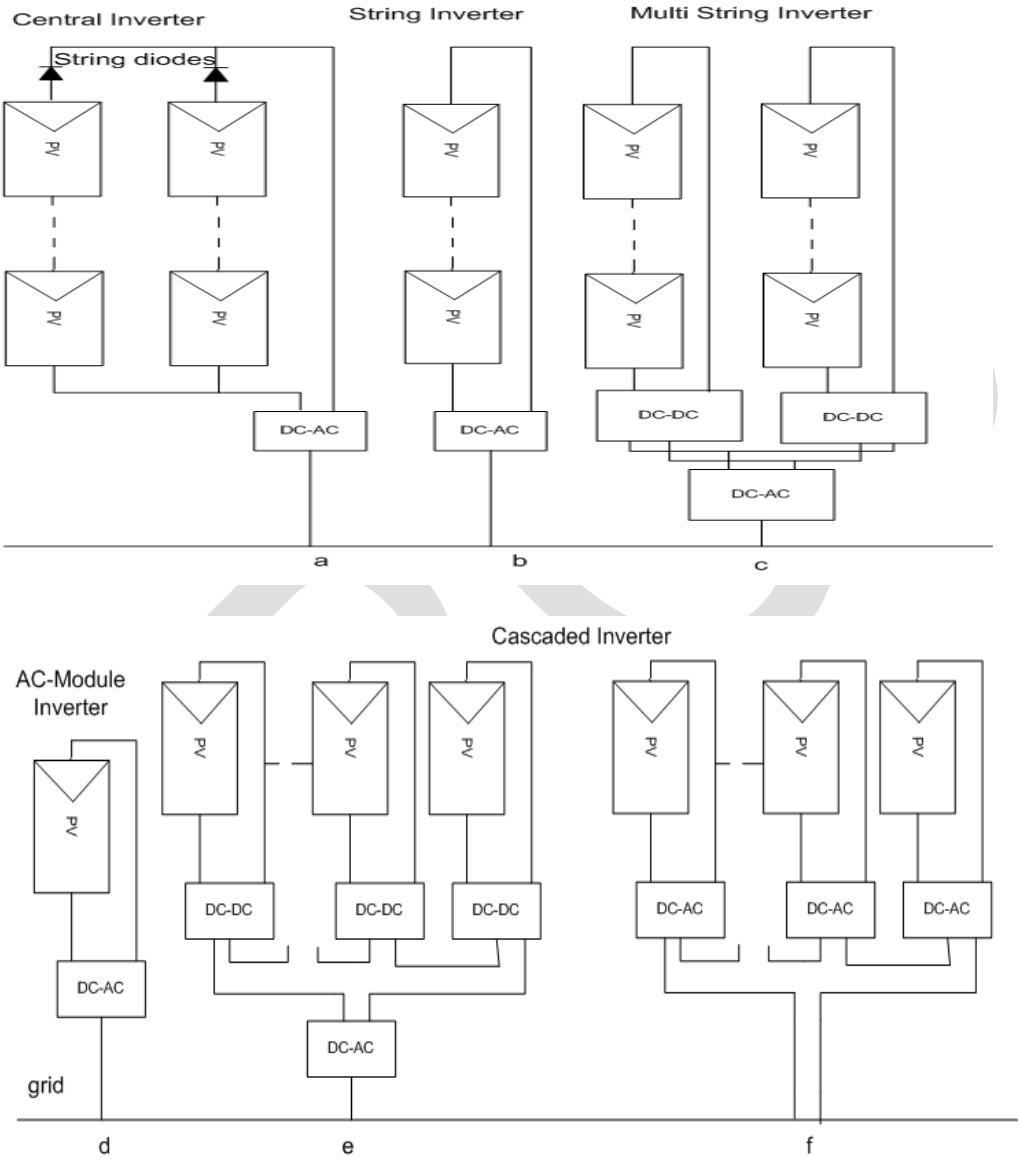

Fig. 1 PV systems configurations

In this project segmental series connected multilevel h-bridge inverter scheme for three phase or single phase grid tied PV system is offered. The panel different topics are shown to describe the requirement of independent MPPT control, and a distributed MPPT control through a control scheme is proposed. And this MPPT control technique is related to single phase as well as three phase systems. Further, individual PV segment is working at its MPP, for the offered three phase grid tied PV systems, unstable power is delivered to the three phase multilevel inverter due to the PV mismatches, leading to unbalanced injected grid current. The modulation compensation technique is additionally added to the control system to balance the three phase grid current. Modular series connected three phase multilevel inverter prototype has been assembled. 185-W solar panel is connected to each h-bridge. This modular design will reduce the cost as well as the flexibility of the system will also increase. And the model results are shown to describe the established control system.

II. EXPLANATION OF PROPOSED SYSTEM

In Fig. 2. Three phase and single phase grid tied PV schemes through modular series connected h-bridge multi-level inverters are shown. n H-bridge converters are tied in series. Through L filters series connected multilevel inverter is tied to the grid, it was used to remove the current harmonics. In each H-bridge module four switches are connected in different combinations, -vdc, 0, or +vdc are the three output voltage levels which are generated. In this type, from n input sources, 2n+1 ac output wave forms will generate. The other advantages of multilevel inverters such as reducing the voltage stresses on the semiconductor switches and it has high frequency

EXPLANATION

III. PANEL MISMATCHES

The significant matter in the PV scheme is PV mismatch. The MPP of individual PV module is diverse due to different temperatures, receiving of unbalanced irradiance and aging of PV panels. To get the better efficiency of PV system, we have to control each PV module independently. Five level two-H-bridge single-phase inverter is simulated in MATLAB/SIMULINK to show the necessity of the individual MPPT control.185-W PV panel is tied as an isolated dc source to each H-bridge. According to the requirement of industrial PV panel, PV panel is modeled from astrometry CHSM-5612M. let an working condition for the each PV panel having various irradiation conditions from the sun; let us consider panel 1 irradiance S = 1000 W/m2 and and panel 2 irradiance is S =600 W/m2. And if the panel 1 is traced and its MPPT controller decides the average voltage of both panels, the power outlet from both the panels P1 is 133W and P2 is 70W as shown in the Fig. 3. The total power harvested from the entire PV system is 203W without individual MPPT control.

PV variance may cause more difficulties in three phase grid tied PV system. By the introducing of unstable power supply to the 3 phase grid tied systems overall efficiency may decreases. Input power individual phase will be different if there are PV mismatches among the phases. Since unbalanced currents will formed in the grid due to the differences in input power but grid voltage is balanced. To resolve the PV mismatch issues, independent MPPT control and modulation compensation are suggested in this paper.

IV CONTROLTECHNIQUES

A. Distributed MPPT Control

To increase the effectiveness of a PV scheme and to remove the opposing effect of the misalliances the PV segments essential to work at various voltage levels to increase the consumption per PV segment. The individual voltage control is feasible by the isolated dc links in the series connected H-bridge multilevel inverter. To realize the each single MPPT control in each PV segment the control technique proposed is reorganized for this application. The three-phase cascaded H-bridge inverter of distributed MPPT control is shown in Fig. 5. An MPPT controller technique is added to produce dc-link voltage references in individual H-bridge module. Single dc-link voltage is matched to their equivalent voltage reference and to determine the current reference then sum of all the mistakes are measure over the voltage controller. The reactive current reference can be set to zero, Iq ref can also be assumed by a reactive current calculator. To find out the phase angle of the grid voltage the synchronous reference frame phase-locked loop (PLL) has been used. The grid currents in abc organizes are modulated to coordinates with the classic control system in three phase system and to produce the modulation index in the coordinates they are measured through proportional integral (PI) controller, which is then changed back to three phases.

For single phase system the distributed MPPT control technique is almost same. The magnitude of the active current reference values given by the total voltage controller, and phase angle and frequency of the active current reference value is provided by the phase-locked loop. Current control loop gives the value of variation index. To make every single PV module work on its own MPP the voltages v_{dca2} to v_{dcan} are managed independently through n-1 loops. In phase a modulation index proportion of single H-bridge module is given by voltage controller. Modulation indices can be acquire by multiplying modulation index of phase a and n-1. The control techniques are same for both b and c phases. Through PI controller, dc-link voltages are regulated. a phase-shifted sinusoidal pulse width modulation switching technique is used to command the switching devices of each H-bridge. Out of N modules there is only one H-bridge module whose modulation index is get by subtraction. The implementation and development of many MPPT techniques have done. We used incremental conductance technique is used in this project.

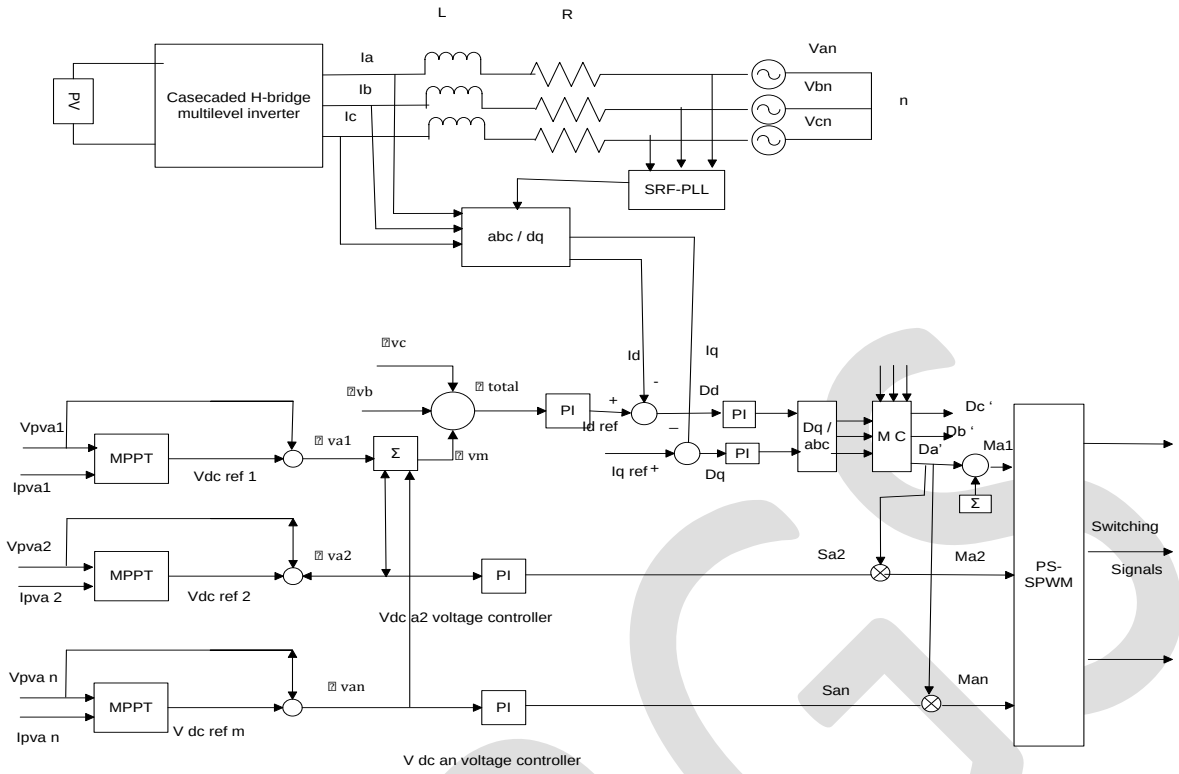

Fig. 3 three-phase modular cascaded H-bridge multilevel PV inverter

B. Modulation Compensation

PV problems may cause many troubles to a three-phase multilevel PV inverter, which brings unstable current to the grid. Zero sequence voltage is inflicting the phase legs in order to strike the current flowing in each phase. Unbalanced current is proportional to output phase voltages, to get the balanced current. Without increasing the difficulty of the control system is used to improve the modulation index of each individual phase. Is the ratio of unbalanced power weight .Where is the phase a, phase b, phase c input powers. The average output power is denoted by Then, a zero sequence modulation index is injected it will be

$$r_j = \frac{P_{inav}}{P_{inj}}$$

Where d_j*the modulation index of phase is* a, phase b, phase c. and these are decided by the current controller.

$$d_j' = d_j - d_0$$

In this scheme easy calculations are needed which are not increases the complications of the control system. To explain the modulation compensation technique, one example is presented in below figure. Here the input powers of each phase is assumed to be unequal.

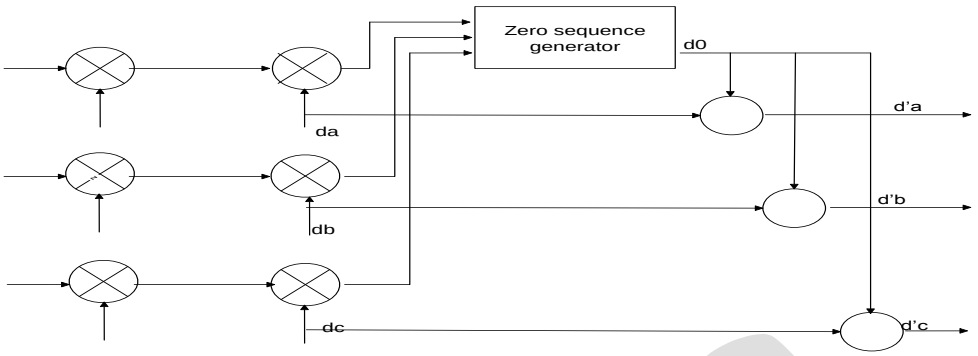

Fig. 4 Modulation compensation scheme

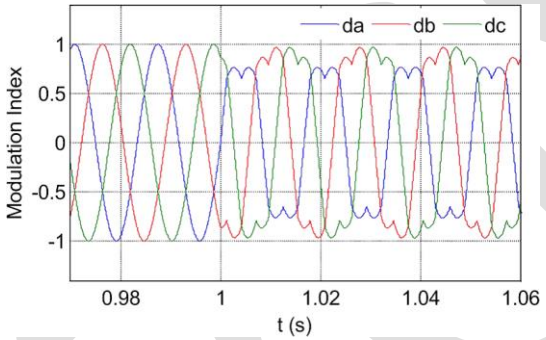

Fig. 5 before and after modulation compensation of modulation indices

V. SIMULATION RESULTS

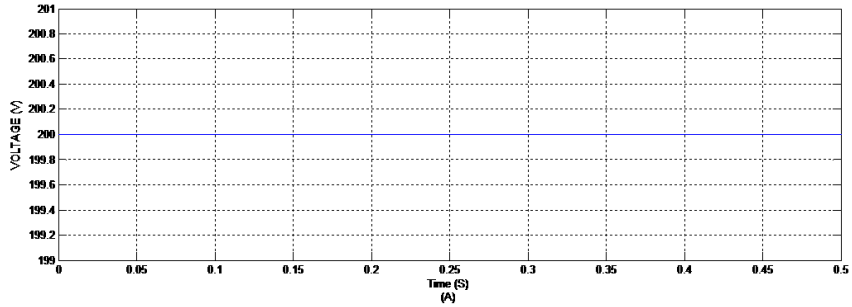

Fig 6. DC-link voltages

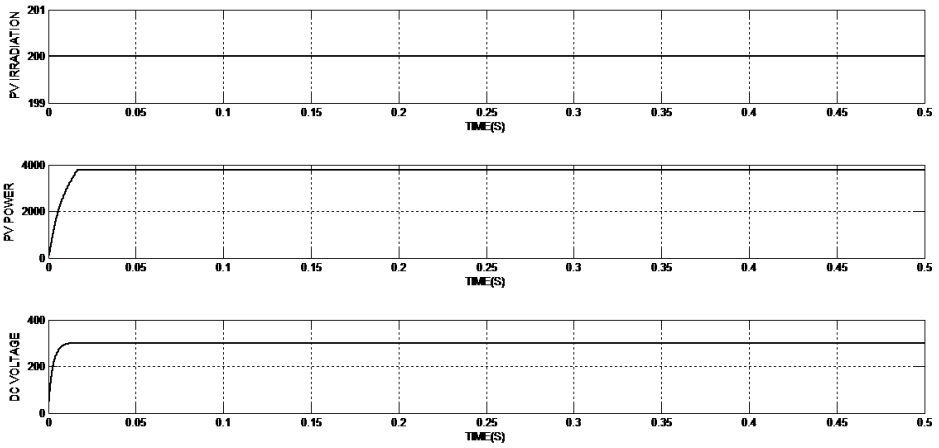

Fig 7. Power outlet from PV panels

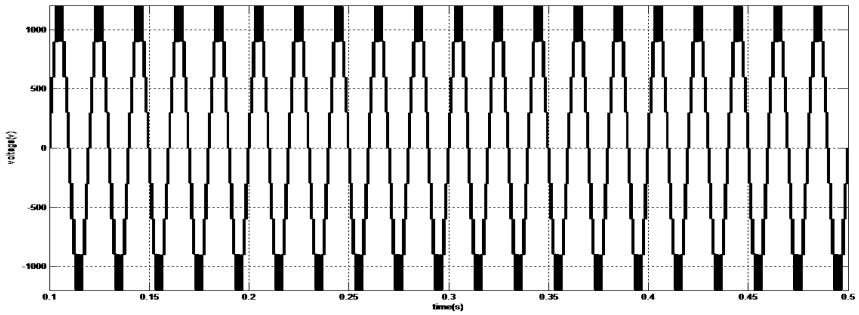

Fig 8. Phase A inverter output voltage waveforms

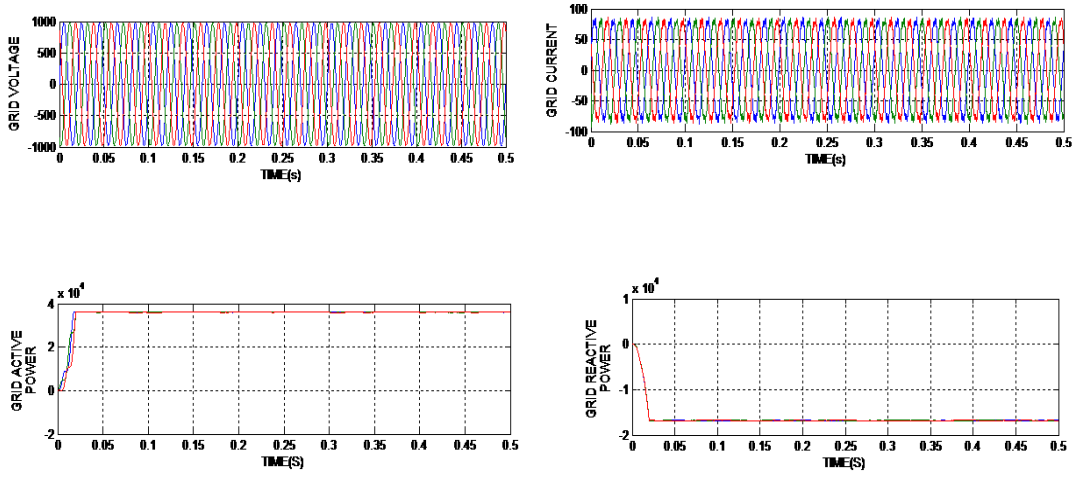

Fig 9. Power introduced to the grid connected PV system Vs Is PQ

VI. CONCLUSION

This project presents a modular cascaded h-bridge multilevel inverter for grid connected PV applications. Each dc link voltages are controlled individually. And PV module utilization will increases by the multilevel inverter topology. By adding the distributed MPPT control scheming for single and three phase PV system, the overall efficiency is increased. In three phase PV systems, PV mismatches may lead to cause unstable supplied power, which result in unstable grid current. So, a modulation compensation technique is used to balance the grid current. It will not increase extra power losses and the difficulty of the control system

REFERENCES:

[1] J. M. Carrasco *et al.*, "Power-electronic systems for the grid integration of renewable energy sources: A survey," *IEEE Trans. Ind. Electron.*, vol. 53, no. 4, pp. 1002–1016, Jun. 2006.

[2] S. B. Kjaer, J. K. Pedersen, and F. Blaabjerg, "A review of single-phase grid connected inverters for photovoltaic modules," *IEEE Trans. Ind. Appl.*, vol. 41, no. 5, pp. 1292–1306, Sep./Oct. 2005.

[3] M. Meinhardt and G. Cramer, "Past, present and future of grid connected photovoltaic- and hybrid power-systems," in *Proc. IEEE PES Summer Meet.*, 2000, vol. 2, pp. 1283–1288.

[4] M. Calais, J. Myrzik, T. Spooner, and V. G. Agelidis, "Inverter for singlephase grid connected photovoltaic systems—An overview," in *Proc. IEEE PESC*, 2002, vol. 2, pp. 1995–2000.

[5] J.M. A.MyrzikandM. Calais, "String and module integrated inverters for single-phase grid connected photovoltaic systems—A review," in *Proc. IEEE Bologna Power Tech Conf.*, 2003, vol. 2, pp. 1–8.

[6] F. Schimpf and L. Norum, "Grid connected converters for photovoltaic, state of the art, ideas for improvement of transformerless inverters," in *Proc. NORPIE*, Espoo, Finland, Jun. 2008, pp. 1–6.

[7] B. Liu, S. Duan, and T. Cai, "Photovoltaic DC-building-module-based BIPV system—Concept and design considerations," *IEEE Trans. Power Electron.*, vol. 26, no. 5, pp. 1418–1429, May 2011.

[8] L. M. Tolbert and F. Z. Peng, "Multilevel converters as a utility interface for renewable energy systems," in *Proc. IEEE Power Eng. Soc. Summer Meet.*, Seattle, WA, USA, Jul. 2000, pp. 1271–1274.

[9] H. Ertl, J. Kolar, and F. Zach, "A novel multicell DC–AC converter for applications in renewable energy systems," *IEEE Trans. Ind. Electron.*, vol. 49, no. 5, pp. 1048–1057, Oct. 2002.

[10] S. Daher, J. Schmid, and F. L. M. Antunes, "Multilevel inverter topologies for stand-alone PV systems," *IEEE Trans. Ind. Electron.*, vol. 55, no. 7, pp. 2703–2712, Jul. 2008.

[11] G. R. Walker and P. C. Sernia, "Cascaded DC–DC converter connection of photovoltaic modules," *IEEE Trans. Power Electron.*, vol. 19, no. 4, pp. 1130–1139, Jul. 2004.

[12] E. Roman, R. Alonso, P. Ibanez, S. Elorduizapatarietxe, and D. Goitia, "Intelligent PV module for grid-connected PV systems," *IEEE Trans. Ind. Electron.*, vol. 53, no. 4, pp. 1066–1073, Jun. 2006.

[13] F. Filho, Y. Cao, and L. M. Tolbert, "11-level cascaded H-bridge grid tied inverter interface with solar panels," in *Proc. IEEE APEC Expo.*, Feb. 2010, pp. 968–972

International Journal of Engineering Research and General Science Volume 6, Issue 4, July-August, 2018
ISSN 2091-2730

FOT CONTROLLED BUCK CONVERTER BASED GRID INTEGRATED SCHEME USING PV SYSTEM

[1]A.Sharmila Begum, PG Scholar, EEE, Lakireddy Balireddy College of Engineering,

Email Id: abdulsharmila9@gmail.com

[2]Mr. P. Deepak Reddy, Assoc. Professor, EEE, Lakireddy Balireddy College of Engineering,

Email Id: pdeepakr@gmail.com

Abstract— Variable frequency voltage based control technique which includes constant- on time (COT) and fixed-off time (FOT) are well suited for wide applications which require fast transient response. In this paper the operation of fixed off -time controlled dc-dc buck converter can be studied in three switching states which includes five operating modes. Here the equivalent or effective series resistance is also taken into consideration because the value of ESR should in permissible limits. Generally the value of ESR should lie in the range of 0-1Ω. Due to improper selection of ESR value of the controlled dc-dc buck converter mode shifting criteria takes place which can be further removed by selecting the suitable ratings of load resistance, inductance values. The behavior of this controlled buck converter with a sudden change in load is also exhibited in this paper. The simulation results for different values of inductance (L), load resistance (R) and effective series resistance ESR (r) and a step change in load are depicted which are obtained using MATLAB SOFTWARE. Here we are using this FOT controlled buck converter for photovoltaic energy generation concept which includes the grid connected system. The simulation results of grid connected PV system using FOT controlled dc-dc buck converter are also shown in this paper.

Keywords— Equivalent series resistance (r), FOT controlled buck converter, PV energy generation concept

INTRODUCTION

Among the chopper control techniques variable frequency control technique [1] has fast transient response and the controlling design is also simple and easy. The operation can also be easily understood. So due to the above advantages the variable frequency operation of choppers have gained large popularity which includes constant-on time control technique [2]-[3] and fixed-off time control technique [4]-[5]. When there is a variation in on-time [T_{on}] then the off-time [T_{off}] is kept constant or fixed and vice-versa. Here in this project we are keeping or maintain the off-time of the dc-dc buck converter to be constant.

Before the operation of fixed-off time dc-dc buck converter the design of filters should be taken into consideration as it plays a vital role in selection of its parameters. Hysteretic control [6]-[7] is also one of the technique among the variable frequency operation technique which have gained more popularity. For the above discussion we can say that the variable frequency control of dc-dc buck converter is quite suitable for its controlling [8]. In this paper we are discussing about the FOT control technique in order to overcome the disadvantages of constant on-time and hysteretic control techniques. The drawbacks of COT and Hysteretic techniques of variable frequency technique were, in COT control the on-time of the switch will be more in which it reduces the life span of the switch and hence the output voltage also decreases than required i.e. the efficiency of the converter will go down. Whereas in case of Hysteretic control it requires two comparators in order to compare the higher level i.e. the output voltage with the lower voltage which is nothing but the reference voltage which increases the cost of the circuit. Therefore, the above limitations are the advantages of the fixed off time buck converter.

From the above discussion it is very clear that we have concentrated more on the variable frequency control technique so we need to know the difference between conventional PWM dc-dc converters and the above mentioned technique. The main difference between them is that the variable frequency control technique depends on the effective series resistance of capacitor output [9] but whereas conventional dc-dc converter does not. During the hardware experiments the value of the ESR of output capacitance should be measured using the ESR meter as it plays a vital role in the circuit. For example if the capacitor with small ESR is chosen such as ceramic capacitor [10] as the output capacitance of buck converter then the inductor current phase may lead behind the phase voltage of output [11]-[12] resulting in the converter to operate in discontinuous mode of operation. All the above discussion is to say that the large ESR of output capacitance is essential to maintain variable frequency controlled buck converter to operate in stable state [5]-[13]. Otherwise the converter operates in unstable state. The above suggestions are very much needed for the design of variable frequency control dc-dc buck converter.

We are also going to discuss about the photovoltaic energy system because our main motive is the grid connected PV system using dc-dc converter. Renewable energy sources play a salient role due to increase of demand for energy. This increase in demand is due to the cause of increase in population. Solar, wind, hydro are the three different types of energy sources which are familiar to the people.

These energy sources do not exhaust. They are pollution free energy sources. Among the above three energy sources we are using the PV energy i.e. Solar energy which depends on the temperature and irradiation of heat. In order to create the interconnection among the PV system and the grid any of the switched mode power circuits need to be developed which is nothing but the fixed off-time controlled buck converter.

I. VARIABLE FREQUENCY FOT CONTROL FOR BUCK CONVERTER

A.Circuit Description

The FOT controlled buck converter essentially consists of source voltage V_s, power electronic switch S, diode D, inductor L, output capacitance C, output capacitance ESR and load resistance R. All the above elements are similar to that of a normal buck converter except the ESR. In addition to this variable frequency control technique also consists of a comparator which is used to compare the output voltage with the reference voltage in order to provide a gating signal. By fulfilling the above components a circuit is depicted in Fig. 1 [10] and the circuit configurations are as shown in table-1.

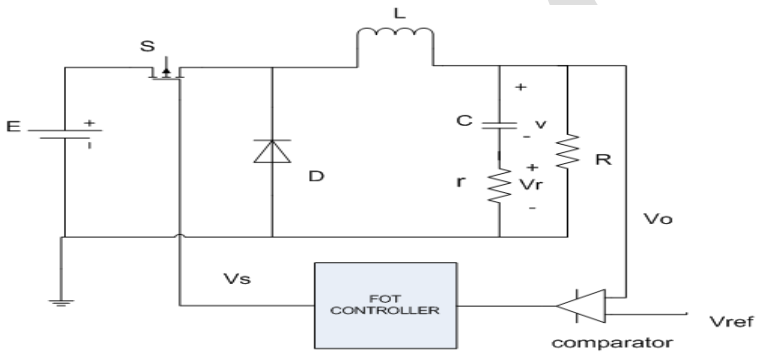

Fig.1 Variable frequency FOT controlled dc-dc buck converter

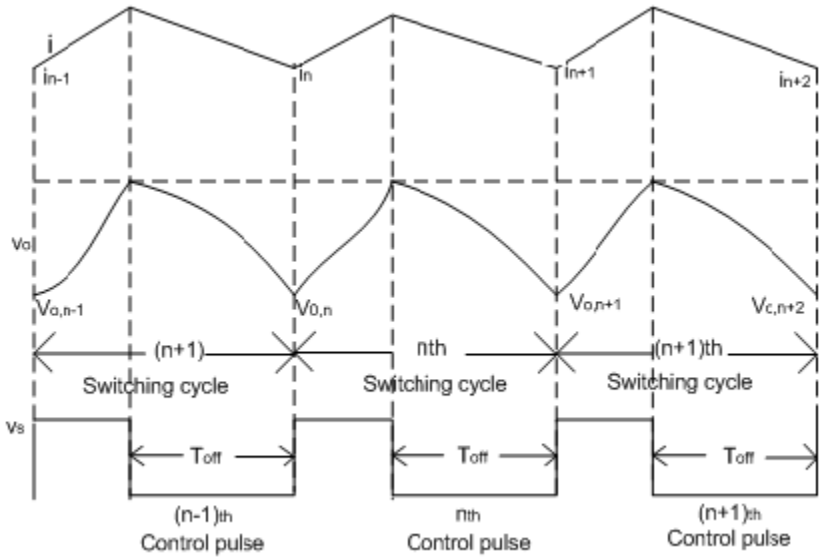

Fig.2 Waveforms of FOT controlled buck converter in continuous conduction mode

The waveforms depicted in Fig. 2 are related to the proposed converter operating in normal state. The operation of FOT controlled buck converter is similar and easily understood as that of the normal buck converter operating in continuous conduction mode. When the ESR of output capacitance is taken into account then the output V_o for the proposed buck converter shown in Fig1 can be derived and written as follows.

$$V_o(t) = r\, i_1 \qquad (1)$$

$$\text{Where } i_1 = i(t) - V_o(t)/R \qquad (2)$$

Now substitute the equation (2)in equation (1) to obtain the output voltage and is given as

$$V_o(t) = r\,[i(t) - V_o(t)/R] + V(t) \quad (3)$$

By rearranging equation (3) the output voltage is written as

$$V_o(t) = [r\,i(t)R + V(t)]/(R+r)$$

Let $R/(R+r) = k$

Therefore finally $V_o(t) = Hx = k[ri(t) + V(t)]$ (4)

$H = [kr \;\; k]$; $x = [i(t) \;\; V(t)]$

For the operation of FOT controlled buck converter two conditions should be taken. Such as the value of ESR is small which can be neglected i.e. r =0 then $V_o(t) = V(t)$. This indicates that the output voltage variation is completely dominated by the capacitor voltage resulting in instability. The other case is if the load resistance R = ∞ Ω then the converter operates in discontinuous mode of operation.

B. Operation Of The Proposed Converter

The operation of the proposed converter depends upon the state of switch S and the diode D. The operation can be described with three switching states which includes five operating modes. As we are having a comparator in Fig.1 it compares the output voltage with the reference voltage. When the reference voltage V_{ref} is less than $V_o(t)$ the output voltage, then the switch S will be in OFF state S_{off} and diode is in ON state D_{on}. During this interval the inductor current $i_L(t)$ discharges through the diode D. When $i_L(t)$ reaches zero then the diode is in OFF state (D_{off}) which leads the converter to operate in discontinuous mode of operation. If not, the converter will undergo the CCM operation. Similarly when the output voltage $V_o(t)$ is beneath the reference voltage V_{ref} then the switch will be in ON state and the diode will be in OFF state. Therefore, the switching states of proposed controlled buck converter can be judged as

$$V_o(t) = V_{ref} \text{ or } i(t) = 0$$

Three switching states or conditions are observed in one switching cycle depending upon the state of switch S and diode D. They are

Condition 1: Switch S ON; Diode D OFF
Condition 2: Switch S OFF; Diode D ON
Condition 3: Switch S OFF; Diode D OFF

The main theme of buck converter is to obtain the constant output voltage with the converter operating in CCM. Here in this proposed converter during the mode of CCM the switch conditions 1 and 2 exists which means the condition 3 does not takes place.

Depending upon the conditions of the switch the state space equations of the proposed fixed off-time dc-dc buck converter can be gleaned as follows.

The five operating modes of fixed off-time of variable frequency operation for buck converter were as follows.

Mode 1: During mode 1 the switching state conditions 1 and 2 takes place and the state space equations can be developed from the main equation i.e. equation (5). The waveforms are shown in Fig. 3(a).The output voltage during this mode of operation can be obtained from equation (4) as

$$v_o(t_1) = Hx(t_1) = k\,[v(t_1) + ri(t_1)] = V_{ref} \quad (6)$$

Mode 2: In this mode of operation all the three switch conditions takes place. Here the current during the time interval t_2 is zero as shown in Fig. 3(b) i.e. $i(t_2) = 0$ and the output voltage during this mode of operation can be obtained similar to that of mode1.

Mode 3: Here in this mode of operation only one switch condition takes place which is nothing but the condition 2 which means the switch S is in OFF state and the diode D is in ON state. In this mode of operation the converter under goes the continuous conduction mode as the inductor current (i) is greater than zero as shown in Fig. 3(c). The output voltage during this mode of is

$$v_o(t_3) = i(t_2)T_{off}x_m \quad (7)$$

Mode 4: During mode 4 the switch conditions 2 and 3 takes place in one cycle of switching. Here in this mode the output voltage is surpassing than the reference voltage and the current and the current i drops to zero as depicted in Fig. 3(d). The output voltage is uttered as

$$v_o(t_4) = i(t_3)\, v_o(t_3)x_m \quad (8)$$

Mode 5: The switch condition 3 only exits in this mode which means both the diode and the switch are in OFF state. Therefore, the current through the inductor is zero during this mode. The output voltage is as follows and the waveforms were as in Fig. 3(e).

$$v_o(t_5) = i(t_3)T_{off}x_m \quad (9)$$

The waveforms of variable frequency FOT controlled dc-dc buck converter for different values as tabulated in table-2 which include load resistance (R), inductance (L), effective series resistance (r) are shown in Fig. 6 and also the waveforms for table-3 which include a change in source (E) were depicted in Fig. 7 of section- 3.

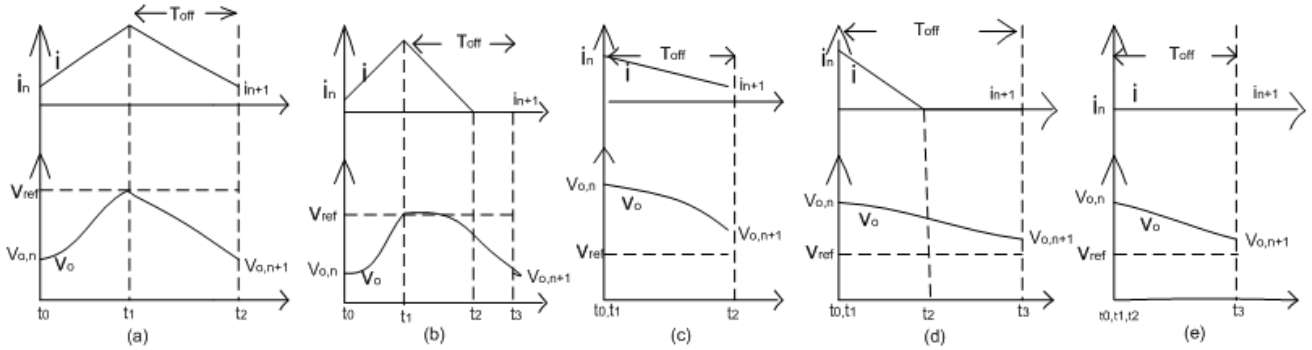

Fig. 3 Modes of operation (a) mode 1: $V_{0,n} \leq V_{ref}$, i > 0 (b) mode 2: $V_{0,n} \leq V_{ref}$, i becomes zero
(c) mode 3: $V_{0,n} > V_{ref}$, i > 0 (d) mode 4: $V_{0,n} > V_{ref}$, i falls to zero (e) mode 5: $V_{0,n} > V_{ref}$, i equals to zero .

C. Introduction And Design For ESR Of Output Capacitance

ESR is nothing but the effective or equivalent series resistance of the capacitors. Before going through the operation of converter one need to pay attention towards the ESR of capacitance as it effects the efficiency and usage of power. Among the non-ideal characteristics of a capacitor ESR is one which plays a vital role in the performance of or in the operation of switched mode power electronic converters. A high value of ESR leads to noise, a large voltage drop and I^2R losses. The heat generated due to ESR of capacitance is low in some cases which is not necessary to be taken into consideration. Without knowing the value of ESR if it is used in portable applications then the heat dissipated will be more which leads to high I^2R losses and hence the efficiency of the device will degrade. In general an ESR meter is used to obtain the value of capacitor in case of hardware experiments. But here we are depending upon the ripple content of output capacitor [3].

$$\frac{d}{dt} V_{ESR} \; / \; t = nT_S = \frac{d}{dt} R I_{ESR} \qquad (10)$$

From Fig. 1, $I_{ESR} = i_L - i_o$ (11)

By substituting equation (10) in (11) and by derivating it we get

$$V_{ESR} = R_{ESR}\left(\frac{Vin}{L} - \frac{Vo}{L}\right)$$

$$= - R_{ESR} \frac{Vo}{L} \qquad (12)$$

Similarly, $\frac{d}{dt} V_{C\_ripple} \; / \; t = nT_S = i_L - i_o/C$

$$V_{C\_ripple} = \frac{-Vo}{2LC} T_{off} \qquad (13)$$

By equating (12) and (13) we get

$$R_{ESR} = \frac{Toff}{2C} \qquad (14)$$

From the above equation we can obtain the value for effective series resistance.

II. GRID CONNECTED PHOTOVOLATIC SYSTEM FOR FOT CONTROLLED BUCK CONVERTER

A. Introduction

The single line diagram for grid connected photovoltaic energy system for variable frequency FOT controlled buck converter is as shown in Fig.4. In order to have a interconnection between PV and grid system we are using a FOT controlled technique for buck converter instead of using MPPT technique.

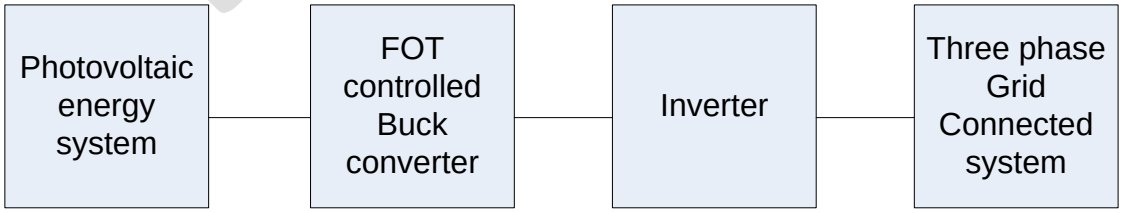

Fig. 4 Single line diagram

Fig. 4 essentially consists of PV energy system, FOT controlled buck converter, inverter and a grid system[2]. In section 2 we have discussed briefly about the FOT controlled buck converter. So in this section let us overcome across photovoltaic module, inverter and the three phase grid.

B. Photovoltaic energy system

RES are non-exhaustible sources and are pollution free. PV energy source is one among the renewable energy sources (RES). Solar panel is the heart of photovoltaic system. It provides the necessary information of PV cells whether they are connected in series or shunt. As we know that PV cells depends on the temperature and irradiation of sun, it converts the solar power into electrical power when there is an interaction between sunlight and the semiconductor materials in the PV cells. Single diode or one diode technique equivalent circuit of PV system is shown in Fig. 5. An array is formed by connecting the cells in series and parallel with desired voltage and power. All the cells together constitute a module to get the required voltage and current in turn power.

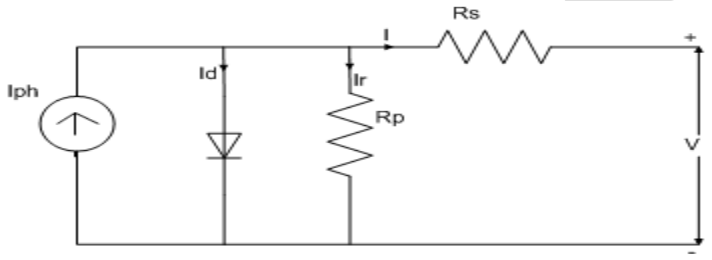

Fig. 5 Equivalent circuit of PV system

Here in this project an inverter is used to convert the DC power coming from the FOT controlled buck converter to required ac power which is the main theme of an inverter. An inverter fundamentally consists of six power electronic switches which are termed as S1-S6. The upper arm of the circuit consists of odd number of switches but whereas the lower arm consists of even number of switches. Each switch conducts for a period of 60^0. The pure sinusoidal alternating current can be obtained from the inverter by proper conduction angle or firing angle of switch or the proper control of ON and OFF of switch. An sinusoidal signal is taken as the reference signal and triangular waveform is chosen as carrier signal. The sequence of switch depends upon the comparison of magnitude of the sinusoidal and triangular waveforms. When the reference signal amplitude is more than the carrier signal then the corresponding upper arm switch will be in conduction.

The three phase ac output power is given or provided to the grid finally.

III. SIMULATION RESULTS

A. Specifications

The project is carried out using MATLAB software. The specifications of parasitic elements used in the converter is given below in Table 1.

Input voltage, E	15V
Reference voltage, V_{ref}	5V
Inductance, L	25Uh
Capacitance, C	100Uf
Output capacitance esr, r	12mΩ

Load resistance, R	10Ω
Fixed off-time, T_{off}	4us

Table-1: Specifications of FOT controlled buck converter

FOT controlled buck converter operation can be studied and understand by the change in parameters of load resistance R, inductance L, output capacitance resistor r, supply voltage E as tabulated in Tables-2 and 3 and the waveforms corresponding to Table-2 are as in Fig. 6 and that of Table-3 are shown in Fig. 7.

a	R = 10Ω, L = 25Uf, r = 12mΩ
b	R = 10Ω, L = 25Uf, r = 24mΩ
c	R = 10Ω, L = 12.48Uf, r =18.6mΩ
d	R = 6Ω, L = 12.48Uf, r = 21.4mΩ
e	R = 6Ω, L = 28.8Uf, r = 14mΩ
f	R = 15Ω, L = 28.8Uf, r = 18mΩ
g	R = 20Ω, L = 20Uf, r = 6mΩ
h	R = 500Ω, L = 20Uf, r = 6mΩ

Table-2: Change in circuit parameters of FOT controlled buck converter

a	E = 3.3V, r = 3mΩ
b	E = 3.3V, r = 6mΩ
c	E = 6V, r = 6mΩ
d	E = 6V, r = 12mΩ

Table-3: Change in source voltage and ESR

B. Simulation Results of FOT controlled buck converter

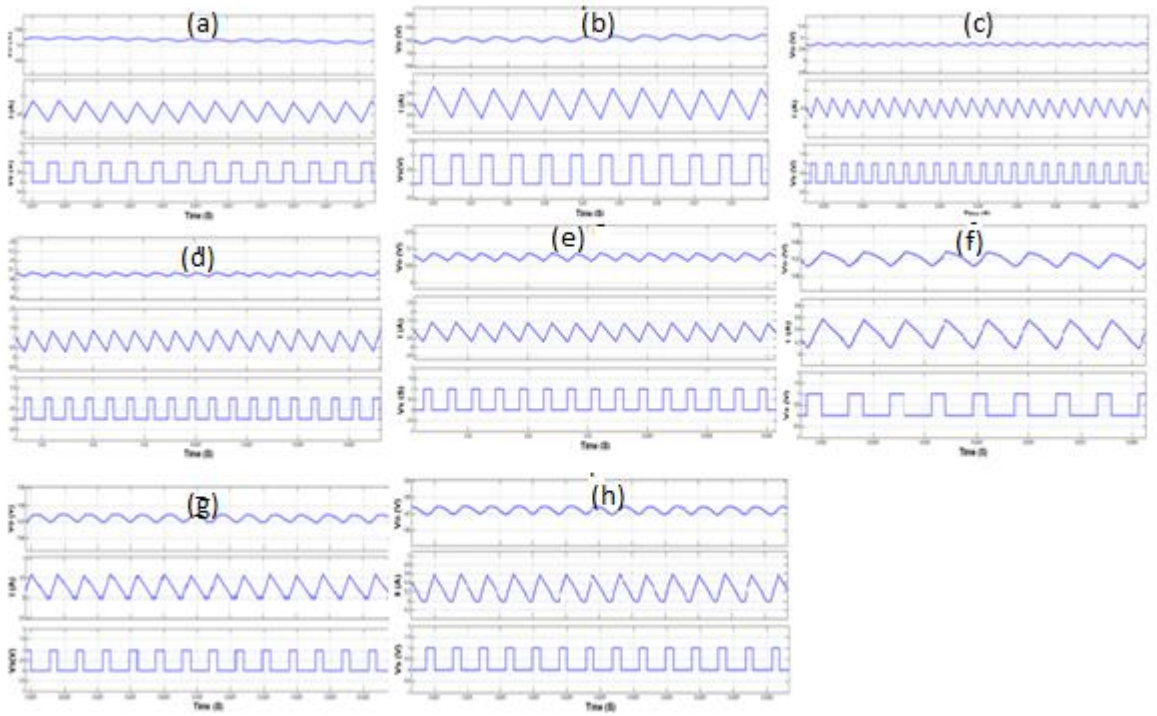

Fig. 6 Simulation results for parameters listed in Table-1 and Table-2

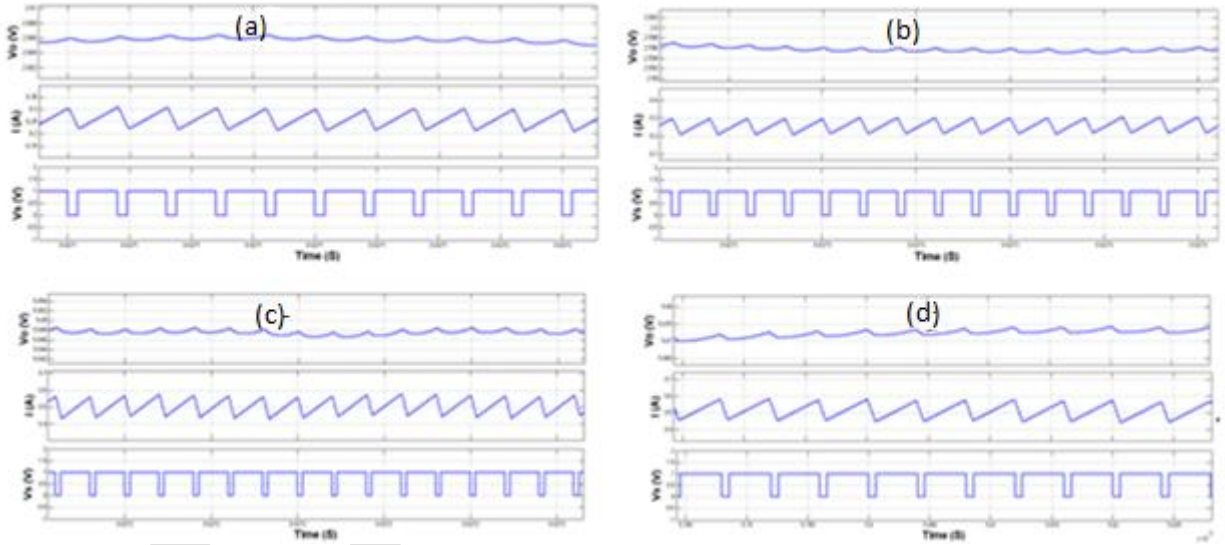

Fig. 7 Circuit simulation results for parameters listed in Table-1 and Table-3

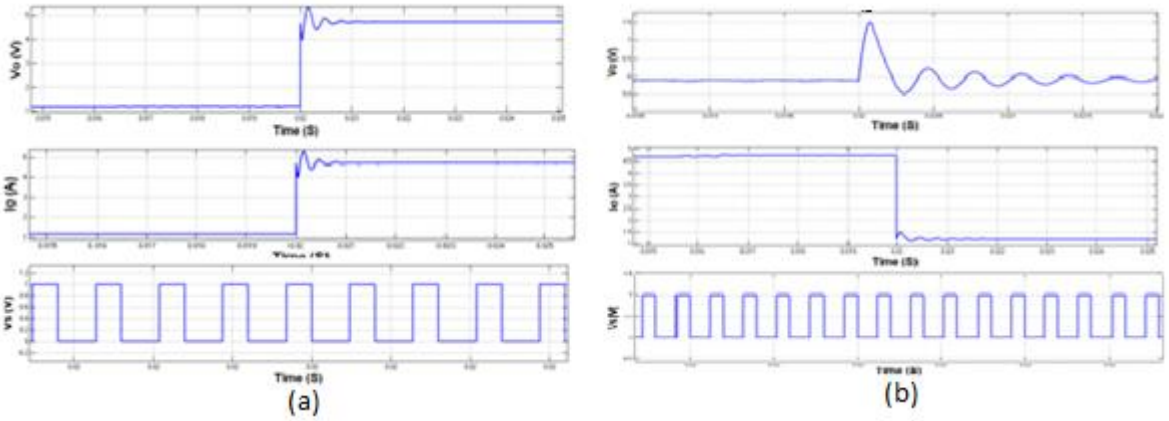

Fig. 8 Results for change in load when L = 10uH, r = 24mΩ and the other specifications as in Table-1

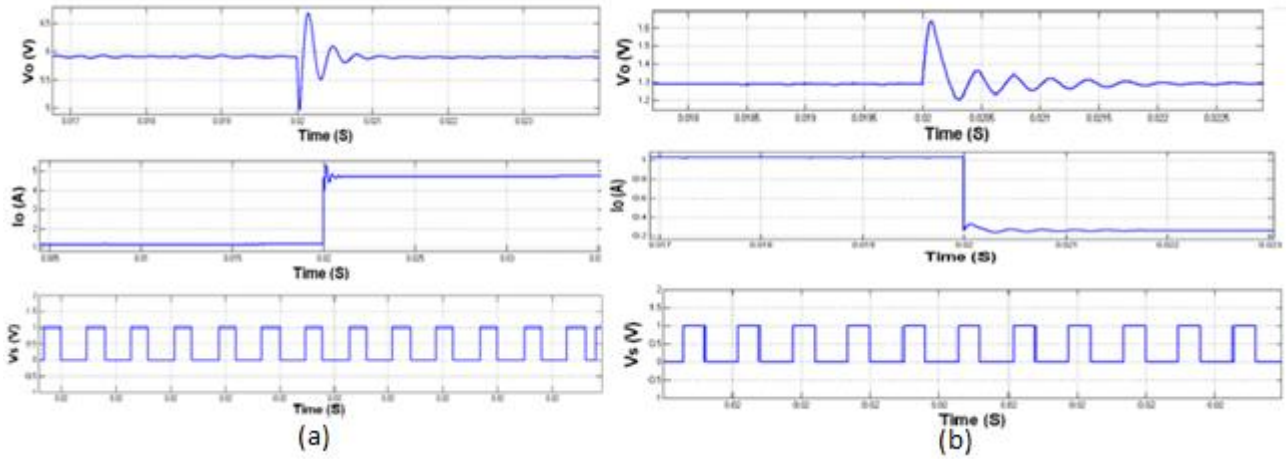

Fig. 9 Simulation results for change in load when E = 3.3V, r = 6mΩ

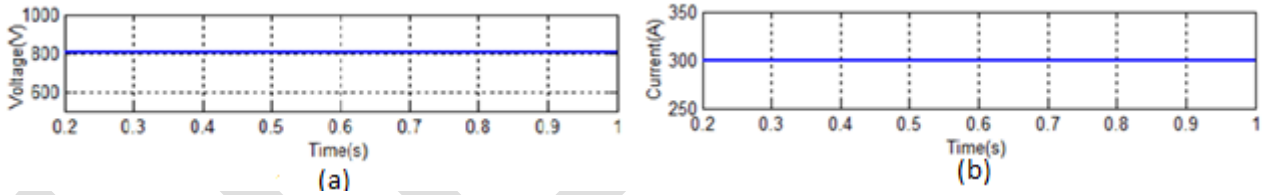

Fig. 10 Results for photovoltaic system (a) PV voltage (b) PV current

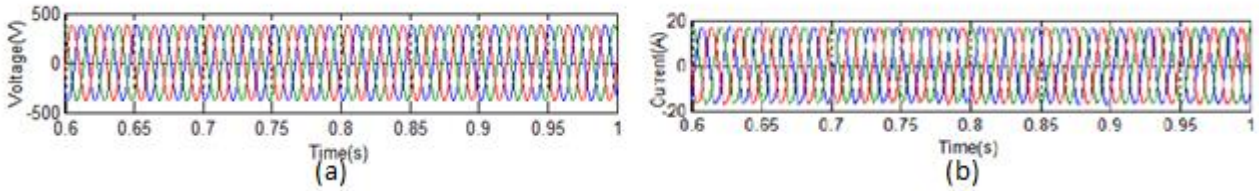

Fig. 11 (a) Three phase grid voltage (b) Three phase grid current

IV.CONCLUSION

Here a variable frequency fixed off time controlled DC- DC buck converter is designed with five operating modes. By taking the ESR of the output capacitance into consideration the FOT controller is studied for different values of load resistance R, inductance L and effective series resistance ESR .Hence the fast transient response of the converter is obtained by choosing the appropriate value of the resistance which is used in series with the output capacitor. Therefore three phase grid connected system is implemented using this technique.

REFERENCES:

1. R. Redl, and J. Sun, "Ripple-based control of switching regulators—an overview," IEEE Trans. Power Electron., vol. 24, no. 12, pp. 2669–2680, Sep. 2009.
2. J. Li and F. C. Lee, "Modeling of V2 current-model control," IEEE Trans. Circuits Syst. I, Reg. Papers, vol. 57, no. 9, pp. 2552–2563, Sep. 2010.
3. T. Qian, W. K. Wu, and W. D. Zhu, "Effect of combined output capacitors for stability of buck converter with constant on-time control," IEEE Trans. Ind. Electron., vol. 60, no. 12, pp. 5585–5592, Dec. 2013.
4. Y. Panov and M. M. Jovanović, "Adaptive off-time control for variable-frequency, soft-switched fly back converter at light loads," IEEE Trans. Power Electron., vol. 17, no. 4, pp. 596–603, Jul. 2002.
5. J. P. Wang, B. C. Bao, J. P. Xu, G. H. Zhou, and W. Hu, "Dynamical effects of equivalent series resistance of output capacitor in constant on-time controlled buck converter," IEEE Trans. Ind. Electron., vol. 60, no. 5, pp. 1759-1768, Mar. 2013.
6. M. Castilla, L. G. de Vicuna, J. M. Guerrero, J. Matas, and J. Miret, "Designing VRM hysteretic controllers for optimal transient response," IEEE Trans. Ind. Electron., vol. 54, no. 3, pp. 1726–1738, Jun. 2007.
7. C. C. Fang, "Critical conditions for a class of switched linear systems based on harmonic balance: applications to DC-DC converters,". Nonlinear Dyn., vol. 70, no. 3, pp. 1767–1789, Sep. 2012.
8. Martin, M. Davis-Marsh, G. Pinto, and I. Jorio. (2012). Capacitor selection for DC-DC converters: What you need to know to prevent early failures, and reduce switching noise. Texas Instruments Corp. ,California.[Online].Available: http://www.kemet.com/Lists/TechnicalArtcles/Attachments/5/Avnet2012PowerForum_CapacitorsSelection.pdf.
9. J. P. Wang, J. P. Xu, and B. C. Bao, "Pulse bursting phenomenon in constant on-time controlled buck converter," IEEE Trans. Ind. Electron., vol. 58, no. 12, pp. 5406–5410, Dec. 2011.
10. B. C. Bao, X. Zhang, J. P. Xu, and J. P. Wang, "Critical ESR of output capacitor for stability of fixed off-time controlled buck converter," Electron. Lett., vol. 49, no. 4, pp. 287–288, Feb. 2013.
11. Y. C. Lin, C. J. Chen, D. Chen, and B. Wang, "A ripple-based constant on-time control with virtual inductor current and offset cancellation for DC power converters," IEEE Trans. Power Electron., vol. 27, no. 10, pp. 4301–4310, Mar. 2012.
12. Y. K. Lo, J. Y. Lin, and C. F. Wang, "Analysis and design of a dual-mode control flyback converter," Int. J. Circuit Theory and Appli., vol. 41, no. 7, pp. 772–778, Jul. 2013
13. J. Singh, "Study and Design of Grid Connected Solar Photovoltaic System at Patiala, Punjab," no. July, 2010.

International Journal of Engineering Research and General Science Volume 6, Issue 4, July-August, 2018
ISSN 2091-2730

FUZZY CONTROLLER BASED LOW COST HIGH EFFICIENCY CONVERTER FOR AUTONOMOUS PHOTOVOLTAIC WATER PUMPING SYSTEM

K.Sudha Rani, PG Scholar, EEE,lakireddyBalireddy College of Engineering, nagarjunasudha01@gmail.com

E.RaghuBabu,Assistant Professor,EEE,lakireddyBalireddyCollegeof Engineering

Abstract—This paper proposes a low cost converter for autonomous photovoltaic water pumping system based on fuzzy controller. The proposed converter i.e. the two inductor boost converter achieves ZVS/ZCS conditions.The operation of two inductor boost converter along with the three phase inverter and three phase induction motor is described.The classic topology of the TIBC has features like high voltage gain and low input current ripple. A solar tracking system is modeled using Matlab/Simulink and a fuzzy logic control is designed to control the duty cycle of TIBC.Simulation results show a power output 210w and efficiency of 98%is achieved for DC-DC converter.

Index Terms—Solar power, DC-DC converter,Voltage source inverter, Photovoltaic Water Pumping System

INTRODUCTION

Now a day's most of the people across the world have not sufficient water to drink. Due to this large amount of people is migrated from one place to another. Where the main source of water is from rain or distant rivers in such place this work is very useful for drinkable, consumption as well as irrigation. There is no need of electric power topump the water and treatment through conventional systems. To solve all these issues PV solar power generation is the best way to eradicate all the problems. This type of energy source is cheaper and these types of systems areexisted from so many years nearly three decades [1].

This system mainly consists of solar panel, an electronic controller, a motor and a water pump. The most important thing in control system has to firstly and most important to obtain the maximum power from the solar panel by tracking the sunlight. The pump [2] in the system isrunning on electricity which is produced by photovoltaic panels or the thermal energy available from collected sunlight. Photovoltaic powered systems are becoming more popular because

(i) In remote areas there is no adequate power lines to water pumping sites due to this reason supply fails to meet the demand.

(ii) Fossil fuel causes lot of environment degradation.

(iii)Gradually increasing the cost of fossil fuel based electricity and

(iv)Decreasing the cost of PV electricity.

Most of the converters available in market are based on an intermediate storage systemuses a lead–acid batteries and DC motors are used drive the water pump. The batteries are used to run the motor even when low climatic conditions. Basically this type of batteries have a low life span approximately two years only, which is comparatelylow with usage of 20 years of a PV module, and also high installation and maintenance cost.Most of the systems use low-voltage DC motors, it does not require boost voltage hence there is no boost stage between the PV module and the motor. But DC motorrequires higher maintenance cost and low efficiency compared to induction motors, due to this reasons it is not suitable for applications in isolated areas.

PUMP CONTROLLERS & STORAGE SYSTEM:

Every system requires a special controller similarly solar pumps also needed a special controller to be powered directly by PV modules (without batteries). The function of the controller is an automatic transmission, which allows the pump to start and run even in low light conditions that means overcast or early morning& evening. With the helpof battery source, the controller may convert 12 Volt

battery power to 30 Volts. The pumps have capable of low flow due to this water must be accumulated in a tank so that it can be released on demand. There are three ways to do this: (1) pumping directly to a pressure tank, (2) using storage tank with a booster pump and pressure tank, (3) using an elevated storage tank with gravity flow. There are different control strategies have been proposed in literature for obtaining maximum power; Perturb & Observe[4], Incremental Conductance, Short-Current Pulse, Constant Voltage, Open Circuit Voltage, Artificial Neural Network [6]etc. The utilization efficiency however, can be further improved by employing a hillclimbing MPPT [5] technique such as the Perturb and Observe (P&O) algorithm [4]. It is a simple algorithm and is easy to implement with analog and digital circuits.The selection of a proper dc–dc converter plays an important role for maximum power point tracking (MPPT) operation. Selection of photovoltaic convertermainly depends on factors such as cost, efficiency, flexibility and energy flow. Flexibility means the ability of the converter to maintain the output with the varying input. Whereas the energy flow means the continuous current to the converter. PV pumping systems without battery can provide a cost effective use of solar energy. Following are the features of current topology: high efficiency due to the low energy available; low cost; no need to manual operating; requires less maintenance, and high life span comparable to the usable life of 20 years of a PV panel.

I. PROPOSED SYSTEM

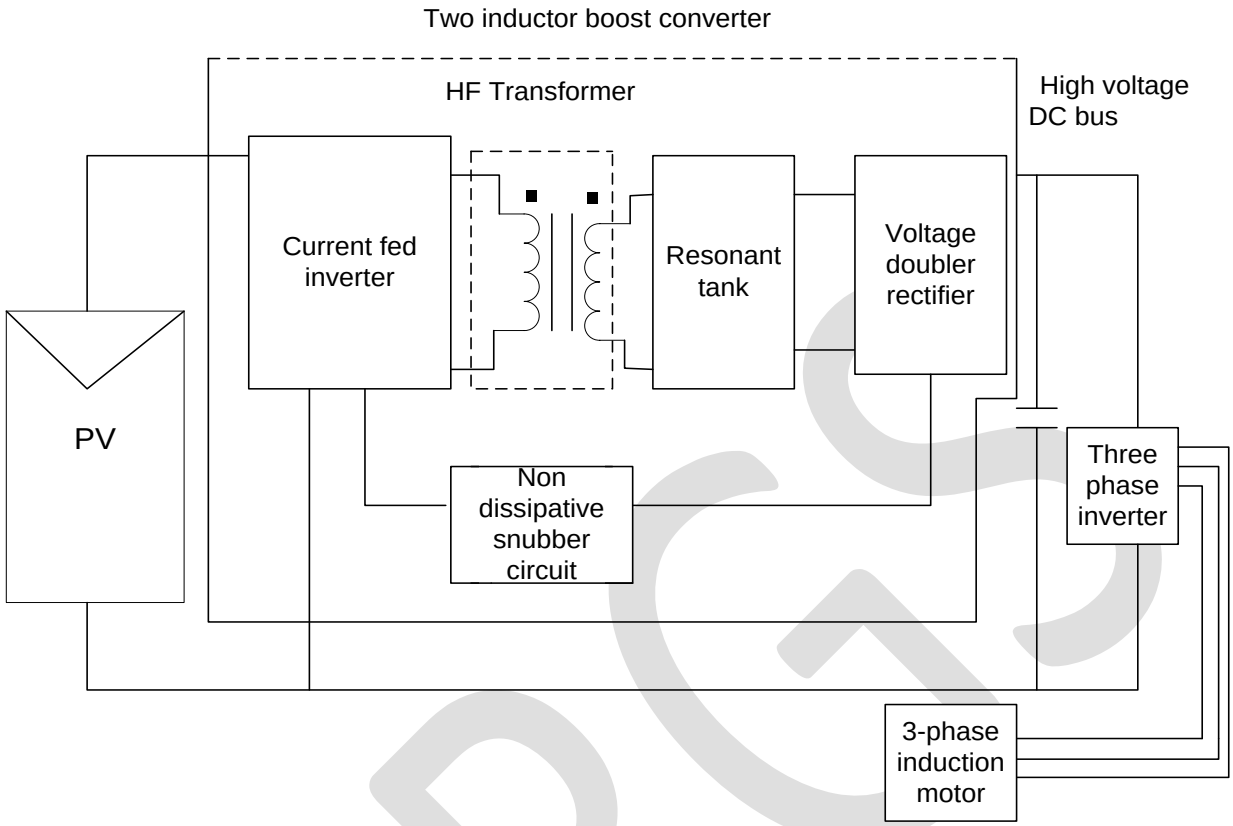

Figure 1: Simplified block diagram of proposed system

The proposed system mainly consists of two inductor boost converter (TIBC) DC-DC converter, three phase inverter and three phase induction motor. The boost converter comprises of current fed inverter, high frequency transformer, non-dissipative snubber circuit, resonant tank and voltage double rectifier. The sunlight directly fell on the PV panel then the solar energy converted into electrical energy. The energy produced by the panel is fed to the motor through a converter withtwo power stages: a DC/DC TIBC stage to boost the voltage of the panels and aDC/AC three-phase inverter to convert the DC voltage to three-phase AC voltage.

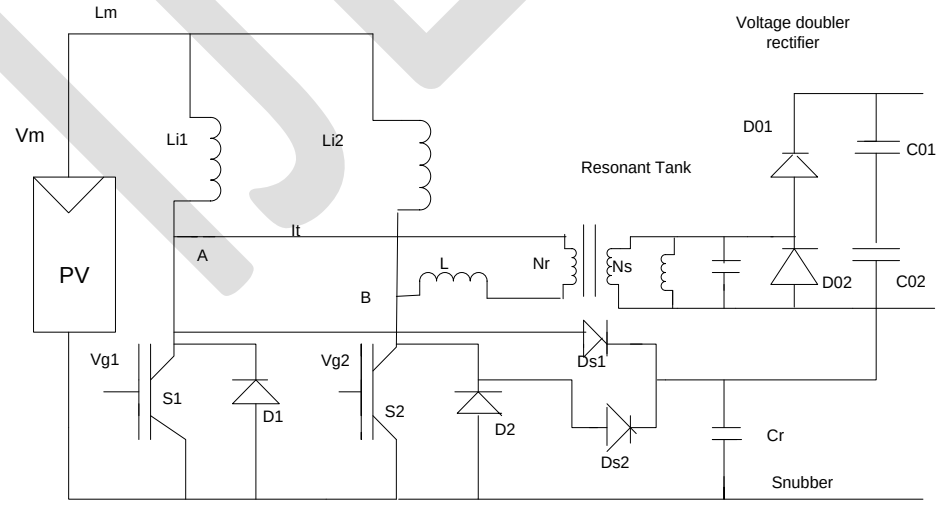

Figure 2: Proposed two inductor boost converter

To analyze the proposed converter some of the assumptions are need to take during switching interval. The input inductors L_{i1},L_{i2} are large so that their current is almost constant. The capacitors C_{o1},C_{o2} and C_s also large enough to maintain constant voltage but the output capacitors C_{o1} and C_{o2} are much larger than C_r to clamp the voltage.

In hard switching operation of TIBC both switches S1 and S2 operates at an overlapped at a duty cycle. When both switches S1 and S2 are turned ON L_{i1}, L_{i2} are charged by the input energy. When S1 is open the energy stores in L_{i1} is transferred to C_{o1} through the transformer and rectifier diode D_{o1}.Similarly when S2 is opened the energy stores in L_{i2} is transferred to C_{o2} through the transformer and rectifier diode D_{o2}.

There are two resonant process occur when multi resonant tank is introduced. They are

1. When both switches are closed the leakageinductance L_r participates along with capacitance C_r in the resonance at the primary current switching and current polarity inversion here the ZCS operation occurs.
2. At the time of conduction time interval.
3. If any switch is on L_r is associated in series with L_{i1} and L_{i2} not participating on the transformers secondary current resonance formed only by L_m and C_r.

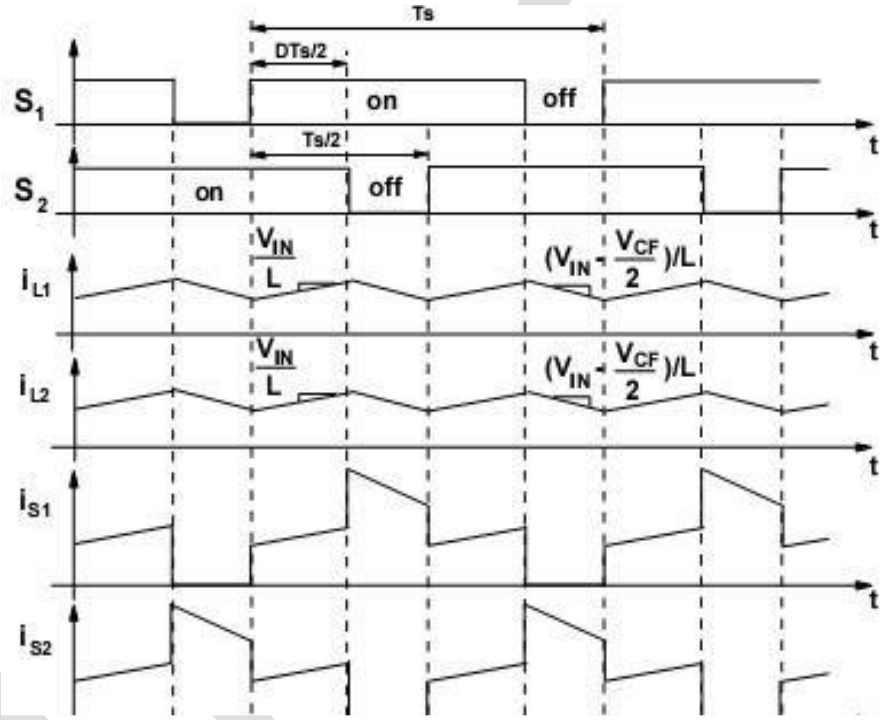

Figure 3: ON & OFF conditions of switches S_1& S_2

III.PROPOSED FUZZY LOGIC CONTROLLER

There are so many logic controllers are used to control the system. Previously there are three main control systems are used they are fixed duty cycle control, MPPT control, Hysteresis control.The operation of fixed duty cycle makes the converter work with the constant voltage gain.

$$\frac{Vout}{Vin} = Kv = \frac{1}{1-D}\left(2\frac{Ns}{Np} + 1\right) \quad \text{----- (1)}$$

Where D represents duty cycle of switch

Ns/Np represents the transformers turns ratio

a. FUZZY LOGIC CONTROLLER APPLIED TODC – DC CONVERTER

In 1975 scientist called Mamdani and Assilian were invented fuzzy inference technique. They first attempt was to control the steam engine and boiler by using set of linguistic rules that are obtained from human operators.

Through a Fuzzy Logic Controller is an expert it can operate by its knowledge and observation without any mathematical equations. The FLC consists of following components:

The fuzzification: It converts the real input values to fuzzy values to be interpreted by the inference mechanism. The rule-base (a set of if-then) it contains the fuzzy values by means of a linguistic approach to attain good control of the converter.

Inference mechanism: It emulates the best way to control the system by taking the experts decision.

The defuzzification:It makes the quite opposite to the fuzzification takes the inference mechanism values and converts them into actual output values. To design the fuzzy logic control it is necessary to define the inputs given below; the first input is the error (e(k)) the equation of error is given by equation (2) and $V_{Ref}$is the voltage reference. The second input is change in error(Δe (k))is given by the equation (3) where *e(k)* is the error at the *k*th sampling and *e(k-1)* is the error at the previous *k*th sampling.

$$e(k) = V_{\mathrm{Re}\,f} - V_0(k) \qquad \text{----- (2)}$$

$$\Delta e(k) = e(k) - e(k-1) \qquad \text{----- (3)}$$

Vo(k)is the sampled output voltage of the boost converter

$V_{Ref}$is the voltage reference.

Those inputs are multiplied by gains g0and g1 respectively and then they are evaluated in the fuzzy controller. The FLC output is the change in the duty cycle Δd (k)which is given by the equation (4)and it is scaled by the gain *h*.

$$d(k) = d(k-1) + h\Delta d(k)T_s \qquad \text{----- (4)}$$

Where $\Delta d(k)$ is the change in duty cycle of the Kthsample.

b. Rule Base

The rule base is defined relation between the inputs and output with the rules of type *IF-THEN*. There are 11 fuzzy sets for each linguistic variable which generates 121 rules that can be expressed as a Mamdani linguistic fuzzy model, the rule base equation is given below

IF *e* is $Ai_1$and Δe *is*Ai_2, THEN Δd_i is B_i -------- (5)

Where *e* and Δeare the input linguistic variables, Δd_i the output linguistic variable, $Ai_1$and $Ai_2$are the values for each input linguistic variables on the universe of discourse and B_i is the value in output in the universe of discourse.

Table I: Fuzzy Rules relating Linguistic Variables

Error	Change in Error (CE)										
	NVB	NB	NM	NS	NVS	ZE	PVS	PS	PM	PB	PVB
NVB	PVB	PVB	PVB	PVB	PVB	PVB	PB	PM	PS	PVS	ZE
NB	PVB	PVB	PVB	PVB	PVB	PB	PM	PS	PVS	ZE	NVS
NM	PVB	PVB	PVB	PVB	PB	PM	PS	PVS	ZE	NVS	NS
NS	PVB	PVB	PVB	PB	PM	PS	PVS	ZE	NVS	NS	NM
NVS	PVB	PVB	PB	PM	PS	PVS	ZE	NVS	NS	NM	NB
ZE	PVB	PB	PM	PS	PVS	ZE	NVS	NS	NM	NB	NVB
PVS	PB	PM	PS	PVS	ZE	NVS	NS	NM	NB	NVB	NVB
PS	PM	PS	PVS	ZE	NVS	NS	NM	NB	NVB	NVB	NVB
PM	PS	PVS	ZE	NVS	NS	NM	NB	NVB	NVB	NVB	NVB
PB	PVS	ZE	NVS	NS	NM	NB	NVB	NVB	NVB	NVB	NVB
PVB	ZE	NVS	NS	NM	NB	NVB	NVB	NVB	NVB	NVB	NVB

IV SYSTEM DESIGNPARAMETERS

A. Specifications:

The project is carried out by using MATLAB software. The specifications of

Parasitic elements used in the converter are given in below table II.

Parameters	**Values**
Converter input current ripple	5%
Nominal bus voltage	350v
TIBC Switching frequency	100KHZ
Inverter switching frequency	7.7KHZ
Constant voltage gain	11.69
Transformers turns ratio N_s/N_p	2.25

Table II: Converter design specifications

The main parameters of the used motor and panel specifications are given in table III.

Parameters	**Values**
PV model	KD210GX
PV power	210W

PV open circuit voltage	29.9v
PV short circuit voltage	6.98A
PV maximum MPP voltage	26.6v
Motor Nominal power	0.2 HP
Motor Nominal Voltage	220V
Motor nominal frequency;	60hz

Table III: Motor and Panel specifications.

B.SIMULATION RESULTS

PV panel outputs:

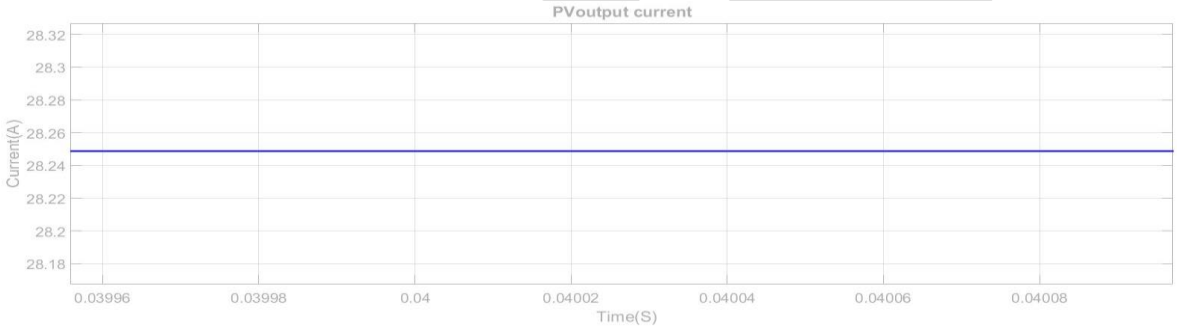

FIGURE 4: Current from PV panel

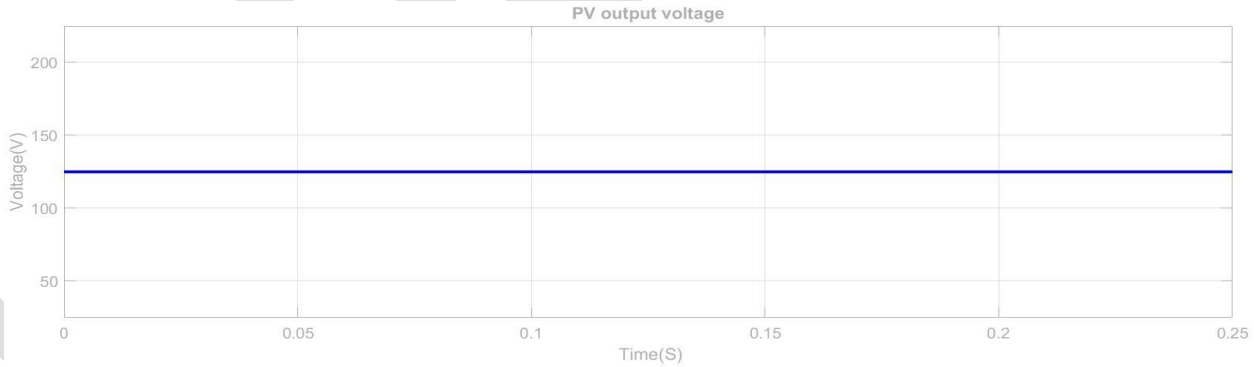

Figure 5: Voltage from PV panel

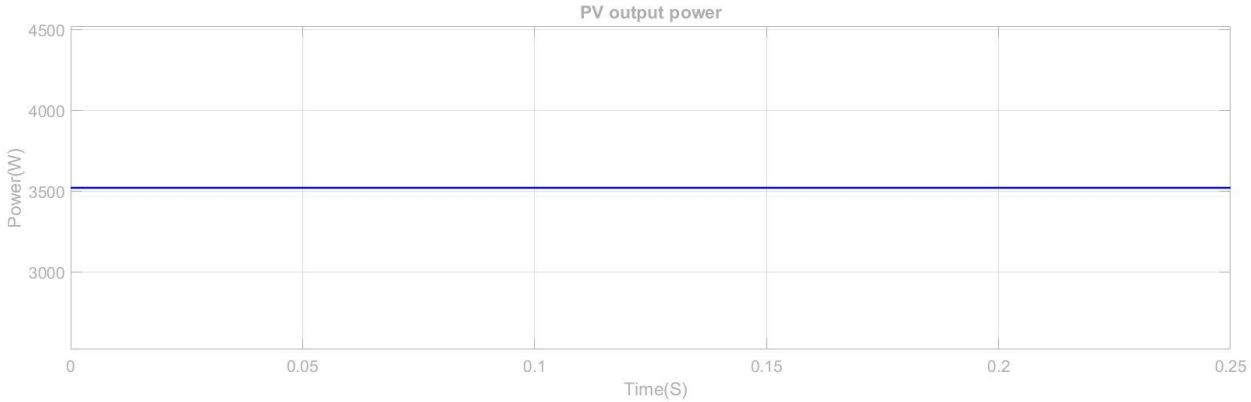

Figure 6: Power from PV panel

MOSFET output waveforms:

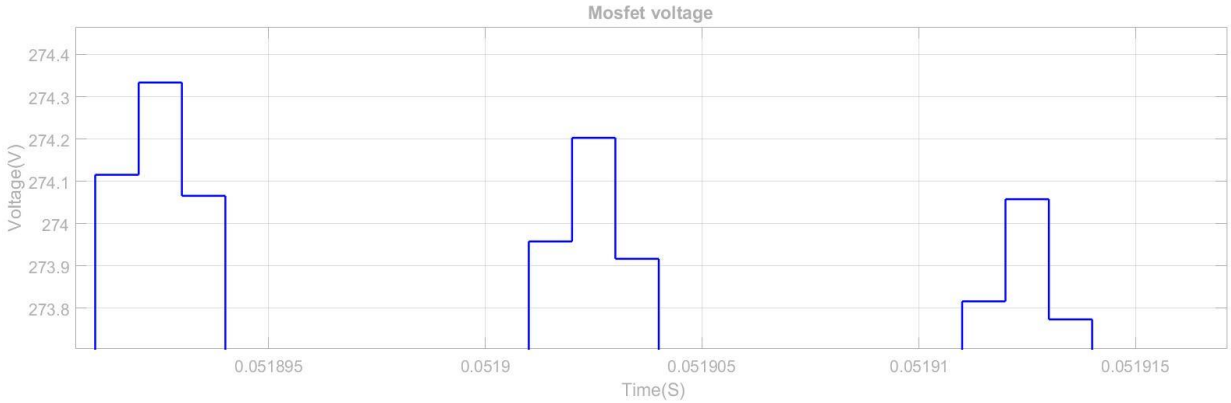

FIGURE 7:MOSFET S_2 Voltage

Figure 8:MOSFETS_2Current

DC output waveforms:

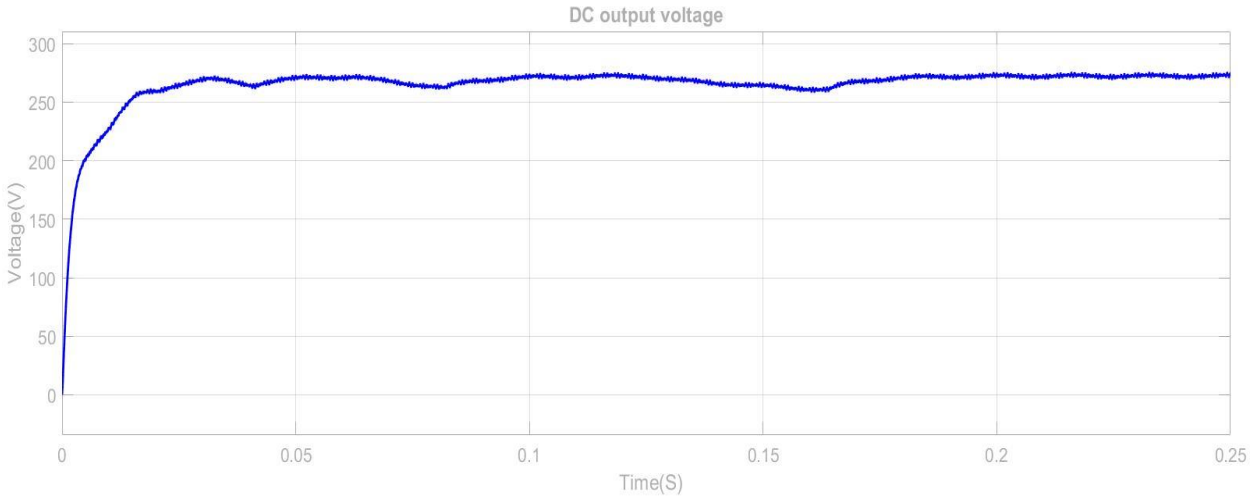

Figure 9:DC output voltage

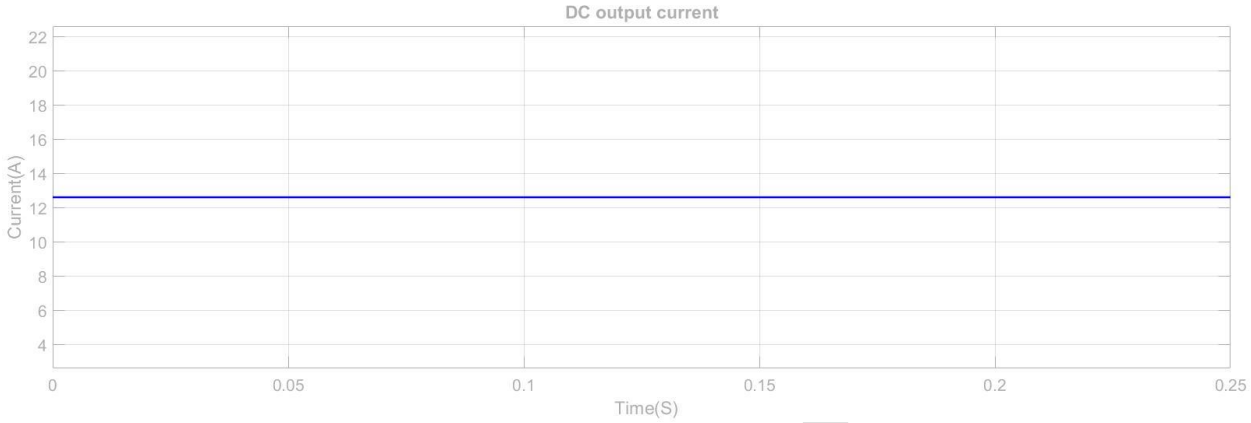

Figure 10:DC output current

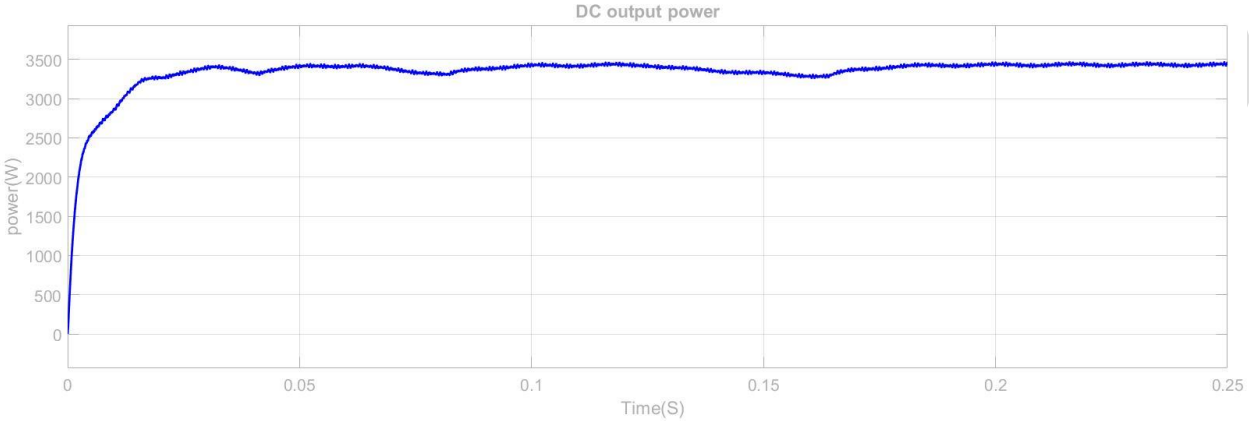

Figure 11: DC output power

Motor output characteristics:

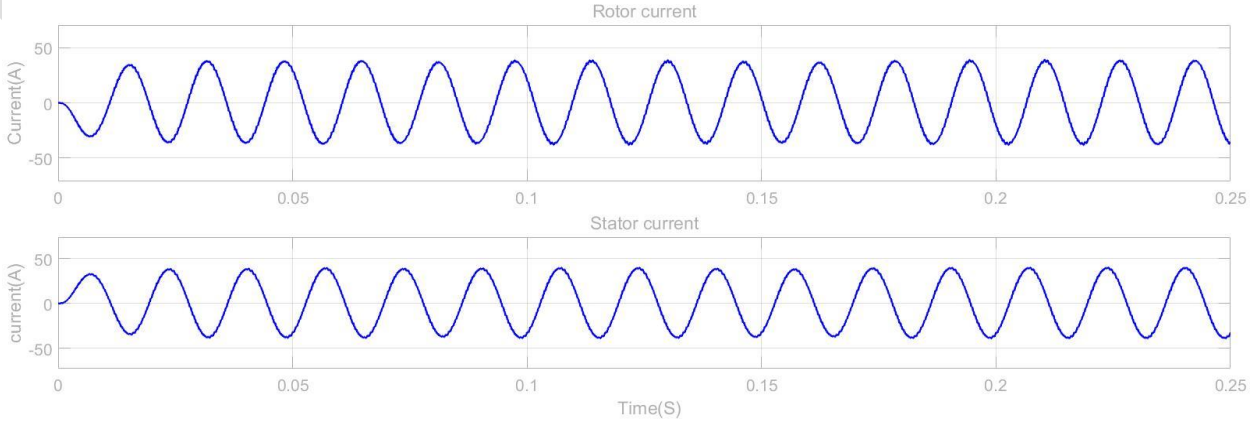

Figure12: Stator rotor current

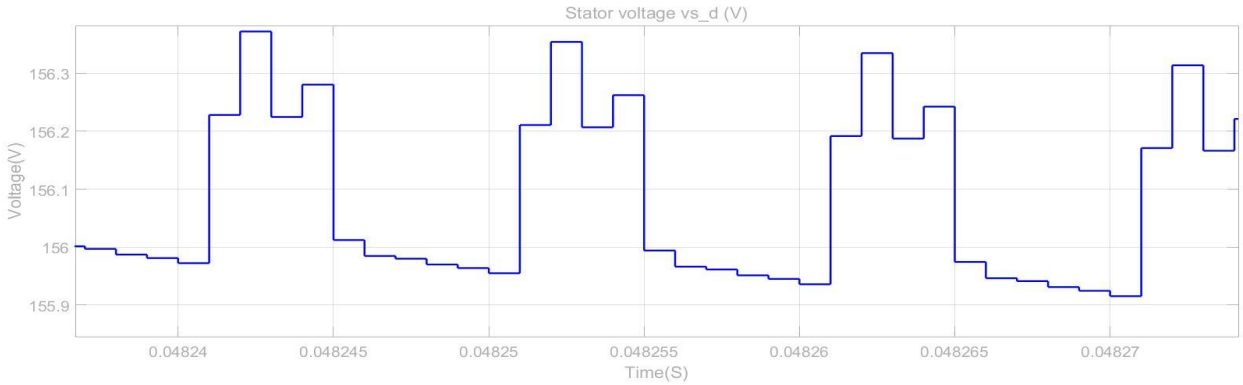

Figure 13:d-axis Stator voltage (v)

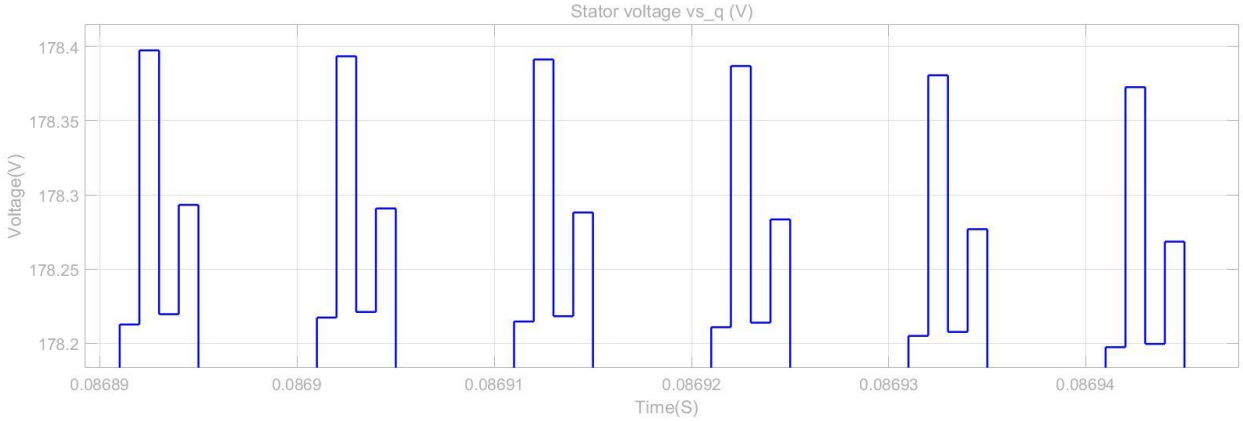

Figure 14:q-axis stator voltage (v)

Three phase inverter waveforms:

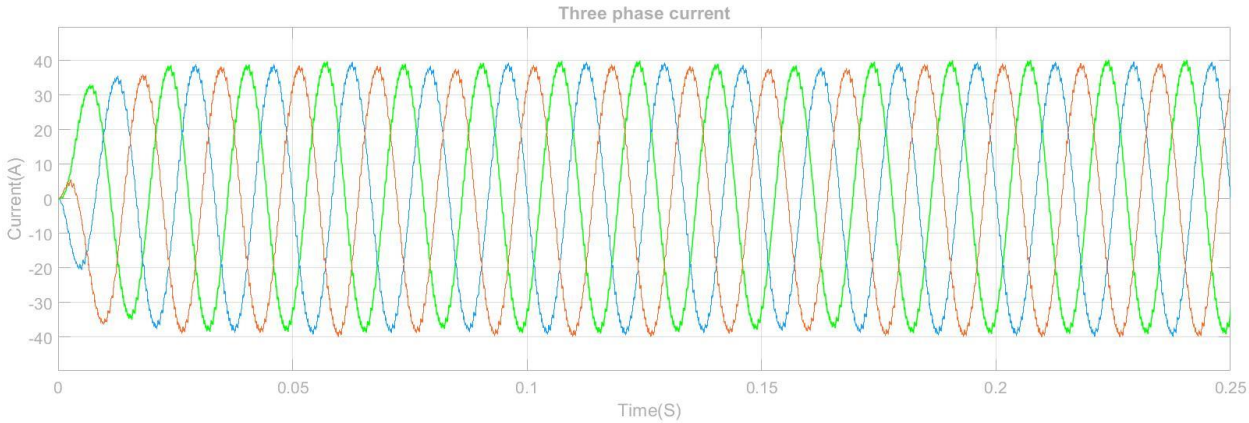

Figure 15: Three phase inverter current

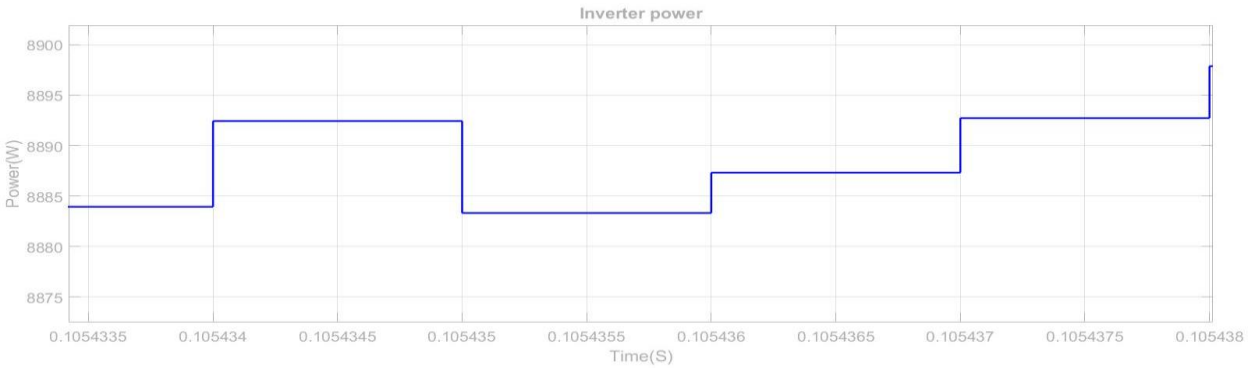

Figure 16: Inverter power

CONCLUSION

This paper presented a converter for photovoltaic water pumping and treatment systems without the use of storage elements. The converter was designed to drive a three-phase induction motor directly from PV solar energy and was conceived to be a commercially viable solution having low cost, high efficiency and robustness.

REFERENCES:

[1] P Sadasivam, MKumaravel, Krishna Vasudevan and Ashok Jhunjhunwala, "Analysis of Subsystems Behaviour and Performance Evaluation of Solar Photovoltaic Powered Water Pumping System", Indian Institute of Technology Madras, Chennai, Tamilnadu, 600036, India 2014.

[2] Author H. Harsono, "Photovoltaic water pump system", Ph.D. dissertation, Dept. Intell. \
Mech. Syst. Eng., Faculty Kochi Univ. Technol., Kochi, Japan, Aug. 2003

[3] M. A. Vitorino and M. B. R. Correa, "High performance photovoltaic pumping system using induction motor", in Proc. Brazilian Power Electron. Conf., 2009, pp. 797804.

[4] Mohammed A. Elgendy, Bashar Zahawi and David J. Atkinson, "Assessment of Perturb and Observe MPPT Algorithm Implementation Techniques for PV Pumping Applications", IEEE Transactions on sustainable Energy, Vol. 3, No. 1, January 2012.

[5] Ali HmidetRabiaaGammoudi and Othman Hasnaoui and RachidDhifaouiHammamet, "Analog MPPT Controller Circuit used in Photovoltaic Pumping Systems", The fifth International Renewable Energy Congress IREC 2014 March 25.

[6] dr. A. Moussi , a. Saadi, a. Betka, g.m. Asher,"photovoltaic pumping system technologies and trends", larhyss journal, issn 1112-3680, june 2003.

[7] b.chittibabu, r. Sudharshankaarthik, nayankumardalei, r.vigneshwaran, rabinarayan das,"pv energy conversion system for water pump applications– modeling & simulation", department of electrical engineering, nit, 13th january 2013.

[8] victorcaracas, guilherme de carvalhofreitas, louisfelipe, "implementation of a high efficiency, lifetime, and low cost converter for an autonomous pv water pumping system"students member ieee, louisantonio de souza, member ieee, 2013 ieee.

[9] v.chitra and r.s.prabhakar, "induction motor speed control using fuzzy logic controller", world academy of science, engineering and technology 23, 2006.

[10]Guilherme De CarvalhoFarias, Student Member, Ieee,Luis Felipe Moreira Teixeira, Student Member, Ieee, And Luiz Antonio De Souza Ribeiro, Member, Ieee,"Implementation Of A High-Efficiency, High-Lifetime And Low-Cost Converter For An Autonomous Photovoltaic Water Pumping System",Ieee Transactions On Industry Applications, Vol. 50, No. 1, January/February 2014.

International Journal of Engineering Research and General Science Volume 6, Issue 4, July-August, 2018
ISSN 2091-2730

INTELLIGENT CONTROL OF DISTRIBUTION GENERATION FOR VOLTAGE SAG MITIGATION IN DISTRIBUTION SYSTEM

B.Jyothi [1], PG scholar EEE Lakireddy Bali Reddy College of Engineering

E-mail : badugujyothi712@gmail.com

Dr. M. Uma Vani[2], Lakireddy Bali Reddy College of Engineering

Abstract—. Voltage dips are most frequent problems occurring in distribution systems. Voltage sags are expansive and are most severe power quality problem. Identification and correction of voltage dip can be done in many ways. Voltage injection by using Distributed Generation (DG) are quite useful in mitigating the voltage sags. This paper addresses correction of voltage sag with solar PV system with inverter side controls using Proportional integral(PI), Fuzzy and ANFIS under balanced and un balanced loading conditions. Usefulness of the proposed controllers is examined through simulation using MATLAB software and the results have shown the validation of the controllers used in the mitigation of voltage dips using DG schemes

Keywords— Voltage sag, Solar PV System, Fuzzy, ANFIS

INTRODUCTION

Power quality issues comprise of a wide range of disturbances such as voltage dip voltage swell , transient voltages harmonics ,flicker and interruptions. In distribution systems voltage dip are most severe than voltage swells. Voltage sag can causes malfunction failure of sensitive equipment and could cause large voltage and current unbalances which lead to tripping of circuit breakers. The voltage dip can be expansive to the consumers and hence there is a need to mitigate voltage dips on the distribution systems[1]. Numerous methods are available in the literature to mitigate voltage dips, but use of custom power device is found to be most effective.

K.J.P. Macken et al. [2] introduce a shunt current or a series voltage into the system is the solution for voltage dip in transmission networks. DG plays a key role during this process. This technique is extended for DG grid connected system, along with power electronic converter and a series compensator. this method has noticeable Disadvantages as follows

i) At the time of interruptions Series compensation do not be used
ii)power electronic components necessity is huge so series compensation is not an profitable solution.

To eliminate voltage dip, KJ.P. Macken et al. [2] also suggested transfer to micro grid operation. In this scheme, the DG system has to be designed for both grid-connected operation and micro grid operation. During grid-connected operation the converter controller of the DG system regulates the current (i.e. current-mode control), whereas m micro grid operation, the controller regulates the voltage (i.e. voltage mode control).

Disadvantage of this method is its operation during voltage dip is less reliable than the series compensator

This paper introduces distribution generation scheme(Solar PV system) and its principle to mitigate voltage sag condition arising in the distribution network with the help of inverter side controls proportional plus integral controller is done to show the effectiveness of the intelligent control techniques.

2.Test system:

Figure 1 shows the test system consisting of a 5-bus radial distribution network and is used to carry out the various simulations with conventional and adaptive controllers for both balanced &un balanced voltage sags. In balanced case all loads are balanced, Load 1 = 24 + j10.2 pu, Load 2 = 21 + j9 pu, Load 3= 30 + j12.6 pu [3][4] .This results in balanced line current and voltages. In unbalanced case, loads are unbalanced which result in unbalance of the line currents and voltages. Here the bus voltage is 25kv.and source voltage is 20kv.

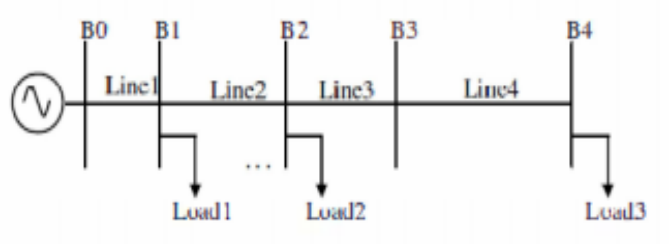

Figure.1:Test system

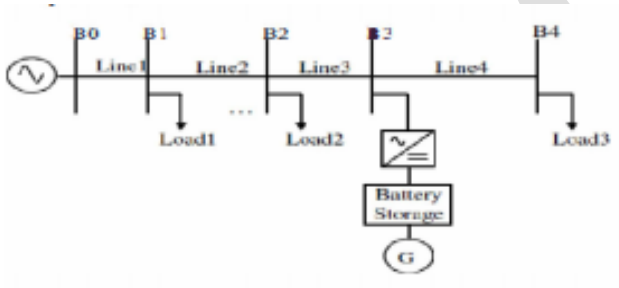

Figure.2: Optimal location of DG

3. Solar PV System

The solar PV array is connected in series with supply load. PV array is connected to grid via a converter a DC-DC boost converter and a three-phase three-level Voltage Source Converter (VSC). Maximum Power Point Tracking (MPPT) is implemented using the 'Incremental Conductance + Integral Regulator' technique. This MPPT system automatically varies the duty cycle in order to generate the required voltage to extract maximum power. The VSC control system uses two control loops: an external control loop which regulates DC link voltage and an internal control loop which regulates I_d and I_q grid currents (active and reactive current components). Id current reference is the output of the DC voltage external controller. Iq current reference is set to zero in order to maintain unity power factor. V_d and V_q voltage outputs of the current controller are converted to three modulating signals U_{abc}.reference used by the PWM Generator. The control system uses a sample time of 100 microseconds for voltage and current controllers as well as for the PLL synchronization unit. Pulse generators of Boost and VSC converters use a fast sample time of 1 microsecond in order to get an appropriate resolution of PWM waveforms.

4.Control Scheme

4.1 PI controller:

The error signal obtained from the reference voltage and the RMS value of the terminal voltage is the input to the PI controller .Such error is handle by a PI controller and the output of a PI controller is the angle which is supply to the pulse with modulation(PWM) signal generator. The pulse signals to the IGBT gates of Voltage Source Converter generated by PWM generator. it is only capable of determining the instantaneous value of the error signal without considering the change of the rise and fall of the error, which in mathematical terms is the derivative of the error signal, denoted as de/dt[5][6].that's why PI controller is its inability to react to sudden changes in the error signal ,this is the main disadvantage of PI controller.

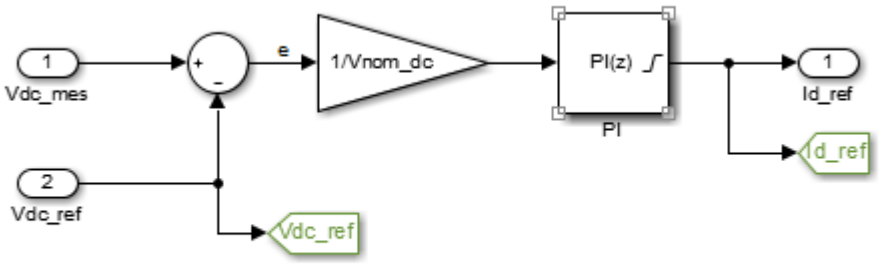

Fig.3:PI controller block in inverter side of solar PV system

4.2 Fuzzy controller:

Error signal and the derivation of the error are the two inputs of the fuzzy controller has. fuzzification, rule execution, and defuzzification are the three stages of a fuzzy logic controller. the inputs e and de/dt are the subsets and these are defined as (NB,NM, NS, Z, PS, PM, PB) Taking into account of the coverage, sensitivity, robustness of universe, the fuzzy subsets of the membership functions use triangular membership function[6][7][8]

Table.1: Fuzzy rule table

e / de/dt	NB	NM	NS	Z	PS	PM	PB
NB	NB	NB	NB	NB	NM	NS	Z
NM	NB	NM	NS	Z	PS	NB	NM
NS	NM	NS	N	PS	PM	NB	NM
Z	NS	Z	PS	PM	PB	NB	NS
PS	Z	PS	PM	PB	PB	NS	Z
PM	PB	PM	PB	PB	PB	Z	PS
PB	PM	PB	PB	PB	PB	NB	NB

4.3 ANFIS controller:

An adaptive neuro-fuzzy inference system or adaptive network-based fuzzy inference system (ANFIS) is a type of artificial neural network that is based on Takagi–Sugeno fuzzy inference system. The method was developed in the early on 1990s. while it integrates equally neural networks and fuzzy logic principles, it has probable to capture the benefits of both in a single framework. Its inference system corresponds to a set of fuzzy IF–THEN rules that have wisdom capability to estimated nonlinear functions. Hence, ANFIS is measured to be a universal estimator[9][10][11][12].

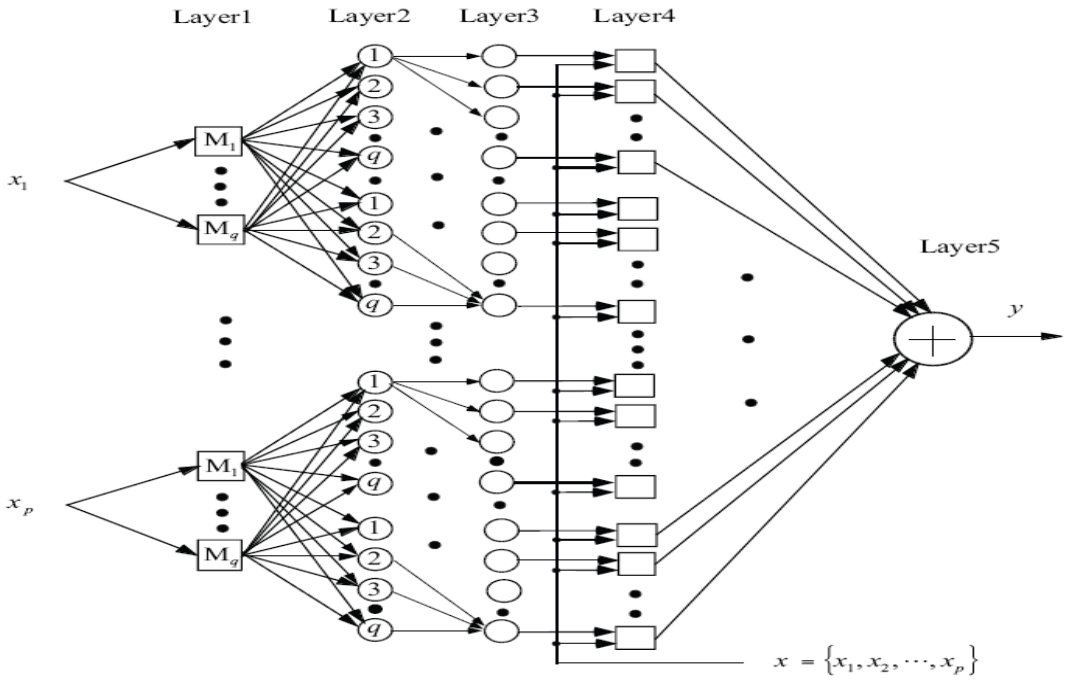

Fig.4: ANFIS Structure

5.Simulation results:

To know the performance of Solar PV System the test system which is shown in Fig.1 is simulated in MATLAB. Simulation results are performed for each case (balanced load and unbalanced) loading conditions. By using PI ,Fuzzy,ANFIS controllers.,

5.1. Balanced load under fault condition

a) With PI controller: The PI controller based DG Scheme: Solar PV System IS able to mitigate the voltage dip for balanced load condition with three phase fault initiated during 0.2ms-0.4ms.as shown in Figures: 5.1.1 and 5.1.2

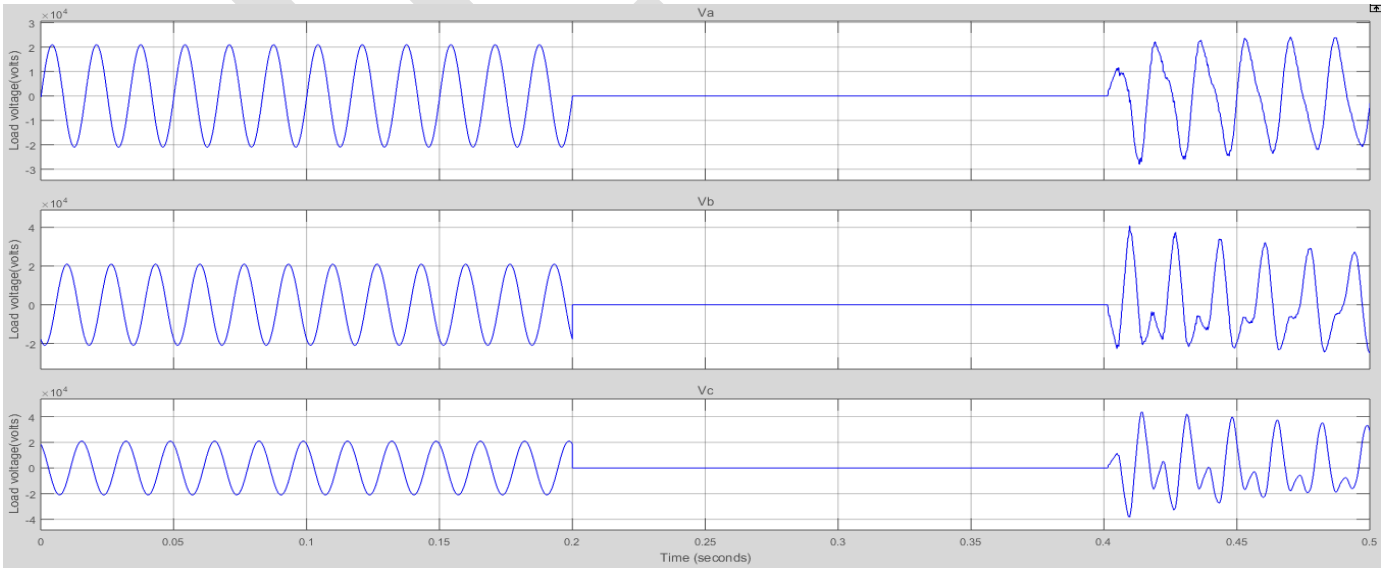

Fig.5.1.1: Fault condition

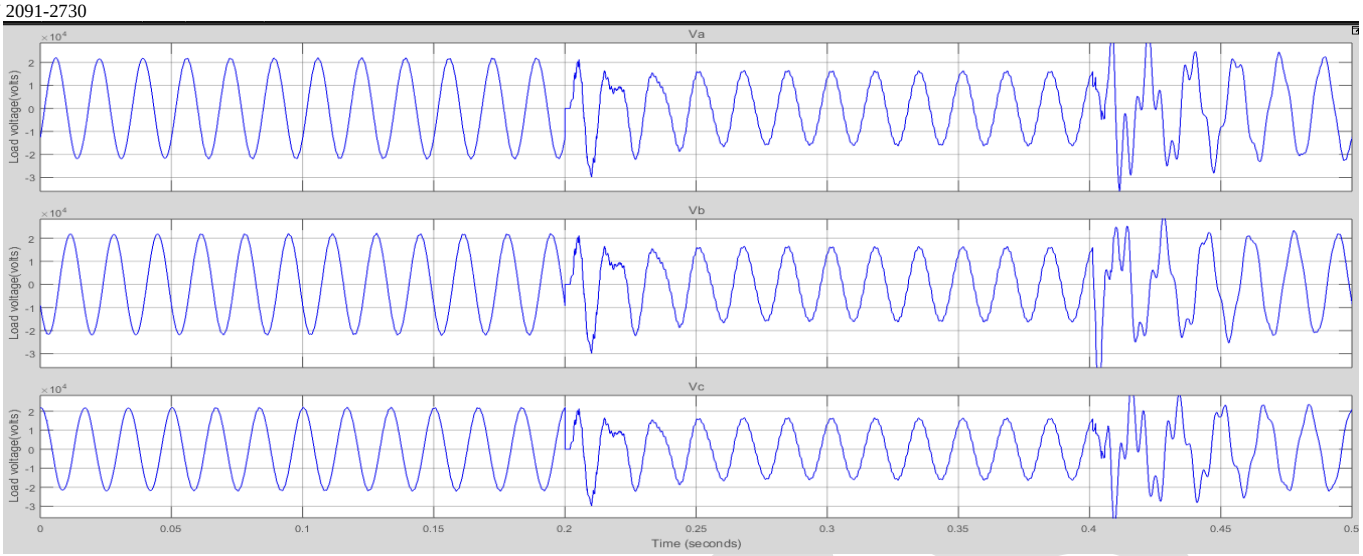

Fig.5.1.2: Solar PV system injected voltage waveforms with PI controller

b) With fuzzy controller: Fuzzy controller based DG Schemes are able to mitigate the voltage dip for balanced condition with three phase fault with fault duration between 0.2ms-0.4ms,results as shown in Figure 5.1.3

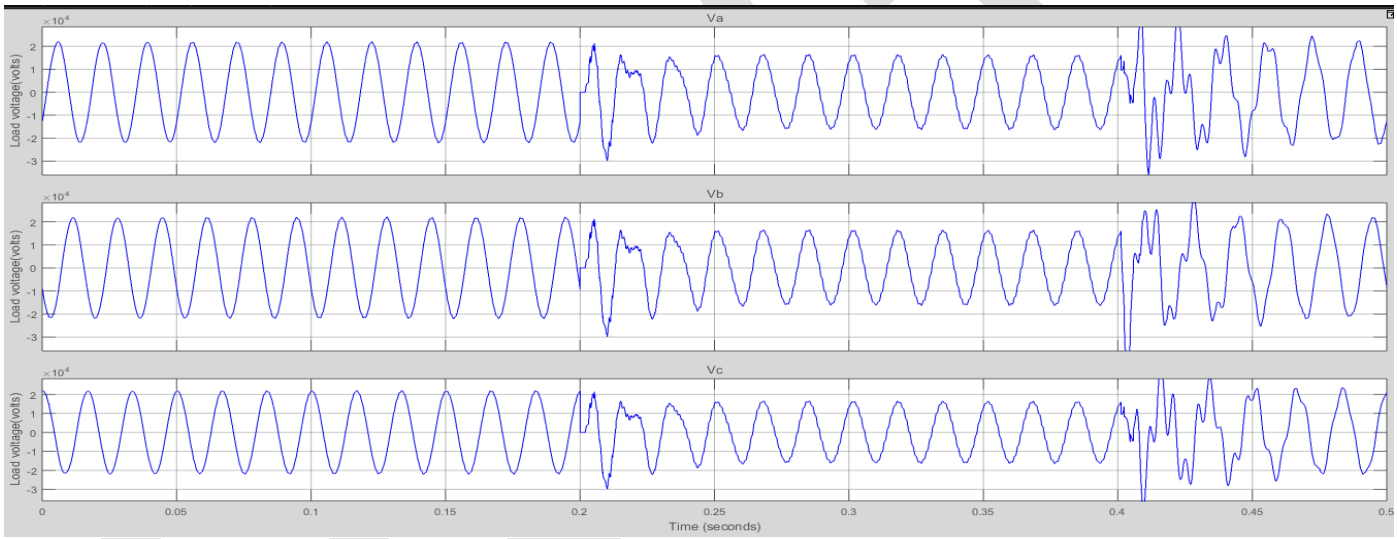

Fig.5.1.3: Solar PV System injected voltage waveforms with Fuzzy controller

C)With ANFIS controller:ANFIS controller based DG Schemes Considered are able to mitigate the voltage dip efficiently for balanced condition with three phase fault with fault duration between 0.2ms-0.4ms,as shown in Figure5.1.4.

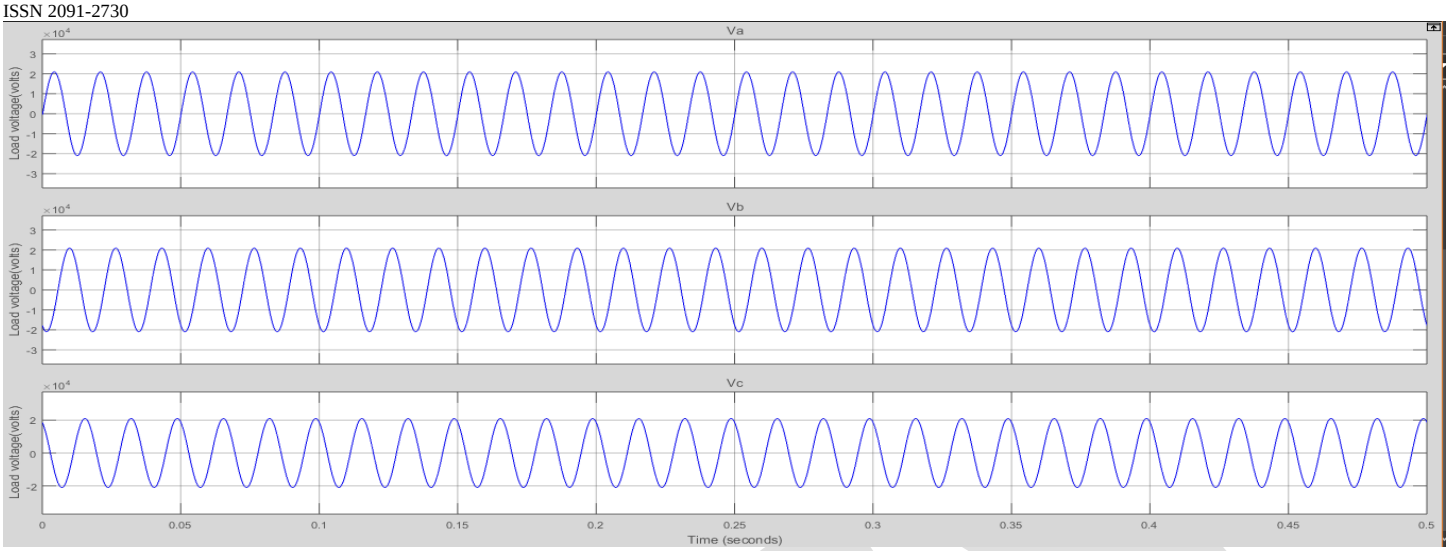

Fig.5.1.4: Solar PV System injected voltage waveforms with ANFIS controller

5.2 Unbalanced load

a) With PI controller:

The PI controlled based solar PV system technique is able to mitigate the voltage dip for unbalanced condition also as shown in figures: 5.2.1&5.2.2

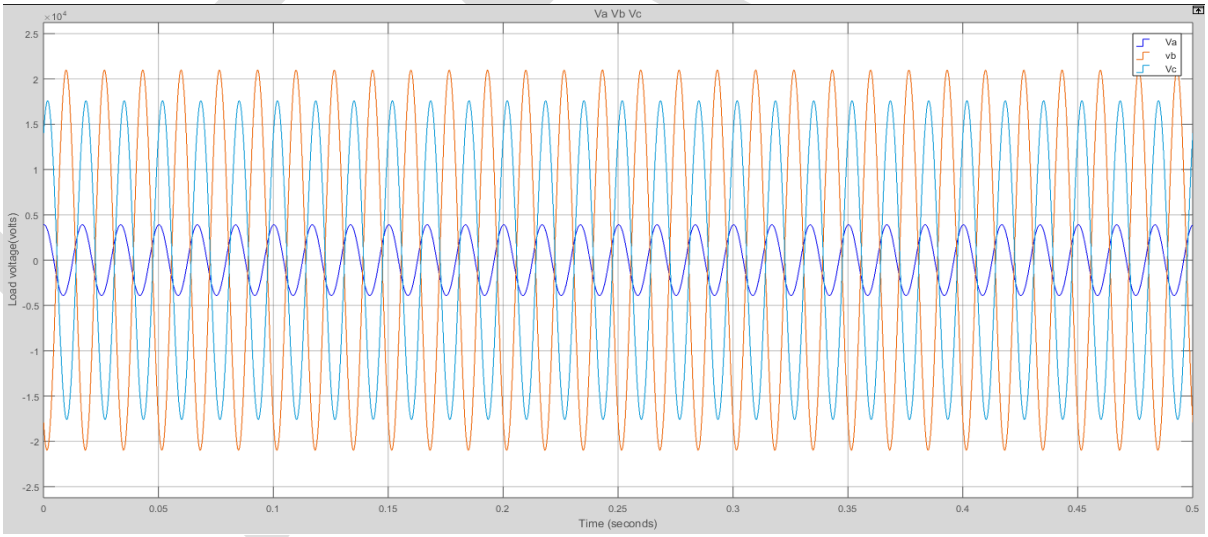

Fig.5.2.1: Unbalanced voltages

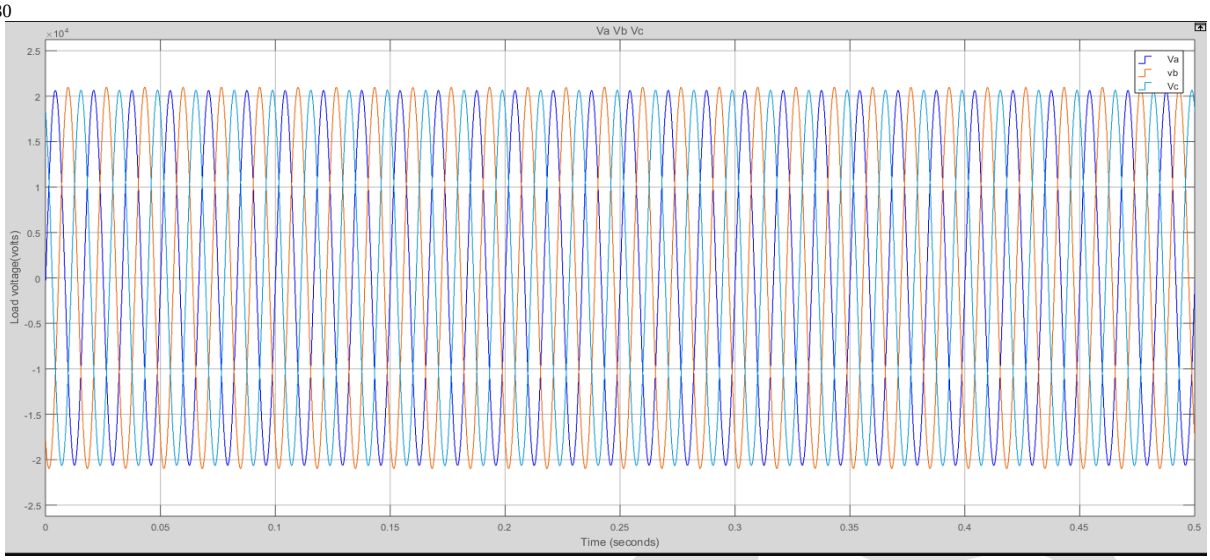

Fig.5.2.2:Solar PV system injected voltage waveforms with PI controller

b) With Fuzzy controller:

The fuzzy controller based DG Scheme is able to mitigate the voltage dip for unbalanced condition as shown in figure 5.2.3.

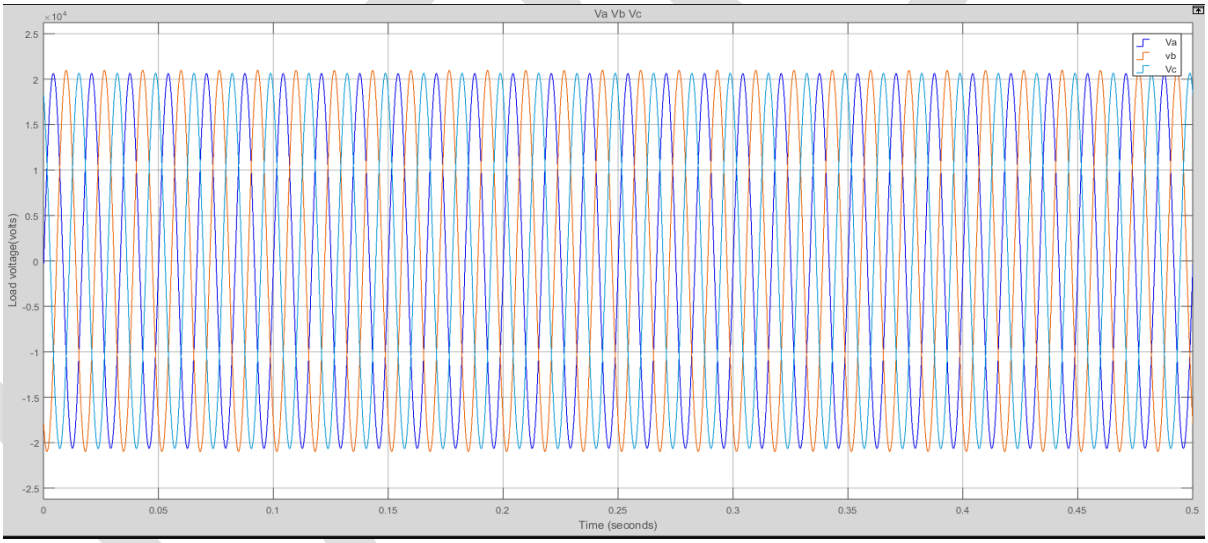

Fig.5.2.3:Sloar PV System injected voltage waveforms with Fuzzy controller

C) With ANFIS controller:

The fuzzy controller based DG Schemes isable to mitigate the voltage dip for unbalanced condition as shown in figure 5.2.4

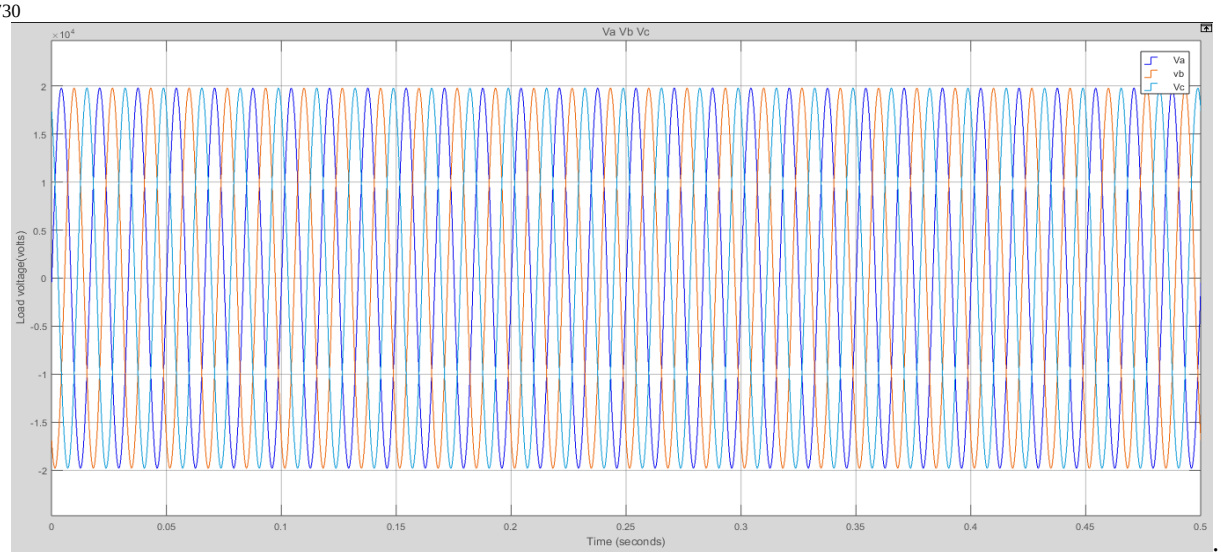

Fig.5.2.4: Solar PV System injected voltage waveforms with ANFIS controller

5.4 Discussion of results: Simulations of the five-bus radial distribution test system to compensate the voltage sag using DG are performed using MATLAB/SIMULINK with balanced and unbalanced loading conditions.

Balanced load with fault: In this case the simulation is performed by considering a three phase fault at bus -2 in the test system delivering power to load. Fault is started at 0.2sec and ends at 0.4sec. DG is connected at bus -3 in the system to inject the voltage during the fault.

Unbalanced load: Simulation is performed with unbalanced loads and the result is presented in Fig 5.2.1. to compensate the voltage sag again DG is connected to the system. Wave forms for this case are shown in figures 5.2.2 to 5.2.4.From the obtained results it is noticed that the output waveforms after compensation is balanced.

CONCLUSION

When DG is directly connected to the distribution system, it influences the background waveform distortions, modifies the harmonic impedances and contributes to modification of voltage harmonic profiles at all of the distribution system buses. Connection through the power electronic interface can inject harmonic currents, which can lead to a voltage distortion increase. The optimal placement and sizing of DG help in loss reduction, voltage profile improvement and voltage dip mitigation, which might lead to undistorted power at the PCC.

This paper presents the analysis of voltage dip mitigation using Solar PV System with balanced and unbalanced voltage sags. The load voltage waveforms clearly indicates that the ANFIS controller is better performance than the PI and Fuzzy controllers to mitigate the voltage sag.

REFERENCES:

[1] Q. Sun, Z. Li, and H. Zhang, "Impact of Distributed Generation on Voltage Profile in Distribution System", in Proc. of International Joint Conference on Computational Sciences and Optimization, 2009.

[2] K.J.P.Macken, H.J.Bollen and RJ.M. Belmans, "Mitigation of voltage dips through distributed generation systems", IEEE Transactions on Industrial Applications, Vol. 40, pp.1686-1693, Nov/ Dec 2004.

[3]O.Ipinnimo, S.Chowdhury "Voltage dip mitigation with DG integration: A Comprehensive Review "International Conference on power electronics and drives ,December 2012.

[4]G.Gupta and Wilfired Fritz"Voltage unbalance for power systems and mitigation techniques a servey", IEEE International Conference on power Electronics, Intelligent Control and Energy Systems, June 2016.

[5]S.V Ravi Kumar, S. Siva Nagaraju "Simulation of DG Schemes in Power Systems" ARPN Journal of engineering and applied sciences, June 2007.

[6]K.Sandhya, A.Jayalaxmi "Design of PI and Fuzzy Controllers for DG Techniques" AASRI Conference on power and energy systems ,January 2012

[7] Alavandar.S,Nigam "Adaptive Neuro-Fuzzy Inference System based control of six DOF robot manipulator" Journal of Engineering Science and Technology Review 1,2008, p. 106-111.

[8]S.V Ravi Kumar,S. Siva Nagaraju "Simulation of DSTATCOM and DVR in Power Systems" ARPN Journal of engineering and applied sciences, June 2007.

[9] Youn Soo-Young Jung, Tae-Hyun Kim, Seung-II Moon and Byng-Moon Han, "Analysis and Control of DSTATCOM for a Line Voltage Regulation" Power Engineering Society Winter Meeting January 2002.

[10] Sng E. K.K., Choi S.S., Vilathga-muwa D.M., "Analysis of Series Compensation and DC-Link Voltage Controls of a Transformer less Self - Charging Dynamic Voltage Restorer", IEEE Transactions on Power Delivery, July 2004.

[11]K.Sandhya, A.Jayalaxmi "Design of PI and Fuzzy Controllers for Dynamic Voltage Restorer (DVR) " AASRI Conference on power and energy systems ,January 2012
[12] Q. Sun, Z. Li, and H. Zhang, "Impact of Distributed Generation on Voltage Profile in Distribution System", in Proc. of International Joint Conference on Computational Sciences and Optimization, 2009.

International Journal of Engineering Research and General Science Volume 6, Issue 4, July-August, 2018
ISSN 2091-2730

INTERLEAVED THREE-PHASE THREE-LEVEL AC-DC SINGLE-STAGE PFC CONVERTER

G. Bindu[1],Mrs. K. S. L. Lavanya [2]
[1]PG Scholar, EEE, lakireddy Balireddy College of Engineering,himabindu0105@gmail.com
[2] Assistant Professor, EEE, lakireddy Balireddy College of Engineering , srilakshmilavanya@gmail.com

ABSTRACT

A new interleaved single-stage three- phase ac-dc power factor correction PFC converter is planned in this paper. The planned converter is based on the soft switching control procedure i.e; zero voltage switching with the intention that some of the switches turned on softly. The planned converter that uses phase-shift pulse width modulation (PWM) is offered at light-load conditions to get better the converters efficiency. Because of its interleaved structure the proposed converter can produce input current lacking harmonics. In this planned paper, the procedure of original converter is clarified and its features are discuss and its function is corresponding to another model converter.

Keywords: AC-DC power supplies, phase-shift pulse width modulation (PWM), three-level converters, three-phase converters, single-stage converters.

1.INTRODUCTION

Power factor correction (PFC) needs ac-dc power supplies to obey with harmonic standards IEC 1000-3-2[1].Some of the pulse width modulation (PWM) techniques are given in below points.

To get the input current more sine wave the earlier methods that uses the filters i.e; the inductors and capacitors to filter out low-frequency input current harmonics while these converters implemented with power factor correction should be expensive and simple so that these converters are also heavy and bulky. So that these applications are used limitedly. Some of the two-stage converters use a pre regulator to get the input current sine wave and the dc-dc converter will produce the desired output voltage and have to control the intermediate dc bus voltage. This converters require two separate switch-mode converters so that overall ac-dc converters price and complication is improved. The dc-dc conversion in a single power converter that can be corrected by a power factor in a single-stage power factor correction (SSPFC) converters. Depending upon two-stage converters, these converters are simple and cheap. some of the single-phase converters(5-7) and the thrre-phase converters(7-18) are planned in this prose.

In the earlier planned papers three-phase single-stage ac-dc converter have the drawbacks that can be classified as follows.

1. Here we are implementing the three separate ac-dc boost converter modules[2], [7]-[9] that can increases the cost and introduce the problems related to the synchronization of all ac-dc boost converter modules.
2. The converters used is resonant-type converters that can need the variable switching frequency control methods to operate so that the converter must be controlled by using very sophisticated techniques and/or nonstandard techniques[3]-[6].
3. Here the ac-dc converter results the output current should be discontinuous and it results a very high output ripple so that the high rating secondary diodes with peak current and large output capacitors are needed to filter out the ripples[7]-[12], [14].
4. The three-phase ac-dc converters can be exposed to very high voltages, because the three-phase ac-dc converters can be implemented with bulk capacitors and switches with very high-voltage ratings [11]-[13].
5. Three-phase converter need to have a large-input filter, that can filter out the large input current ripples as this current is discontinuous with high peaks.
6. The converter planned in [18] mitigates the above following drawbacks. Even though the proposed converter in [18] [20] these papers were an advance more than earlier planned three-phase single-stage converters, then also these converters require to operate at light-load conditions that have a irregular output inductor current to keep the dc link

capacitor below 450v and these converters will require to operate with input current that which is discontinuous which results high component stress and for the reason that of large amount of ripples in the input there is need to have a considerable filtering in the input.

The paper that which is proposed in [21] is shown in figure 1, is a new three-phase single-stage PFC AC-DC converter which is having the interleaved construction in the modern power electronics this interleaved construction is more popular[22]-[23].

The converter proposed in the paper [21] has some of the disadvantage, that the center tapped transformer is very costly to construct, which results same voltage lying on every half of the secondary windings. And the output is half of the secondary voltage, as each and every diode utilizes simply one half of the transformers secondary voltage. So that the output voltage of secondary winding of the transformer is double the times of the magnetizing voltage i.e; $2v_m$ when compared to the input power supply. Hence from the above discussion it is very clear that the cost of the circuit become expensive.

In the planned paper, interleaved three-phase three-level AC-DC single stage PFC converter with standard phase-shifted pulse width modulation (PWM) is explained and procedure of original converter is clarified and its features are discuss and its function is corresponding to another model converter.

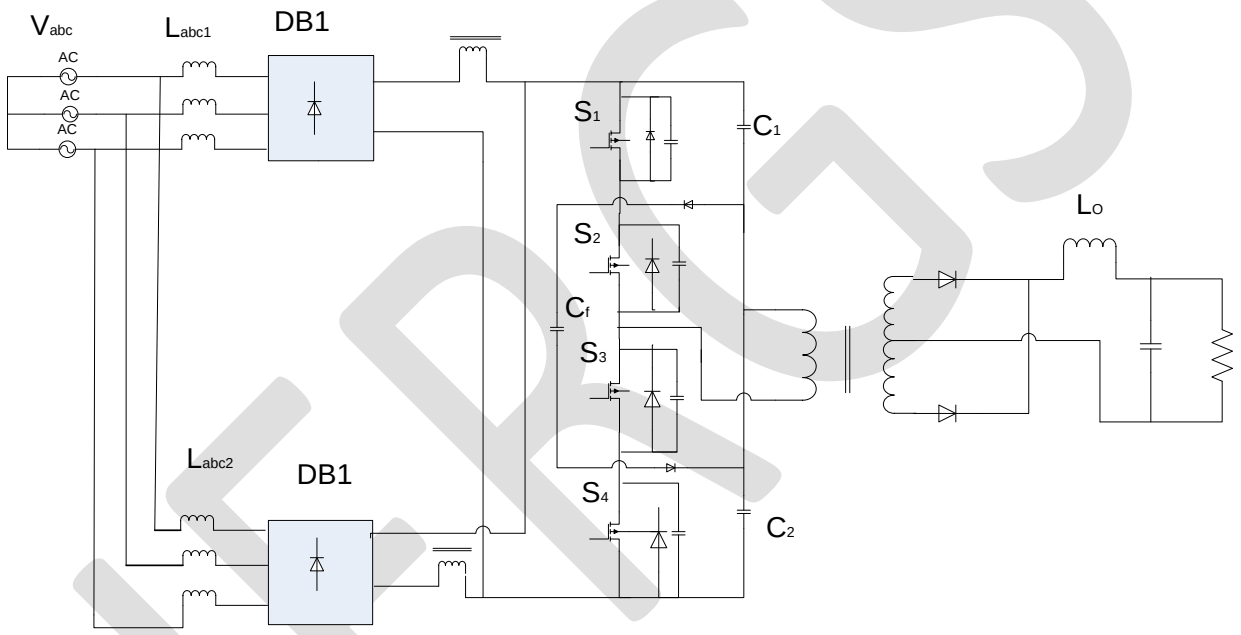

Fig. 1. Interleaved single-stage three-level converter**.**

2. CIRCUIT DESCRIPTION

The basic diagram of proposed converter is shown in figure . The basic drawing is related to that of three-phase single-stage PFC AC-DC converter as presented in the earlier paper[21]. Here v_{abc} is the three-phase ac supply voltage. The three input inductors L_{abc1} are coupled to each other to a diode bridge rectifier $DB_1$and the other three input inductors L_{abc2} are connected to each other to a diode bridge rectifier DB_2. The proposed converter can be taken from the converter transformer of additional windings that can be capable to work like a magnetic switches that can cancels the output voltage of dc-link capacitor after that this output voltage of diode bridge is zip. Here four power MOSFETs are connected with the aim of which can be termed as switches S_1,S_2,S_3,S_4 and D_1, D_2,D_3, D_4 can be reffered as the full bridge rectifier.

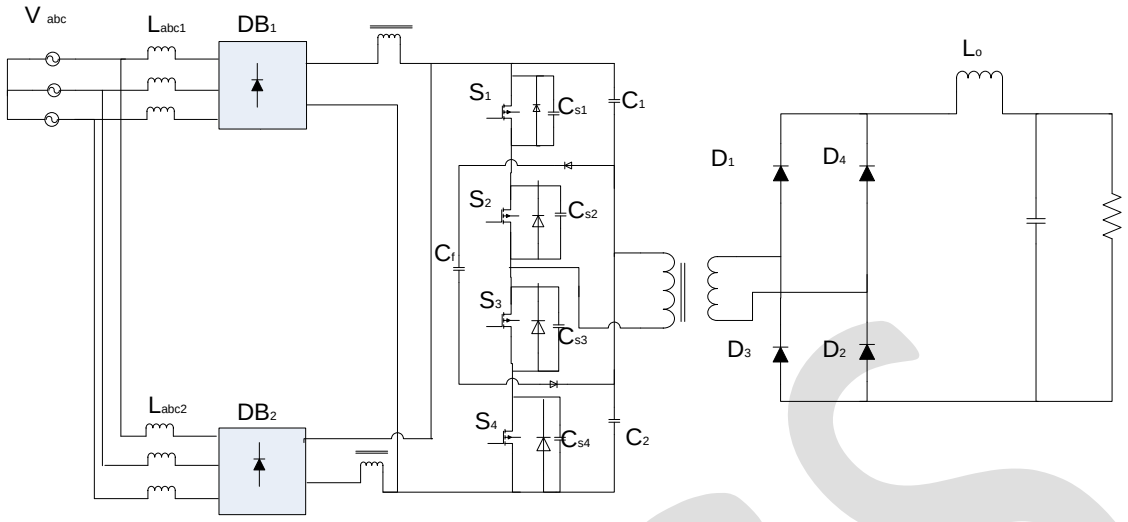

Fig. 2. Proposed topology of Three-phase three-level converter**.**

3.OPERATION OF THE CONVERTER

Mode 1($t_o \leq t \leq t_1$): In this mode of operation the switches s_1 and s_2 are turned ON. During this interval the flying capacitor C_f and both the dc bus capacitors C_1 and C_2 are charged to half of the dc bus voltage, and then the dc bus capacitor C_1 flows to the load output. Because of magnetic coupling, voltage appears from corner to corner the additional windings is equal to dc bus voltage and then this voltage totally cancels the dc bus voltage at the capacitor; then the output of the diode bridge voltage is zip so that the inductor currents iL_{a1} , iL_{b1} , iL_{C1} at the input will increase. And at the secondary side of the transformer the diodes D_1 and D_2 starts conducting at the same time to flow the energy into load.

Mode 2($t_1 \leq t \leq t_2$): In this mode of operation the switch s_1 is in turned off condition and the switch s_2 will remains ON. In the earlier mode of operation power stored in the input additional inductor starts being transferred into the dc bus capacitors then this energy will transfers into the capacitor c_{s1} charges and capacitor c_{s4} discharges through the flying capacitor c_f until the voltage across c_{s4}, the capacitance output of s_4 is clamped to zero. When switch s_4 turns ON with zero voltage switching then this mode ends, from the previous mode of operation the diodes are still conducting in the secondary side of the transformer.

Mode 3($t_2 \leq t \leq t_3$): In this mode of operation still the switch s_1 is in turned off condition and the switch s_2 will remains ON. In the earlier mode of operation stored power in the additional inductor input L_1 transfers to the dc bus capacitors. In the additional winding 1 the voltage that can be appeared is zip. The main transformer of the primary current can be passed through the diode D_1 and switch s_2. With the help of converters load side section, the output inductor current free wheels the main transformers secondary side, then the output inductor voltage is equal to $-V_L$.

Mode 4($t_3 \leq t \leq t_4$): In this mode of operation both the switches S_1 and S_2 are turned OFF. The power stored in the additional inductor input L_1 is still transferred to the dc bus capacitors. The main transformers prime current can be discharge throughout the remains diode of switch S_3 due to the enough power in the outflow inductance. With respect to the capacitor C_2 this prime current will be charged through the body diodes of switches S_3 and S_4. Whenever the switch S_3 will be switched ON then this mode ends. And the diodes D_3 D_4 are conducting at the same time in the secondary side of the transformer to flow the energy to load.

Mode 5($t_4 \leq t \leq t_5$): In this mode of operation both the switches S_3 and S_4 are turned ON and the power flows from capacitor C_2 to the load and the voltage results from corner to corner additional winding is same to that of dc bus voltage however by means of reverse polarity that can nullify the dc bus voltage. The voltage at boost inductors L_2 becomes only the rectified supply voltage of every phase and the current flowing through the each inductor increases. The energy stored in the inductor L_1 is completely discharges into the dc link capacitor then this mode will be ended. For the remaining switching cycle, the planned converter under goes S_4 through Modes 6-

10, which are equal to the Modes1-5 as an alternative of S_1 and S_2 the switches S_3 and S_4 are ON and the diode bridge DB_2 starts conducting the current as an alternative of DB_1.

As there are two sets of inductors, there will be two sets of input inductor currents which will operate in discontinuous mode. As we know that the input is sum of i_{l1} and i_{l2} this current will be produced by two sets of inductors. In order to make the current flow to converters proper selection of $L_{a1} = L_{b1} = L_{c1}$ and $L_{a2} = L_{b2} = L_{c2}$ should be made in order to obtain the currents i_{la1} and i_{la2} to overlap each other. The currents i_{l1} and i_{l2} are produced by 180 phase difference in which one of the currents has obtained by impressing the transformer primary with a positive voltage and the other by the negative voltage.

In order to generate the gating signals a standard phase shift PWM IC is used which was S_2 S_2 implemented in this paper. During one mode of operation the switches S_2 and S_3 are not acceptable to be ON at the same time as well. When the switches S_1 S_2 or S_3 S_4 are ON then the converter will be under energy-transfer mode. Similarly when S_1 S_3 or S_2 S_4 are ON then the operation will be under freewheeling mode. In one switching cycle an alternating energy-transfer and freewheeling modes takes place in a standard two-level phase shift PWM full bridge converter that corresponds to same sequence or modes.

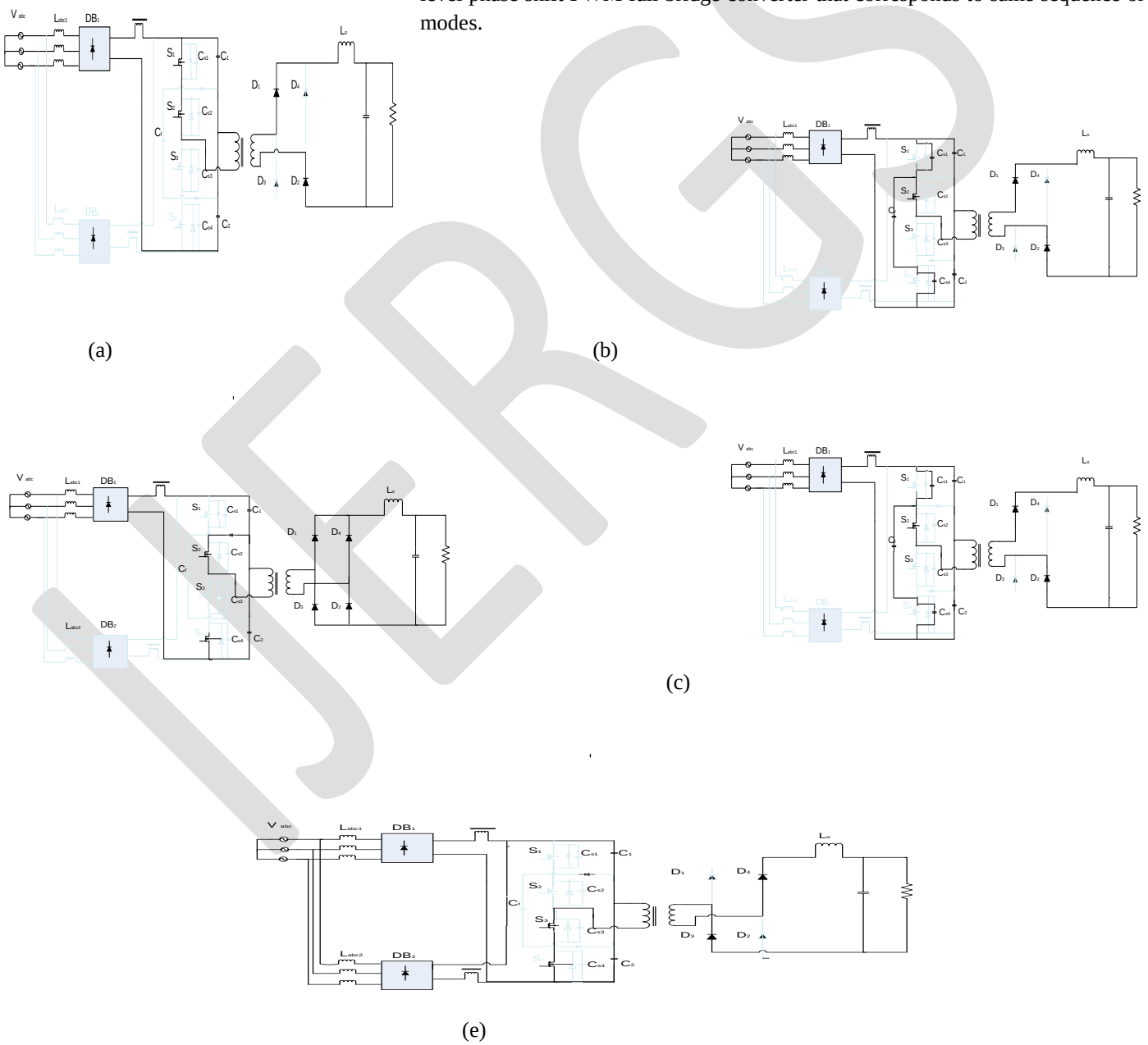

(a) (b) (c) (d) (e)

Fig. 3. Operating stages of circuit for time intervals from (a) [t_0-t_1] to (e) [t_4-t_5].

4. Design considerations

To design the planned paper the following considerations that should be taken into the account are discussed in this paper. The key parameters and its values in the planned converter are transformer turns ratio, output inductor, and input inductor are explained.

A. Transformer Turns Ratio N

The dc bus voltage at primary side is effected by the value of number of turns ratio (N). In order to discharge the bus capacitors, the turns ratio determines the load current that was presented at the primary side of the transformer. The conduction losses will be high when the number of turns ratio is low which indicates the current at primary side will be too great. And the conduction losses will be low when the number of turns ratio is high which indicates the current at primary side will be too low. In this case the converter can produce that can need the output voltage and can operate with discontinuous input and continuous output currents.

B. Output Inductor L_o

The selection of inductor should in such a that the flow of current to be in continuous modes under normal operating conditions. The voltage at the dc bus converter will be excessive when the parameter of L_o can not be too high under light-load conditions.

C. Input Inductor L_{in}

In order to maintain the discontinuous operating mode for all conditions, the parameters for L_1 and L_2 should be sufficiently less, but it should not be very less in order to result in more peak currents. The input current is obtained by addition of currents flowing through the inductors i_{L1} and i_{L2}.

D. Flying Capacitor C_f

The flying capacitor is charged to half of the dc bus voltage. Whenever the converter is operated with phase-shift PWM control, flying capacitor is in general decoupled from the converter with the exception of at some stage in assured switching transitions, for instance switch S_1 stops conducting to start Mode 2 and whenever the switch S_4 starts conducting during the equivalent mode later in switching cycle; hence there is slight chance for C_f to charge and discharge through a switching cycle. Therefore, the converter can be intended according to the design procedure given in [21] as the operation of the two converters is identical.

5.SIMULATIONRESULTS

Table 1:

Input voltage V_{in}	208±10%v
Output voltage V_o	48v
Output power P_o	1.1 KW
Switching frequency f_{sw}	100kHz
Input inductor L_{in}	140uH
Output inductor L_o	100uH
Capacitors C_1 C_2 C_f	2200uF

The planned converter is implemented with phase-shift modulation using a UC 2879 phase-shift PWM IC. The main switches were IRFP27N60KPbF, and the diodes were UF1006DICT. The converters typical waveforms are shown in Fig. 4.

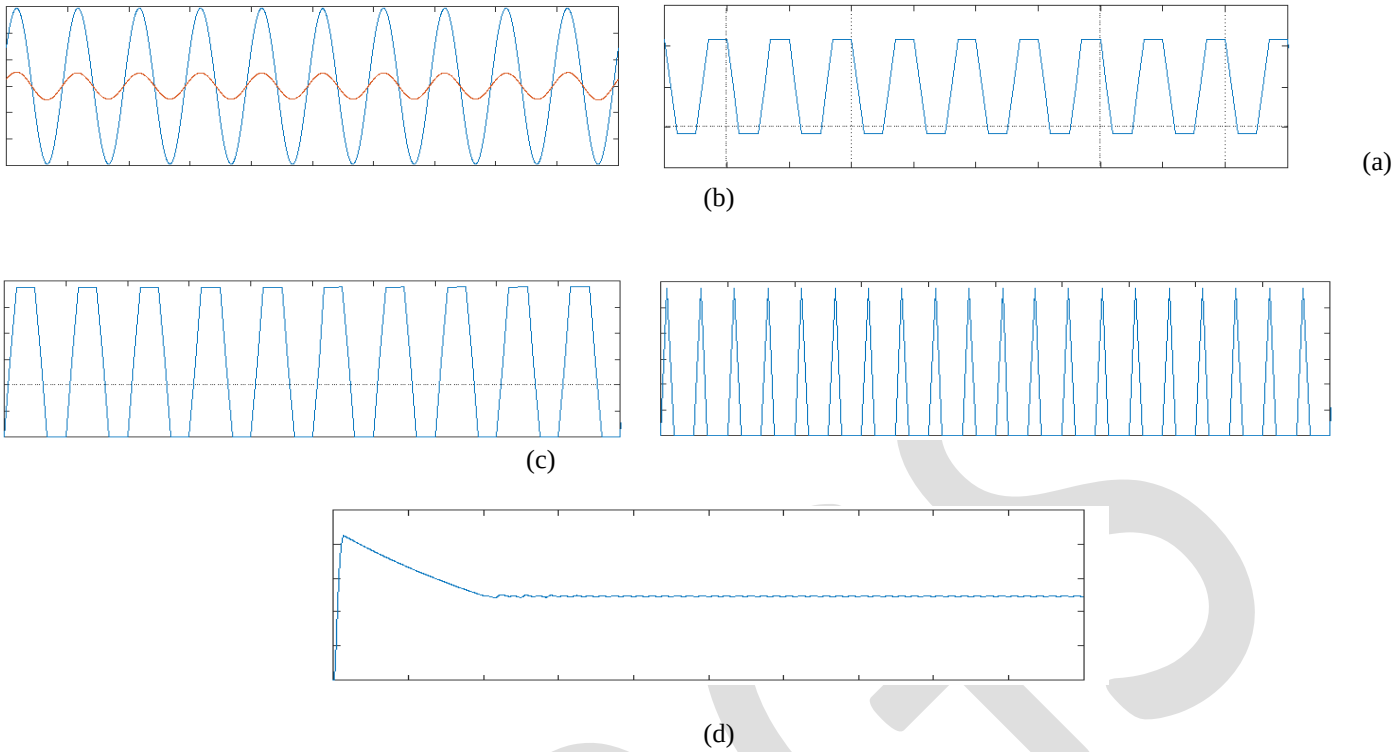

(a)

(b)

(c)

(d)

Fig.4. (a). Input voltage and current (b). Primary voltage of main transformer

(c).voltage and current at switchS_3. (d). output voltage

6.CONCLUSION

Interleaved three-phase three-level AC-DC single-stage PFC converter by using a standard phase-shift pulse width modulation was explained in this paper. . In this planned paper, the procedure of original converter is clarified and its features are discuss and its function is corresponding to another model converter. that the center tapped transformer is very costly to construct, which results same voltage lying on every half of the secondary windings. And the output is half of the secondary voltage, as each and every diode utilizes simply one half of the transformers secondary voltage. So that the output voltage of secondary winding of the transformer is double the times of the magnetizing voltage i.e; $2v_m$ when compared to the input power supply. Hence from the above discussion it is very clear that the cost of the circuit become expensive.

REFERENCES:

[1] Limits for Harmonic Current Emission (Equipment Input Current> 16A per Phase), IEC 1000-3-2, 1995.

[2] G. Spiazzi and F. C. Lee, “Implementation of single-phase boost power-factor correction circuits in three-phase applications,” IEEE Trans, Ind, Electron., vol. 44, no. 3, pp. 365-371, Jun. 1997.

[3] J. M. Kwon, W. Y. Choi, and B. H. Kwon, “Single-stage quasi-resonant flyback converter for a cost-effective PDP sustain power module,” IEEE Trans. Ind. Electron., vol. 58, no. 6, pp. 2372-2377, Jun. 2011.

[4] H. L. Cheng, Y. C. Hsieh, and C. S. Lin, “A novel single-stage high-power-factor ac/dc converter featuring high circuit efficiency,” IEEE Trans. Ind. Electron., vol. 58, no. 2, pp. 524-532, Feb. 2011.

[5] H. S. Ribeiro and B. V. Borges, “New optimized full-bridge single-stage ac/dc converters,” IEEE Trans. Ind. Electron., vol. 58, no. 6, pp. 2397-2409, Jun. 2011.

[6] N. Golbon and G. Moschopoulos, "A low-power ac-dc single-stage converter with reduced dc bus voltage variation," IEEE Trans. Power Electron., vol. 27 , no. 8, pp. 3714-3724, Jan. 2012.

[7] H. M. Suraywanshi, M. R. Ramteke, K. L. Thakre, and V. B. Borghate, "Unity-power-factor operation of three phase ac-dc soft switched converter based on boost active clamp topology in modular approach," IEEE Trans. Power Electron., vol. 23, no. 1, pp. 229-236, Jan. 2008.

[8] U. Kamnarn and V. Chunkag, "Analysis and design of a modular three-phase ac-to-dc converter using CUK rectifier module with nearly unity power factor and fast dynamic response," IEEE Trans. Power Electron., vol. 24, no. 8, pp. 2000-2012, Aug. 2009.

[9] U. Kamnarn and V. Chunkag, "A power balance control technique for operating a three-phase ac to dc converter using single-phase CUK rectifier modules," in Proc. IEEE Conf. Ind. Electron. Appl., 2006, pp. 1-6.

[10] J. Contreas and I. Barbi, "A three-phase high power factor PWM ZVS power supply with a single power stage," in Proc. IEEE Power Electron. Spec. Conf. Rec., 1994, pp. 356-362.

[11] F. Cannales, P. Barbosa, C. Aguilar, and F. C. Lee, "A quasi-integrated AC/DC three-phase dual-bridge converter," in Proc. IEEE Power Electron. Spec. Conf. Rec., 2001, pp. 1893-1898.

[12] F. S. Hamdad and A. K. S. Bhat, "A novel soft-switching high-frequency transformer isolated three-phase AC to DC converter with low harmonic distortion" IEEE Trans. Power Electron., vol. 19, no. 1, pp. 35-45, Jan. 2004.

[13] P. M. Barbosa, J. M. Burdio, and F. C. Lee, "A three-level converter and its application to power factor correction," IEEE Trans. Power Electron., vol. 20, no. 6, pp. 1319-1327, Nov. 2005.

[14] C. M. Wang, "A novel single-stage high-power-factor electronic ballast with symmetrical half-bridge topology," IEEE Trans. Ind. Electron., vol. 55, no. 2, pp. 969-972, Feb. 2008.

[15] P. M. Barbosa, J. M. Burdio, and F. C. Lee, "A three-level converter and its application to power factor correction," IEEE Trans. Power Electron., vol. 20, no. 6, pp. 1319-1327, Nov. 2005.

[16] Y. Xie, Y. Fang, and H. Li, "Zero voltage-switching three-level three-phase high-power-factor rectifier," in Proc. IEEE Ind. Electron. Soc. Conf. Rec., 2007, pp. 1962-1967.

[17] B. Tamyurek and D. A. Torrey, "A three-phase unity power factor single stage ac-dc converter based on interleaved flyback topology," IEEE Trans.Power Electron., vol. 26, no. 1, pp. 308-318, Jan. 2011.

[18] M. Narimani and G. Moschopoulos "A novel single-stage multilevel type full-bridge converter," IEEE Trans. Ind. Electron., vol. 60, no. 1, pp. 31-42, Jan. 2013.

[19] A. M. Cross and A. J. Forsyth, "A high-power-factor, three-phase isolated ac-dc converter using high-frequency current injection," IEEE Trans. Power Electron., vol. 18, no. 4, pp. 1012-1019, Jul. 2003.

[20] M. Narimani and G. Moschopoulos "A new interleaved three-phase single-stage PFC AC-DC converter," IEEE Trans. Ind. Electron., vol. 60, no. 1, pp. 648-654, Feb. 2014.

[21] M. Narimani and G. Moschopoulos "A new interleaved three-phase single-stage PFC AC-DC converter," IEEE Trans. Ind. Electron., vol. 30, no. 7, July. 2015.

[22] B. Tamyurek and D. A. Torrey, "A three-phase unity power factor single-stage ac-dc converter based on an interleaved flyback topology," IEEE Trans. Power Electron., vol. 26, no.1, pp. 308-318, Jan. 2011.

[23] N. Rocha, C. B. Jacobina, and C. D. Santos, "parallel connection of two single-phase ac-dc-ac three-leg converter with interleaved technique," in Proc. IEEE Ind. Electron. Soc. Conf., 2012, pp. 639-644.

Load 1 and load 2 are operating from t=0.5 to 1.5 and 1 to 1.5 at 3kw power. At this time interval power from comes from the grid to load. So grid power is negative at this time it means load was feed by the grid. After t=2 sec grid was continuously in off state. From this time battery power was come into picture which was shown in Fig5.2 (b). From t=2sec to t=2.5sec solar generated power was stored in battery. Now at 2kw power, at the time t=2.5sec load 1 was started and operates continuously till t=3.5 sec .t=3sec to t=3.5sec load 2 was operating with the power of 2kw. At this time interval these 2 loads feed by the battery power.

Results

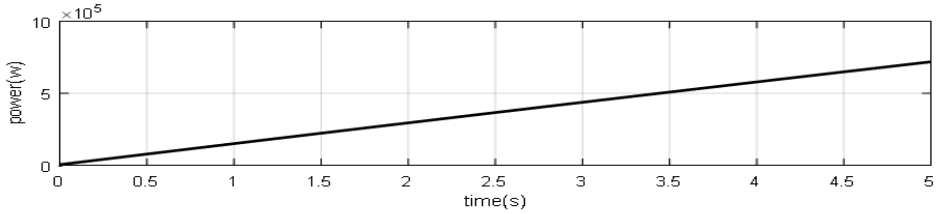

(a)

Fig 5.1 a. Dc power

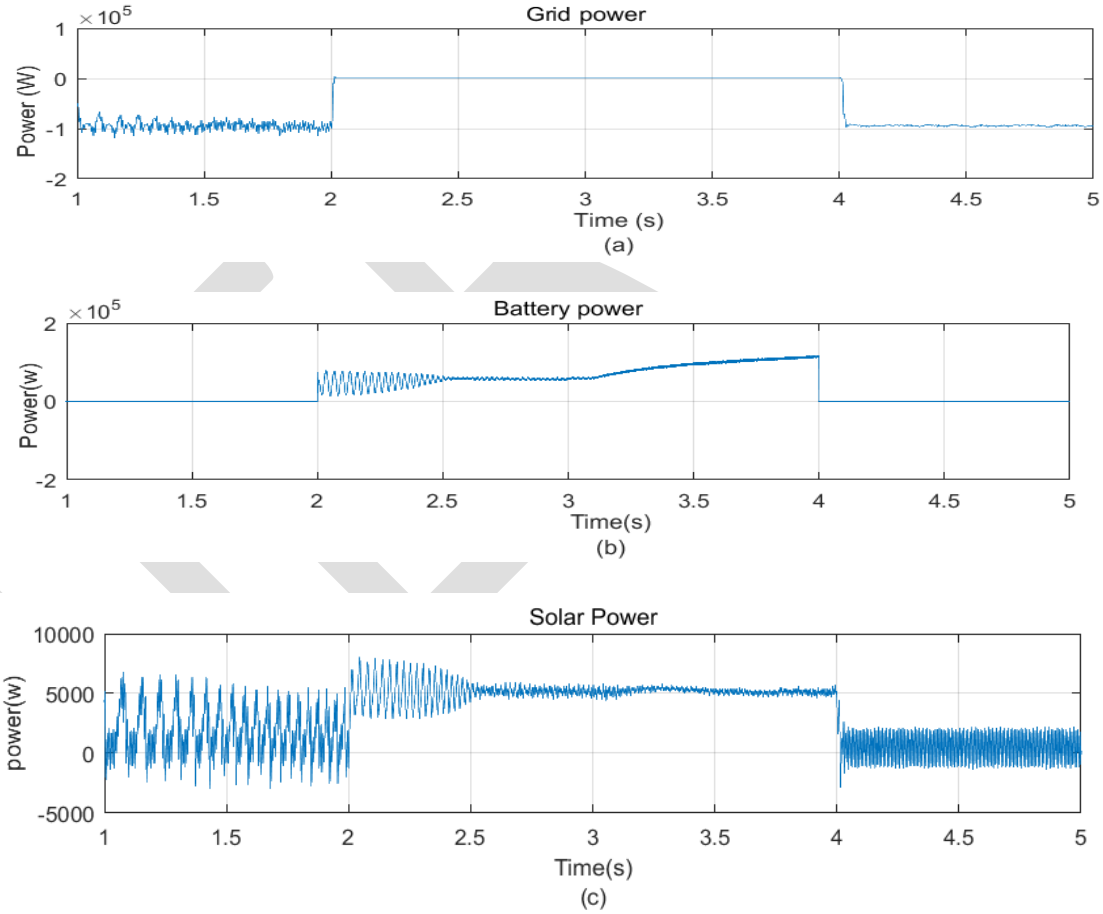

Fig 5.2: a. grid power, b. battery power, c. solar power.

International Journal of Engineering Research and General Science Volume 6, Issue 4, July-August, 2018
ISSN 2091-2730

MODELLING AND IMPLIMENTATION OF HYBRID AC/LVDC MICRO GRID

G.Supriya[1], K.Nagalinga Chary[2]

[1]PG Scholar, EEE, Lakireddy Balireddy College of Engineering,supriyasree777@gmail.com

[2] Asst.Professor, EEE, lakireddy Balireddy College of Engineering.

Abstract— AC or DC micro grid consists of different renewable sources, converters and loads connected to the power system. These have multiple reverse connections. To overcome such problems we are going through hybrid micro grid. But power management, control over the grid, and function of the hybrid grid are further difficult than an independent ac or dc grid. A hybrid ac/dc micro grid consists of various operating modes. Each converter has its controlling technique to collect optimum power from renewable energy sources. These converters will reduce the power transformation among the networks, maintain the stable operation under different supply and demand conditions. This hybrid micro-grid is outlined to operate with renewable energy sources. And it is interconnection of large AC and LVDC networks, with a bi-directional AC/DC/AC converter. And this system has radial distribution among the networks. Here wind power and solar power are the renewable sources. In the wind power, we have a wind turbine along with DFIG, same as solar power has PV farm along with boost converter which is works on MPPT technique. The system has been simulated in Simulink. The result shows the effective operation of the grid with different sources.

Keywords: PV Panel, MPPT Technique, Boost converter, LVC bus, Bi-directional converter, Wind based system, DFIG, AC/DC/AC converters.

1. LITARATURE SURVEY

We have many household items which are working on dc power. For this reason we have to convert ac power into dc power so we need to adopt another converter to convert ac to dc. Dc power utilizing drives has a problem of speed regulation. For this reason further ac/dc conversions are employed. Due to the increasing of these conversion stages, efficiency was decreased (ref 3) .To decrease these conversion stages, we have to install the small grids near by the load centers. It leads the concept of ac or dc micro grids (ref 4). AC micro grids feed the ac loads from the available ac or by converting available dc into ac (ref 4, 5). To feed the dc loads, we have to convert ac into dc which leads another conversion stages and dc power use drives has the problem of speed control so to compensate these problems we have to go through the concept of dc grids (Ref 6, 7). Due to the presence of ac loads in both cases (ac grids and dc grids), we have the problem of multiple conversions. To reduce these conversions we have to go through the concept of hybrid ac/dc micro grids. Ref (8, 9). The solution for this problem is we have to inter connect the separate ac and dc buses through a bidirectional problem to reduce the multiple conversions. The design of bidirectional converter with different control schemes was discussed in (ref 10). These all has various power quality issues those are discussed in (ref11). A main control technique is proposed to deal with the renewable energy sources (ref 16). A micro controller based controlling to balance the power in micro grid with renewable energy sources (ref 17). A hybrid ac-dc micro grid topology consists generally two sources. PV plant with battery store house and grid connected system was discussed in (ref 18). A new technique to manage PV-wind system was discussed in (ref 19). A hybrid ac-dc micro grid with different sources like diesel generator, wind farms, PV farms with battery banks was discussed in (ref 20). In case of optimization problems, hybrid ac-dc micro grid designed with the robust optimal power management system which is discussed in (ref 21). Later, low voltage concept is introduced. In case of household, office spaces and data centers usage of LVDC was increased. So for this purpose we are introduced the concept of LVDC micro grids discussed in (ref 22). These LVDC micro grids decrease the problem of multiple conversions by direct usage of the generated dc power. Household Appliances works on the voltage levels of 12v, 24v, 48v, this doesn't exceeds the level of 50v (ref 23, 24). But the concept of LVDC was extended to office appliances (ref 25).

For voltage drop analysis, different voltage levels such as 326v, 230v, 120v, 48v are done. From this detailed study we can know that 326v is more suitable for office appliances than 48v (ref 26). A hybrid grid means it is the connection of two different sources, with

their controlling networks. These 2 sources are renewable energy sources like solar irradiation, fuel cell stack, battery etc. in dc side and wind speed, ultra capacitor, diesel generator etc. in ac side.

The major cause for going through renewable energy sources is:

Nowadays we are generating electricity using non renewable energy sources like natural gas, coal, and oil and so on, these have inordinate effect on the environment as it releases huge amount of carbon dioxide to the earth's atmosphere, it causes increased amount of temperature on earth's surface, which is named as greenhouse effect. Hence, by using advanced technology, no.of ways are developed to generate electricity using renewable energy sources such as the wind and solar etc. Coming to the representation of a hybrid grid, it has two types of sources. Dc source and ac source. These both are renewable sources. These sources are connected to loads along with their converters.

2. System configuration

The system configuration was shown in below figure. It was connected with different ac and dc sources. Ac and dc loads are tied to its individual ac and dc systems. These converters are connected together with a bidirectional converter. Ac network have its corresponding sources, connected to its corresponding loads and energy storage elements. Same as dc network. In this suggested system, PV system connected to the boost converter which is works on P&O MPPT technique and it is tied to the dc bus to simulate dc source. A DFIG based wind system is tied along with their converters to ac bus to simulate ac sources. Solar irradiation and temperature, MPPT decides the output power of PV panel. A shunt capacitor is connected to PV terminals to decrease the high frequency ripples from the solar output. After this a dc-dc converter is present to boost up the low output obtain from the PV panel and now we have to maintain a dc link voltage. Three converters (boost converter, main converter, and bi-directional converter) connected to the common dc bus. Wind generating system consists of DFIG with back to back ac/dc/ac converter which is connected to a bus. These ac and dc networks are tied with a bidirectional converter to maintain the power flow between ac and dc sources.

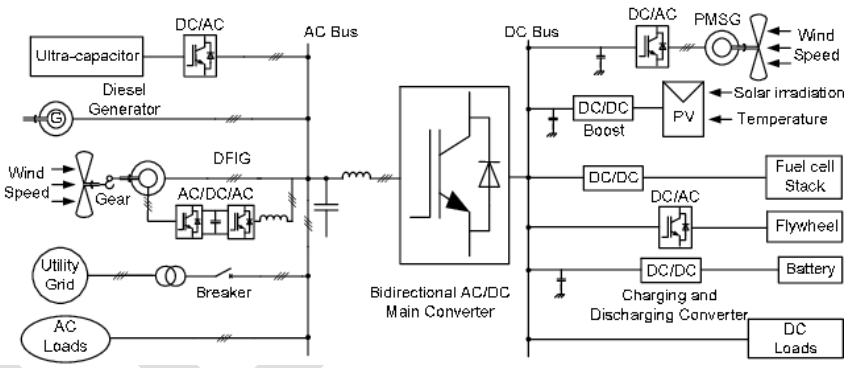

Fig.1 Proposed System

3. SYSTEM ODELLING AND DESIGNING

3.1. SOURCES:

A. Wind based system:

Wind is the main source of wind based system. Wind is caused by differences in the atmospheric pressure. Due to this differences wind moves from higher pressure to lower pressure areas. It causes different wind speeds. This system has wind turbines consisting of large no. of propellers. Propellers or blades turn around rotor due to the wind speed. Now the kinetic energy of wind is converter into rotational energy or mechanical energy. It was used to grinding grins or pumping water. The rotor was connected to the main shaft which spins the generator to generate electrical energy.

Power in the wind (P) = $\frac{1}{2}\rho\pi R^2 AV^3$

R =Radius of the blade ρ = Density of Air

A = Wind turbine rotor area V = average wind speed

A.1. Modeling of DFIG based wind generator

DFIG stator circuit directly connected to the transformer primary side and secondary side tied with the transmission line to make a common coupling point (PCC).DFIG rotor circuit tied to the ac-dc-ac converter. Here shunt capacitor to remove harmonics which are entering into the transmission system. Transformer is to provide voltage matching. DFIG based wind system has two converters. Rotor side converter and Grid side converter. Both are tied in parallel with dc link capacitor. Rotor side converter is to regulate the developed torque in DFIG by controlling the rotor current. However grid side connected converter prevents the dc bus voltage.

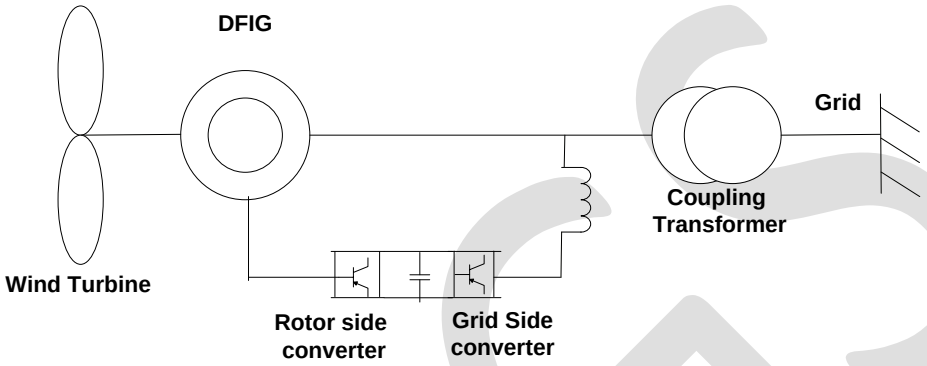

Fig.2.1 Wind Based generating station connected to the grid.

B. Solar System

Generally we have two types of technologies. Photovoltaic technology and thermal technology. Photovoltaic technology converts directly sun light into electricity. Thermal technology has dangerous amount of heat which is harmful. So here we are using photovoltaic technology. In this system we have solar panels which are connected to a converter. And Sun light is the main source. Each solar panel has no. Of PV cells and some are connected in series and some are in parallel. When sun light hits the panel, pv cells converts the solar energy into dc current. The converter is an inverter. This inverter will convert's dc power into ac power. The system can operate in two configurations – stand-alone mode and grid-connected mode. In the first method, Independent work of PV system was done that means it doesn't depends on any other power supply. And it feeds the loads by supplying electricity. So these are also called as autonomous systems. It has a storage ability (e.g. battery) it will store electricity to feed the loads during the night time or at times of poor sunlight levels and in second method, grid-connected PV system works along with the conventional distribution system. This combination is used to give electricity into grid or the loads which are connected to grid.

B.1. Modelling of PV array

Basic design of photovoltaic system consists of PV panel, dc-dc converter which is tied in series with the PV array, and a controller. This controller is used to trace the maximum power. It is essential ion photovoltaic system and it maximizes the output power and efficiency of PV system.

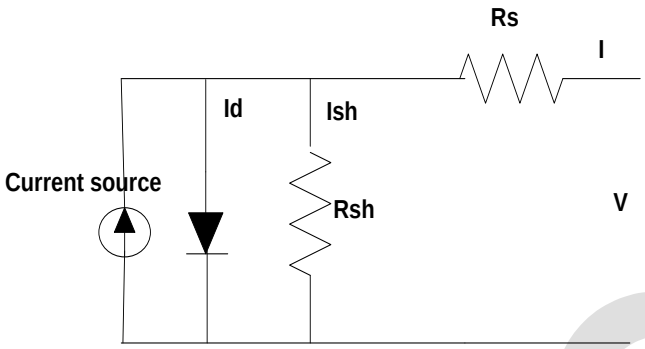

Fig.2.2.single diode PV array equivalent circuit

Basic equation to model PV array:

$$I_{PV} = I_{PH} - [I_S\left(exp\frac{q(V_{PV} + I_{PV}R_S)}{kT_CA}\right) - 1] - (V_{PV} + I_{PV}R_S)/R_P$$

We have many methods to mark out MPP. Here we are using P&O MPPT method to outline the maximum power.

Perturb & Observe MPPT technique:

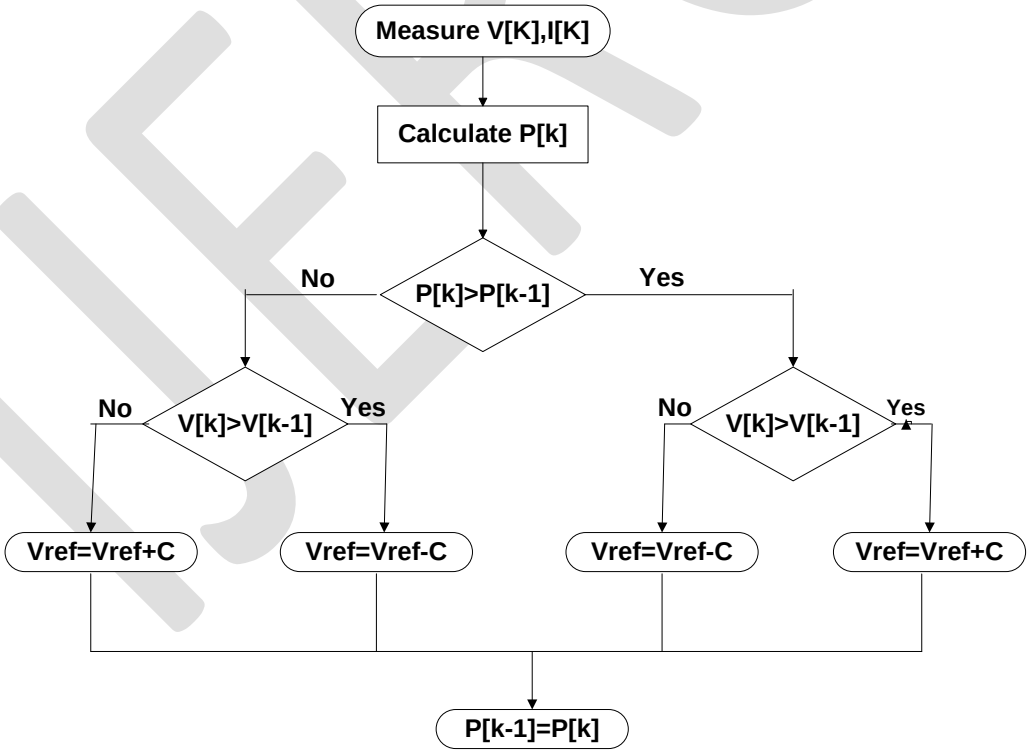

Fig.2.2 (a). P&O MPPT Technique Flow chart

4. MODELLING OF CONVERTERS:

In this hybrid grid we have three types of converters. First one is boost converter which is coupled with the PV array to trace maximum power point. To inter connect DFIG with grid ac/dc/ac converter is used. And there is a bidirectional converter which is accountable for dc bus voltage in the grid.

A. Modelling of boost converter: Commonly, in more cases boost converter is used as the MPPT converter. We may use this converter by using two control techniques. Direct duty cycle control (DDC) technique, current mode control (CMC) technique.

Direct duty cycle method:

In these both cases some resistance is added as electrical load to examine the two methods. Duty cycle of the converter switch was calculated from the previous value of duty cycle. New value of duty cycle of the converter switch is calculated by adding or subtracting the previous value of the duty cycle with the help of perturb & observation technique.

Current mode control method:

In this control variable is current. And it is obtained from the P&O method. In this method also mppt based on previous perturb value. the previous perturb value moved towards or far from the point of maximum power and from this value we can discuss that operation.

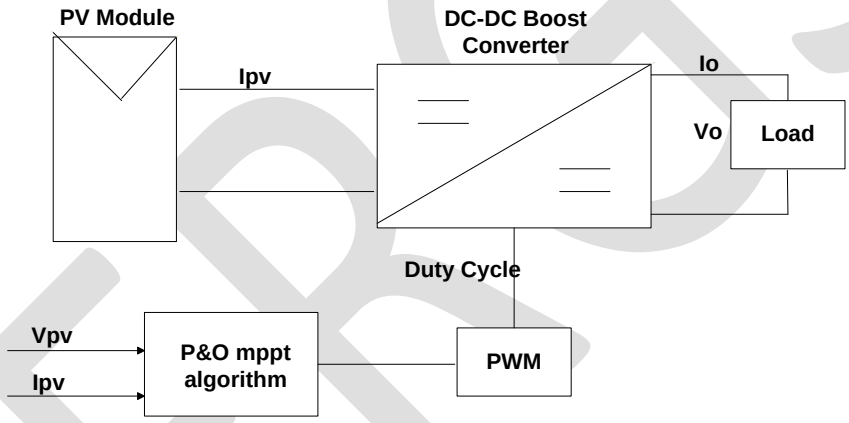

(a) Direct duty cycle control technique

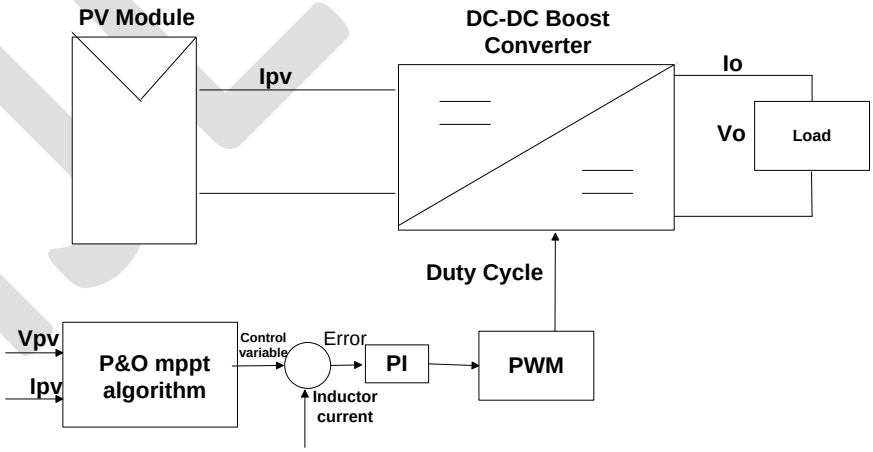

(b) Current mode control method

Fig. 3 Block diagram of P&O MPPT technique

Output voltage and current of boost converter:

$$V_0 = \frac{1}{(1-D)} V_{in}$$

$$\mathrm{I}_0 = \frac{1}{(1-D)} I_{in}$$

Where,

V_0= boost converter output voltage

I_0 = boost converter output converter

D = Duty cycle

B. Modelling of DFIG controllers:

Wind turbine system has a generator named as doubly fed induction generator (DFIG). This DFIG secondary winding is tied to the secondary winding of three phase transformer. Rotor converter which is connected to the DFIG controls the rotor current which is present in stator flux reference frame. Direct current component and quadrature current component permit the decoupling effect of torque. Direct rotor current is used in such a way as field current in synchronous generator. Quadrature rotor current, controls the generator torque to get the desired rotational speed in fluctuated speed systems.

Supply side converter named as current controlled converter. It is used to deliver rotor power to the grid at synchronous speed .vector control of grid side converter allows reactive power compensation.

C. Modelling of bi directional converter

The major aim of bi-directional converter is to interconnect ac and dc networks of the micro grid. This converter is modeled in d-q reference frame for decoupling control effect. This converter has two control loops.

Power control loop:

After power invariant conversion in d-q reference, we have to calculate the real and reactive powers. This operation describes the decoupling control. From the decoupled equations, we can derive that real power and reactive powers which are controlled by q-axis and d-axis currents.

Dc bus voltage control loop:

A voltage loop is modeled for the modulation of dc-bus voltage to the reference value. And it has a constant dc link voltage throughout the process.

f

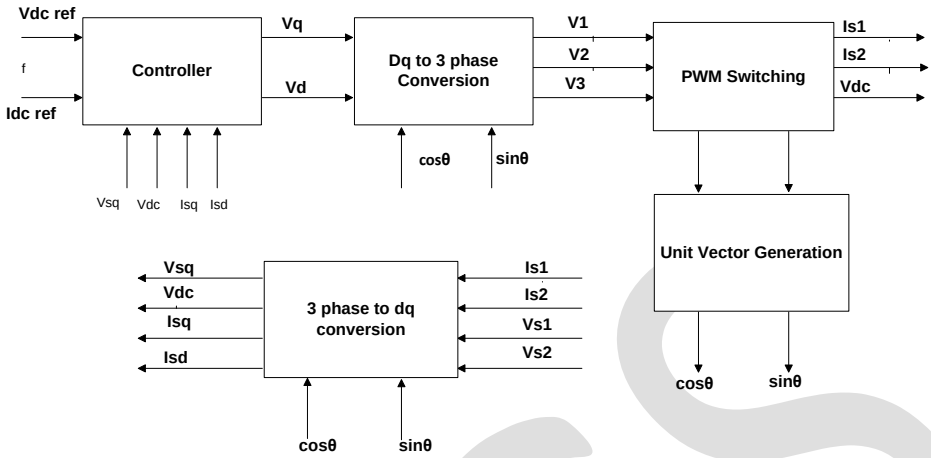

Fig.4 Block diagram of bi-directional converter

5. Simulation and results discussion:

A test system of hybrid micro grid design was done. Performance and simulation analysis of the system were studied. In this system ac network as well as dc networks are present. These both networks may have any no. of buses. Solar panel operating with the irradiance and temperature is 600w/ and c room temperature. Solar panel output graph was shown in Fig5.1 (a).From the boost converter we get the output as 850kw power shown in Fig 5.1(b). Finally after connect the LVDC bus finally from the dc side output is 8kw shown in fig 5.2(c).Ac side we have a wind turbine which is connected to the grid through DFIG and its converters. From the grid we get real power and reactive power. Here grid delivered 100kw power to the load shown in the fig5.2 (a). In this paper we have 2 loads operating from t=0 to t=5 sec. these 2 loads are single phase ac loads which are connected in parallel operating at the voltage of 200v. Load 1 and load 2 consuming the power of 3kw and 2 KW at different times. 2 loads are tie up with the grid through transformers shown in Fig 5.3(a), 5.3(b).

Now the designed mat lab file was simulated. First load operate from t=0.5sec to t=1.5sec with consuming power of 30kw. And t=2.5sec to t=3.5sec consuming the power of 20kw. Second load operate from t=1 sec to t=1.5 sec with consuming power of 30kw. And t=3sec to t=3.5sec with the power of 20kw. These two loads are operated by giving the gate signals. Solar was continuously in operating mode. Sometimes it will give the power to battery and sometimes feed the load.

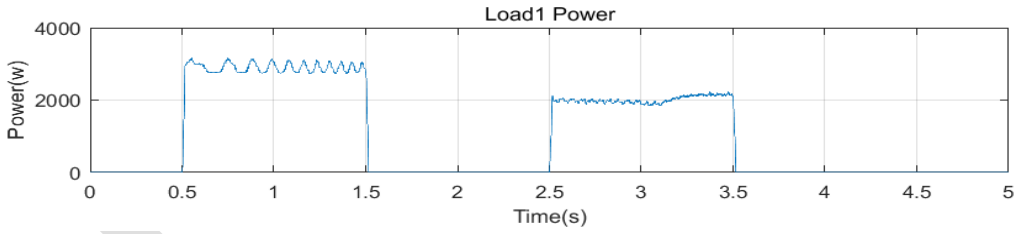

(a)

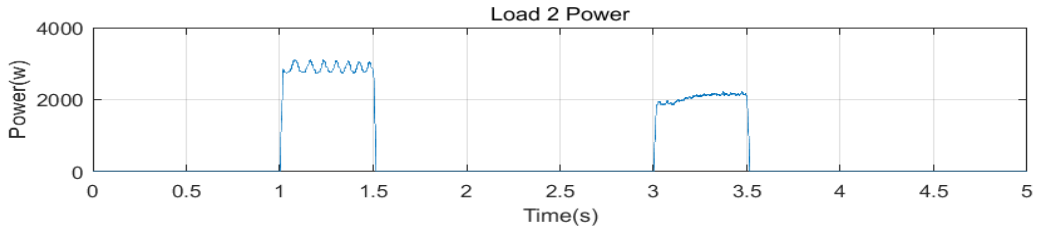

(b)

Fig 5.3. a. load 1 power. b. load 2 power

6. Conclusion

Thus, a smart hybrid AC/LVDC micro grid was considered in this paper. In the test system the design was simulated. Results are executed; verified the concept of proposed system operation and controlling. The achievement of such type of hybrid micro grids gives the more importance for the development of renewable generating systems. This paper explains complete design of sources with their controllers, and modeling of boost converter, bi directional converter with their control techniques.

REFERENCES:

- Lasseter, R.H.:'MicroGrids'.Proc.IEEE Power Engineering Society Winter Meeting, 2002.
- Baran, M.E., Mahajan, N.R.: 'DC distribution for industrial systems: opportunities and challenges', *IEEE Trans. Ind. Appl.*, 2003.
- Hammerstrom, D.J.: 'AC versus DC distribution systems – did we get it right?'. Proc. IEEE Power Engineering Society General Meeting, June 2007.
- Ito, Y., Yang, Z., Akagi, H.: 'DC micro-grid based distribution power generation system'. Proc. IEEE Int. Power Electronics and Motion Control Conf., August 2004.
- Sannino, A., Postiglione, G., Bollen, M.H.J.: 'Feasibility of a DC network for commercial facilities', *IEEE Trans. Ind. Appl.*, 2003.
- Liu, X., Wang, P., Loh, P.C.: 'A hybrid AC/DC microgrid and its coordination control', *IEEE Trans. Smart Grid*, 2011.
- Baharizadeh, M., Karshenas, H.R., Guerrero, J.: 'New control strategy of interlinking converters as the key segment of hybrid AC–DC microgrids', *IET. Gener. Transm. Distrib.*, 2016.
- Mohamed, A., Elshaer, M., Mohammed, O.: 'Bi-directional AC–DC/DC–AC converter for power sharing of hybrid AC/DC systems'. Proc. IEEE Power Engineering Society General Meeting, July 2011.
- Guerrero, J.M., Loh, P.C., Lee, T.-L., *et al.*: 'Advanced control architectures for intelligent microgrids – part II: power quality, energy storage, and AC/DC microgrids', *IEEE Trans. Ind. Electron.*, 2013.
- Akbari, M., Golkar, M.A., Tafreshi, S.M.M.: 'A PSO solution for improved voltage stability of a hybrid AC–DC microgrid'. Proc. IEEE PES Innovative Smart Grid Technologies – India (ISGT India), Kerala, December 2011.

Belvedere, B., Bianchi, M., Borgetti, A., *et al.*: 'A microcontroller based power management system for standalone micro-grids with hybrid power supply', *IEEE Trans. Sustain. Energy*, 2012

- Nilsson, D.: 'DC distribution systems'. *Licentiate of Engineering thesis, Division of Electric Power Engineering, Department of Energy and Environment*, Chalmers University of Technology, 2005.
- Ma, T., Cintuglu, M.H., Mohammed, O.: 'Control of hybrid AC/DC microgrid involving energy storage, renewable energy and pulsed loads'. 2015 IEEE Industry Applications Society Annual Meeting, Addison, TX, 2015.
- Paliwal, P., Patidar, N.P., Nema, R.K.: 'A novel method for reliability assessment of autonomous PV-wind-storage system using probabilistic storage model', *Int. J. Electr. Power Energy Syst., Elsevier*, 2014.
- Hosseinzadeh, M., Salmasi, F.R.: 'Power management of an isolated hybrid AC/DC micro-grid with fuzzy control of battery banks', *IET Renew. Power Gener.*, 2015.
- Sannino, A., Postiglione, G., Bollen, M.H.J.: 'Feasibility of a DC network for commercial facilities', *IEEE Trans. Ind. Appl.*, 2003.
- Vaessen, P.: 'Direct-current voltage (DC) in households', September 2005.
- Rodriguez, Otero, M.A., O'Neill, C.E.: 'Efficient home appliances for a future DC residence'. IEEE Conf. Energy 2003.
- Postiglione, G.: 'DC distribution system for home and office'. *MS thesis, Department of Electric Power Engineering*, Chalmers University of Technology, 2001

- Arafat, Y., Amin, M.: 'Feasibility study of low voltage DC house and compatible home appliance design'. *MS thesis, Division of Electric Power Engineering, Department of Energy and Environment*, Chalmers University of Technology, 2011

International Journal of Engineering Research and General Science Volume 6, Issue 4, July-August, 2018
ISSN 2091-2730

SINUSOIDAL PULSE WIDTH MODULATION BASED ADAPTIVE DC LINK VOLTAGE FOR CPI VOLTAGE VARIATIONS

K.RAVIKUMAR REDDY, K.SUDHEER KUMAR
[1]PG Student, Department of EEE, LBRCE College of Engineering, rkreddy1992@gmail.com,
[2] Sr. Assistant Professor, Department of EEE, LBRCE College of Engineering, ksudheerofc@gmail.com.

Abstract— This proposed model has a three-phase two step grid tied SPV (solar photo voltaic) topology. The main step is the boost converter, which fills the need of MPPT (maximum power point tracking) and sustaining the solar dc voltage to input of the PV inverter, while the second step is a two-level VSC (voltage source converter) serving as PV inverter which transfers power from a boost converter into the grid. The model likewise utilizes an adaptive voltage at DC link which is made adaptive by modifying reference DC interface voltage as per CPI (common point of intersection) voltage. Reduction of switching power losses are done through adaptive DC link voltage control. A sustained forward term for solar contribution is utilized to improve the dynamic response and the system is verified considering realistic grid voltage changes for under voltage and over voltage. The performance of proposed system is tested through MATLAB/Simulink.

Keywords— PV array, MPPT, SPWM, CPI voltage variations, DC-DC Boost Converter, Adaptive DC Link, Voltage source converter.

1. INTRODUCTION

Now a day's the majority countries are focusing on non-conventional energy sources as yield beneficial of pollution free, less cost and sufficient in nature. The process and repairs cost of generating power with non-conventional energy sources involves less difficult operation as well easy organization with grid. The non-conventional energy sources like solar and wind are being widely used as cogeneration to meet the needs of housing and commercial uses. These distributed sources have require new power electronic coherence and control techniques for rising efficiency and power quality [1-2].PV solar energy systems are classified into 2 types; there are grid interfaced and standalone system. In standalone PV systems different problems are related to battery storage energy [3-4]. As compared to standalone systems grid connected system has some advantages of effective power utilization. A grid side and PV system side need technical requirements to fulfill the safety of the PV installer and grid reliability. PV grid connected systems with some techniques are solving the issues like electromagnetic interference and harmonics distortion necessities, islanding [5-6]. Inverter is the main equipment in Grid connected system for converting DC into AC power. Only 30% -40% of power is produced from the PV panel so, for producing more power from PV panel MPPT techniques are required. In current years, no. of methods has been developed for detecting peak power [7]. Perturb and observe technique is easy implement and easy control mechanism. Main problem of P&O technique is unable to identify the peak power during unexpected changes in climate condition [8]. Frictional open-circuit voltage (FOCV) and short-circuit current (FSCC) [9-10] methods are simple and effective to obtain the peak power. Both FSCC & FOCV methods are results more power loss. INC (Incremental Conductance) MPPT is quick, accurate and easy to implement.INC conductance MPPT gives best results during unexpected changes in climate conditions. The grid connected PV system causes for generation loss by tripping case. From under and over voltages grid connected VSCs is protected. The under and over voltages nominal range is around 0.9 to 1.1 pu respectively [11]. For converter may lose control, voltage losses at converter and converter grade etc. for this reason the range of under and over voltages are small. Generally the under voltage is observed at peak load conditions. Several researchers proposed a two stage PV generation scheme [12], [15]. The chopper circuit can used a primary step which works for the determination of MPPT. The PV system works at MPP point by changing converter duty cycle. The step two is 3-phase VSC which provide the power into the distribution system. The DC link voltage maintain as constant for1-phase two step grid tied PV systems is proposed in [12]. Moreover, voltage at DC link maintains constant for 3-phase PV generation system is proposed in [13] [14]. In [15] hybrid filters losses are compact by making adaptive DC link. According to reactive power requirements of filters the voltage at DC link can be altered [16]. The 3-phase peak line voltages are less than the reference voltage of DC link for VSC current control. The 1-phase grid linked current control converter has some limitation is represented in [17]. The DC link voltage reference is retained above the maximum acceptable CPI voltage variation. For CPI voltage variations the constant voltage at DC link gives worst resultant. This paper represents a modest control structure for grid linked PV array with adaptive voltage at DC link for voltage changes at CPI. The primary stage is boost converter and secondary stage two level VSC. The constant DC link voltage has some limitations so adaptive voltage at dc link for VSC is proposed. The interfacing inductor losses at high frequency and switching power losses are reducing by adaptive DC link voltage. By introducing PVFF word in VSC to get a quick dynamic response in DC link voltage.

This paper is methodized as follows: Section 2 illustrates the system topology. In Section 3 control configuration is presented. Discussion on simulation results are clarified in Section 4. Lastly, conclusions are presented in Section 5.

2. System Topology

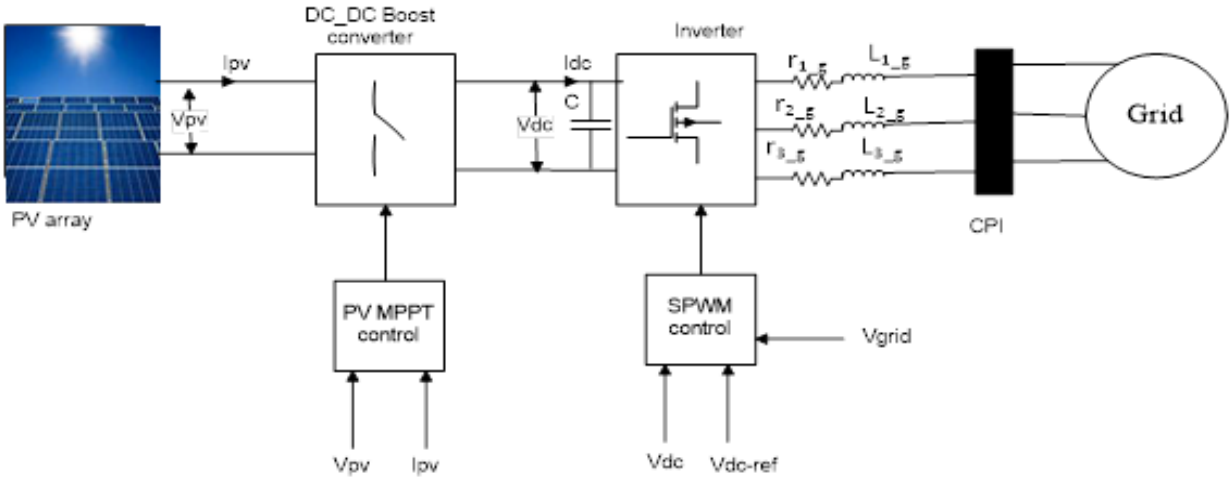

Fig.1. Block diagram of proposedSinusoidal Pulse Width Modulation based Adaptive voltage at DC Link.

The projected system configuration is shown in fig1. A sinusoidal pulse width modulation of an adaptive voltage at DC link for CPI voltage changes is divided into two stages. The primary stage is DC-DC converter with helping of MPPT. The secondary stage is DC-AC converter with two-level 3-phase VSC. The boost converter input is linked to PV array, and then the maximum power from PV array is obtained by using INC MPPT. The VSC input can connect an output of the boost converter at DC link. Based on the CPI voltage variations the DC link voltage at VSC can be slowly varied. The IGBT switches are used in 3-phase VSC. For reducing high frequency switching ripples, ripple filter can be placed between output of VSC and CPI.

3. Control Configuration

Control approach of the scheme is divided into two portions. The PV array output terminals are given to the input of boost converter. Boost converter input voltage is obtained from the MPPT algorithm then transfer to input of VSC. Maximum power at the DC link is inverted to CPI at UPF (Unity Power Factor). The system is controlled on boost converter input and output voltages are varying according to detected variable of the circuit. The INC MPPT is used to predict the reference voltage PV system voltage. The PLL (phase lock loop) fewer control is suggested for the VSC control. By using PVFF term reference grid current amplitudes are estimated and voltage error is produced by PI controller. The 3-phase VSC output currents and predictable grid voltages must be synchronized. The impedance voltage (V_p) and Irg are used in SPWM voltage controller for generating the switching pulses to VSC. The control approach of sinusoidal pulse width modulation with an adaptive voltage at DC link for CPI voltage changes with and without PVFF is shown in fig2, fig3.

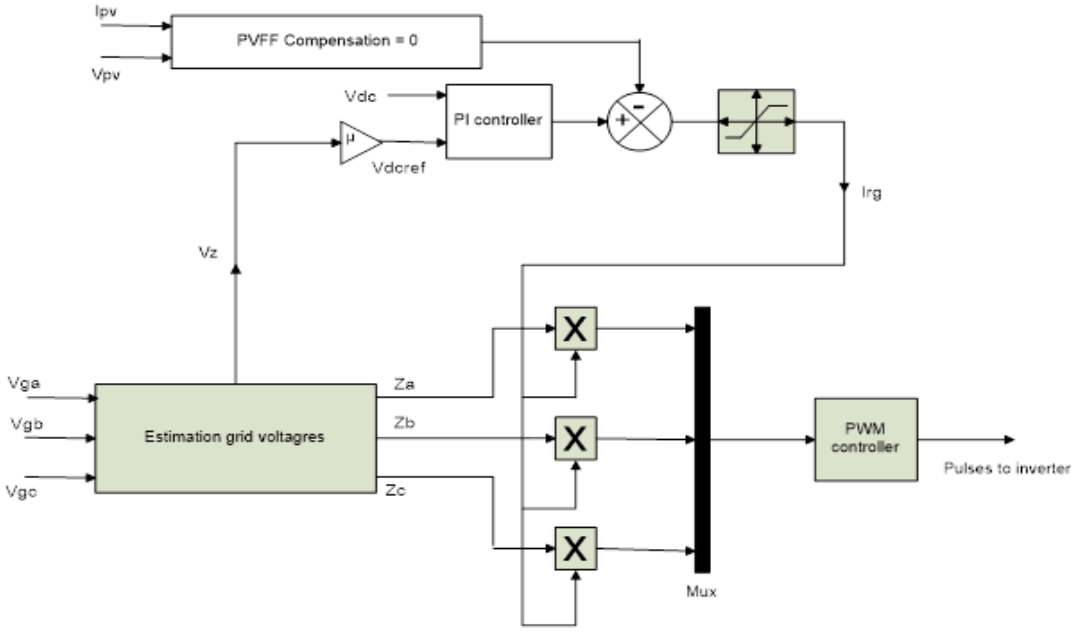

Fig2. Sinusoidal Pulse Width Modulation technique without PVFF

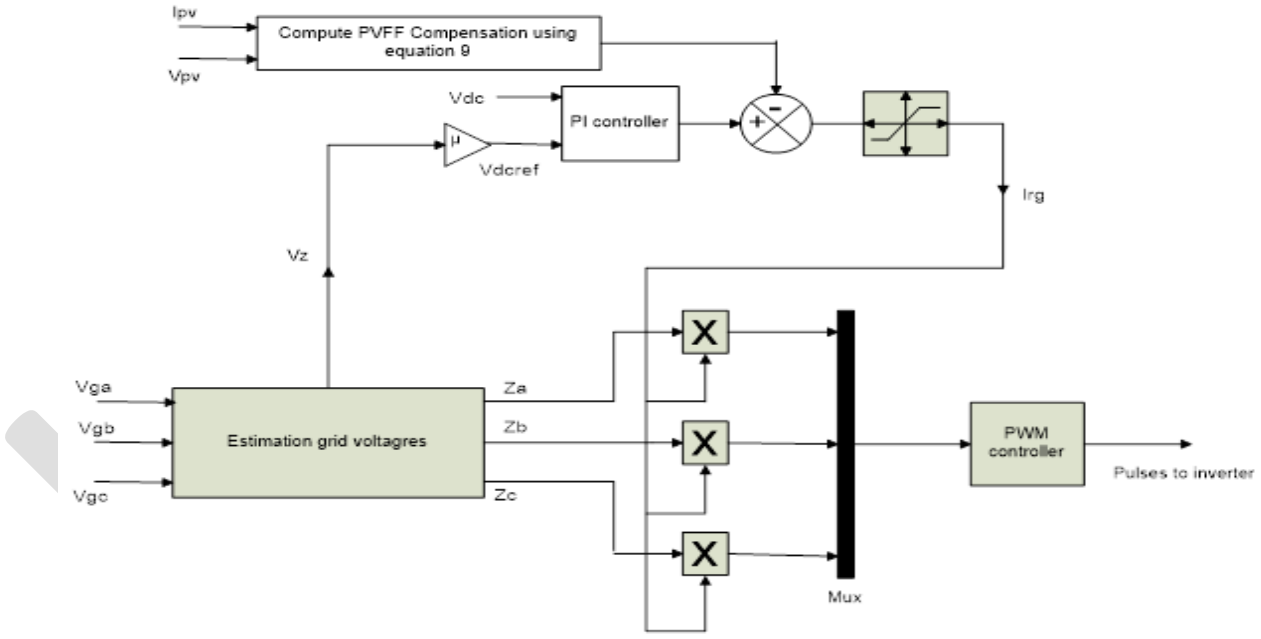

Fig3. Sinusoidal Pulse Width Modulation technique with PVFF

I. Incremental Conductance MPPT

The INC algorithm is reducing error between instantaneous conductance and INC conductance of PV array. INC MPPT algorithm estimate the peak power by differentiate the power output of PV panel with PV voltage is shown in equation 1

$$\frac{dP_{pv}}{dV_{pv}} = \frac{d(I_{pv} * V_{pv})}{dV_{pv}} = I_{pv} + V_{pv}\frac{dI_{pv}}{dV_{pv}} \qquad (1)$$

At MPP solution of the above equation is zero, negative solution gives right of the MPP and positive gives left side of the MPP are shown in equation 2, 3 and 4.

$$\frac{\Delta I_{pv}}{\Delta V_{pv}} = \frac{-I_{pv}}{V_{pv}} \qquad (2)$$

$$\frac{\Delta I_{pv}}{\Delta V_{pv}} < \frac{-I_{pv}}{V_{pv}} \qquad (3)$$

$$\frac{\Delta I_{pv}}{\Delta V_{pv}} > \frac{-I_{pv}}{V_{pv}} \qquad (4)$$

II. VSC control approach

The VSC control algorithm is presented in fig2and fig3. The VSC control algorithm main objective is maintain DC link voltage to set reference value. The maximum power at DC link voltage is inject into the grid at UPF with the respect CPI. The grid currents are estimated for controlling the VSC output currents. In phase unit vectors are multiplied with estimated grid currents to keep stable and sinusoidal grid currents. The voltage at DC link (Vdc), line voltages at CPI (Vga, Vgb and Vgc) and the grid currents (Iga, Igb and Igc) are detected. The in-phase unit vectors are expected from phase voltages (V_p) and it is expected from line voltages at CPI. Za, Zb and Zc are the estimated unit vectors.

Estimated CPI voltage amplitudes are,

$$V_p = \sqrt{\frac{2(Vga^2 + Vgb^2 + Vgc^2)}{3}} \qquad (5)$$

Estimated 3-phase unit vectors,

$$Z_a = \frac{V_{ga}}{V_p}, Z_b = \frac{V_{gb}}{V_p}, Z_c = \frac{V_{gc}}{V_p} \qquad (6)$$

For output current of VSC is properly control, the line voltage must be less than the DC link voltage of VSC. The voltage at DC link $V_{dc\,ref}$ is varies with respect to the CPI voltage.

$$V_{dc\,ref} = \mu\sqrt{3V_z}, \quad \text{where } \boldsymbol{\mu}>1 \qquad (7)$$

The CPI voltage must be less than the 10% of DC reference voltage. Drip through switches, interfacing inductor resistances are considered for appropriate current control. Later in the projected work $\boldsymbol{\mu}$ is considered as 1.1.The DC link voltage is set to reference of DC link voltage by PI controller. The difference between reference voltage and DC voltage are given to PI controller. For study state PI controller output is considered as loss component, grid currents amplitudes are contain of 2 quantities which are the input from the PV array and loss components. Estimated loss component is,

$$I_{loss}(k) = I_{loss}(k=1) + K_p\{(V_e(k) - V_e(k-1)\} + K_i V_e(k) \qquad (8)$$

The PVFF word for PV system impact on grid currents is predictable for various changes in PV irradiation and grid voltages and gets quick dynamic response. The estimated PVFF word as,

$$I_{PVg} = \frac{2P_{pv}}{3V_z} \qquad (9)$$

The CPI output currents can expected and considered grid currents direction. Grid loss is drawn where PVFF is served into grid. Estimated grid currents amplitude is,

$$I_{rg} = I_{loss} - I_{PVg} \qquad (10)$$

The amplitude of grid current is estimated I_{rg} is multiplied with the grid voltages, amplitude of 3-phase(V_p)is given to unit delay 1/z then connected to pulse generator for generating the switching pulse to VSC.

4. Discussion on Simulation results

I. Case 1(PV system without feed forward loop)

The system act below sudden change in irradiation from 1000 w/m^2 to 500 w/m^2 without the PV feed forward compensation. Shown in fig4 (a), the scheme under steady state condition with solar PV irradiation change at time t=0.3s. The grid power can balanced and sinusoidal but the Ig(A) are decreased due to irradiation change at time t=0.3s are shown in fig4 (a). The PV array current Ipv(A) and voltage Vpv(V) are shown in fig4 (a) for PV irradiation can changed 1000 w/m^2 to 500 w/m^2. The PV array power for different irradiation at time t=0.3s as shown in fig4 (a). It can be detected that the dynamic response PV array system for unexpected change in irradiation level to well suggested system. The PI controller constructed system have been show more deviation and lengthier time to settle as compare suggested system in DC link voltage without PV feed forward based control approach with compensation. The voltage at Dc link Vdc (V) is reformed from 620V to 585Vfor different irradiation at time t=0.3s is shown in fig4 (a). The suggested system control approach as soon as reached the next formal and it's reducing the grid power.

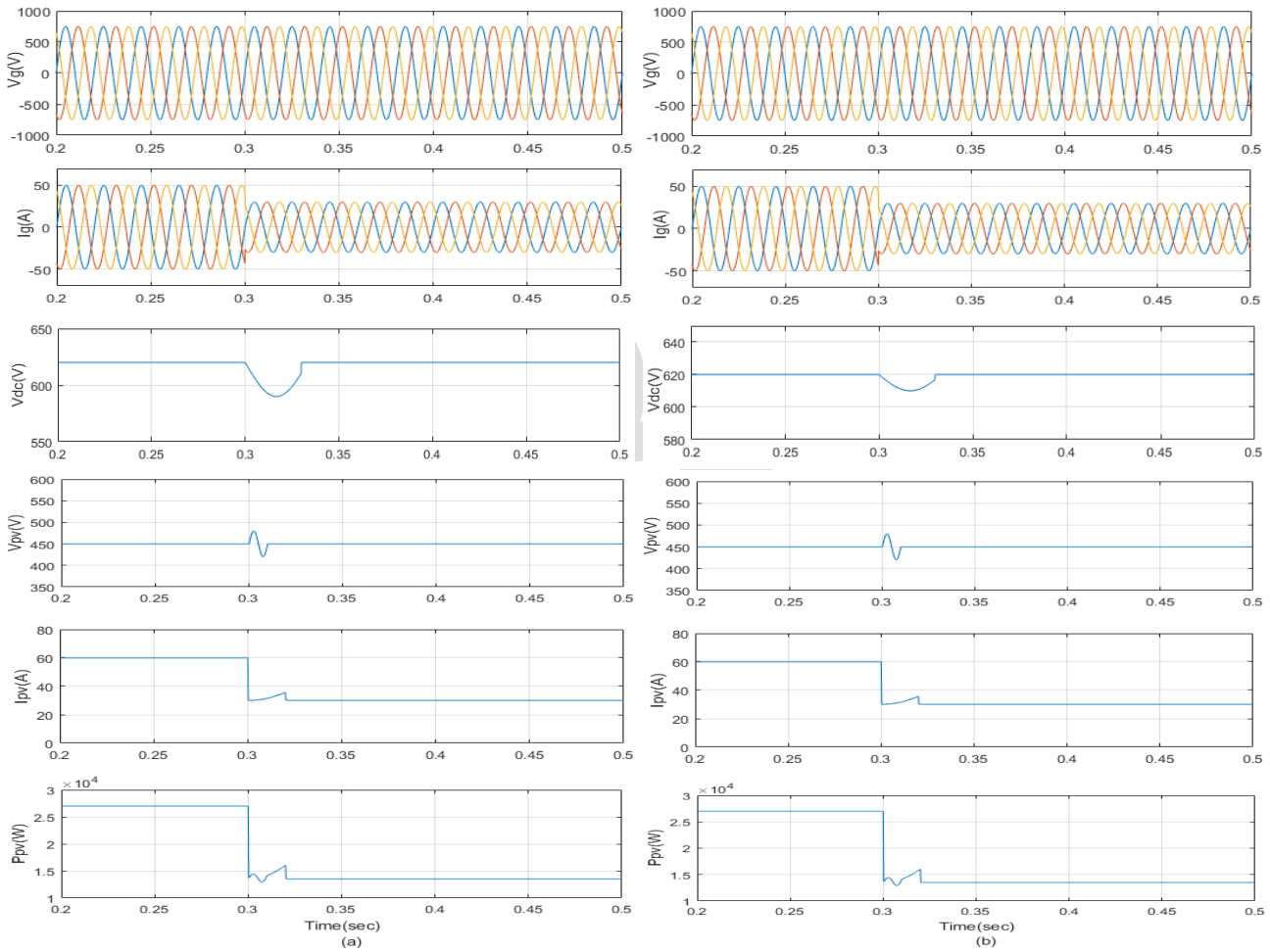

Fig.4simulation results for (a) variation in irradiation of PV array without PV feedforward loop, (b) variation in irradiation of PV array with PV feedforward loop.

II. Case2 (PV system with feed forward loop)

The system act as under sudden change in irradiation from 1000 w/m^2 to 500 w/m^2 with the PV feed forward compensation. Shown in fig4 (b), the scheme under steady state condition with solar PV irradiation change at time t=0.3s. The grid power can balanced and sinusoidal but the Ig(A) are decreased due to irradiation change at time t=0.3s are shown in fig4 (b). The PV array current Ipv(A) and voltage Vpv(V) are shown in fig4 (b) for PV irradiation can changed 1000 w/m^2 to 500 w/m^2. The PV array power for different irradiation at time t=0.3s as shown in fig4 (b). It can be detected that the dynamic response PV array system for sudden change in

irradiation level to well suggested system. The PI controller based system have been show less deviation and settling time is less as compare suggested system in DC link voltage with PV feed forward based control approach with compensation. The voltage at Dc link Vdc (V) is changed from 620V to 610V for different irradiation at time t=0.3s is shown in fig4 (b). The suggested system control approach as soon as reached the next formal and it's reducing the grid power.

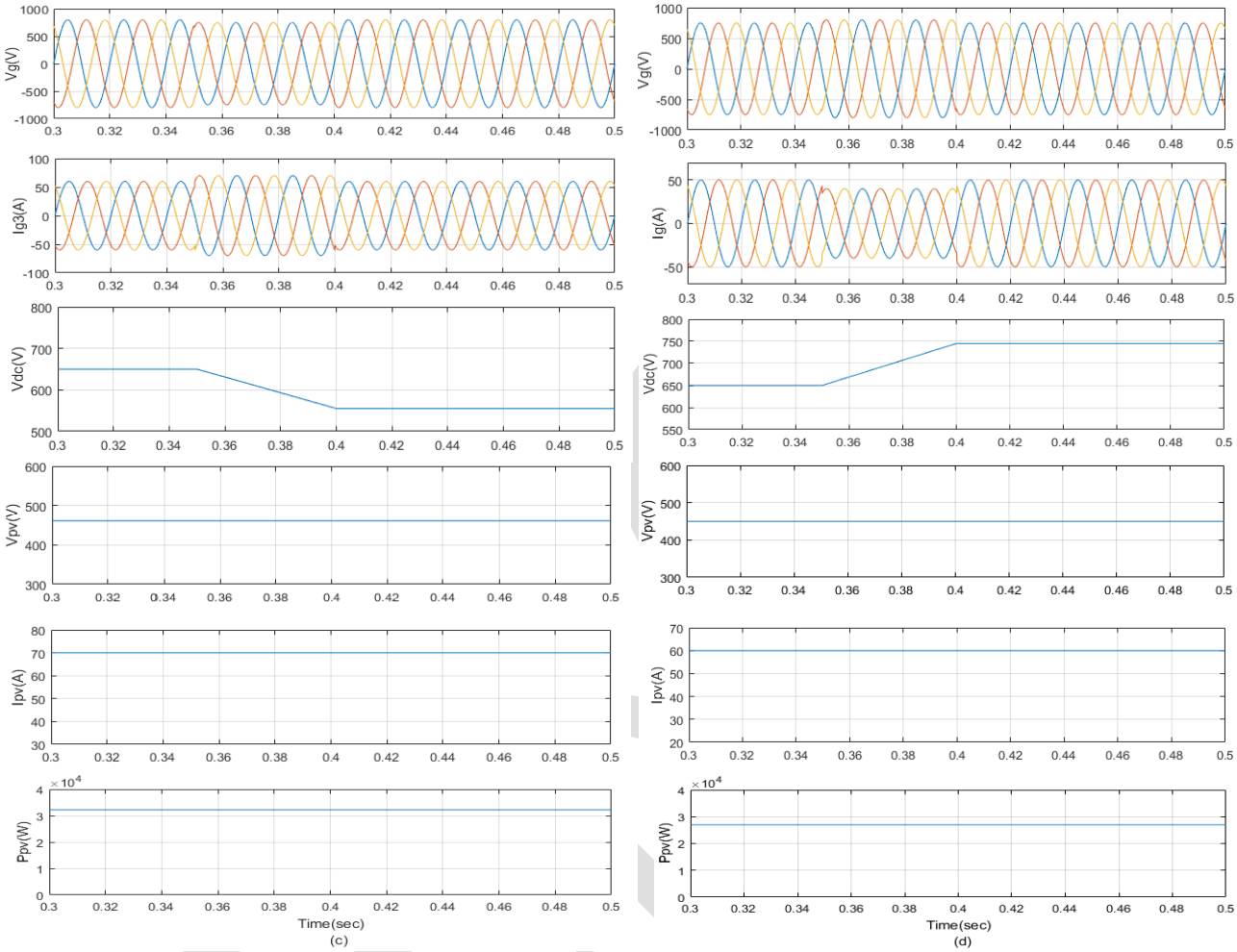

Fig.5simulation results for (a) Under voltage at CPI (415 V to 350 V), (b) Over voltage at CPI (415 V to 480 V).

III. Case 3 (Under Voltage Operation)

The system act as under voltage operation at CPI in steady state and dynamics. The CPI operating voltage is 415V up to time t=0.35s. At CPI the voltage Vg (V), will be decreased to 350V after the time t=0.35s are shown in fig5 (a). The CPI voltage variation is effect on the DC link voltage. The sinusoidal and balanced grid currents Ig (A) are maintained however the grid currents can be increased at time t=0.35s are shown in fig5 (a). No variations is observed at PV system voltage Vpv(V), PV system current Ipv(A), PV system power Ppv(W) are shown in fig5 (a).

IV. Case 4 (Over Voltage Operation)

The system act as over voltage operation at CPI in steady state and dynamics. The CPI operating voltage is 415V up to time t=0.35s. At CPI the voltage Vg(V), will be increased to 480V after the time t=0.35s are shown in fig5 (b). The CPI voltage variation is effect on the voltage at DC link. The sinusoidal and balanced grid currents Ig(A) are maintained however the grid currents can be decreased at time t=0.35s are shown in fig5 (b). No variations is detected at PV system voltage Vpv(V), PV system current Ipv(A), PV system power Ppv(W) are shown in fig5 (b).

5. CONCLUSION

A three-phase grid connected two-stage system has been developed for solar PV system. To control the boost converter composite InC based MPPT algorithm is used. The CPI voltage variation for the different ranges can be demonstrated by proposed topology. Control of grid tied VSC has been proposed by using a modest and novel adaptive DC link voltage control. The CPI voltage changes makes

voltage at dc link is adaptive which helps in reduction of losses in the system. For obtains fast dynamic response a PV array feed forward term is used. A feed forward compensation of DC link voltage control loop has been established and evaluated. The PV array feed forward term is selected for the change in PV power and CPI voltage changes. The grid tied VSC strategy is tested on the knowledge of adaptive voltage at DC link, for the given PV array and the same control mechanism can be extended to connected grid interfaces to devices such as, STATCOM, D-STATCOM etc. The simulation results have established the feasibility of suggested control algorithm.

REFERENCES:

[1] Jinwei He, Yun Wei Li, Blaabjerg, F., "Flexible Microgrid Power Quality Enhancement Using Adaptive Hybrid Voltage and Current Controller," IEEE Trans. Ind. Electron., vol.61, no.6, pp.2784-2794, June 2014

[2] Weiwei Li, Xinbo Ruan, Chenlei Bao, Donghua Pan, Xuehua Wang, "Grid Synchronization Systems of Three-Phase Grid-Connected Power Converters: A Complex-Vector-Filter Perspective," IEEE Trans. Ind. Electron., vol.61, no.4, pp.1855-1870, April 2014.

[3] H.Wang and D. Zhang, "The stand-alone PV generation system with parallel battery charger," in *Proc. Int. Conf. Elect. Control Eng. (ICECE'10)*, 2010, pp. 4450–4453.

[4] D. Debnath and K. Chatterjee, "A two stage solar photovoltaic based standalone scheme having battery as energy storage element for rural deployment," *IEEE Trans. Ind. Electron.*, vol. 62, no. 7, pp. 4148–4157, Jul. 2015.

[5] I. J. Balaguer-Álvarez and E. I. Ortiz-Rivera, "Survey of distributed generation islanding detection methods," *IEEE Latin Amer. Trans.*, vol. 8, no. 5, pp. 565–570, Sep. 2010.

[6] W. Xiao, F. F. Edwin, G. Spagnuolo, and J. Jatskevich, "Efficient approaches for modeling and simulating photovoltaic power systems," *IEEE J. Photovoltaics*, vol. 3, no. 1, pp. 500–508, Jan. 2013.

[7] B. Subudhi, R. Pradhan, "A Comparative Study on Maximum Power Point Tracking Techniques for Photovoltaic Power Systems," IEEE Trans. Sustain. Energy. vol. 4, no. 1, pp.89-98, Jan 2013.

[8] A. Pandey, N. Dasgupta, and A. K. Mukerjee, "Design issues in implementing MPPT for improved tracking and dynamic performance," in *Proc. IEEE IECON*, 2006, pp. 4387–4391.

[9] B. Bekker and H. J. Beukes, "Finding an optimal PV panel maximum power point tracking method," in *Proc. 7th AFRICON Conf. Africa*, 2004, pp. 1125–1129.

[10] N. Mutoh, T. Matuo, K. Okada, and M. Sakai, "Prediction-databased maximum-power-point-tracking method for photovoltaic power generation systems," in *Proc. 33rd Annu. IEEE Power Electron. Spec. Conf.*, 2002, pp. 1489–1494.

[11] M. E. Ropp, J. G. Cleary, and B. Enayati, "High penetration and antiislanding analysis of multi-single phase inverters in an apartment complex," in *Proc. IEEE Conf. Innovative Technol. Efficient Reliab. Electr.Supply (CITRES'10)*, 2010, pp. 102–109.

[12] S. Deo, C. Jain, and B. Singh "A PLL-Less scheme for single-phase grid interfaced load compensating solar PV generation system," *IEEE Trans.Ind. Informat.*, vol. 11, no. 3, pp. 692–699, Jun. 2015.

[13] B. Singh, D. T. Shahani, and A. K. Verma, "Neural network controlled grid interfaced solar photovoltaic power generation," *IET PowerElectron.*, vol. 7, no. 3, pp. 614–626, Jul. 2013.

[14] C. Jain and B. Singh "A frequency shifter based simple control for multifunctional solar PV grid interfaced system," in *Proc. 37th Nat. Syst. Conf.*, 2013, pp. 363–374.

[15] C.-S. Lam,W.-H. Choi, M.-C.Wong, and Y.-D. Han, "Adaptive DC-Link voltage-controlled hybrid active power filters for reactive power compensation," *IEEE Trans. Power Electron.*, vol. 27, no. 4, pp. 1758–1772, Apr. 2012.

[16] C.-S. Lam, M.-C. Wong, W.-H. Choi, X.-X. Cui, H.-M. Mei, and J.-Z. Liu, "Design and performance of an adaptive low-DC-voltagecontrolled LC-hybrid active power filter with a neutral inductor in threephase four-wire power systems," *IEEE Trans. Ind. Electron.*, vol. 61, no. 6, pp. 2635–2647, Jun. 2014.

[17] Y.-M. Chen, H.-C. Wu, Y.-C. Chen, K.-Y. Lee, and S.-S. Shyu, "The AC line current regulation strategy for the grid-connected PV system," *IEEETrans. Power Electron.*, vol. 25, no. 1, pp. 209–218, Jan. 2010.

International Journal of Engineering Research and General Science Volume 6, Issue 4, July-August, 2018
ISSN 2091-2730

Sequential Work Place Layout Planning to Achieve Rapid Production Rate

Jitendra Yadav, Prakash Girewal, K.K.Shahu

Vikrant Institute of Technology and Management Indore, jitendrayadav1690@gmail.com

Abstract— In this modern world, we are well aware about the Manufacturing technologies and methodologies. Industries are to adjusting new and more and more machineries and methods but by these approaches, Sequential Work Place Layout Planning to Achieve Rapid Production Rate Abstract In this modern world, we are well aware about the Manufacturing technologies and methodologies. Industries are to adjusting new and more and more machineries and methods but by these approaches, industries are adopting this method for profit. Some of the methodologies is completely changing the world and this kind of technologies companies are adapting too quick and responsively. In this thesis, we are exploring and integrating some of the methodology such as Six Sigma approach and Sequential Operational Production Planning. For controlling this process, we are integrating sequential operational production planning to achieve rapid production rate and higher sigma level. It is alarmed with changing materials into things and services, as professionally it is possible to make maximum profit for it also contains that the management generate the maximum level of Sigma imaginable within a body.

Keywords— Operation Management; Production Process; Sequential Planning; Manufacturing; Sigma Level, Work place layout.

INTRODUCTION

This paper belongs to generate maximum output from a process, which involves about well-designed sequenced planning process these are unified plans to reach maximum productivity. We are incorporating three process together in sequenced planning process first we practical a proper disreputable as operation management it will work like a platform for the other executing technologies in which we are effecting work place layout planning/management/design which will requirement we will relate as per supplies for. In resulting we will use the inbounds supply chain for supervision arrangement for the avoiding lack of the raw measureable and it will also assistance for the save store quickly managed and it will uphold a lowest level of inventory for controlling the over roster, short stock time of raw material and over inventory. In additional next preparation, we are applying the inventory management for the inventory consumption and decreasing inventory-carrying cost. Inventory carrying cost can help to boost the financing conditions of the company it will help to achieve higher productivity. These methodologies will perform the planning under the platform of the operation management the function of operation management is in that dissertation is to only control the complete process which can result on preparation in Work place design/planning/management, Inbound organized supply chain supervision and inventory controlling. After successfully implementation, this methodology can achieve the highest productivity. Rosters that are mishandled can create important financial glitches for a commercial, whether the mishandling results in an inventory glut or an inventory shortage. To regulatory this procedure, we are mixing Operations management is worried with materials into things and facilities as professionally as likely to maximize the income of a Body. It also consists that the management of commercial performs to make the uppermost level of competence likely within an institute. The methods they are attainment at an incomplete fraction of output and effectiveness. We performing for an appearance of Methodical process &

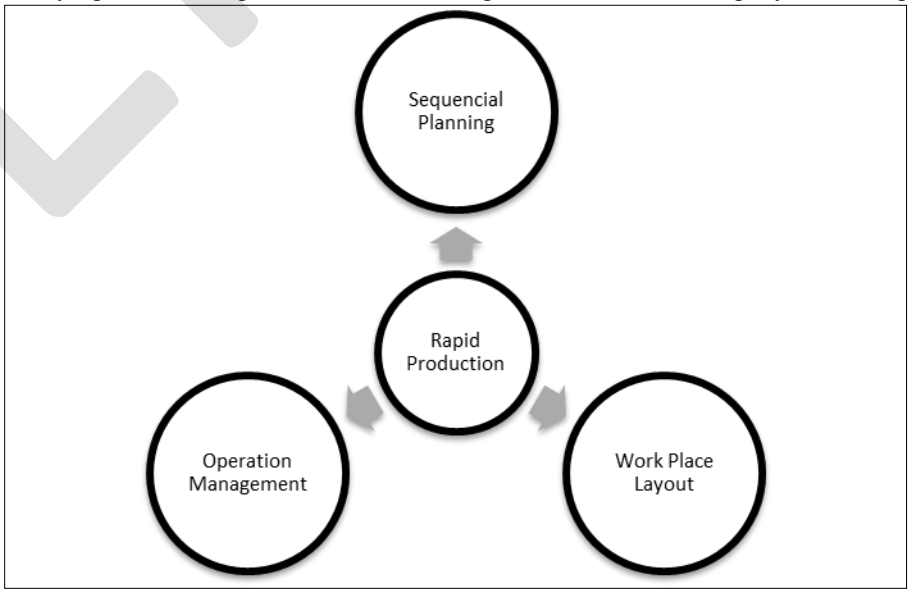

Figure 1- Rapid Production System

mixing these major plans for the better efficiency and the productivity. We are merging preparation of production over a scheme of Operation Running amalgamation through subsystems of this progression as Work Place Layout, Incoming Supply Chain and Schedule Management Scheme for the better output.

LITERATURE REVIEW

Chris Voss, Nikos Tsikriktsis and Mark Frohlich, International Journal of Operations & Production Management - Research based on the investigation of the Pure Case investigation and the limited quantitative consequences of the research can be made; the best only limited statistical analysis. Which is widely used in Europe, although it is the North American agency (Drezer et al., Paneerselvann et al., 1999) published a case study and field study at 4.94% and 3.80%. However, there is a cumulative number of documents based on CASE RESEARCH: The case research has many challenges: it takes time, requires expert observers, and requires follow-up in concomitant findings and in a strict investigation of incomplete cases. However, Case's collapse Research has a much more important effect. It is innovative and creative ideas, a new theory is developed and doctors have great credibility - the ultimate consumer of research because it suppressed by the strictest limits of surveys and models.

ALEDA V. ROTH AND LARRY J. MENOR, PRODUCTION AND OPERATIONS MANAGEMENT Vol. 12, No. 2, summer 2003 Printed in U.SA.- This document provides a search calendar for the Operations Management Service (SOM). First, we need an SOM program to stimulate. The challenges of the service sector and the connection management of our growing and rapidly evolving national economy drive the urgency of SOM research. Second, we offer a theoretical form that illustrates a broad picture of the key architectural elements in the SOM study landscape. The writing based on research and development prior to the design, development and evaluation of services. Finally, we use our agenda to develop a testing program to stimulate future research in SOM, focus on understanding academic research, and refine developing areas. The operating principles, the theoretical expansion and the development of research techniques in the SOM must increase the monetary significance.

Ibrahim H. Garbie, -Proceedings of the 41st International Conference on Computers & Industrial Engineering, 2008 Vol 7, Issue 13-Be anxiously willing to work effectively, safely and conveniently. The effective demand for ergonomics in the design of the work system can balance the materialistic and professional requirements of the worker. This improves the productivity of the operator, ensures worker safety and physical and mental well-being and job satisfaction. Several research studies have shown positive results that apply to effective value in design, machine and tool design, environment and facilities. Research Studies at Ergonomics has also created data and guidelines for industrial applications. The ergonomic design features of machines, workstations and facilities are well recognized. However, there are still companies in developing countries, especially weak approval and limited application. The main concern of the design of the work system is the development of machines and devices in general. Does not work properly or think. Therefore, poor design work systems are a commonplace in business. Ignorance of ergonomic principles brings disability and pain to the workers. Physical and expressive stress, low productivity, and poor quality of work can result in an unproductive workplace. By reducing the worker's work, the worker can use fewer gestures and reduce the workspace by spending less energy and reducing fatigue. Das and Grady developed the design and demand for anthropometric data. This suggests that an adaptive chair in the office is the most essential for the standard sized workbench. However, the standard height of the workbench not well defined without the anthropometric data of the user population. Most users do not have anthropometric data. This is why the meter is adjustable. Improve productivity in the printing circuit assembly (PCA) plant and seriously consider the health and safety of employees

INTEGRATION OF WORKPLACE LAYOUT, SEQUENTIAL PLANNING, OPERATION MANAGEMENT

Integration of these three methodologies are can provide quite impressive results. Design a new work place can lead the better material flow and better machine arrangements. When we are planning to implement work place layout plan so that we have to design that plan which is suitable to a particular industries. We are incorporating three process together in sequenced planning process first we practical a proper disreputable as operation management it will work like a platform for the other executing technologies in which we are effecting work place layout planning / management / design which will requirement we will relate as per supplies. . The methods they are attainment at an incomplete fraction of output and effectiveness. We performing for an appearance of Methodical process & mixing these major plans for the better efficiency and the productivity. We are merging preparation of production over a scheme or a repetitive product.

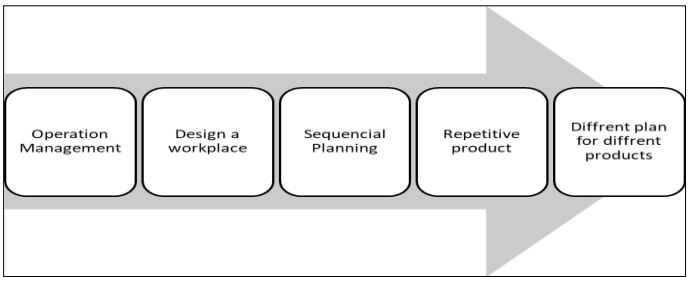

Figure 2- Integration of process

EXISTING METHODOLOGY

In existing technology, we are talking about the processes, methods and operations, which are using by local workshop in micro scale industries. All big companies are using various methodologies like Six Sigma, project management in most of the mechanical industries who belongs to repetitive Products they are using automation. Automation are very costly and it is very high in capital so micro scale industries are cannot adopt these kinds of high stacks Automation. They are following their own beliefs to create a product, so we need to educate them for betterment of production, quality and their growth. Some big companies have the sub vendors, which are using their own old tactics to perform a product. An important job of Product Manager Planning and Product Control. This determines the production process in advance and done according to the plan. The products linked to the complete exchange of raw materials. Productive planning is the transmission, prevention and elimination of prevention difficulties. A technique predicts each step of the product's long-term process. Taking them at the right time and at the right level, and trying to complete the operations to their maximum capacity. The job of control is to facilitate the work and to see everything going according to the plans. The whole process should conducted in the best way and at the lowest cost. The plans of the product manager must anticipate the plans. It is a work of control and planning. Product planning and control requires both good quality products to produce at affordable prices and in the most systematic way. The conversion process is about making decisions about what to produce, how to produce, produce, etc. These decisions are part of the production plan. Deciding to work it is just not enough.

PROPOSED METHODOLOGY

In proposed methodology, we are applying this for the increasing manufacture with the help of three major tools

- Work Place Layout
- Inventory Management
- Operation Management

On the platform of Operation Organization for control, this tools activities. Operation Management is a very vast field but we are using it like a supervisory tool to these three above-itemized tools. If we follow the Principle of Planning and Switch, we have a mechanical store shop and have discussed. "Production of the necessary product in the production of the necessary product can be achieved with the highest efficiency of production through the best and inexpensive method" - PPC is a product of coordinating all manufacturing activities in a manufacturing company playing. Production planning and control mainly involve planning in an engineering company, production, quality, and quality before production and start of training activities. The production plan consists of an organization of the entire manufacturing / operating system to produce a product. Many programs involved in the manufacturing process design the product, determine the needs of equipment and capacity, physical facilities and physical and physical management system, determine the range of processes, and the nature of the operations to be carried out with time requirements and some product size and quality levels. The objective mechanism of the manufacturing plan is to provide a set of guidelines for completing the efficient exchange of raw resources, human resources, and other products together with the physical system. Volume of the product:

Items to decide the product preparation methods: Used product planning, from business to company. Production planning for the production and production of production plan and production of the entire production / operating system will begin production plan. It also works for an industrial plan of revised version of the current product using existing facilities. The vast difference between one company and another manufacturing process is mainly the differences in the financial and technical conditions existing in the management of the enterprises. The three main factors are decisive production-planning processes:

The amount and intensity of production preparation determined by the size and nature of character and industrial processes. The production plan expected to cut industrial costs. In the case of a custom order job store the preparation plan is limited to the preparation of raw materials and parts and components of the production industry and the creation of the works pieces of the production industry.

RESULT COMPARISON OF METHODOLOGY

We observed that the better sequence could drive better performance of the company. No planning can drive low efficiency. No single instruction. The data for each operation is existing to the operator using many generic process papers, which they have to understand! This leads to several different working methods and entire lack of adjustment. No standard layout for paper and data not presented in a user-friendly format. Operation not broken down into clear separate tasks. Not sufficient detail in the method explanation.

This can lead more travel time and distance of the Martial.

Total travel distance of material =

19+21+17+24+9+13

Total travel distance of material = 103 m

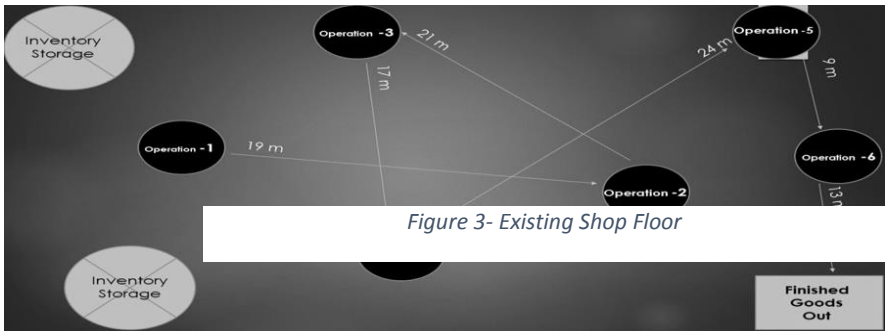

Figure 3- Existing Shop Floor

Proposed Shop Floor Plan

Now implemented Methodology can leads to high efficiency. Thoroughly linked with the method plan are the operators working commands, which describe how to execute the operation. The satisfied and arrangement of the work commands are critical and can have a huge influence on the product excellence. Some businesses (e.g. automotive) focus deeply on this point and many OEM corporations have set values for suppliers. The work training is so important because it is a critical tool for standardizing working methods, which is a key factor in promising consistent product excellence. A good work shop floor should be like.

This can lead less travel time and distance of the Martial.

Total travel distance of material = 5+7+6+9+9+10

Total travel distance of material = 46 m

Figure 4- Proposed Shop Floor

ADVANTAGES OF PROPOSED METHODOLOGY

1. Improving Production Rate and quality

How several times has a manager brainstormed ways to growth the frequency with which personnel perform quality control drafts? New floor layouts are the perfect chance to reduce the footsteps/effort mandatory to QC products while care key personnel at or close their primary workplaces.

2. Operator Efficiency

Reviewing machine-manning supplies by looking at the current mix also can factored hooked on new floor layouts. That does small runs may advantage from having an operator that can change repeatedly to the next job. A shop that does very extended runs, or has been clever to schedule parallel size work to lines, can bring prime operator work positions to within a few steps of each other to decrease redundant people.

3. Planning for Expansion

Planning for future machine developments and elevations can pay massive dividends when the time taken to factor in floor planetary.

4. Less travel time of Material Layout Concepts

In each layout, it must be strongminded where the incomplete product arrives the and wherever finished goods leave. Machine arrangement comes next. Typically, the highest layout chance/variable is the conveyor transfer among the equipment, so careful consideration should give to this capital expense.

ACKNOWLEDGMENT

I take the opportunity to express my cordial gratitude to Mr.Prakash Girewal Asst. Prof. of Mechanical Engg. Dept. and HOD Mr.K.K Shahu Vikrant Institute of Technology and Management Indore, for this kind support . I feel thankful for their innovative idea.

CONCLUSION

In Countries like India small scale industries are short of skilled person and not afford automation .for such kind of industries this methodology helps a lot. In sum, the available research determines that openings can have both direct and indirect belongings on worker's strength and well-being. Product will travel less and dispatch will be possible before delivery date. There is collecting evidence that the appearances of the physical work location can function as a coping reserve and provide many opportunities for renovation. Workplace design is a much-referenced catchword when it comes to following and civilizing employee efficiency. Whatever the field called that achieves product flows, which at the instant is inbound supply chain management, the movement is usual. , it is one of the most significant aspects of any professional. The characteristic of this part of the professional is whether you can content the mandate of your clients if you are not sure if you take all the materials accessible to make the final invention. It clearly shows in results that the proposed methodology is performing well.

REFERENCES:

1. Mehta, S., R. Uzsoy. 1999. Predictable schedule of a single machine with failures. International Review of Computer-Integrated Manufacturing 12 15-38.
2. Mercier, L., P. Van Hentenryck. 2008. Contour detection for a grouped calendar. INFORMS Journal on Computing 20 143-153.
3. Milano, M., P. Van Hentenryck. 2010. Hybrid optimization: ten years of CPAIOR. Jumper. Milgrom, P., J. Roberts. 1990. Rationalization, learning and balance in games with strategic complementarity. Econometrica 58 1255-1277.
4. Moin, N.H., S. Salhi. 2007. Inventory Routing Issues: Logistics Overview. The Journal of the Operational Research Society 58 1185-1194.
5. Morton, T. E., D.W. Pentico. 1993. Heuristic planning systems. Wiley.

6. Mosheiov, G., A. Sarig. 2009. Scheduling maintenance and assigning windows to the window on a single machine. Computers and Operations Research 36 2541-2545.
7. MODAPTS International Association, Inc., 2000, MODAPTS Manual, Southern Shores, NC, 4th edition, second printing, February 2007.
8. Kanawaty, George, 1996, "Introduction to the Study of Work" 4th Edition (Revised), International Labor Office, Geneva Konz, Stephan, 1995, "Work Project: Industrial Ergonomics, Fourth Edition, Horizon Publishing, Inc. .
9. Niebel, Benjamin W., Freivalds, Andris, 2009, Industrial Engineering: Methods, Standards and Work Project "12th Edition, McGraw-Hill Education, August 1st.
10. Bowman D.A., Kruijff E., LaViola J.J. and Poupyrev I. "3D User Interface: Theory and Practice". pp. 87-134.
11. Addison-Wesley / Pearson Education, 2005. Bowman D.A., Coquillart S., Froehlich S., Hirose M., Kitamura Y., Kiyokawa K. "3D User Interfaces: New Directions and Prospects". Annals of the History of IEEE Computing, pp. 20-36, 2008.
12. Dang N., Tavanti M., Rankin I. and Cooper M. "Comparison of various input devices to the 3D environment". in Proceedings of ECCE Conference 2007, pp. 153-160, 2008Galambos P., and Baranyi P. “VirCA as Virtual Intelligent Space for RT-Middleware”, in Proceedings of 2011 IEEE/ASME International Conference on Advanced Intelligent Mechatronics (AIM2011), pp. 140-145, 2011. Gallo L. and Pietro G.D.. “Input Devices and Interaction
13. Expanded Medicine VR Techniques, "Multimedia Techniques for Device and Environmental Analysis, Part 2, pp. 115-134, 2009.
14. Komlodi A., Jozsa E., Hercegfi K., Kucsora Borics SD, "An Empirical Evaluation of the Wii Controller Utility as an Input Device for a Realistic VirC Virtual Space" in Proceedings of Cognitive International Conference on Infocommunications (CogInfoCom) p 1-6, 2011.
15. Korondi P., Baranyi P., Hashimoto H., Solvang B. "3D communication and control over the Internet". Computer Intelligence in Engineering, Springer-Verlag, pp. 47-60., 2010.
16. Lewis, J.J. J. Sauro "The Current Structure of the Large-Scale Utility System", Proceedings of the 1st International Conference on Human Centered Design: under HCI Held International 2009, pp. 94-103, 2009.
17. D. Vincze, Kovács Sz., M. Gacsi, K. Korondi, A. Miklósi, P. Baranyi "A new application of environmental modeling Virca 3D standard test ethical interaction between dog and man." ACTA POLYTECHNICA HUNGARICA 9: (1) pp. 107-120, 2012.
18. Gabor Sziebig, Andor Gaudia, Peter Korondi, Ando Noriaki, Video Processing System for RT-middleware. In: Proc VII International Symposium of Hungarian Intelligence Investigators (HUCI'06). Budapest, Hungary, 24/11 / 2006-25 / 11/2006. pp. 461-472.
19. Bjørn Solvang, Peter Korondi, Gabor Sziebig, Noriaki Ando, SAPIR: Adaptive Supervised Programming and Industrial Robots. In: 11th IEEE International Conference on Intelligent Engineering Systems (INES'07). Budapest, Hungary, 29/06 / 2007-02 / 07/2007. (IEEE) pp 281-286. (ISBN: 1-4244-1147-5)
20. Gabor Sziebig, Chen Hao, Lorant Nagy, Peter Korondi, Comprehensive DC Multimedia Learning Program for Remote Servo Learning. In: Proceeding of Computational Intelligence and Computing (Cintia), 8th International Symposium of Hungarian Researchers, Budapest, Hungary, 15/10 / 2007-17 / 10/2007. pp. 283-293. Article 25. (ISBN: 978 963 7154 65 2)
21. Gabor Sziebig, Andor Gaudia, Peter Korondi, Noriaki Ando, Bjørn Solvang, Robot Vision RT-Middleware Framework. In: Proceedings of the IEEE Instrumentation and Measurement Technologies Conference, IMTC '07. Warsaw, Poland, 01/05 / 2007-03 / 05/2007. Piscataway: IEEE, pp. 1-6. (ISBN: 1-4244-0588-2)
22. Gabor Sziebig, Bela Takarics, Viliam Fedak, Peter Korondi, virtual master device. In: Proc V Joint Slovak-Hungarian Symposium on the Applied Intelligence of Machines (SAMI'07). Poprad, Slovakia, 25/01 / 2007-26 / 01 / 2007.pp. 29-40. Article 4
23. Gabor Sziebig, Istvan Nagy, R K Jardan, Peter Korondi, Integrated DC Learning Program for DC Servo for Distance Learning. In: Materials from the 13th Power Electronics and Motion Control Conference (EPE-PEMC 2008). Poznań, Poland, 01/09/2009 / 09/2008. pp. 2360-2367. (ISBN: 978-1-4244-1741-4)
24. Peter Korondi, Bjørn Solvang, Gabor Sziebig, Peter Baranyi, Interactive Programming Methodology of People and Robots. In: Manufacturing 2008. International 19 International Conference. Budapest, Hungary, 06/11 / 2008-07 / 11/2008. Budapest: pp. 125-133. (ISBN: 978-963-9058-24-8)
25. Zoltan Suto, Peter Stumpf, Kalman R. Jardan, Istvan Nagy, Integrated eLearning Projects in the European Union. In: IECON 2008. Orlando, United States, 10/11 / 2008-13 / 11/2008. IEEE, pp. 3524-3529. (ISBN: 978-1-4244-1767-4)

International Journal of Engineering Research and general science is an open access peer review publication which is established for publishing the latest trends in engineering and give priority to quality papers which emphasis on basic and important concept through which there would be remarkable contribution to the research arena and also publish the genuine research work in the field of science, engineering and technologies